

CECW-EH-D Engineer Manual 1110-2-1601	Department of the Army U.S. Army Corps of Engineers Washington, DC 20314-1000	EM 1110-2-1601 1 July 1991/ 30 June 1994
	Engineering and Design HYDRAULIC DESIGN OF FLOOD CONTROL CHANNELS	
	Distribution Restriction Statement Approved for public release; distribution is unlimited.	

**Engineering and Design
 HYDRAULIC DESIGN OF FLOOD CONTROL CHANNELS**

1. This Change 1 to EM 1110-2-1601, 1 Jul 91:


- a.* Updates Chapter 2.
- b.* Updates Chapter 3.
- c.* Adds Chapter 5, which describes methods for predicting n values for the Manning equation.
- d.* Updates the Table of Contents to reflect the changes in Chapters 2 and 3 and the addition of Chapter 5.
- e.* Updates the preceding chapters to reflect the addition of Chapter 5.
- f.* Adds references in Chapters 3 and 5 to Appendix A.
- g.* Adds updated plates in Chapter 3 to Appendix B.
- h.* Inserts page F-18, which was inadvertently omitted.
- i.* Updates Appendix H.
- j.* Adds symbols in Chapter 5 to Appendix I.

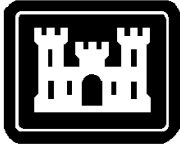
2. Substitute the attached pages as shown below:

Chapter	Remove page	Insert page
Table of Contents	i and ii	i and ii
2	2-1 and 2-2	2-1 and 2-2
3	3-1 thru 3-10	3-1 thru 3-12
5	—	5-1 thru 5-16
Appendix A	A-1 thru A-7	A-1 thru A-8
Appendix B	B-35 thru B-60	B-35 thru B-61
Appendix F	F-17	F-17 and F-18
Appendix H	H-1 and H-2	H-1 and H-2
Appendix I	I-1 thru I-4	I-1 thru I-4

3. File this change sheet in front of the publication for reference purposes.

FOR THE COMMANDER:


WILLIAM D. BROWN
Colonel, Corps of Engineers
Chief of Staff



EM 1110-2-1601
1 July 1991

**US Army Corps
of Engineers**

ENGINEERING AND DESIGN

Hydraulic Design of Flood Control Channels

ENGINEER MANUAL

DEPARTMENT OF THE ARMY
U.S. Army Corps of Engineers
Washington, D.C. 20314-1000

EM 1110-2-1601

CECW-EH-D

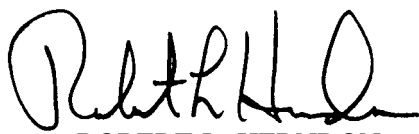
Engineer Manual
No. 1110-2-1601

1 July 1991

Engineering and Design
HYDRAULIC DESIGN OF FLOOD CONTROL CHANNELS

- 1. Purpose.** This manual presents procedures for the design analysis and criteria of design for improved channels that carry rapid and/or tranquil flows.
- 2. Applicability.** This manual applies to major subordinate commands, districts, and laboratories having responsibility for the design of civil works projects.
- 3. General.** Procedures recommended herein are considered appropriate for design of features which are usable under most field conditions encountered in Corps of Engineers projects. Basic theory is presented as required to clarify presentation and where the state of the art, as found in standard textbooks, is limited. In the design guidance, where possible, both laboratory and prototype experimental test results have been correlated with current theory.

FOR THE COMMANDER:



ROBERT L. HERNDON
Colonel, Corps of Engineers
Chief of Staff

CECW-EH-D

Engineer Manual
No. 1110-2-1601

30 June 1994

**Engineering and Design
HYDRAULIC DESIGN OF FLOOD CONTROL CHANNELS**

Table of Contents

Subject	Paragraph	Page	Subject	Paragraph	Page
Chapter 1			<i>Section III</i>		
Introduction			<i>Design Guidance for Stone Size</i>		
Purpose	1-1	1-1	General	3-5	3-4
Scope	1-2	1-1	* Design Conditions	3-6	3-5*
References	1-3	1-1	Stone Size	3-7	3-5
Explanation of Terms	1-4	1-1	* Revetment Top and End		
Channel Classification	1-5	1-1	Protection	3-8	3-8*
Preliminary Investigations for Selection			<i>Section IV</i>		
of Type of Improvement	1-6	1-1	<i>Revetment Toe Scour Estimation and Protection</i>		
Chapter 2			* General	3-9	3-9*
Open Channel Hydraulic Theory			* Revetment Toe Protection		
Physical Hydraulic			Methods	3-10	3-10*
Elements	2-1	2-1	* Revetment Toe Protection		
Hydraulic Design			Design	3-11	3-10*
Aspects	2-2	2-1	* Delivery and Placement	3-12	3-11*
Flow Through Bridges	2-3	2-5	<i>Section V</i>		
Transitions	2-4	2-8	<i>Ice, Debris, and Vegetation</i>		
Flow in Curved Channels	2-5	2-12	* Ice and Debris	3-13	3-11*
Special Considerations	2-6	2-14	* Vegetation	3-14	3-12*
Stable Channels	2-7	2-15	<i>Section VI</i>		
Chapter 3			<i>Quality Control</i>		
Riprap Protection			* Quality Control	3-15	3-12*
<i>Section I</i>			Chapter 4		
<i>Introduction</i>			Special Features and Considerations		
General	3-1	3-1	Sediment Control Structures	4-1	4-1
Riprap Characteristics	3-2	3-1	Air Entrainment	4-2	4-3
<i>Section II</i>			Hydraulic Jump in Open		
<i>Channel Characteristics</i>			Channels	4-3	4-3
Side Slope Inclination	3-3	3-4	Open Channel Junctions	4-4	4-5
Channel Roughness, Shape,			Hydraulic Model Studies	4-5	4-8
Alignment, and Gradient.	3-4	3-4			

**EM 1110-2-1601
Change 1
30 Jun 94**

Subject	Paragraph	Page	Subject	Paragraph	Page
* Chapter 5			Appendix D		
Methods for Predicting n Values for the Manning Equation			Computer Program for Designing Banked Curves for Supercritical Flow in Rectangular Channels		
Introduction	5-1	5-1	Appendix E		
Approach	5-2	5-1	Theory of Combining Flow at Open Channel Junctions (Confluences)		
Hydraulic Roughness by Handbook Methods	5-3	5-1	Appendix F		
Base n Values (n_b) for Channels	5-4	5-1	Report on Standardization of Riprap Gradations		
Hydraulic Roughness by Analytical Methods	5-5	5-2	Appendix G		
Composite n Values and Hydraulic Radius	5-6	5-12	Velocity Estimation Based on Field Observations		
Expansion and Contraction in a 1-D Model	5-7	5-14	Appendix H		
Unforeseen Factors	5-8	5-14 *	Examples of Stone Size Calculations		
Appendix A			Appendix I		
References			Notation		
Appendix B					
Plates					
Appendix C					
Notes on Derivation and Use of Hydraulic Properties by the Alpha Method					

Chapter 1 Introduction

1-1. Purpose

This manual presents procedures for the design analysis and criteria of design for improved channels that carry rapid and/or tranquil flows.

1-2. Scope

Procedures are presented without details of the theory of the hydraulics involved since these details can be found in any of various hydraulic textbooks and publications available to the design engineer. Theories and procedures in design, such as flow in curved channels, flow at bridge piers, flow at confluences, and side drainage inlet structures, that are not covered fully in textbooks are discussed in detail with the aid of Hydraulic Design Criteria (HDC) charts published by the US Army Engineer Waterways Experiment Station (USAEWES). The charts and other illustrations are included in Appendix B to aid the designer. References to HDC are by HDC chart number. The use of models to develop and verify design details is discussed briefly. Typical calculations are presented to illustrate the principles of design for channels under various conditions of flow. Electronic computer programming techniques are not treated in this manual. However, most of the basic hydraulics presented herein can be adapted for computer use as illustrated in Appendix D.

1-3. References

References are listed in Appendix A.

1-4. Explanation of Terms

Abbreviations used in this manual are explained in the Notation (Appendix I). The symbols employed herein conform to the American Standard Letter Symbols for Hydraulics (American Society of Mechanical Engineers 1958) with only minor exceptions.

1-5. Channel Classification

In this manual, flood control channels are considered under two broad classifications: rapid- and tranquil-flow channels. The most important characteristics that apply to rapid and tranquil flows are listed below:

a. Velocities. Rapid flows have supercritical

velocities with Froude numbers greater than 1 ($F > 1$), and tranquil flows have subcritical velocities with Froude numbers less than 1 ($F < 1$).

b. Slopes. Invert slopes in general are greater than critical slopes ($S_o > S_c$) for rapid flow and less than critical slopes ($S_o < S_c$) for tranquil flow.

c. Channel storage. Channel storage is usually negligible in rapid flow, whereas it may be appreciable in natural rivers with tranquil flow.

d. Discharge. All discharges are normally confined within the channel for rapid flow (no overbank flow).

Other characteristics such as standing waves, surges, and bed configuration that differ under the influence of rapid- or tranquil-flow conditions should be recognized and considered as the occasion demands. Rapid and tranquil flows can occur within a longitudinal reach of a channel with changes in discharge, roughness, cross section, or slope. Channel improvements may bring about changes in flow characteristics.

1-6. Preliminary Investigations for Selection of Type of Improvement

The investigation required in selecting the type of channel improvement to be adopted involves three considerations: physical features of the area, hydraulic and hydrologic aspects, and economy.

a. Physical features. The topography of the area controls in a general way the channel alignment and invert grades. Of prime importance, also, are width of available right-of-way; location of existing channel; and adjacent existing structures, such as bridges, buildings, transportation facilities, utility structures, and outlets for local drainage and tributaries. Invert slopes may be controlled by elevations of existing structures as well as by general topography, elevations at ends of improvements, and hydraulic features.

b. Historical and observed elements. The flow characteristics noted in historical records and indicated from detailed observation of existing conditions will usually be basic to the selection of type of improvement or design. With the flood discharges determined, the interdependent factors that determine improvement methods and general channel alignment are slope of invert, width and depth of flow, roughness coefficient, the presence or nature of aggradation and degradation processes, debris transportation, bank erosion, cutoffs, and bar formations.

c. Preliminary layout. A preliminary map or aerial mosaic of the area showing the topography and other control factors to a scale satisfactory for plotting the center line of the channel should be obtained. A scale of 1 inch (in.) to 100 feet (ft) with 2-ft-contour interval is suggested, although judgment based on local conditions should be used. A preliminary profile should be prepared that will show all pertinent elevations of the ground and existing structures along the banks and along the center line of the proposed channel.

d. Preliminary alternative designs. From a study of the preliminary plan, profiles, and available widths, tentative channel cross sections are adopted. These are generally rectangular or trapezoidal sections. Low velocity flows can usually be carried in natural-bottom trapezoidal channels with or without stone-revetted side slopes. High-velocity flows normally would be carried in concrete-lined channels. Preliminary hydraulic analyses

of the proposed channels are then made with a view toward establishing the most efficient channel improvement from the standpoint of hydraulic efficiency and economic feasibility.

e. Economy. Approximate cost estimates are prepared, including costs of channel construction, appurtenant works and bridges, and rights-of-way. It may be necessary to consider several channel alignments, cross sections, and construction materials before the least-cost design consistent with sound engineering principles is determined. Assured performance, consistent with project formulation based on sound engineering judgment, is a necessary part of economic consideration. With an optimum general design thus tentatively established, and provided the cost is economically feasible for the project as a whole, the detailed hydraulic design is presented in Chapter 2.

Chapter 2 Open Channel Hydraulic Theory

2-1. Physical Hydraulic Elements

a. General. The physical hydraulic elements concerned in hydraulic design of channels consist of invert slope (S_o), cross-sectional area (A), wetted perimeter (P), and equivalent boundary surface roughness (k). The hydraulic radius (R) used in resistance formulae is the ratio A/P . The invert slope of proposed channel improvement is controlled primarily by elevations of the ground along the alignment as determined by preliminary layout discussed in paragraph 1-6d. A center-line profile between controlling elevations along the proposed alignment will indicate a preliminary channel slope.

b. Channel cross section.

(1) The proper channel cross section for a given reach is the one that has adequate hydraulic capacity for a minimum cost of construction and maintenance. The economics must include the costs of right-of-way and structures such as bridges. In rural areas a trapezoidal cross section may be least costly, whereas in urban areas a rectangular cross section is often the least costly.

(2) Plate 1¹ shows a sample cost computation and related cost curve for a reach of curved rectangular concrete channel. Similar procedures may be applied to compute the cost for any type of cross section considered for design. Special types of concrete channel cross sections are shown in Plate 2: the V-bottom channel and the modified trapezoidal channel. The latter has a small low-flow channel in the center.

(a) In the V-bottom channel, low flows are concentrated along the channel center line. This prevents moderate flow from meandering over the entire channel width, which would result in random deposition of material across the invert as in the case of a horizontal bottom. Deposition in the center of the V-bottom is removed by larger flows. Because the wear caused by bed load is also concentrated near the center line, maintenance cost is reduced.

(b) In the modified trapezoidal cross section, vertical sidewalls reduce the top width. This design is desirable

when the width of the right-of-way is limited. A small, low-flow channel in the center of the cross section provides a flow way into which subdrainage can be emptied. In cold climates, the low-flow channel reduces the invert area subjected to the deleterious effects of freezing and thawing. In some cases the low-flow channel may serve as a fishway.

c. Roughness. The concept of surface roughness as the basic parameter in flow resistance (friction) is almost universally accepted. Absolute roughness is determined from the physical dimensions of the wetted surface irregularities and is normally of theoretical interest only. Equivalent roughness is a linear dimension (effective roughness height) directly related to the boundary resistance of the channel (Plate 3). The relations between roughness and the various coefficients for friction formulae are adequately covered by Chow (1959, chap 8).

* Friction formulae and their uses are discussed in paragraph 2-2, and methods for predicting Manning's roughness coefficient n are discussed in Chapter 5. *

d. Composite roughness. Where there is material variation in roughness between various portions of the wetted perimeter such as might be found in natural channels or channels with protected banks and natural inverts, an equivalent or effective roughness or friction coefficient for each stage considered should be determined. Appendix C illustrates a method for determining a composite value of k for each stage. Plates 4 and 5 give the relation between k and Manning's n for flows in the rough flow zone shown in Plate 3. HDC sheets 631-4 and 631-4/1 also give a procedure for determining an effective Manning's n .

e. Hydraulic efficiency. The problem of the most efficient cross section is treated by Brater and King (1976, see pp 7-5 to 7-7) and Chow (1959, see paragraph 7-6).

2-2. Hydraulic Design Aspects

a. General. This presentation assumes that the design engineer is fully acquainted with the hydraulic theories involved in uniform and gradually varied flows, steady and unsteady flows, energy and momentum principles, and other aspects such as friction related to hydraulic design normally covered in hydraulic texts and handbooks such as those by Brater and King (1976) and Chow (1959). The following is presented as guidance in the method of application of textbook material and to give additional information not readily available in reference

¹ Plates mentioned in this and succeeding chapters are included in Appendix B as Plates B-1, B-2, etc.

material. The use of k is emphasized herein because computational results are relatively insensitive to errors in assigned values of k . However, use of Manning's n has been retained in several procedures because of its wide acceptance and simplicity of use. This applies particularly to varied flow profiles, pulsating flow, and the design of free-surface hydraulic models.

b. Friction losses.

(1) The importance that friction plays in the determination of flow characteristics in channels cannot be overstressed. Three equations (Chezy's, Manning's, and Darcy's) are in general use for the determination of losses due to friction. These equations expressed as friction slope S_f , i.e., slope of the energy grade line, are

(a) Chezy:

$$S_f = \frac{V^2}{C^2 R} \quad (2-1)$$

(b) Manning:

$$S_f = \frac{V^2 n^2}{2.21 R^{4/3}} \quad (2-2)$$

(c) Darcy:

$$S_f = \frac{f V^2}{8 R g} \quad (2-3)$$

where

V = velocity

C = Chezy coefficient

f = Darcy-Weisbach resistance coefficient

g = acceleration of gravity

*

The relation between the coefficients in these equations can be expressed as

$$\frac{C}{1.486} = \frac{R^{1/6}}{n} = \frac{10.8}{f^{1/2}} \quad (2-4)$$

(2) When determining friction coefficients, it should be recognized that the energy grade line and therefore the friction coefficient include uniformly occurring turbulence and eddy losses as well as the friction loss. Equivalent roughness for the same reason. Special, locally occurring turbulence and eddy losses are to be determined separately as covered in hydraulic textbooks and elsewhere in this manual.

c. Friction coefficients.

(1) The equations for using equivalent roughness to determine friction coefficients (Plate 3) are

(a) For hydraulically smooth channels

$$C = 32.6 \log_{10} \left(\frac{5.2 R_n}{C} \right) \quad (2-5)$$

(b) For hydraulically rough channels

$$C = 32.6 \log_{10} \left(\frac{12.2 R}{k} \right) \quad (2-6)$$

where R_n is the Reynolds number.

(2) For the channel surface to be hydraulically smooth, the equivalent roughness must be less than the critical value given by paragraph 8-12 of Chow (1959).

$$k_c = \left(\frac{5C}{\sqrt{g}} \right) \left(\frac{v}{V} \right) \quad (2-7)$$

where v is the kinematic viscosity of water.

*

(3) Most channels (including concrete-lined channels) with appreciable velocity are hydraulically rough. Plates 4 and 5 are furnished as an aid for determining friction coefficients from equivalent roughness. Irrigation and power canals generally fall in the transition zone shown in Plate 3.

(4) Table 2-1, extracted from HDC sheets 631 to 631-2, provides acceptable equivalent roughness values for straight, concrete-lined channels.

(5) See Chapter 3 for friction coefficients for riprap.

(6) Values of k for natural river channels usually fall between 0.1 and 3.0 ft (see Table 8-1 of Chow

Table 2-1
Acceptable Equivalent
Roughness Values

Design Problem	k , ft
Discharge Capacity	0.007
Maximum Velocity	0.002
Proximity to Critical Depth ¹	
Tranquil Flow	0.002
Rapid Flow	0.007

Note:

1. To prevent undesirable undulating waves, ratios of flow depth to critical depth between 0.9 and 1.1 should be avoided where economically feasible.

1959). These values will normally be much larger than the spherical diameters of the bed materials to account for boundary irregularities and sand waves. When friction coefficients can be determined from experienced flow information, k values should then be computed using the relations described in Equation 2-6. The k values so determined apply to the surfaces wetted by the experienced flows. Additional wetted surfaces at higher stages should be assigned assumed k values and an effective roughness coefficient computed by the method outlined in Appendix C if the increased wetted surfaces are estimated to be appreciably smoother or rougher. Values of k for natural channels may also be estimated from Figures 8 and 9 of Chow (1959) if experimental data are not available.

d. Flow classification. There are several different types of flow classification. Those treated in this paragraph assume that the channel has a uniform cross-sectional rigid boundary. The concepts of tranquil and rapid flows are discussed in (1) below. The applicability of the newer concepts of steady rapid flow and pulsating rapid flow to design problems are treated in (2) below. All of these concepts are considered from the viewpoint of uniform flow where the water-surface slope and energy grade line are parallel to the bottom slope. Flow classification of nonuniform flow in channels of uniform solid boundaries or prismatic channels is discussed in (3) below. The design approaches to flow in nonprismatic channels are treated in other portions of this manual.

(1) Tranquil and rapid flows.

(a) The distinction between tranquil flow and rapid flow involves critical depth. The concept of specific energy H_e can be used to define critical depth. Specific energy is defined by

$$H_e = d + \alpha \frac{V^2}{2g} \quad (2-8)$$

where

d = depth

α = energy correction factor

$V^2/2g$ = velocity head

Plate 6 shows a specific energy graph for a discharge q of 100 cubic feet per second (cfs) (two-dimensional flows). Each unit discharge has its own critical depth:

$$d_c = \left(\frac{q^2}{g} \right)^{1/3} \quad (2-9)$$

The development of this equation is given by pp 8-8 and 8-9 of Brater and King (1976). It may be noted that the critical depth occurs when the specific energy is at a minimum. Flow at a depth less than critical ($d < d_c$) will have velocities greater than critical ($V > V_c$), and the flow is described as rapid. Conversely, when $d > d_c$ and $V < V_c$, the flow is tranquil.

(b) It may be noted in Plate 6 that in the proximity of critical depth, a relatively large change of depth may occur with a very small variation of specific energy. Flow in this region is unstable and excessive wave action or undulations of the water surface may occur. Experiments by the US Army Engineer District (USAED), Los Angeles (1949), on a rectangular channel established criteria to avoid such instability, as follows:

Tranquil flow: $d > 1.1d_c$ or $F < 0.86$

Rapid flow: $d < 0.9d_c$ or $F > 1.13$

where F is the flow Froude number. The Los Angeles District model indicated prototype waves of appreciable height occur in the unstable range. However, there may be special cases where it would be more economical to provide sufficient wall height to confine the waves rather than modify the bottom slope.

(c) Flow conditions resulting with Froude numbers near 1.0 have been studied by Boussinesq and Fawer. The results of their studies pertaining to wave height with unstable flow have been summarized by Jaeger (1957, pp 127-131), including an expression for approximating the wave height. The subject is treated in more detail in paragraph 4-3d below. Determination of the critical depth instability region involves the proper selection of high and low resistance coefficients. This is demonstrated by the example shown in Plate 6 in which the depths are taken as normal depths and the hydraulic radii are equal to depths. Using the suggested equivalent roughness design values of $k = 0.007$ ft and $k = 0.002$ ft, bottom slope values of $S_o = 0.00179$ and $S_o = 0.00143$, respectively, are required at critical depth. For the criteria to avoid the region of instability ($0.9d_c < d < 1.1d_c$), use of the smaller k value for tranquil flow with the bottom slope adjusted so that $d \geq 1.1d_c$ will obviate increased wall heights for wave action. For rapid flow, use of the larger k value with the bottom slope adjusted so that $d \leq 0.9d_c$ will obviate increased wall heights should the actual surface be smoother. Thus, the importance of equivalent roughness and slope relative to stable flow is emphasized. These stability criteria should be observed in both uniform and nonuniform flow design.

(2) Pulsating rapid flow. Another type of flow instability occurs at Froude numbers substantially greater than 1. This type of flow is characterized by the formation of slugs particularly noticeable on steep slopes with shallow flow depth. A Manning's n for pulsating rapid flow can be computed from

$$\frac{0.0463R^{1/6}}{n} = 4.04 - \log_{10} \left(\frac{F}{F_s} \right)^{2/3} \quad (2-10)$$

The limiting Froude number F_s for use in this equation was derived by Escoffier and Boyd (1962) and is given by

$$F_s = \frac{\xi}{\sqrt{g} \zeta^{3/2} (1 + Z\zeta)} \quad (2-11)$$

where ξ , the flow function, is given by

$$\xi = \frac{Q}{b^{5/2}}$$

where Q is the total discharge and ζ , the depth-width ratio, is given by

$$\zeta = \frac{d}{b}$$

where b is the bottom width.

Plate 7 shows the curves for a rectangular channel and trapezoidal channels with side slopes Z of 1, 2, and 3.

(3) Varied flow profiles. The flow profiles discussed herein relate to prismatic channels or uniform cross section of boundary. A complete classification includes bottom slopes that are horizontal, less than critical, equal to critical, greater than critical, and adverse. However, the problems commonly encountered in design are mild slopes that are less than critical slope and steep slopes that are greater than critical slope. The three types of profiles in each of these two classes are illustrated in HDC 010-1. Chow (1959) gives a well-documented discussion of all classes of varied flow profiles. It should be noted that tranquil-flow profiles are computed proceeding upstream and rapid-flow profiles downstream. Flow profiles computed in the wrong direction result in divergences from the correct profile. Varied-flow computations used for general design should not pass through critical depth. Design procedures fall into two basic categories: uniform and nonuniform or varied flow. Many

graphs and tables have been published to facilitate computation of uniform flow. Brater and King (1976) have specially prepared tables for trapezoidal channels based on the Manning equation. HDC 610-1 through 610-4/1-1 give graphs that afford rapid solution for the normal depth in trapezoid channels. Nonuniform or varied flow in prismatic channels can be solved rapidly by use of the varied flow function. (It should be noted that different authors have used the terms "nonuniform" flow and "varied" flow to mean the same thing; "varied flow" is used in this manual.) Varied flow in nonprismatic channels, such as those with a gradually contracting or a gradually expanding cross section, is usually handled by "step methods." It should be noted that short, rapidly contracting or expanding cross sections are treated in this manual as transitions.

(a) Prismatic channels. A prismatic channel is characterized by unvarying cross section, constant bottom slope, and relatively straight alignment. There are three general methods of determining flow profiles in this type of channel: direct integration, direct step, and standard step, as discussed in Chow (1959, pp 252-268). The direct integration and direct step methods apply exclusively to prismatic channels, whereas the standard step method applies not only to prismatic channels but is the only method to be applied to nonprismatic channels. The direct integration method (with certain restrictions as to the constancy of hydraulic exponents) solves the varied flow equation to determine the length of reach between successive depths. Use is made of varied-flow-function tables to reduce the amount of computations. This method is not normally employed unless sufficient profiles and length of channel are involved to warrant the amount of precomputational preparation. The direct step method determines the length of reach between successive depths by solution of the energy and friction equations written for end sections of the reach. The standard step method is discussed in (b) below.

(b) Nonprismatic channels. When the cross section, alignment, and/or bottom slope changes along the channel, the standard step method (Chow 1959, p 265) is applied. This method determines the water-surface elevation (depth) at the reach extremity by successive approximations. Trial water-surface elevations are assumed until an elevation is found that satisfies the energy and friction equations written for the end sections of the reach. Cross sections for this method should, in general, be selected so that velocities are increasing or decreasing continuously throughout the reach. EM 1110-2-1409 contains further information on this method. Plate 8 shows a sample computation for a gradually contracting trapezoidal

channel where both bottom width and side slope vary. Successive approximations of water-surface elevations are made until a balance of energy is obtained. Friction losses h_f are based on the Manning equation.

$$S_f = \frac{n^2 V^2}{2.21R^{4/3}} = \frac{V^2}{C^2 R} \quad (2-1 \text{ and } 2-2 \text{ bis})$$

For the sample computation a mild slope upstream and steep slope downstream of sta 682+40 have been assumed. Critical depth would occur in the vicinity of sta 682+40 and has been assumed as the starting condition. Initially, column 21 has the same value as column 10. The computations proceed downstream as the flow is rapid. The length of reach is chosen such that the change in velocity between the ends of the reach is less than 10 percent. The energy equation is balanced when column 21 checks column 10 for the trial water surface of column 5. Plate 9 repeats the computation, substituting $k = 0.002 \text{ ft}$ for $n = 0.014$. For rough channel conditions

$$C = 32.6 \log_{10} \left(\frac{12.2R}{k} \right) \quad (2-6 \text{ bis})$$

2-3. Flow Through Bridges

Bridge piers located in channels result in energy losses in the flow and create disturbances at the bridge section and in the channel sections immediately upstream and downstream. As bridge pier losses materially affect water-surface elevations in the vicinity of the bridge, their careful determination is important. Submergence of bridge members is not desirable.

a. Abutment losses. Bridge abutments should not extend into the flow area in rapid-flow channels. In tranquil-flow channels they should be so designed that the flow depth between abutments or between the abutment and an intermediate pier is greater than critical depth. The Bureau of Public Roads (BPR) (Bradley 1978) has published design charts for computing backwater for various abutment geometries and degrees of contraction. The design procedure and charts developed by BPR are recommended for use in channel designs involving bridge abutments. For preliminary designs, a step backwater computation using abrupt expansion and contraction head losses of 1.0 and 0.5, respectively, times the change in

velocity head may be used. This method under the same circumstances may be applied to bridge openings containing piers.

b. Pier losses. Rapid, tranquil, or a combination of rapid- and tranquil-flow conditions may occur where only bridge piers are located in the flow area. Flow through bridge piers for this condition is classified as class A, B, or C, according to the depth of flow in relation to critical depth occurring upstream, between piers, and downstream. Plate 10 is a graphic description of these classes, which are discussed below. Plate 11 is useful in determining the class of flow in rectangular channels.

(1) Class A flow (energy method). Chow (1959, paragraph 17-10) presents a discussion and several energy loss formulae with appropriate coefficients that may be used for computing bridge pier losses for tranquil flow (class A). While the momentum method presented below may also be used for class A flow, the energy method usually gives better results.

(2) Classes B and C flows (momentum method).

(a) A graph (example shown in Plate 12) constructed from the equation proposed by Koch and Carstanjen (Chow 1959) and based on the momentum relation can be used for determining graphically the flow classification at constrictions due to bridge piers. In addition, the graph can be used for estimating unknown flow depths. A summary of the equation derivation follows.

(b) In a given channel section the momentum per unit time of the flow can be expressed by

$$M = \beta \left(\frac{\gamma QV}{g} \right) \quad (2-12)$$

where

M = momentum per unit time, pounds (lb)
(from pounds-second per second
(lb-sec/sec))

β = momentum correction coefficient

γ = specific weight of water, pounds per
cubic foot (pcf)

Q = total discharge, cfs

V = average channel velocity, feet per
second (fps)

g = acceleration of gravity, ft/sec²

In Equation 2-12 β is generally assumed to be equal to 1.0. Since

$$Q = AV \quad (2-13)$$

Equation 12 can be written

$$M = \frac{\gamma Q^2}{gA} \quad (2-14)$$

(c) The total hydrostatic force m (in pounds) in the channel section can be expressed as

$$m = \gamma \bar{y}A \quad (2-15)$$

where \bar{y} is the distance from the water surface to the center of gravity (centroid) of the flow section.

(d) Combining Equations 14 and 15 results in

$$m + M = \gamma \bar{y}A + \frac{\gamma Q^2}{gA} \quad (2-16)$$

By the momentum principle in an unconfined channel

$$m_a + \frac{\gamma Q_a^2}{gA_a} = m_b + \frac{\gamma Q_b^2}{gA_b} \quad (2-17)$$

where m_a and m_b are the total hydrostatic forces of water in the upstream and downstream sections, respectively, lb.

(e) Based on experiments under all conditions of open-channel flow where the channel was constricted by short, flat surfaces perpendicular to the flow, such as with

bridge piers, Koch and Carstanjen (Koch 1926) found that the upstream momentum force had to be reduced by $(A_p/A_1)(\gamma Q^2/gA_1)$ to balance the total force in the constriction.

(f) Equating the summation of the external forces above and below the structures with those within the contracted section yields

$$m_1 + \frac{\gamma Q^2}{gA_1} - \left[\left(\frac{A_p}{A_1} \right) \left(\frac{\gamma Q^2}{gA_1} \right) \right] = m_2 + m_p + \frac{\gamma Q^2}{gA_2} \quad (2-18)$$

and

$$m_2 + m_p + \frac{\gamma Q^2}{gA_2} = m_3 + \frac{\gamma Q^2}{gA_3} \quad (2-19)$$

Combining these equations results in

$$m_1 + \frac{\gamma Q^2}{gA_1} - \left[\left(\frac{A_p}{A_1} \right) \left(\frac{\gamma Q^2}{gA_1} \right) \right] = m_2 + m_p + \frac{\gamma Q^2}{gA_2} = m_3 + \frac{\gamma Q^2}{gA_3} \quad (2-20)$$

This reduces to the Koch-Carstanjen equation

$$m_1 - m_p + \frac{\gamma Q^2}{gA_1^2}(A_1 - A_p) = m_2 + \frac{\gamma Q^2}{gA_2} = m_3 - m_p + \frac{\gamma Q^2}{gA_3} \quad (2-21)$$

where

γ = specific weight of water, pounds per cubic foot (pcf)

Q = total discharge, cfs

m_1 = total hydrostatic force of water in upstream section, lb

m_2 = total hydrostatic force of water in pier section, lb

m_3 = total hydrostatic force of water in downstream section, lb

m_p = total hydrostatic force of water on pier ends, lb

A_1 = cross-sectional area of upstream channel, square feet, ft²

A_2 = cross-sectional area of channel within pier section, ft²

A_3 = cross-sectional area of downstream channel, ft²

A_p = cross-sectional area of pier obstruction, ft²

(g) Curves based on the Koch-Carstanjen equation (Equation 2-21) are illustrated in Plate 12a. The resulting flow profiles are shown in Plate 12b. The necessary computations for developing the curves are shown in Plate 13. The downstream depth is usually known for tranquil-flow channels and is greater than critical depth. It therefore plots on the upper branch of curve III in Plate 12a. If this depth A is to the right of (greater force than) the minimum force value B of curve II, the flow is class A and the upstream design depth C is read on curve I immediately above point A . In this case, the upstream depth is controlled by the downstream depth A plus the pier contraction and expansion losses. However, if the downstream depth D plots on the upper branch of curve III to the left of (less force than) point B , the upstream design depth E is that of curve I immediately above point B , and critical depth within the pier section B is the control. The downstream design depth F now is that given by curve III immediately below point E . A varied flow computation in a downstream direction is required to determine the location where downstream channel conditions effect the depth D .

(h) In rapid-flow channels, the flow depth upstream of any pier effect is usually known. This depth is less than critical depth and therefore plots on the lower branch of curve I. If this depth G is located on curve I to the

right of point *B*, the flow is class C. The downstream design depth *H* and the design flow depth within the pier section *I* are read on curves III and II, respectively, immediately above depth *G*. A varied flow computation is required to determine the location where downstream channel conditions again control the depth. However, if the unaffected upstream rapid-flow depth *J* plots on the lower branch of curve I to the left of point *B*, the design upstream depth *K* is read on curve I immediately above point *B*. The design downstream depth *L* is read on curve II immediately below point *B*. In this case, class B flow results with a hydraulic jump between depths *J* and *K* (Plate 12b) upstream of the pier as controlled by critical depth within the pier section *B*. A varied flow computation is again required to determine the location where downstream channel conditions control the flow depth.

(3) Design charts, rectangular sections. A graphic solution for class A flow in rectangular channels, developed by USAED, Los Angeles (1939), and published as HDC 010-6/2, is reproduced in Plate 14. The drop in water surface H_3 in terms of critical depth is presented as a function of the downstream depth d_3 and critical depth in the unobstructed channel. Separate curves are given for channel contraction ratios of between 0.02 and 0.30. In rectangular channels, α is the horizontal contraction ratio. The basic graph is for round nose piers. The insert graph provides correction factors (γ) for other pier shapes. Use of the chart is illustrated in Plate 15. Plate 16 (HDC 010-6/3) presents the USAED, Los Angeles, (1939), solution for class B flow using the momentum method. Plate 17 (HDC 010-6/4) presents the USAED, Chicago, solution for class B flow by the energy method. The use of these charts for rectangular channel sections is shown in Plate 15.

c. Bridge pier extension. Upstream pier extensions are frequently used to reduce flow disturbance caused by bridge piers and to minimize collection of debris on pier noses. In addition, it is often necessary and economical to make use of existing bridge structures in designing flood channels. In some instances there is insufficient vertical clearance under these structures to accommodate the design flow. With class B flow, the maximum flow depth occurs at the upstream end of the pier and the critical depth occurs within the constriction. Field observations and model studies by USAED, Los Angeles (1939), indicate that the minimum depth within the constricted area usually occurs 15 to 25 ft downstream from the upstream end of the pier. Pier extensions are used to effect an upstream movement of the control section, which results in a depth reduction in the flow as it enters the constricted pier section. The use of bridge pier

extensions to accomplish this is illustrated in USAED, Los Angeles (1943), and USAEWES (1957). The general statements relative to bridge pier extensions for class B flow also apply to class C flow. However, in the latter case, the degree and extent of the disturbances are much more severe than with class B flow. Excellent illustrations of the use of bridge pier extensions in high-velocity channels are given in USAED, Los Angeles (1943), and USAED, Walla Walla (1960). The bridge pier extension geometry shown in Plate 18 was developed by USAED, Los Angeles, and pier extensions of this design have been found to perform satisfactorily.

d. Model studies. Where flow conditions at bridge piers are affected by severe changes in channel geometry and alignment, bridge abutments, or multiple bridge crossings, consideration should be given to obtaining the design flow profile from a hydraulic model study.

2-4. Transitions

a. General. Transitions should be designed to accomplish the necessary change in cross section with as little flow disturbance as is consistent with economy. In tranquil flow, the head loss produced by the transition is most important as it is reflected as increased upstream stages. In rapid flow, standing waves produced by changes of direction are of great concern in and downstream from the transition. Streamlined transitions reduce head losses and standing waves. As transition construction costs exceed those of uniform channel cross section and tend to increase with the degree of streamlining, alternative transition designs, their costs, and the incremental channel costs due to head losses and/or standing waves should be assessed.

b. Types. The three most common types of transitions connecting trapezoidal and rectangular channels are cylindrical quadrant, warped, and wedge, as shown in Plate 19. For comparable design, the wedge-type transition, although easier to construct, should be longer than the warped because of the miter bends between channel and transition faces. Warped and wedge types can be used generally for expansions or contractions.

(1) Tranquil flow. Each of these three transition types may be used for tranquil flow in either direction. The cylindrical quadrant is used for expansions from rectangular to trapezoidal section and for contractions from trapezoidal to rectangular section. An abrupt or straight-line transition as well as the quadrant transition can be used in rectangular channels.

(2) Rapid flow. The cylindrical quadrant is used for transitions from tranquil flow in a trapezoidal section to rapid flow in a rectangular section. The straight-line transition is used for rectangular sections with rapid flow. Specially designed curved expansions (c(2)(b) below) are required for rapid flow in rectangular channels.

c. Design.

(1) Tranquil flow. Plate 20 gives dimensions of plane surface (wedge type) transitions from rectangular to trapezoidal cross section having side slopes of 1 on 2; 1 on 2.5, and 1 on 3. In accordance with the recommendations of Winkel (1951) the maximum change in flow line has been limited to 6.0 degrees (deg). Water-surface profiles should be determined by step computations with less than 20 percent (less than 10 percent in important instances) change in velocity between steps. Adjustments in the transition should be made, if necessary, to obtain a water-surface profile that is as nearly straight as practicable.

(2) Rapid flow. In rapid flow, stationary waves result with changes in channel alignment. These disturbances may necessitate increased wall height, thereby appreciably increasing construction costs. USAED, Los Angeles, uses the criterion in Table 2-2 for the design of straight-line or wedge-type transitions to confine flow disturbances within the normal channel freeboard allowance:

Table 2-2
Recommended Convergence and Divergence Transition Rates

Mean channel velocity, fps	Wall flare for each wall (horizontal to longitudinal)
10-15	1:10
15-30	1:15
30-40	1:20

(a) Rectangular contractions. Ippen (1950), Ippen and Dawson (1951), and Ippen and Harleman (1956) applied the wave theory to the design of rectangular channel transitions for rapid flow and developed the following equations for computing flow depths in and downstream from the convergence:

$$\tan \theta = \frac{\tan \beta_1 \left(\sqrt{1 + 8F_1^2 \sin^2 \beta_1} - 3 \right)}{2 \tan^2 \beta_1 + \sqrt{1 + 8F_1^2 \sin^2 \beta_1} - 1} \quad (2-22)$$

$$\frac{y_2}{y_1} = \frac{1}{2} \left(\sqrt{1 + 8F_1^2 \sin^2 \beta_1} - 1 \right) \quad (2-23)$$

and

$$F_2^2 = \frac{y_1}{y_2} \left[F_1^2 - \frac{1}{2} \frac{y_1}{y_2} \left(\frac{y_2}{y_1} - 1 \right) \left(\frac{y_2}{y_1} + 1 \right)^2 \right] \quad (2-24)$$

where

θ = wall deflection angle

F = Froude number

β = wave front angle

y = flow depth

The subscripts 1, 2, and 3 refer to the flow areas indicated on the sketches in Plate 21. For straight-line convergence (Plate 21b), the maximum flow disturbance results when the initial wave front intersection, point *B*, occurs at the downstream transition *CC'*. When the reflected waves *BD* and *BD'* intersect the channel walls below or above section *CC'*, diamond-shaped cross waves develop in the channel. However, the change in wall alignment at section *CC'* results in negative wave disturbances that should tend to decrease the downstream effects of positive wave fronts. This should result in somewhat lower depths where the waves meet the downstream walls. The minimum disturbance occurs when the reflected waves *BD* and *BD'* meet the channel walls at section *CC'*. This, theoretically, results in the flow filaments again becoming parallel to the channel center line. If the reflected waves meet the walls upstream from section *CC'*, the waves would be deflected again with a resulting increase in depth. Graphic plots of Equations 2-22 through 2-24 have been published (Ippen 1950, Ippen and Dawson 1951, and

Ippen and Harleman 1956). Plate 22 presents design curves based on these equations. The extent of the curves has been limited to flow conditions normally occurring in rapid-flow flood control channels. The required length of the transition is a function of the wall deflection angle θ and the channel contraction $b_1 - b_3$, or

$$L = \frac{b_1 - b_3}{2 \tan \theta} \quad (2-25)$$

where

b_1 = upstream channel width, ft

b_3 = downstream channel width, ft

The theory indicates that the surface disturbances are minimized when $L = L_1 + L_2$ (Plate 21). The equations for L_1 and L_2 are

$$L_1 = \frac{b_1}{2 \tan \beta_1} \quad (2-26)$$

and

$$L_2 = \frac{b_3}{2 \tan (\beta_2 - \theta)} \quad (2-27)$$

The correct transition design for a given change in channel width and Froude number involves selection of a value of θ so that $L = L_1 + L_2$. A computation illustrating the design procedure is given in Plate 23.

(b) Rectangular expansions. In channel expansions the changes in flow direction take place gradually in contrast to the steep wave front associated with contractions. In 1951, Rouse, Bhoota, and Hsu (1951) published the results of a study of expanding jets on a horizontal floor. A graphical method of characteristics, described in Ippen (1951), was used for the theoretical development of flow depth contours. These results were verified experimentally. The following equation based on theoretical and experimental studies was found to give the most satisfactory boundary shapes for the expansion of a high-velocity jet on a horizontal floor.

$$\frac{Z}{b_1} = \frac{1}{2} \left(\frac{X}{b_1 F_1} \right)^{3/2} + \frac{1}{2} \quad (2-28)$$

where

Z = transverse distance from channel center line

b_1 = approach channel width

X = longitudinal distance from beginning of expansion

F_1 = approach flow Froude number

Equation 2-28 is for an infinitely wide expansion. Optimum design of expansions for rapid flow necessitates control of wall curvature so that the negative waves generated by the upstream convex wall are compensated for by positive waves formed by the downstream concave wall. In this manner, the flow is restored to uniformity where it enters the downstream channel. A typical design of a channel expansion is shown in Plate 24b. Plate 24a reproduces generalized design curves presented in Rouse, Bhoota, and Hsu (1951). It is to be noted that the convex wall curve equation is appreciably less severe than that indicated by Equation 2-28. Equations for laying out the transition and a definition sketch are given in Plate 24b. The data given in Plate 24 should be adequate for preliminary design. In cases where the wave effects are critical, the design should be model tested. Laboratory experiments based on the generalized curves have indicated that the downstream channel depths may be appreciably in excess of those indicated by the simple wave theory. The simple wave theory can be applied to the design of straight-line transitions. An illustration of the computation procedure is given on pages 9-10 through 9-12 of Brater and King (1976). It is to be noted that this computation does not include any wave effects reflected from one sidewall to the other. Also, an abrupt positive wave exists where the expanding wall intersects the downstream channel wall. Application of this method of characteristics is illustrated on pages 9-12 through 9-16 of Brater and King (1976).

(c) Nonrectangular transitions. The necessary techniques for applying the wave theory to channel transitions involving both rectangular and trapezoidal sections have not been developed, and generalized design curves are not available. Limited tests on straight-line and warped-wall

channel transitions for trapezoidal to rectangular sections and for rectangular to trapezoidal sections have been made at Pennsylvania State University (Blue and Shulits 1964). Tests were limited to three different transition shapes for Froude numbers of 1.2 to 3.2. Each shape was tested for five different transition lengths. The trapezoidal channel invert was 0.75 ft wide. The rectangular channel was 1.071 ft wide. Generalized design curves were not developed. However, the study results should be useful as design guides.

(3) Rapid to tranquil flow.

(a) The design of rapid-flow channels may require the use of transitions effecting flow transformation from rapid to tranquil flow. Such transitions normally involve channel expansions in which the channel shape changes from rectangular to trapezoidal.

(b) Channel expansions in which the flow changes from rapid to tranquil are normally of the wedge type. The flow transformation can be accomplished by means of the abrupt hydraulic jump or by a gradual flow change involving an undular-type jump. In either case, it is necessary that the flow transformation be contained in the transition section. The use of a stilling-basin type of transition to stabilize the hydraulic jump is illustrated in USAED, Los Angeles (1961) and USAEWES (1962). A typical example of this type of transition is given in Plate 25.

(c) USAED, Los Angeles (1958, 1961, 1962) has designed and model tested a number of transitions transforming rapid flow in rectangular channels to tranquil flow in trapezoidal channels without the occurrence of an abrupt hydraulic jump. The high-velocity jet from the rectangular channel is expanded in the transition by means of lateral and boundary roughness control in such a manner that an undular-type jump occurs in the downstream reach of the transition. Plate 26 illustrates a typical design developed through model tests.

d. Transition losses.

(1) Tranquil flow. Transitions for tranquil flow are designed to effect minimum energy losses consistent with economy of construction. Transition losses are normally computed using the energy equation and are expressed in terms of the change in velocity head Δh_v from upstream to downstream of the transition. The head loss h_1 between cross sections in the step computation may be expressed as

$$h_1 = C_c \Delta h_v \tag{2-29}$$

for contractions and as

$$h_1 = C_e \Delta h_v \tag{2-30}$$

where

C_c = contraction coefficient

C_e = expansion coefficient

for expansions. Equations 2-29 and 2-30 have been obtained and published (Chow 1959, Brater and King 1976, US Bureau of Reclamation (USBR) 1967). The values in Table 2-3 are generally accepted for design purposes.

Table 2-3
Transition Loss Coefficients

Transition Type	C_c	C_e	Source
Warped	0.10	0.20	Chow 1959, Brater and King 1976
Cylindrical Quadrant	0.15	0.20	Chow 1959
Wedge	0.30	0.50	USBR 1967
Straight Line	0.30	0.50	Chow 1959
Square End	0.30	0.75	Chow 1959

(2) Rapid flow. Transition losses may be estimated for rapid-flow conditions from the information supplied in (1) above. However, the effects of standing waves and other factors discussed in c(2) above make exact

determinations of losses difficult. Model tests should be considered for important rapid-flow transitions.

2-5. Flow in Curved Channels

a. General.

(1) The so-called centrifugal force caused by flow around a curve results in a rise in the water surface on the outside wall and a depression of the surface along the inside wall. This phenomenon is called superelevation. In addition, curved channels tend to create secondary flows (helical motion) that may persist for many channel widths downstream. The shifting of the maximum velocity from the channel center line may cause a disturbing influence downstream. The latter two phenomena could lead to serious local scour and deposition or poor performance of a downstream structure. There may also be a tendency toward separation near the inner wall, especially for very sharp bends. Because of the complicated nature of curvilinear flow, the amount of channel alignment curvature should be kept to a minimum consistent with other design requirements.

(2) The required amount of superelevation is usually small for the channel size and curvature commonly used in the design of tranquil-flow channels. The main problem in channels designed for rapid flow is standing waves generated in simple curves. These waves not only affect the curved flow region but exist over long distances downstream. The total rise in water surface for rapid flow has been found experimentally to be about twice that for tranquil flow.

(3) Generally, the most economical design for rapid flow in a curved channel results when wave effects are reduced as much as practical and wall heights are kept to a minimum. Channel design for rapid flow usually involves low rates of channel curvature, the use of spiral transitions with circular curves, and consideration of invert banking.

b. *Superelevation.* The equation for the transverse water-surface slope around a curve can be obtained by balancing outward centrifugal and gravitational forces (Woodward and Posey 1941). If concentric flow is assumed where the mean velocity occurs around the curve, the following equation is obtained

$$\Delta y = C \frac{V^2 W}{gr} \quad (2-31)$$

where

Δy = rise in water surface between a theoretical level water surface at the center line and outside water-surface elevation (superelevation)

C = coefficient (see Table 2-4)

V = mean channel velocity

W = channel width at elevation of center-line water surface

g = acceleration of gravity

r = radius of channel center-line curvature

Use of the coefficient C in Equation 2-31 allows computation of the total rise in water surface due to superelevation and standing waves for the conditions listed in Table 2-4. If the total rise in water surface (superelevation plus surface disturbances) is less than 0.5 ft, the normally determined channel freeboard (paragraph 2-6 below) should be adequate. No special treatment such as increased wall heights or invert banking and spiral transitions is required.

Table 2-4
Superelevation Formula Coefficients

Flow Type	Channel Cross Section	Type of Curve	Value of C
Tranquil	Rectangular	Simple Circular	0.5
Tranquil	Trapezoidal	Simple Circular	0.5
Rapid	Rectangular	Simple Circular	1.0
Rapid	Trapezoidal	Simple Circular	1.0
Rapid	Rectangular	Spiral Transitions	0.5
Rapid	Tapezoidal	Spiral Transitions	1.0
Rapid	Rectangular	Spiral Banked	0.5

(1) Tranquil flow. The amount of superelevation in tranquil flow around curves is small for the normal channel size and curvature used in design. No special treatment of curves such as spirals or banking is usually necessary. Increasing the wall height on the outside of the curve to contain the superelevation is usually the most economical remedial measure. Wall heights should be increased by Δy over the full length of curvature. Wall heights on the inside of the channel curve should be held

to the straight channel height because of wave action on the inside of curves.

(2) Rapid flow. The disturbances caused by rapid flow in simple curves not only affect the flow in the curve, but persist for many channel widths downstream. The cross waves generated at the beginning of a simple curve may be reinforced by other cross waves generated farther downstream. This could happen at the end of the curve or within another curve, provided the upstream and downstream waves are in phase. Wall heights should be increased by the amount of superelevation, not only in the simple curve, but for a considerable distance downstream. A detailed analysis of standing waves in simple curves is given in Ippen (1950). Rapid-flow conditions are improved in curves by the provision of spiral transition curves with or without a banked invert, by dividing walls to reduce the channel width, or by invert sills located in the curve. Both the dividing wall and sill treatments require structures in the flow; these structures create debris problems and, therefore, are not generally used.

(a) Spiral transition curves. For channels in which surface disturbances need to be minimized, spiral transition curves should be used. The gradual increase in wall deflection angles of these curves results in minimum wave heights. Two spiral curves are provided, one upstream and one downstream of the central circular curve. The minimum length of spirals for unbanked curves should be determined by (see Douma, p 392, in Ippen and Dawson 1951)

$$L_s = 1.82 \frac{VW}{\sqrt{gy}} \quad (2-32)$$

where y is the straight channel flow depth.

(b) Spiral-banked curves. For rectangular channels, the invert should be banked by rotating the bottom in transverse sections about the channel center line. Spirals are used upstream and downstream of the central curve with the banking being accomplished gradually over the length of the spiral. The maximum amount of banking or difference between inside and outside invert elevations in the circular curve is equal to twice the superelevation given by Equation 2-31. The invert along the inside wall is depressed by Δy below the center-line elevation and the invert along the outside wall is raised by a like amount. Wall heights are usually designed to be equal on both sides of the banked curves and no allowance needs

to be made for superelevation around the curve. The minimum length of spiral should be 30 times the amount of superelevation (Δy) (USAED, Los Angeles, 1950).

$$L_s = 30\Delta y \quad (2-33)$$

The detailed design of spiral curves is given in Appendix D. A computer program for superelevation and curve layout is included. Banked inverts are not used in trapezoidal channels because of design complexities and because it is more economical to provide additional free-board for the moderate amount of superelevation that usually occurs in this type of channel.

c. Limiting curvature. Laboratory experiments and field experience have demonstrated that the helicoidal flow, velocity distribution distortion, and separation around curves can be minimized by properly proportioning channel curvature. Woodward (1920) recommends that the curve radius be greater than 2.5 times the channel width. From experiments by Shukry (1950) the radius of curvature should be equal to or greater than 3.0 times the channel width to minimize helicoidal flow.

(1) Tranquil flow. For design purposes a ratio of radius to width of 3 or greater is suggested for tranquil flow.

(2) Rapid flow. Large waves are generated by rapid flow in simple curves. Therefore a much smaller rate of change of curvature is required than for tranquil flow. A 1969 study by USAED, Los Angeles (1972), of as-built structures shows that curves with spiral transitions, with or without banked inverts, have been constructed with radii not less than

$$r_{\min} = \frac{4V^2W}{gy} \quad (2-34)$$

where

r_{\min} = minimum radius of channel curve
center line

V = average channel velocity

W = channel width at water surface

y = flow depth

The amount of superelevation required for spiral-banked curves (b above) is given by

$$\Delta y = C \frac{V^2 W}{gr} \quad (2-35)$$

However, this study indicates that the maximum allowable superelevation compatible with Equation 2-34 is

$$2\Delta y = W \tan 10 = 0.18W \quad (2-36)$$

or

$$\Delta y = 0.09W$$

d. Bend loss. There has been no complete, systematic study of head losses in channel bends. Data by Shukry (1950), Raju (1937), and Bagnold (1960) suggest that the increased resistance loss over and above that attributable to an equivalent straight channel is very small for values of $r/W > 3.0$. For very sinuous channels, it may be necessary to increase friction losses used in design. Based on tests in the Tiger Creek Flume, Scobey (1933) recommended that Manning's n be increased by 0.001 for each 20 deg of curvature per 100 ft of channel, up to a maximum increase of about 0.003. The small increase in resistance due to curvature found by Scobey was substantiated by the USBR field tests (Tilp and Scrivner 1964) for $r/W > 4$. Recent experiments have indicated that the channel bend loss is also a function of Froude number (Rouse 1965). According to experiments by Hayat (Rouse 1965), the free surface waves produced by flow in a bend can cause an increase in resistance.

2-6. Special Considerations

a. Freeboard.

(1) The freeboard of a channel is the vertical distance measured from the design water surface to the top of the channel wall or levee. Freeboard is provided to ensure that the desired degree of protection will not be reduced by unaccounted factors. These might include erratic hydrologic phenomena; future development of urban areas; unforeseen embankment settlement; the accumulation of silt, trash, and debris; aquatic or other growth

in the channels; and variation of resistance or other coefficients from those assumed in design.

(2) Local regions where water- surface elevations are difficult to determine may require special consideration. Some examples are locations in or near channel curves, hydraulic jumps, bridge piers, transitions and drop structures, major junctions, and local storm inflow structures. As these regions are subject to wave-action uncertainties in water-surface computations and possible overtopping of walls, especially for rapid flow, conservative freeboard allowances should be used. The backwater effect at bridge piers may be especially critical if debris accumulation is a problem.

(3) The amount of freeboard cannot be fixed by a single, widely applicable formula. It depends in large part on the size and shape of channel, type of channel lining, consequences of damage resulting from overtopping, and velocity and depth of flow. The following approximate freeboard allowances are generally considered to be satisfactory: 2 ft in rectangular cross sections and 2.5 ft in trapezoidal sections for concrete-lined channels; 2.5 ft for riprap channels; and 3 ft for earth levees. The freeboard for riprap and earth channels may be reduced somewhat because of the reduced hazard when the top of the riprap or earth channels is below natural ground levels. It is usually economical to vary concrete wall heights by 0.5-ft increments to facilitate reuse of forms on rectangular channels and trapezoidal sections constructed by channel pavers.

(4) Freeboard allowances should be checked by computations or model tests to determine the additional discharge that could be confined within the freeboard allowance. If necessary, adjustments in freeboard should be made along either or both banks to ensure that the freeboard allowance provides the same degree of protection against overtopping along the channel.

b. Sediment transport. Flood control channels with tranquil flow usually have protected banks but unprotected inverts. In addition to reasons of economy, it is sometimes desirable to use the channel streambed to percolate water into underground aquifers (USAED, Los Angeles, 1963). The design of a channel with unprotected inverts and protected banks requires the determination of the depth of the bank protection below the invert in regions where bed scour may occur. Levee heights may depend on the amount of sediment that may deposit in the channel. The design of such channels requires estimates of sediment transport to predict channel conditions under given flow and sediment characteristics. The subject of

sediment transport in alluvial channels and design of canals has been ably presented by Leliavsky (1955). Fundamental information on bed-load equations and their background with examples of use in channel design is given in Rouse (1950) (see pp 769-857). An excellent review with an extensive bibliography is available (Chien 1956). This review includes the generally accepted Einstein approach to sediment transport. A comparative treatment of the many bed-load equations (Vanoni, Brooks, and Kennedy 1961) with field data indicates that no one formula is conclusively better than any other and that the accuracy of prediction is about ± 100 percent. A recent paper by Colby (1964b) proposes a simple, direct method of empirically correlating bed-load discharge with mean channel velocity at various flow depths and median grain size diameters. This procedure is adopted herein for rough estimates of bed-load movement in flood control channels.

c. Design curves. Plate 27 gives curves of bed-load discharge versus channel velocity for three depths of flow and four sediment sizes. The basic ranges of depths and velocities have been extrapolated and interpolated from the curves presented in Colby (1964a) for use in flood control channel design. Corrections for water temperature and concentration of fine sediment (Colby 1964a) are not included because of their small influence. The curves in Plate 27 should be applicable for estimating bed-load discharge in channels having geologic and hydraulic characteristics similar to those in the channels from which the basic data were obtained. The curves in this plate can also be used to estimate the relative effects of a change in channel characteristics on bed-load movement. For example, the effect of a series of check dams or drop structures that are provided to decrease channel slope would be reflected in the hydraulic characteristics by decreasing the channel velocity. The curves could then be used to estimate the decrease in sediment load. The curves can also be used to approximate the equilibrium sediment discharge. If the supply of sediment from upstream sources is less than the sediment discharge computed by the rating curves, the approximate amount of streambed scour can be estimated from the curves. Similarly, deposition will occur if the sediment supply is greater than the sediment discharge indicated by the rating curves. An example of this is a large sediment load from a small side channel that causes deposition in a major flood channel. If the location of sediment deposition is to be controlled, the estimated size of a sediment detention facility can be approximated using the curves. An example of the use of a sediment discharge equation in channel design is given in USAED, Los Angeles (1963).

2-7. Stable Channels

a. General.

(1) The design of stable channels requires that the channel be in material or lined with material capable of resisting the scouring forces of the flow. Channel armor-ing is required if these forces are greater than those that the bed and bank material can resist. The basic principles of stable channel design have been presented by Lane (1955) and expanded and modified by Terrell and Borland (1958) and Carlson and Miller (1956). An outline of the method of channel design to resist scouring forces has been given in Simons (1957). The most common type of channel instability encountered in flood control design is scouring of the bed and banks. This results from relatively large discharges, steep channel slopes, and normally limited channel right-of-way widths. These factors frequently require the use of protective revetment to prevent scouring.

(2) While clay and silt are fairly resistant to scour, especially if covered with vegetation, it is necessary to provide channel revetment when tractive forces are sufficiently high to cause erosion of channels in fine material. Little is known about the resistance of clay and silt to erosion as particles in this size range are influenced to a large extent by cohesive forces. A summary of some of the effects is given by the Task Committee on Preparation of Sedimentation Manual (1966). Suggested maximum limiting average channel velocities for noncohesive materials are listed in c below and plotted in Plate 28.

b. Prevention of scour. Scour and deposition occur most commonly when particle sizes range from fine sand to gravel, i.e., from about 0.1 mm through 50 mm (Plate 28). Erosion of sands in the lower range of sizes is especially critical as the sand particle weight is small, there is no cohesion between grains, and there is usually little vegetation along the channel. This particle size range comprises the majority of the bed and suspended load in many streams. Paragraph 2-6 above discusses sediment movement and presents a sediment rating curve as a guide to predicting channel stability.

c. Permissible velocity and shear. The permissible velocity and shear for a nonerodible channel should be somewhat less than the critical velocity or shear that will erode the channel. The adoption of maximum permissible velocities that are used in the design of channels has been widely accepted since publication of a table of values by Fortier and Scobey (1926). The latest information on

critical scour velocities is given by the Task Committee on Preparation of Sedimentation Manual (1966). Table 2-5 gives a set of permissible velocities that can be used as a guide to design nonscouring flood control channels. Lane (1955) presents curves showing permissible channel shear stress to be used for design, and the Soil Conservation Service (1954) presents information on grass-lined channels. Departures from suggested

permissible velocity or shear values should be based on reliable field experience or laboratory tests. Channels whose velocities and/or shear exceed permissible values will require paving or bank revetment. The permissible values of velocity and/or shear should be determined so that damage exceeding normal maintenance will not result from any flood that could be reasonably expected to occur during the service life of the channel.

Table 2-5
Suggested Maximum Permissible Mean Channel Velocities

Channel Material	Mean Channel Velocity, fps
Fine Sand	2.0
Coarse Sand	4.0
Fine Gravel ¹	6.0
Earth	
Sandy Silt	2.0
Silt Clay	3.5
Clay	6.0
Grass-lined Earth (slopes less than 5%) ²	
Bermuda Grass	
Sandy Silt	6.0
Silt Clay	8.0
Kentucky Blue Grass	
Sandy Silt	5.0
Silt Clay	7.0
Poor Rock (usually sedimentary)	10.0
Soft Sandstone	8.0
Soft Shale	3.5
Good Rock (usually igneous or hard metamorphic)	20.0

Notes:
1. For particles larger than fine gravel (about 20 millimetres (mm) = 3/4 in.), see Plates 29 and 30.
2. Keep velocities less than 5.0 fps unless good cover and proper maintenance can be obtained.

Chapter 3 Riprap Protection

Section I Introduction

3-1. General

* The guidance presented herein applies to riprap design for open channels not immediately downstream of stilling basins or other highly turbulent areas (for stilling basin riprap, use HDC 712-1, Plates 29 and 30). The ability of riprap slope protection to resist the erosive forces of channel flow depends on the interrelation of the following factors: stone shape, size, weight, and durability; riprap gradation and layer thickness; and channel alignment, cross-section, gradient, and velocity distribution. The bed material and local scour characteristics determine the design of toe protection which is essential for riprap revetment stability. The bank material and groundwater conditions affect the need for filters between the riprap and underlying material. Construction quality control of both stone production and riprap placement is essential for successful bank protection. Riprap protection for flood control channels and appurtenant structures should be designed so that any flood that could reasonably be expected to occur during the service life of the channel or structure would not cause damage exceeding nominal maintenance or replacement (see ER 1110-2-1150). While the procedures presented herein yield definite stone sizes, results should be used for guidance purposes and revised as deemed necessary to provide a practical protection design for the specific project conditions.

3-2. Riprap Characteristics

The following provides guidance on stone shape, size/weight relationship, unit weight, gradation, and layer thickness. Reference EM 1110-2-2302 for additional guidance on riprap material characteristics and construction.

a. Stone shape. Riprap should be blocky in shape rather than elongated, as more nearly cubical stones “nest” together best and are more resistant to movement. The stone should have sharp, angular, clean edges at the intersections of relatively flat faces. Stream rounded stone is less resistant to movement, although the drag force on a rounded stone is less than on angular, cubical stones. As rounded stone interlock is less than that of equal-sized angular stones, the rounded stone mass is

more likely to be eroded by channel flow. If used, the rounded stone should be placed on flatter side slopes than angular stone and should be about 25 percent larger in diameter. The following shape limitations should be specified for riprap obtained from quarry operations:

- (1) The stone shall be predominantly angular in shape.
- (2) Not more than 30 percent of the stones distributed throughout the gradation should have a ratio of a/c greater than 2.5.
- (3) Not more than 15 percent of the stones distributed throughout the gradation should have a ratio of a/c greater than 3.0.
- (4) No stone should have a ratio of a/c greater than 3.5.

To determine stone dimensions a and c , consider that the stone has a long axis, an intermediate axis, and a short axis, each being perpendicular to the other. Dimension a is the maximum length of the stone, which defines the long axis of the stone. The intermediate axis is defined by the maximum width of the stone. The remaining axis is the short axis. Dimension c is the maximum dimension parallel to the short axis. These limitations apply only to the stone within the required riprap gradation and not to quarry spalls and waste that may be allowed.

b. Relation between stone size and weight. The ability of riprap revetment to resist erosion is related to the size and weight of stones. Design guidance is often expressed in terms of the stone size $D_{\%}$, where $\%$ denotes the percentage of the total weight of the graded material (total weight including quarry wastes and spalls) that contains stones of less weight. The relation between size and weight of stone is described herein using a spherical shape by the equation

$$D_{\%} = \left(\frac{6W_{\%}}{\pi\gamma_s} \right)^{1/3} \quad (3-1)$$

where

$D_{\%}$ = equivalent-volume spherical stone diameter, ft

$W_{\%}$ = weight of individual stone having diameter of $D_{\%}$

γ_s = saturated surface dry specific or unit weight of stone, pcf

Plate 31 presents relations between spherical diameter and weight for several values of specific or unit weight. Design procedures for determining the stone size required to resist the erosive forces of channel flow are presented in paragraph 3-5 below.

c. Unit weight. Unit weight of stone γ_s generally varies from 150 to 175 pcf. Riprap sizing relations are relatively sensitive to unit weight of stone, and γ_s should be determined as accurately as possible. In many cases, the unit weight of stone is not known because the quarry is selected from a list of approved riprap sources after the construction contract is awarded. Riprap coming from the various quarries will not be of the same unit weight. Under these circumstances, a unit weight of stone close to the minimum of the available riprap sources can be used in design. Contract options covering specific weight ranges of 5 or 10 pcf should be offered when sufficient savings warrant.

d. Gradation.

(1) The gradation of stones in riprap revetment affects the riprap's resistance to erosion. Stone should be reasonably well graded throughout the in-place layer thickness. Specifications should provide for two limiting gradation curves, and any stone gradation as determined from quarry process, stockpile, and in-place field test samples that lies within these limits should be acceptable. Riprap sizes and weights are frequently used such as $D_{30}(\text{min})$, $D_{100}(\text{max})$, $W_{50}(\text{min})$, etc. The D or W refers to size or weight, respectively. The number is the percent finer by weight as discussed in b above. The (max) or (min) refers to the upper or lower limit gradation curves, respectively. Engineer Form 4794-R is a standard form for plotting riprap gradation curves (Plate 32). The gradation limits should not be so restrictive that production costs would be excessive. The choice of limits also depends on the underlying bank soils and filter requirements if a graded stone filter is used. Filters may be required under riprap revetments. Guidance for filter requirements is given in EM 1110-2-1901. Filter design is the responsibility of the Geotechnical Branch in each District.

(2) Standardized gradations having a relatively narrow range in sizes (D_{85}/D_{15} of 1.4-2.2) are shown in Table 3-1. Other gradations can be used and often have a wider range of allowable sizes than those given in Table 3-1. One example is the Lower Mississippi Valley

Division (LMVD) Standardized Gradations presented in Appendix F. The LMVD gradations are similar to the gradations listed in Table 3-1 except the LMVD $W_{50}(\text{max})$ and $W_{15}(\text{max})$ weights are larger, which can make the LMVD gradations easier to produce. Most graded ripraps have ratios of D_{85}/D_{15} less than 3. Uniform riprap ($D_{85}/D_{15} < 1.4$) has been used at sites in the US Army Engineer Division, Missouri River, for reasons of economy and quality control of sizes and placement.

(3) Rather than a relatively expensive graded riprap, a greater thickness of a quarry-run stone may be considered. Some designers consider the quarry-run stone to have another advantage: its gravel- and sand-size components serve as a filter. The gravel and sand sizes should be less by volume than the voids among the larger stone. This concept has resulted in considerable cost savings on large projects such as the Arkansas and Red River Navigation Projects. Not all quarry-run stone can be used as riprap; stone that is gap graded or has a large range in maximum to minimum size is probably unsuitable. Quarry-run stone for riprap should be limited to $D_{85}/D_{15} \leq 7$.

(4) Determining optimum gradations is also an economics problem that includes the following factors:

- (a) Rock quality (durability under service conditions)
- (b) Cost per ton at the quarry (including capability of quarry to produce a particular size)
- (c) Number of tons required
- (d) Miles transported
- (e) Cost of transportation per ton-mile
- (f) Cost per ton for placement
- (g) Need for and cost of filter
- (h) Quality control during construction (it is easier to ensure even coverage with a narrow gradation than with a wide gradation)

(i) Number of different gradations required. Sometimes cost savings can be realized by using fewer gradations.

See EM 1110-2-2302 for further discussion of these factors.

Table 3-1
Gradations for Riprap Placement in the Dry, Low-Turbulence Zones

Limits of Stone Weight, lb¹, for Percent Lighter by Weight

D ₁₀₀ (max) in.	100		50		15		D ₃₀ (min) ft	D ₉₀ (min) ft	
	Max	Min	Max ²	Min	Max ²	Min			
Specific Weight = 155 pcf									
* 9	34	14	10	7	5	2	0.37	0.53	*
12	81	32	24	16	12	5	0.48	0.70	
15	159	63	47	32	23	10	0.61	0.88	
18	274	110	81	55	41	17	0.73	1.06	
21	435	174	129	87	64	27	0.85	1.23	
24	649	260	192	130	96	41	0.97	1.40	
27	924	370	274	185	137	58	1.10	1.59	
30	1,268	507	376	254	188	79	1.22	1.77	
33	1,688	675	500	338	250	105	1.34	1.94	
36	2,191	877	649	438	325	137	1.46	2.11	
42	3,480	1,392	1,031	696	516	217	1.70	2.47	
48	5,194	2,078	1,539	1,039	769	325	1.95	2.82	
54	7,396	2,958	2,191	1,479	1,096	462	2.19	3.17	
Specific Weight = 165 pcf									
* 9	36	15	11	7	5	2	0.37	0.53	*
12	86	35	26	17	13	5	0.48	0.70	
15	169	67	50	34	25	11	0.61	0.88	
18	292	117	86	58	43	18	0.73	1.06	
21	463	185	137	93	69	29	0.85	1.23	
24	691	276	205	138	102	43	0.97	1.40	
27	984	394	292	197	146	62	1.10	1.59	
30	1,350	540	400	270	200	84	1.22	1.77	
33	1,797	719	532	359	266	112	1.34	1.96	
36	2,331	933	691	467	346	146	1.46	2.11	
42	3,704	1,482	1,098	741	549	232	1.70	2.47	
48	5,529	2,212	1,638	1,106	819	346	1.95	2.82	
54	7,873	3,149	2,335	1,575	1,168	492	2.19	3.17	
Specific Weight = 175 pcf									
* 9	39	15	11	8	6	2	0.37	0.53	*
12	92	37	27	18	14	5	0.48	0.70	
15	179	72	53	36	27	11	0.61	0.88	
18	309	124	92	62	46	19	0.73	1.06	
21	491	196	146	98	73	31	0.85	1.23	
24	733	293	217	147	109	46	0.97	1.40	
27	1,044	417	309	209	155	65	1.10	1.59	
30	1,432	573	424	286	212	89	1.22	1.77	
33	1,906	762	565	381	282	119	1.34	1.94	
36	2,474	990	733	495	367	155	1.46	2.11	
42	3,929	1,571	1,164	786	582	246	1.70	2.47	
48	5,864	2,346	1,738	1,173	869	367	1.95	2.82	
54	8,350	3,340	2,474	1,670	1,237	522	2.19	3.17	

Notes:

1. Stone weight limit data from ETL 1110-2-120 (HQUSACE, 1971 (14 May), "Additional Guidance for Riprap Channel Protection, Ch 1," US Government Printing Office, Washington, DC). Relationship between diameter and weight is based on the shape of a sphere.
2. The maximum limits at the W₅₀ and W₁₅ sizes can be increased as in the Lower Mississippi Valley Division Standardized Gradations shown in Appendix F.

e. Layer thickness. All stones should be contained within the riprap layer thickness to provide maximum resistance against erosive forces. Oversize stones, even in isolated spots, may result in riprap failure by precluding mutual support and interlock between individual stones, causing large voids that expose filter and bedding materials, and creating excessive local turbulence that removes smaller size stone. Small amounts of oversize stone should be removed individually and replaced with proper size stones. The following criteria apply to the riprap layer thickness:

(1) It should not be less than the spherical diameter of the upper limit W_{100} stone or less than 1.5 times the spherical diameter of the upper limit W_{50} stone, whichever results in the greater thickness.

(2) The thickness determined by (1) above should be increased by 50 percent when the riprap is placed underwater to provide for uncertainties associated with this type of placement. At one location in the US Army Engineer Division, Missouri River, divers and sonic sounders were used to reduce the underwater thickness to 1.25 times the dry placement thickness.

Section II Channel Characteristics

3-3. Side Slope Inclination

The stability of riprap slope protection is affected by the steepness of channel side slopes. Side slopes should ordinarily not be steeper than 1V on 1.5H, except in special cases where it may be economical to use larger hand-placed stone keyed well into the bank. Embankment stability analysis should properly address soils characteristics, groundwater and river conditions, and probable failure mechanisms. The size of stone required to resist the erosive forces of channel flow increases when the side slope angle approaches the angle of repose of a riprap slope protection. Rapid water-level recession and piping-initiated failures are other factors capable of affecting channel side slope inclination and needing consideration in design.

3-4. Channel Roughness, Shape, Alignment, and Gradient

As boundary shear forces and velocities depend on channel roughness, shape, alignment, and invert gradient, these factors must be considered in determining the size of stone required for riprap revetment. Comparative cost estimates should be made for several alternative channel

plans to determine the most economical and practical combination of channel factors and stone size. Resistance coefficients (Manning's n) for riprap placed in the dry should be estimated using the following form of Strickler's equation:

$$n = K [D_{90}(\text{min})]^{1/6} \quad (3-2)$$

where

K = 0.036, average of all flume data

= 0.034 for velocity and stone size calculation

= 0.038 for capacity and freeboard calculation

$D_{90}(\text{min})$ = size of which 90 percent of sample is finer, from minimum or lower limit curve of gradation specification, ft

The K values represent the upper and lower bounds of laboratory data determined for bottom riprap. Resistance data from a laboratory channel which had an irregular surface similar to riprap placed underwater show a Manning's n about 15 percent greater than for riprap placed in the dry. Equation 3-2 provides resistance losses due to the surface roughness of the riprap and does not include form losses such as those caused by bends. Equation 3-2 should be limited to slopes less than 2 percent. *

Section III Design Guidance for Stone Size

3-5. General

Riprap protection for open channels is subjected to hydrodynamic drag and lift forces that tend to erode the revetment and reduce its stability. Undermining by scour beyond the limits of protection is also a common cause of failure. The drag and lift forces are created by flow velocities adjacent to the stone. Forces resisting motion are the submerged weight of the stone and any downward and lateral force components caused by contact with other stones in the revetment. Stone availability and experience play a large part in determining size of riprap. This is particularly true on small projects where hydraulic parameters are ill-defined and the total amount of riprap required is small.

3-6. Design Conditions

Stone size computations should be conducted for flow conditions that produce the maximum velocities at the riprapped boundary. In many cases, velocities continue to increase beyond bank-full discharge; but sometimes back-water effects or loss of flow into the overbanks results in velocities that are less than those at bank-full. Riprap at channel bends is designed conservatively for the point having the maximum force or velocity. For braided channels, bank-full discharges may not be the most severe condition. At lesser flows, flow is often divided into multiple channels. Flow in these channels often impinges abruptly on banks or levees at sharp angles.

3-7. Stone Size

This method for determining stone size uses depth-averaged local velocity. The method is based on the idea that a designer will be able to estimate local velocity better than local boundary shear. Local velocity and local flow depth are used in this procedure to quantify the imposed forces. Riprap size and unit weight quantify the resisting force of the riprap. This method is based on a large body of laboratory data and has been compared to available prototype data (Maynard 1988). It defines the stability of a wide range of gradations if placed to a thickness of $1D_{100}(\text{max})$. Guidance is also provided for thickness greater than $1D_{100}(\text{max})$. This method is applicable to side slopes of 1V on 1.5H or flatter.

a. Velocity estimation. The characteristic velocity for side slopes V_{SS} is the depth-averaged local velocity over the slope at a point 20 percent of the slope length from the toe of slope. Plate 33 presents the ratio V_{SS}/V_{AVG} , where V_{AVG} is the average channel velocity at the upstream end of the bend, as a function of the channel geometry, which is described by R/W , where R is the center-line radius of bend and W is the water-surface width. V_{AVG} , R , and W should be based on flow in the main channel only and should not include overbank areas. The trapezoidal curve for V_{SS}/V_{AVG} shown in Plate 33 is based on the STREMR numerical model described in Bernard (1993). The primary factors affecting velocity distribution in riprap-lined, trapezoidal channel bendways are R/W , bend angle, and aspect ratio (bottom width/depth). Data in Maynard (1992) show a trapezoidal channel having the same bottom width but side slopes ranging from 1V:1.5H to 1V:3H to have the same maximum V_{SS}/V_{AVG} at the downstream end of the bend. Plate 33 should be used for side slopes from 1V:3H to 1V:1.5H. For straight channels sufficiently far ($>5W$) from

upstream bends, large values of R/W should be used, resulting in constant values of V_{SS}/V_{AVG} . Very few channels are straight enough to justify using $V_{SS}/V_{AVG} < 1$. A minimum ratio of $V_{SS}/V_{AVG} = 1$ is recommended for side slopes in straight channels. Rock stability should be checked for both side slopes and the channel bottom. In bendways, the outer bank side slope will generally require the largest rock size. In straight reaches, the channel bottom will often require the largest stone size. Velocities in the center of a straight channel having equal bottom and side slope roughness range from 10 to 20 percent greater than V_{AVG} . Plate 34 describes V_{SS} and Plate 35 shows the location in a trapezoidal channel bend of the maximum V_{SS} . Velocity downstream of bends decays at approximately the following rate: No decay in first channel width downstream of bend exit; decay of $V_{SS}/V_{AVG} = 0.1$ per channel width until $V_{SS}/V_{AVG} = 1.0$. Plate 36 shows the variation in velocity over the side slope in a channel. The straight channel curve in Plate 36 was found applicable to both 1V:2H and 1V:3H side slopes. The bend curve for $R/W = 2.6$ was taken from a channel having strong secondary currents and represents a severe concentration of high velocity upon the channel side slope. These two curves represent the extremes in velocity distribution to be expected along the outer bank of a channel bend having a riprap side slope from toe of bank to top of bank. Knowing V_{SS} from Plate 33, the side slope velocity distribution can be determined at the location of V_{SS} . An alternate means of velocity estimation based on field observation is discussed in Appendix G. The alpha method (Appendix C), or velocities resulting from subsections of a water-surface profile computation, should be used only in straight reaches. When the alpha method is used, velocity from the subsection adjacent to the bank subsection should be used as V_{SS} in design of bank riprap.

b. Stone size relations. The basic equation for the representative stone size in straight or curved channels is

$$D_{30} = S_f C_s C_v C_T d \left[\left(\frac{\gamma_w}{\gamma_s - \gamma_w} \right)^{1/2} \frac{V}{\sqrt{K_1 g d}} \right]^{2.5} \quad (3-3)$$

where

D_{30} = riprap size of which 30 percent is finer by weight, length

EM 1110-2-1601

Change 1

30 Jun 94

- S_f = safety factor (see c below)
- * C_s = stability coefficient for incipient failure,
 $D_{85}/D_{15} = 1.7$ to 5.2
 - = 0.30 for angular rock
 - * = 0.375 for rounded rock
 - C_v = vertical velocity distribution coefficient
 - = 1.0 for straight channels, inside of bends
 - = $1.283 - 0.2 \log (R/W)$, outside of bends (1 for $(R/W) > 26$)
 - = 1.25, downstream of concrete channels
 - = 1.25, ends of dikes
 - C_T = thickness coefficient (see $d(1)$ below)
 - * = 1.0 for thickness = $1D_{100}(\text{max})$ or $1.5 D_{50}(\text{max})$, whichever is greater
 - * d = local depth of flow, length (same location as V)
 - γ_w = unit weight of water, weight/volume
 - * V = local depth-averaged velocity, V_{SS} for side slope riprap, length/time
 - K_1 = side slope correction factor (see $d(1)$ below)
 - g = gravitational constant, length/time²
 - * Some designers prefer to use the traditional D_{50} in riprap design. The approximate relationship between D_{50} and D_{30} is $D_{50} = D_{30} (D_{85}/D_{15})^{1/3}$. Equation 3-3 can be used with either SI (metric) or non-SI units and should be limited to slopes less than 2 percent.
- c. Safety factor.* Equation 3-3 gives a rock size that should be increased to resist hydrodynamic and a variety of nonhydrodynamic-imposed forces and/or uncontrollable physical conditions. The size increase can best be accomplished by including the safety factor, which will be a value greater than unity. The minimum safety factor is
- * $S_f = 1.1$. The minimum safety factor may have to be increased in consideration for the following conditions:

(1) Imposed impact forces resulting from logs, uprooted trees, loose vessels, ice, and other types of large

floating debris. Impact will produce more damage to alighter weight riprap section than to a heavier section. For moderate debris impact, it is unlikely that an added safety factor should be used when the blanket thickness exceeds 15 in.

- (2) The basic stone sizing parameters of velocity, unit weight of rock, and depth need to be determined as accurately as possible. A safety factor should be included to compensate for small inaccuracies in these parameters. If conservative estimates of these parameters are used in the analysis, the added safety factor should not be used. The safety factor should be based on the anticipated error in the values used. The following discussion shows the importance of obtaining nearly correct values rather than relying on a safety factor to correct inaccurate or assumed stone sizing parameters. The average velocity over the toe of the riprap is an estimate at best and is the parameter to which the rock size is the most sensitive. A check of the sensitivity will show that a 10 percent change in velocity will result in a nearly 100 percent change in the weight limits of the riprap gradation (based on a sphere) and about a 30 percent change in the riprap thickness. The riprap size is also quite sensitive to the unit weight of the rock to be used: a 10 percent change in the unit weight will result in a 70 percent change in the weight limits of the riprap gradation (based on a sphere) and about a 20 percent change in the riprap thickness. The natural variability of unit weight of stone from a stone source adds to the uncertainty (EM 1110-2-2302).
- * The rock size is not nearly as sensitive to the depth parameter.

(3) Vandalism and/or theft of the stones is a serious problem in urban areas where small riprap has been placed. A $W_{50}(\text{min})$ of 80 lb should help prevent theft and vandalism. Sometimes grouted stone is used around vandalism-prone areas.

- (4) The completed revetment will contain some pockets of undersized rocks, no matter how much effort is devoted to obtaining a well-mixed gradation throughout the revetment. This placement problem can be assumed to occur on any riprap job to some degree but probably more frequently on jobs that require stockpiling or additional handling. A larger safety factor should be considered with stockpiling or additional hauling and where placement will be difficult if quality control cannot be expected to address these problems.

(5) The safety factor should be increased where severe freeze-thaw is anticipated.

The safety factor based on each of these considerations should be considered separately and then the largest of these values should be used in Equation 3-3.

d. Applications.

(1) The outer bank of straight channels downstream of bends should be designed using velocities computed for the bend. In projects where the cost of riprap is high, a channel model to indicate locations of high velocity might be justified. Equation 3-3 has been developed into Plate 37, which is applicable to thicknesses equal to $1D_{100}(\max)$, γ_s of 165 pcf, and the S_f of 1.1. Plate 38 is used to correct for values of other than γ_s of 165 pcf (when D_{30} is determined from Plate 37). The K_1 side slope factor is normally defined by the relationship of Carter, Carlson, and Lane (1953)

$$K_1 = \sqrt{1 - \frac{\sin^2 \theta}{\sin^2 \phi}} \quad (3-4)$$

where

θ = angle of side slope with horizontal

ϕ = angle of repose of riprap material (normally 40 deg)

Results given in Maynard (1988) show Equation 3-4 to be conservative and that the repose angle is not a constant 40 deg but varies with several factors. The recommended relationship for K_1 as a function of θ is given in Plate 39 along with Equation 3-4 using $\phi = 40$ deg. Using the recommended curve for side slope effects, the least volume of rock per unit length of bank line occurs on a 1V:1.5H to 1V:2H side slope. Also shown on Plate 39 is the correction for side slope when D_{30} is determined from Plate 37. Correction for the vertical velocity distribution in bends is shown in Plate 40. Testing has been conducted to determine the effects of blanket thickness greater than $1D_{100}(\max)$ on the stability of riprap. Results are shown in Plate 40. The thickness coefficient C_T accounts for the increase in stability that occurs when riprap is placed thicker than the minimum thickness of $1D_{100}(\max)$ or $1.5 D_{30}(\max)$, whichever is greater.

(2) The basic procedure to determine riprap size using the graphical solution of this method is as follows:

(a) Determine average channel velocity (HEC-2 or other uniform flow computational methods, or measurement).

(b) Find V_{ss} using Plate 33.

(c) Find D_{30} using Plate 37.

(d) Correct for other unit weights, side slopes, vertical velocity distribution, or thicknesses using Plates 38 through 40.

(e) Find gradation having $D_{30}(\min) \geq$ computed D_{30} . Alternately Equation 3-3 is used with Plates 39 and 40 to replace steps (c) and (d).

(3) This procedure can be used in both natural channels with bank protection only and prismatic channels having riprap on bed and banks. Most bank protection sections can be designed by direct solution. In these cases, the extent of the bank compared to the total perimeter of the channel means that the average channel velocity is not significantly affected by the riprap. The first example in Appendix H demonstrates this type of bank protection.

(4) In some cases, a large part of the channel perimeter is covered with riprap; the average channel velocity, depth, and riprap size are dependent upon one another; and the solution becomes iterative. A trial riprap gradation is first assumed and resistance coefficients are computed using Equation 3-2. Then the five steps described in (2) above are conducted. If the gradation found in paragraph (e) above is equal to the assumed trial gradation, the solution is complete. If not, a new trial gradation is assumed and the procedure is repeated. The second example in Appendix H demonstrates this type of channel riprap.

(5) In braided streams and some meandering streams, flow is often directed into the bank line at sharp angles (angled flow impingement). For braided streams having impinged flow, the above stone sizing procedures require modification in two areas: the method of velocity estimation and the velocity distribution coefficient C_v . All other factors and coefficients presented are applicable.

(a) The major challenge in riprap design for braided streams is estimating the imposed force at the impingement point. Although unproven, the most severe bank

* attack in braided streams is thought to occur when the water surface is at or slightly above the tops of the mid-channel bars. At this stage, flow is confined to the multiple channels that often flow into or “impinge” against bank lines or levees. At lesser flows, the depths and velocities in the multiple channels are decreased. At higher flows, the channel area increases drastically and streamlines are in a more downstream direction rather than into bank lines or levees.

(b) The discharge that produces a stage near the tops of the midchannel bars is Q_{tmcb} . Q_{tmcb} is probably highly correlated with the channel-forming discharge concept. In the case of the Snake River near Jackson, Wyoming, Q_{tmcb} is 15,000-18,000 cfs, which has an average recurrence interval of about 2-5 years. Using cross-section data to determine the channel area below the tops of the midchannel bars and Q_{tmcb} allows determination of the average channel velocity at the top of the midchannel bars, V_{tmcb} .

(c) Field measurements at impingement sites were taken in 1991 on the Snake River near Jackson, Wyoming, and reported in Maynard (1993). The maximum observed ratio $V_{\text{SS}}/V_{\text{tmcb}} = 1.6$, which is almost identical to the ratio shown in Plate 33 for sharp bendways having $R/W = 2$ in natural channels, and this ratio is recommended for determining V_{SS} for impinged flow. The second area of the design procedure requiring modification for impinged flow is the velocity distribution coefficient C_v , which varies with R/W in bendways as shown in Plate 40. Impinged flow areas are poorly aligned bends having low R/W , and $C_v = 1.25$ is recommended for design.

(6) Transitions in size or shape may also require riprap protection. The procedures in this paragraph are applicable to gradual transitions where flow remains tranquil. In areas where flow changes from tranquil to rapid and then back to tranquil, riprap sizing methods applicable to hydraulic structures (HDC 712-1) should be used. In converging transitions, the procedures based on Equation 3-3 can be used unaltered. In expanding transitions, flow can concentrate on one side of the expansion and design velocities should be increased. For installations immediately downstream of concrete channels, a vertical velocity distribution coefficient of 1.25 should be used due to the difference in velocity profile over the two surfaces.

* e. *Steep slope riprap design.*

In cases where unit discharge is low, riprap can be used on steep slopes ranging from 2 to 20 percent. A typical application is a rock-lined chute. The stone size equation is

$$D_{30} = \frac{1.95 S^{0.555} q^{2/3}}{g^{1/3}} \quad (3-5)$$

where

S = slope of bed

q = unit discharge

Equation 3-5 is applicable to thickness = $1.5 D_{100}$, angular rock, unit weight of 167 pcf, D_{85}/D_{15} from 1.7 to 2.7, slopes from 2 to 20 percent, and uniform flow on a down-slope with no tailwater. The following steps should be used in application of Equation 3-5:

(1) Estimate $q = Q/b$ where b = bottom width of chute.

(2) Multiply q by flow concentration factor of 1.25. Use greater factor if approach flow is skewed.

(3) Compute D_{30} using Equation 3-5.

(4) Use uniform gradation having $D_{85}/D_{15} \leq 2$ such as Table 3-1.

* (5) Restrict application to straight channels with side slope of 1V:2.5H or flatter.

(6) Use filter fabric beneath rock.

The guidance for steep slope riprap generally results in large riprap sizes. Grouted riprap is often used instead of loose riprap in steep slope applications. *

3-8. Revetment Top and End Protection

Revetment top and end protection requirements, as with all channel protective measures, are to assure the project benefits, to perform satisfactorily throughout the project economic life, and not to exceed reasonable maintenance

costs. Reference is made to ER 1110-2-1405, with emphasis on paragraph 6c.

a. Revetment top. When the full height of a levee is to be protected, the revetment will cover the freeboard, i.e., extend to the top of the levee. This provides protection against waves, floating debris, and water-surface irregularities. Similar provisions apply to incised channel banks. A horizontal collar, at the top of the bank, is provided to protect against escaping and returning flows as necessary. The end protection methods illustrated in Plate 41 can be adapted for horizontal collars. Plate 36 provides general guidance for velocity variation over channel side slopes that can assist in evaluating the economics of reducing or omitting revetment for upper bank areas. Revetment size changes should not be made unless a sufficient quantity is involved to be cost effective. Many successful revetments have been constructed where the top of the revetment was terminated below the design flow line. See USACE (1981) for examples.

b. Revetment end protection. The upstream and downstream ends of riprap revetment should be protected against erosion by increasing the revetment thickness or extending the revetment to areas of noneroding velocities and relatively stable banks. A smooth transition should be provided from where the end protection begins to the design riprap section. The keyed-in section should satisfy filter requirements. The following guidance applies to the alternative methods of end protection illustrated in Plate 41.

(1) Method A. For riprap revetments 12 in. thick or less, the normal riprap layer should be extended to areas where velocities will not erode the natural channel banks.

(2) Method B. For riprap revetments exceeding 12 in. in thickness, one or more reductions in riprap thickness and stone size may be required (Plate 41) until velocities decrease to a noneroding natural channel velocity.

(3) Method C. For all riprap revetments that do not terminate in noneroding natural channel velocities, the ends of the revetment should be enlarged, as shown in Plate 41. The decision to terminate the revetment in erosive velocities should be made with caution since severe erosion can cause the revetment to fail by progressive flanking.

c. Length. Riprap revetment is frequently carried too far upstream and not far enough downstream of a channel

bend. In a trapezoidal channel, the maximum velocities along the outer bank are often located in the straight reach immediately downstream of the bend for relatively large distances downstream. In a natural channel, the limit of protection on the downstream end should depend on where the flow crosses to the opposite bank, and should consider future bar building on the opposite bank, resulting in channel constriction and increased velocities. Guidance is generally lacking in this area, but review of aerial photographs of the subject location can provide some insight on where the crossover flow occurs. Model tests in a sand bed and bank flume (USACE 1981) were conducted to determine the limits of protection required to prevent scour that would lead to destruction of the revetment. These tests were conducted in a 110-deg bend having a constant discharge. The downstream end of the revetment had to be 1.5 channel widths downstream of the end of the bend. Geomorphic studies to determine revetment ends should be considered.

Section IV *Revetment Toe Scour Estimation and Protection*

3-9. General

Toe scour is probably the most frequent cause of failure of riprap revetments. This is true not only for riprap, but also for a wide variety of protection techniques. Toe scour is the result of several factors, including these three:

a. Meandering channels, change in cross section that occurs after a bank is protected. In meandering channels the thalweg often moves toward the outer bank after the bank is protected. The amount of change in cross section that occurs after protection is added is related to the erodibility of the natural channel bed and original bank material. Channels with highly erodible bed and banks can experience significant scour along the toe of the new revetment.

b. Meandering channels, scour at high flows. Bed profile measurements have shown that the bed observed at low flows is not the same bed that exists at high flows. At high flows the bed scours in channel bends and builds up in the crossings between bends. On the recession side of the flood, the process is reversed. Sediment is eroded from the crossings and deposited in the bends, thus obscuring the maximum scour that had occurred.

c. Braided channels. Scour in braided channels can reach a maximum at intermediate discharges where flow in the channel braids attacks banks at sharp angles.

Note that local scour is the mechanism being addressed herein. When general bed degradation or headcutting is expected, it must be added to the local scour. When scour mechanisms are not considered in the design of protection works, undermining and failure may result.

* Plate 42 may be used for depth of scour estimates. The design curve in Plate 42 represents an upper limit for scour in channels having irregular alignments. For bendways having a relatively smooth alignment, a 10 percent reduction from the design curve is recommended. Neill (1973) provides additional information on scour depth estimation.

3-10. Revetment Toe Protection Methods

Toe protection may be provided by two methods:

a. Extend to maximum scour depth. Place the lower extremity below the expected scour depth or found it on nonerrodible material. These are the preferred methods, but they can be difficult and expensive when underwater excavation is required.

b. Place launchable stone. Place sufficient launchable stone to stabilize erosion. Launchable stone is defined as stone that is placed along expected erosion areas at an elevation above the zone of attack. As the attack and resulting erosion occur below the stone, the stone is undermined and rolls/slides down the slope, stopping the erosion. This method has been widely used on sand bed streams. Successful applications include:

(1) Windrow revetments: riprap placed at top of bank.

(2) Trench-fill revetments: riprap placed at low water level.

(3) Weighted riprap toes: riprap placed at intersection of channel bottom and side slope.

Trench-fill revetments on the Mississippi River have successfully launched to protect for a vertical scour depth of up to 50 ft. On gravel bed streams, the use of launchable stone is not as widely accepted as in sand bed streams. Problems with using launchable stone in some gravel bed rivers may be the result of underestimating stone size, scour depth, or launchable stone volume because the concept of launchable stone has been successful on several gravel bed rivers.

3-11. Revetment Toe Protection Design

The following guidance applies to several alternative methods of toe protection illustrated in Plate 43.

a. Method A. When toe excavation can be made in the dry, the riprap layer may be extended below the existing groundline a distance exceeding the anticipated depth of scour. If excavation quantities are prohibitive, the concept of Method D can be adapted to reduce excavation.

b. Method B. When the bottom of the channel is nonerrodible material, the normal riprap should be keyed in at streambed level.

c. Method C. When the riprap is to be placed underwater and little toe scour is expected (such as in straight reaches that are not downstream of bends, unless stream is braided), the toe may be placed on the existing bottom with height a and width c equal to $1.5T$ and $5T$, respectively. This compensates for uncertainties of underwater placement.

d. Method D. An extremely useful technique where water levels prohibit excavation for a toe section is to place a launchable section at the toe of the bank. Even if excavation is practicable, this method may be preferred for cost savings if the cost of extra stone required to produce a launched thickness equal to or greater than T plus the increase shown in Table 3-2 is exceeded by the cost of excavation required to carry the design thickness T down the slope. This concept simply uses toe scour as a substitute for mechanical excavation. This method also has the advantage of providing a "built-in" scour gage, allowing easy monitoring of high-flow scour and the need for additional stone reinforcement by visual inspection of the remaining toe stone after the high flow subsides or by surveyed cross sections if the toe stone is underwater. It is readily adaptable to emergency protection, where high flow and the requirement for quick action make excavation impractical. Shape of the stone section before launching is not critical, but thickness of the section is important because thickness controls the rate at which rock is released in the launching process. For gradual scour in regular bendways, the height of the stone section before launching should be from 2.5 to 4.0 times the bank protection thickness (T). For rapid scour in impinged flow environments or in gravel bed streams, the stone section height before launching should be 2.5 to 3.0 T . In

* **Table 3-2**
Increase in Stone Volume for Riprap Launching Sections

Vertical Launch Distance, ft ¹	Volume Increase, Percent	
	Dry Placement	Underwater Placement
≤ 15	25	50
> 15	50	75

Note:

¹ From bottom of launch section to maximum scour.

any case, the thinner and wider rock sections represented by the lower values of thickness have an apparent advantage in that the rock in the stream end of the before-launch section has a lesser distance to travel in the launching process. Providing an adequate volume of stone is critical. Stone is lost downstream in the launching process; and the larger the scour depth, the greater the percentage of stone lost in the launching process. To compute the required launchable stone volume for Method D, the following assumptions should be used:

(1) Launch slope = 1V on 2H. This is the slope resulting from rock launched on noncohesive material in both model and prototype surveys. Launch slope is less predictable if cohesive material is present, since cohesive material may fail in large blocks.

(2) Scour depth = existing elevation - maximum scour elevation.

* (3) Thickness after launching = thickness of the bank revetment T .

* To account for the stone lost during launching and for placement underwater, the increases in stone volume listed in Table 3-2 are recommended. Using these assumptions, the required stone volume for underwater placement for vertical launch distance less than 15 ft = 1.5T times launch slope length

$$= 1.5T \text{ times scour depth times } \sqrt{5}$$

$$= 3.35T \text{ (scour depth)}$$

Add a safety factor if data to compute scour depth are unreliable, if cohesive bank material is present, or if monitoring and maintenance after construction cannot be guaranteed. Guidance for a safety factor is lacking, so to some extent it must be determined by considering consequences of failure. Widely graded ripraps are recommended because of reduced rock voids that tend to

* prevent leaching of lower bank material through the launched riprap. Launchable stone should have $D_{85}/D_{15} \geq 2$.

prevent leaching of lower bank material through the launched riprap. Launchable stone should have $D_{85}/D_{15} \geq 2$. *

3-12. Delivery and Placement

Delivery and placement can affect riprap design. See EM 1110-2-2302 for detailed guidance. The common methods of riprap placement are hand placing; machine placing, such as from a skip, dragline, or some form of bucket; and dumping from trucks and spreading by bulldozer. Hand placement produces the most stable riprap revetment because the long axes of the riprap particles are oriented perpendicular to the bank. It is the most expensive method except when stone is unusually costly and/or labor unusually cheap. Steeper side slopes can be used with hand-placed riprap than with other placing methods. This reduces the required volume of rock. However, the greater cost of hand placement usually makes machine or dumped placement methods and flatter slopes more economical. Hand placement on steep slopes should be considered when channel widths are constricted by existing bridge openings or other structures when rights-of-way are costly. In the machine placement method, sufficiently small increments of stone should be released as close to their final positions as practical. Rehandling or dragging operations to smooth the revetment surface tend to result in segregation and breakage of stone. Stone should not be dropped from an excessive height or dumped and spread as this may result in the same undesirable conditions. However, in some cases, it may be economical to increase the layer thickness and stone size somewhat to offset the shortcomings of this placement method. Smooth, compact riprap sections have resulted from compacting the placed stone sections with a broad-tracked bulldozer. This stone must be quite resistant to abrasion. Thickness for underwater placement should be increased by 50 percent to provide for the uncertainties associated with this type of placement. Underwater placement is usually specified in terms of weight of stone per unit area, to be distributed uniformly and controlled by a "grid" established by shoreline survey points. *

Section V

Ice, Debris, and Vegetation

3-13. Ice and Debris

Ice and debris create greater stresses on riprap revetment by impact and flow concentration effects. Ice attachment to the riprap also causes a decrease in stability. The Cold Regions Research Engineering Laboratory, Hanover, NH, should be contacted for detailed guidance relative to ice

effects on riprap. One rule of thumb is that thickness should be increased by 6-12 in., accompanied by appropriate increase in stone size, for riprap subject to attack by large floating debris. Riprap deterioration from debris impacts is usually more extensive on bank lines with steep slopes. Therefore, riprapped slopes on streams with heavy debris loads should be no steeper than 1V on 2.5H.

3-14. Vegetation

The guidance in this chapter is based on maintaining the riprap free of vegetation. When sediment deposits form lowflow berms on riprap installations, vegetation may be allowed on these berms under the following conditions: roots do not penetrate the riprap; failure of the riprap would not jeopardize project purposes prior to repairs; and the presence of the berm and vegetation does not significantly reduce the discharge capacity of the project. For riprap areas above the 4 or 5 percent exceedence flow line, consideration may be given to overlaying the riprap with soil and sod to facilitate maintenance by mowing rather than by hand or defoliant. This may be particularly appropriate for riprap protecting against eddy action around structures such as gate wells and outlet works in levees that are otherwise maintained by mowing.

*

Recognizing that vegetation is, in most instances, inimical to riprap installations, planned use of vegetation with riprap should serve some justifiable purpose, be accounted for in capacity computations, be controllable throughout the project life, have a strengthened riprap design that will withstand the additional exigencies, and account for increased difficulty of inspection.

Section VI *Quality Control*

3-15. Quality Control

Provisions should be made in the specifications for sampling and testing in-place riprap as representative sections of revetment are completed. Additional sample testing of in-place and in-transit riprap material at the option of the Contracting Officer should be specified. The primary concern of riprap users is that the in-place riprap meets specifications. Loading, transporting, stockpiling, and placing can result in deterioration of the riprap. Coordination of inspection efforts by experienced staff is necessary. Reference EM 1110-2-2302 for detailed sampling guidance and required sample volumes for in-place riprap.

*

Chapter 4 Special Features and Considerations

4-1. Sediment Control Structures

a. General. Two basic types of control structures are used:

(1) stabilizers designed to limit channel degradation and

(2) drop structures designed to reduce channel slopes to effect nonscouring velocities.

These structures also correct undesirable, low-water-channel meandering. Gildea (1963) has discussed channel stabilization practice in USAED, Los Angeles. Debris basins and check dams are special types of control structures that are used to trap and store bed-load sediments.

b. Stabilizers.

(1) A stabilizer is generally placed normal to the channel center line and traverses the channel invert. When the stabilizer crest is placed approximately at the elevation of the existing channel invert, it may consist of grouted or ungrouted rock, sheet piling, or a concrete sill. The stabilizer should extend into or up the channel bank and have adequate upstream and downstream bed and bank protection. Plate 44 illustrates the grouted stone type of stabilizer used in USAED, Los Angeles. Stabilizers may result in local flow acceleration accompanied by the development of scour holes upstream and downstream. As indicated in Plate 44, dumped stone should be placed to anticipated scour depths. Maximum scour depths usually occur during peak discharges.

(2) Laboratory tests on sheet piling stabilizers for the Floyd River Control Project were made by the University of Iowa for USAED, Omaha (Linder 1963). These studies involved the development of upstream and downstream bed and bank riprap protection for sheet piling stabilizers in a channel subject to average velocities of 14 fps. The final design resulting from these tests is shown in Plate 45. Plate 46 is a general design chart giving derrick stone size required in critical flow areas as a function of the degree of submergence of the structure. Plate 47 presents design discharge coefficients in terms of the sill submergence T and critical depth d_c for the channel section. Use of Plates 46 and 47 is predicated on the condition that the ratio T/d_c is greater than 0.8. For smaller values the high-velocity jet plunges beneath the water surface, resulting in excessive erosion. The top of

the sheet piling is set at an elevation required by the above-mentioned criteria. Plate 47 is used with the known discharge to compute the energy head at $5d_c$ upstream of the structure. The head H on the structure is determined from the energy equation and used with Plate 46 to estimate the required derrick stone size. The curves in Plates 29 and 30 should be used as guides in the selection of riprap sizes for the less critical flow area.

c. Drop structures.

(1) Description and purpose. Drop structures are designed to check channel erosion by controlling the effective gradient, and to provide for abrupt changes in channel gradient by means of a vertical drop. They also provide a satisfactory means for discharging accumulated surface runoff over fills with heights not exceeding about 5 ft and over embankments higher than 5 ft provided the end sill of the drop structure extends beyond the toe of the embankment. The hydraulic design of these structures may be divided into two general phases, design of the notch or weir and design of the overpour basin. Drop structures must be so placed as to cause the channel to become stable. The structure must be designed to preclude flanking.

(2) Design rules. Pertinent features of a typical drop structure are shown in Plate 48. Discharge over the weir should be computed from the equation $Q = CLH^{3/2}$, using a C value of 3.0. The length of the weir should be such as to obtain maximum use of the available channel cross section upstream from the structure. A trial-and-error procedure should be used to balance the weir height and width with the channel cross section. Stilling basin length and end sill height should be determined from the design curves in Plate 48. Riprap probably will be required on the side slopes and on the channel bottom immediately downstream from the structure.

d. Debris basins and check dams.

(1) General. Debris basins and check dams are built in the headwaters of flood control channels having severe upstream erosion problems in order to trap large bed-load debris before it enters main channels. This is done to prevent aggradation of downstream channels and deposition of large quantities of sediment at stream mouths. Also, the passage of large debris loads through reinforced concrete channels can result in costly erosion damage to the channel. Such damage also increases hydraulic roughness and reduces channel capacity. A general summary of data on the equilibrium gradient of the deposition profile above control structures has been presented by

Woolhiser and Lenz (1965). The principles of design and operation of large debris basins as practiced by USAED, Los Angeles, have been presented by Dodge (1948). Ferrell and Barr (1963) discuss the design, operation, and effects of concrete crib check dams used in the Los Angeles County Flood Control District on small streams.

(2) Debris storage. Debris basins, usually located near canyon mouths at the upper end of alluvial fans, are designed to settle out and provide storage space for debris produced from a single major storm. In the Los Angeles area, the debris basin design capacity has been based on 100,000 cubic yards (cu yd) per square mile of drainage area, or 62 acre-feet per square mile. This quantity was obtained as an envelope curve of observed debris production during the storm of 1938 (Dodge 1948). Later estimates by Tatum (1963), taking into account factors affecting debris production such as fire history of the area, indicated a value of about twice this amount. Debris storage in the basin is usually maintained by reexcavation after a major storm period. The debris stored in the basin after any one flood should not be allowed to exceed 25 percent of the basin capacity. When permanent debris storage is more economical than periodic excavation, the average annual rate of debris accumulation multiplied by the project life should be used for storage capacity. Data from the Los Angeles County Flood Control District (Moore, Wood, and Renfro 1960) on 49 debris dams and basins give a mean annual debris production of 5,500 cu yd per square mile of drainage basin. This figure applies in the Los Angeles and similar areas, and can be used to determine the economic feasibility of long-term storage versus periodic debris removal.

(3) Debris basin elements. A debris basin consists of five essential basic parts:

(a) A bowl-shaped pit excavated in the surface of the debris cone.

(b) An embankment, usually U-shaped in plan, constructed from pit material, located along the two sides and the downstream end of the pit, and joining the hillside at each end where possible.

(c) One or more inlet chutes at the upstream end of the pit, when necessary to prevent excessive streambed degradation upstream of the debris basin.

(d) A broad-crested spillway at the downstream end of the basin leading to a flood control channel.

(e) An outlet tower and conduit through the embankment at the spillway for basin draining.

Plate 49 shows general design plans for a debris basin. The basin shape, the inlets, and the outlet should be located so that the debris completely fills the basin before debris discharge occurs over the spillway.

(4) Design criteria. The slope of the upper surface of the debris deposit must be estimated to determine the proper basin shape and to estimate the total debris capacity of the basin. A value of 0.5 times the slope of the natural debris cone at the basin site has been used for design. The basin side embankments should be of sufficient height and extend far enough upstream to confine the maximum debris line slope projected upstream from the spillway crest. The spillway should be designed to pass the design flood discharge with the basin filled with debris. The tops of the basin embankments should provide 5 ft of freeboard with the foregoing conditions. The design criteria for debris basins in the Los Angeles area should be used only for general guidance because of large differences in geology, precipitation patterns, land use, and economic justification in different parts of the country. The following conditions are peculiar to the Los Angeles area:

(a) Phenomenal urban growth in the desirable land area of the lower alluvial fans.

(b) Large fire potential.

(c) Hot, dry climate over a large portion of the year which inhibits vegetative growth.

(d) Sudden torrential rainfall on precipitous mountain slopes during a short rainy season.

(e) Unstable soil conditions subject to voluminous slides when saturated.

Debris and sediment production rates vary throughout the country depending on many factors, some of which are controllable by man. Extensive construction, strip mining operations, intensive agricultural use, and timber cutting operations are only a few examples of land uses that can have a profound local effect on sediment production and thus determine the type of sediment control necessary. Formulation of a sediment control plan and the design of associated engineering works depend to a large extent on local conditions.

4-2. Air Entrainment

a. General. Air entrainment should be considered in the design of rapid-flow channels. The entrainment of air may result in bulking of the flow and necessitate increased wall heights. Presently available data indicate that appreciable air entrainment should not occur with Froude numbers less than about 1.6.

b. Early design criteria. The USAED, Sacramento, developed the following equation based on data reported by Hall (1943):

$$m = \frac{V^2}{200gd} \quad (4-1)$$

where

m = air-water ratio

V = theoretical average flow velocity
without air

d = flow depth including air

The term V^2/gd is the Froude number squared. Equation 4-1 with minor differences in the definition of terms has been published by Gumensky (1949). The basic equation has been used extensively for design purposes in the past.

c. Modern investigations. The mechanics of self-aerated flow in open channels with sand grain surfaces has been studied at the University of Minnesota by Straub and Anderson (1960). The results of the Minnesota tests have been combined with selected Kittitas chute prototype data (Hall 1943) and published as HDC 050-3. The chart includes the following suggested design equation:

$$\bar{C} = 0.701 \log_{10} \left(\frac{S}{q^{1/5}} \right) + 0.971 \quad (4-2)$$

where

\bar{C} = ratio of experimentally determined
air volume to air plus water volume

S = sine of angle of chute inclination

q = discharge per unit width of channel

d. Design criteria. Use of Equation 4-2 or HDC 050-3 requires the assumption that the experimental water flow depth d_w in the term $\bar{C} = d_a/(d_a + d_w)$ where d_a is depth of air-water mixture, ft, is the same as the theoretically computed flow depth. The Minnesota data indicate that this assumption is valid only for small Froude numbers. For large Froude numbers, the theoretically computed depths for nonaerated flow were found to be 50 to 75 percent greater than the observed experimental flow depth. For this reason and for convenience of design, the Minnesota and Kittitas data have been computed and plotted in terms of the observed total flow depth (air plus water) and the theoretical flow depth and Froude number for nonaerated flow (Plate 50a). The resulting design curve has been extrapolated for low Froude numbers and replotted as Plate 50b. This plate should be used for air-entrained flows in flood control channels. A comparison of HDC 050-3 and Plate 50b indicates that this plate results in more conservative design for low Froude numbers.

4-3. Hydraulic Jump in Open Channels

a. General. Flow changes from the rapid to tranquil state will usually occur in the form of a hydraulic jump. The hydraulic jump consists of an abrupt rise of the water surface in the region of impact between rapid and tranquil flows. Flow depths before and after the jump are less than and greater than critical depth, respectively. The zone of impact of the jump is accompanied by large-scale turbulence, surface waves, and energy dissipation. The hydraulic jump in a channel may occur at locations such as:

- (1) The vicinity of a break in grade where the channel slope decreases from steep to mild.
- (2) A short distance upstream from channel constrictions such as those caused by bridge piers.
- (3) A relatively abrupt converging transition.
- (4) A channel junction where rapid flow occurs in a tributary channel and tranquil flow in the main channel.
- (5) Long channels where high velocities can no longer be sustained on a mild slope.

b. Jump characteristics.

(1) The momentum equation for the hydraulic jump is derived by setting the hydrodynamic force plus momentum flux at the sections before and after the jump equal, as follows:

$$A_1 \bar{y}_1 + \frac{Q^2}{gA_1} = A_2 \bar{y}_2 + \frac{Q^2}{gA_2} \quad (4-3)$$

where \bar{y} is the depth to the center of gravity of the stream cross section from the water surface. For a rectangular channel the following jump height equation can be obtained from Equation 4-3:

$$\frac{y_2}{y_1} = \frac{1}{2} \left(\sqrt{1 + 8F_1^2} - 1 \right) \quad (4-4)$$

where the subscripts 1 and 2 denote sections upstream and downstream of the jump, respectively. Equation 4-3 also gives good agreement for trapezoidal channels as shown by tests reported by Posey and Hsing (1938). However, flood channels should not be designed with jumps in trapezoidal sections because of complex flow patterns and increased jump lengths.

(2) The energy loss in the hydraulic jump can be obtained by use of the energy equation and the derived jump height relation (Chow 1959). This results in an equation that is a function only of the upstream Froude number. The relations between the Froude number, the jump height (Equation 4-4), and the energy loss (Equation 15-1, Brater and King 1976) are presented in Plate 51. The relation between the Froude number and the jump length, based on the data by Bradley and Peterka (1957) for rectangular channels, is also presented in this plate.

c. Jump location.

(1) The location of the hydraulic jump is important in determining channel wall heights and in the design of bridge piers, junctions, or other channel structures, as its location determines whether the flow is tranquil or rapid. The jump will occur in a channel with rapid flow if the initial and sequent depths satisfy Equation 4-3

(Equation 4-4 for rectangular channels). The location of the jump is estimated by the sequent depths and jump length. The mean location is found by making backwater computations from upstream and downstream control points until Equation 4-3 or 4-4 is satisfied. With this mean jump location, a jump length can be obtained from Plate 51 and used for approximating the location of the jump limits. Because of the uncertainties of channel roughness, the jump should be located using practical limits of channel roughness (see paragraph 2-2c). A trial-and-error procedure is illustrated on page 401 of Chow (1959).

(2) The wall height required to confine the jump and the backwater downstream should extend upstream and downstream as determined by the assumed limits of channel roughness. Studies also should be made on the height and location of the jump for discharges less than the design discharge to ensure that adequate wall heights extend over the full ranges of jump height and location.

(3) In channels with relatively steep invert slopes, sequent depths are somewhat larger than for horizontal or mildly sloping channels and jump lengths are somewhat smaller than those given in Plate 51. Peterka (1957) summarizes the available knowledge of this subject. This reference and HDC 124-1 should be used for guidance when a jump will occur on channel slopes of 5 percent or more.

d. Undular jump. Hydraulic jumps with Froude numbers less than 1.7 are characterized as undular jumps (Bakhmeteff and Matzke 1936) (see Plate 52). In addition, undulations will occur near critical depth if small disturbances are present in the channel. Jones (1964) shows that the first wave of the undular jump is considerably higher than given by Equation 4-4. The height of this solitary wave is given by

$$\frac{a}{y_1} = F_1^2 - 1 \quad (4-5)$$

where a is the undular wave height above initial depth y_1 . Additional measurements were also made by Sandover and Zienkiewicz (1957) verifying Equation 4-5 and giving the length of the first undular wave. Other measurements with a theoretical analysis have been reported by Komura (1960). Fawer (Jaeger 1957) has also given a formula for the wavelength based on experimental data; Lemoine (Jaeger 1957) used small-amplitude wave theory to give the wavelength of the undular jump. The

results of these investigations are summarized in Plate 52, which gives the undular jump surge height, breaking surge height (Equation 4-4), and the wavelength of the first undular wave. Also shown in this plate is a relation given by Keulegan and Patterson (1940) for the height of the first undulation

$$\frac{a}{y_1} = \frac{3}{2} \left(\frac{y_2 - y_1}{y_1} \right) \quad (4-6)$$

Experiment and theory indicate that the undular wave will begin to spill at the first crest when the Froude number exceeds about 1.28. Undulations persist, however, until the Froude number exceeds about $\sqrt{3}$ (≈ 1.7). This is the limit for breaking waves when Equation 4-4 gives a value of $y_2/y_1 = 2$. Further configuration information on undular jumps may be obtained from Figures 44, 45, and 46 of USBR (1948).

e. Stilling basins. Stilling basin design for high Froude numbers is covered in EM 1110-2-1603. The design of stilling basins in the range of Froude numbers from 1.0 to about 1.3 is complicated by undular waves that are dissipated only by boundary friction with increasing distance downstream. This range of Froude numbers should be avoided whenever possible because of flow instability. The hydraulic jump with Froude numbers of 1.3 to 1.7 is characterized by breaking undulations with very little energy dissipation (see Plate 51). Wall heights in this range of Froude numbers should be designed to contain waves up to the value given by the Keulegan and Patterson (1940) limit.

4-4. Open Channel Junctions

a. General. The design of channel junctions is complicated by many variables such as the angle of intersection, shape and width of the channels, flow rates, and type of flow. Appendix E presents a theoretical analysis, based on the momentum principle, that can be used for several types of open channel junctions. The design of large complex junctions should be verified by model tests.

b. Wave effects.

(1) Standing waves (Ippen 1951) in rapid flow at open channel junctions complicate flow conditions. These waves are similar to those created in channel curves described in paragraph 2-4, and may necessitate increased wall heights in the vicinity of the junction. The studies

by Bowers (1950) indicate that a hydraulic jump may form in one or both of the inlet channels, depending on the flow conditions.

(2) Wave conditions that may be produced by rapid flow in and downstream of a typical junction are shown in Plate 53. One area of maximum wave height can occur on the side channel wall opposite the junction point and another on the main channel right wall downstream from the junction. Behlke and Pritchett (1966) have conducted a series of laboratory tests indicating that wave pileup against the channel walls can be up to 7 times the initial depth with a flow Froude number of 4. The design of walls to contain these wave heights over long channel distances is usually not economical. The practical remedy is to reduce or minimize standing waves.

(3) Peak flows from the side channel may not occur simultaneously with peak flows in the main channel. Laboratory tests by Behlke and Pritchett (1966) indicate that occurrence of the design flow in one of the channels with zero flow in the other can result in very high wave pileup on the junction walls. Plates 54a and b show maximum wave height as a function of upstream Froude number for conditions of zero flow in the side channel and main channel, respectively. This plate demonstrates the need for keeping the angle of the junction intersection relatively small. The data are also useful in designing wall heights; for example, the maximum wave pileup on the main channel wall would be greater than twice the side channel flow depth for $F_2 = 3.0$, a junction angle of 15 deg, and no flow in the main channel.

c. Wave height criteria. Behlke and Pritchett's (1966) recommended criteria for the design of channel junctions in rapid flow to minimize wave effects are listed below:

(1) Enlarge the main channel below the junction apex to maintain approximately constant flow depths throughout the junction.

(2) Provide equal water-surface elevations in the side and main channels in the vicinity of the junction.

(3) Ensure that the side channel wave originating at the junction apex impinges on the opposite side channel wall at its intersection with the enlarged main channel wall.

(4) Provide tapered training walls between the main channel and the side channel flows.

(5) Ensure that maximum wave heights occur with maximum flows. Plate 55 illustrates typical design examples for rectangular and trapezoidal channels using these criteria. Important junctions in rapid flow designed to reduce wave effects should be model tested at all probable flow combinations as well as at design flow.

d. Confluence design criteria.

(1) The results of several model studies in USAED, Los Angeles, indicate that some general guides can be adopted for the design of confluence junctions. Gildea and Wong (1967) have summarized some of these criteria:

(a) The design water-surface elevations in the two joining channels should be approximately equal at the upstream end of the confluence.

(b) The angle of junction intersection should be preferably zero but not greater than 12 deg.

(c) Favorable flow conditions can be achieved with proper expansion in width of the main channel below the junction.

(d) Rapid flow depths should not exceed 90 percent of the critical depth (Froude number should be greater than 1.13) to maintain stable rapid flow through the junction (paragraph 2-2d(1)).

(2) Model tests of many confluence structures indicate very little crosswave formation and turbulence at the junction if these criteria are followed. Moreover, experience has shown that the momentum equation approach given in Appendix E can be used for junctions involving small angles and equal upstream water-surface elevations.

(3) Typical confluence layouts model tested by USAED, Los Angeles, and proven to have good flow characteristics are shown in Plate 56. The design with the offset in the main channel center line is normally used (Plate 56a). When the main channel center-line alignment cannot be offset, a layout with a transition on the wall opposite the inlet side should be used (Plate 56b). The proper amount of expansion in the main channel downstream of the confluence is very important in maintaining good flow conditions. Plate 57 gives the USAED, Los Angeles, empirical curve for the required increase in channel width, Δb_3 , as a function of the discharge ratio. If the junction angle is zero, the width of the channel at the confluence will be equal to the sum of the widths of the main and side channels plus the thickness of the dividing wall between the channels. If a reduction in

width is required downstream from the confluence, the transition should be made gradually.

e. Design procedure. The design procedure for the typical open channel confluence shown in Plate 56 involves the following steps:

(1) Determine side-channel requirements relative to discharge, alignment, and channel size.

(2) Select junction point to obtain an entrance angle less than 12 deg. This angle requirement may necessitate a long, spiral curve for the side channel upstream from the junction.

(3) Determine the increase of channel width Δb_3 from the Q_2/Q_3 ratio curve in Plate 57. Compute the required downstream channel width $b_3 = b_1 + \Delta b_3$ and the confluence width $b_c = b_1 + 2\Delta b_3$.

(4) Make the confluence layout on a straight-line basis by setting the main channel walls parallel to and at distances of $(1/2)b_3$ and $b_c - (1/2)b_3$ from the center line as shown in Plate 56a.

(5) Connect the left walls of the side and the main channels by a curve determined by the apex angle θ and a radius r_L given by

$$r_L = \frac{4V^2 b_2}{gy} + 400 \quad (4-7)$$

Equation 4-7 results from a study of a number of confluences built by USAED, Los Angeles. The term $(4V^2 b_2)/gy$ is the same as that used in Equation 2-34.

(6) Make the right wall of the side channel concentric with the left wall and locate the junction intersection point. The right wall radius r_R is given by

$$r_R = r_L + b_2 \quad (4-8)$$

(7) Determine the average depth of flow at midpoint of the confluence by the momentum method (Appendix E) assuming $b_m = (1/2)(b_1 + b_2 + b_c)$.

(8) Set the side-channel invert elevation so that the design water-surface levels in both channels approximate

each other. A stepped invert in either of the channels may be required.

(9) Determine the length of transition and invert slope required to reduce the channel width from b_2 to b_3 without exceeding the criterion $y/y_c \leq 0.90$ in the transition. Convergence rates should be in agreement with those recommended in paragraph 2-4.

f. Side drainage inlets. Flow disturbances occur where storm drains or industrial waste lines discharge into flood control channels, commonly referred to as "inlets." Small side-drainage flows are commonly conveyed in a pipe storm drain system. Criteria for box and pipe culvert inlet design are given in h below. Economical design for intermediate tributary flows normally requires free surface structures. A side-channel spillway type of inlet for this range of discharge has been developed by USAED, Los Angeles, which reduces disturbances to a minimum in the main channel. This type of junction is described in g below. The conventional confluence structure described in d above should be used for large tributary discharges.

g. Side-channel drainage inlet.

(1) The side-channel spillway type of drainage inlet was developed and model tested by USAED, Los Angeles (1960b). The recommended structure consists of a common wall between the side channel and the main channel. A weir notched in this wall allows the tributary flow to enter the main channel with minimum disturbance. A typical design of this type of structure is illustrated in Plate 58. A small drain should be placed at the lowest point of the side channel. The objective of this design is to discharge the side flow with reduced velocity into the main channel gradually over a relatively long spillway inlet. Model tests (USAED, Los Angeles, 1960b) indicate that this effectively reduces wave action and disturbances in the main channel for all flow combinations. Satisfactory operation may require periodic sediment removal from behind the weir.

(2) The procedure for designing the side-channel spillway inlet structure follows:

(a) Set the spillway crest 0.5 ft above the parallel to the design watersurface level in the main channel.

(b) Determine the required length L of the crest by the equation, $L = Q/(CH^{3/2})$, so that the maximum H is not greater than 1.5 ft with critical depth over the crest C equal to 3.097.

(c) Determine the side-channel flow depth d at the upstream end of the spillway.

(d) Set the side-channel invert so that the spillway approach depth is equal to $d - H$.

(e) Determine the side-channel convergence required to maintain a constant flow depth in the side channel behind the spillway. This should result in a reasonably constant unit discharge over the spillway equal to that computed by the equation in (b) above.

(f) Plot the computed side-channel alignment points obtained from step (e) on the channel plan and connect them by a smooth curve or straight line to intersect the main channel wall so that the side channel has a minimum width of 2 ft behind the spillway.

(g) Adjust the side-channel convergence and repeat step (e) if the spillway length in step (f) does not approximate that determined in step (b).

h. Box and pipe culvert inlets. Gildea and Wong (1967) have determined design criteria for pipe inlets. The variables to be considered in the design are width of the main channel, angle of entrance of the storm drain, size of the storm drain, volume and velocity of flow, and elevation of the storm drain with respect to the channel bottom. Model tests (USAED, Los Angeles, 1960b, 1964) have shown that flow disturbances in the main channel are minimized when side-drain openings are small and side-drainage flows are introduced reasonably parallel to the main flow. The following criteria should be used for design:

(1) The maximum angle of entrance for side culverts should be:

(a) 90 deg for diameters of 24 in. or less.

(b) 45 deg for diameters from 24 to 60 in.

(c) 30 deg for diameter 60 in. or greater.

(2) The culvert invert should be placed no more than 18 in. above the main channel invert to give the maximum submergence practicable.

(3) Automatic floodgates or flap gates should be installed when damage from backflooding from the main channel would exceed that resulting from local pondage caused by gate operation. These gates should be recessed

to prevent projecting into the main channel flow when in a full-open position. Head loss coefficients for flap gates are given in HDC 340-1.

4-5. Hydraulic Model Studies

a. General. The use of hydraulic models has become a standard procedure in the design of complex open channels not subject to analytical analyses or for which existing design criteria based on available model and field tests are inadequate. Hydraulic models afford a means of checking performance and devising modifications to obtain the best possible design at minimum cost. Model tests should be used to supplement but not replace theoretical knowledge, good judgment, and experience of the design engineer. They often indicate design changes that save substantial amounts in construction costs as well as effect improvements in operation. Model tests of large flood control channels are generally desirable where supercritical flow results in standing waves and other major disturbances in channels containing junctions, transition structures, alignment curvature, multiple bridge piers, or stilling basins.

b. Model design.

(1) The theory of model design is treated in EM 1110-2-1602 and other publications (Rouse 1950, Davis and Sorenson (1969), American Society of Civil Engineers (ASCE) 1942). For open channel models, the gravity force will dominate the flow and similitude will require equality of Froude number in the model and prototype. The Froudian scale relations (model-to-prototype) in Table 4-1 apply to undistorted models. The length ratio L_r is the model-to-prototype ratio L_m/L_p . These transfer relations are based on equal force of gravity and density of fluid in model and prototype. The procedure for initiation of model studies is discussed in EM 1110-2-1602.

(2) Model scale ratios for flood control channels have ranged from 1:15 to 1:70, depending on the type of problem being studied, the relative roughness of the model and prototype, and the size of the prototype

structure. Scale ratios of 1:15 to 1:30 are usually employed where supercritical flow wave problems are involved. They are also used for sectional models of drop structures, spillways, etc. The smaller scale ratios (1:30 to 1:70) are used for general model studies where long channel lengths are reproduced. The accuracy of possible model construction and flow measurements may control the permissible scale ratios. Most models of channels are generally built to give depths of flow about 0.5 ft or more and channel widths of about 1 to 2 ft. The most common scale ratios used by the USAED, Los Angeles, Hydraulic Laboratory for channel model studies are from 1:25 to 1:40.

c. Model roughness. Turbulent flow will prevail with model channel velocities and depths commonly used in testing. In most cases, the channel flow is rough-turbulent or nearly so; therefore, hydraulic resistance is determined primarily by the relative size of the roughness elements. However, the model Reynolds number will always be smaller than the prototype, and this will to some extent cause scale distortion of certain phenomena such as zones of separation, wave dissipation, flow instability, and turbulence in the model. Particular care should be taken in interpreting those effects that are known to be strongly dependent on viscous forces.

d. Slope distortion. An empirical equation of the Manning type may be used to give the required model roughness (Rouse 1950) for large-scale models where fully rough-turbulent flow prevails. This condition is expressed by the equation

$$n_r = L_r^{1/6} \tag{4-9}$$

If this roughness criterion cannot be fulfilled, slope adjustment or distortion must be applied to the model so that prototype flow conditions can be simulated in the model. The amount of additional slope required is given by the equation (Rouse 1950)

Table 4-1
Scale Relations

Length	Area	Volume	Time	Velocity	Discharge	Manning's n
L_r	L_r^2	L_r^3	$L_r^{1/2}$	$L_r^{1/2}$	$L_r^{5/2}$	$L_r^{1/6}$

$$S_r = \frac{n_r^2}{L_r^{1/3}} \quad (4-10)$$

$$n_r = \frac{R_r^{2/3}}{L_r^{1/2}} \quad (4-12)$$

Equation 4-10 applies only when the model and prototype channels are geometrically similar in cross section. Without slope distortion ($S_r = 1$), this equation would reduce to Equation 4-9.

For a wide channel Equation 4-12 reduces to

$$n_r = \frac{y_r^{2/3}}{L_r^{1/2}} \quad (4-13)$$

e. Scale distortion.

(1) Distorted scales are generally used in models of river channels, floodways, harbors, and estuaries. Movable-bed models are distorted in order to ensure the movement of particle-size bed material under model flow conditions. Flood control projects for the improvement of river channels through urbanized areas often require the reproduction of long channel lengths and wide floodway widths. Most such channels have mild slopes and the flows are tranquil at very low Froude numbers. In order to fit this type of model in a reasonably economical space, the horizontal scale ratio has to be limited and vertical scale distortion selected to give measurable depths and slopes as well as to ensure turbulent flow in the model. The use of distorted models should be generally limited to problems involving tranquil flows. A number of reports (USAEWES 1949a, 1949b, 1953) have been published that illustrate the application of distorted models for the solution of complex local flood protection problems and channel improvements.

The required roughness in the model can be computed by Equation 4-12 and used as a guide in designing the model. Distorted models should be verified using measured field data or computed prototype data prior to testing of improvement plans. Flood control channel models should be built to as small a distortion as is economically feasible. A distortion of 3 or less is desirable, but depends to some extent on the type of information needed from the model study. It may sometimes be economically feasible to divide a long channel study into several problem areas and model each one independently. In this manner different scales could be used as required by the problem to be studied in each reach.

(2) The scale relations for distorted models are given in ASCE (1942). If the bed slope ratio is made equal to the energy slope ratio, the slope ratio will also be equal to the amount of model distortion.

f. Movable-bed models. Open channel studies involving problems of sediment erosion, transportation, or deposition require a bed of sand or other material that will move when subjected to flow. Rouse (1950), Davis and Sorenson (1969), and ASCE (1942) give considerable detail on design, construction, verification, and use of movable-bed models. Qualitative indication of bed movement has been used in flood control channel models for design purposes. For example, the effectiveness of a hydraulic jump to dissipate energy is often obtained through the relative extent of downstream scour. The stability of riprap protection can also be obtained from model studies. A typical example of a study to determine the relative scour and design of riprap protection at inlet and outlet channels is given in USAED, Los Angeles (1960a).

$$S_r = \frac{y_r}{L_r} \quad (4-11)$$

where y_r is the vertical scale ratio and L_r is the horizontal scale ratio, model to prototype. The Manning equation can then be used to obtain a roughness criteria for model design (Rouse 1950).

* **Chapter 5**
Methods for Predicting n Values for the Manning Equation

5-1. Introduction

This chapter describes the prediction of the total Manning's roughness coefficient (n value) for a reach by establishing physically based component parts and determining the contribution from each. The following component parts were selected: bed roughness, bank roughness, surface irregularities, obstructions, vegetation roughness, and expansion/contraction losses.

5-2. Approach

Hydraulic roughness is a major source of uncertainty in water surface profile calculations. Field data at each project are required to confirm selected values. When field data are not available, the traditional approach is to use handbook methods or analytical methods to predict the hydraulic roughness values.

a. Handbook method. In this approach the engineer uses "calibrated photographs" and other subjective methods to associate hydraulic roughness values with conditions observed and anticipated in the project reach. Chow (1959) and Barnes (1967) are the dominant sources of calibrated photographs. More recently, Arcement and Schneider (1989) extended the work to include floodplains. Other sources, like hydraulics and agricultural handbooks, add variation but not much additional insight.

b. Analytical methods. A second approach for predicting roughness coefficients is to relate hydraulic roughness to the effective surface roughness and irregularity of the flow boundaries. This approach is called analytical methods in this chapter. The classic example is the Moody-type diagram for hydraulic roughness in open channel flow (Plate 3). The procedure shown in paragraph 2-2c is still the state of the art in n values for concrete-lined channels. It is based on the Keulegan equations for velocity distribution (Chow 1959). The Iwagaki relationship has been included in the determination of the coefficients for the roughness equations.

c. Grass-lined channels. Manning's n values for grass-lined channels were reported by the Soil Conservation Service (Chow 1959).

d. Mobile boundary channels. Simons and Richardson (1966) related bed forms in mobile boundary

channels to stream power. These data indicate that a significant change can occur in n values as the stream bed changes from ripples to dunes to plane bed to antidune. Subsequently, work by Limerinos (1970) and Brownlie (1983) provided regression equations for calculating bed roughness in mobile boundary channels. Note that channel bed roughness is just one component of the total n value for a reach.

e. Compositing. The procedure for combining different roughnesses across a section into a single value for hydraulic computations is called compositing. The composited value may change if a different method for compositing is chosen. Therefore, the handbook methods are probably more dependable as sources of n values than the analytical methods because the compositing is included in the field observation.

5-3. Hydraulic Roughness by Handbook Methods

Arcement and Schneider (1989) summarize the state of the art in selecting n values for natural channels and flood plains. This work was performed for the U.S. Department of Transportation and subsequently will be called the USDT method in this chapter. The basic approach follows that proposed by Cowan (Chow 1959):

$$n = (n_b + n_1 + n_2 + n_3 + n_4)m \quad (5-1)$$

where

n_b = base n value

n_1 = addition for surface irregularities

n_2 = addition for variation in channel cross section

n_3 = addition for obstructions

n_4 = addition for vegetation

m = ratio for meandering

5-4. Base n Values (n_b) for Channels

On page 4 of their report, Arcement and Schneider state, "The values in [their] Table 1 for sand channels are for upper regime flows and are based on extensive laboratory and field data obtained by the U.S. Geological Survey. When using these values, a check must be made to ensure that the stream power is large enough to produce upper

*

* regime flow.” Although the base n values given in Table 5-1 for stable channels are from verification studies, the values have a wide range because the effects of bed roughness are extremely difficult to separate from the effects of other roughness factors. The choice of n values from Table 5-1 will be influenced by personal judgment and experience. The n values for lower and transitional regime flows are much larger generally than the values given in Table 5-1 for upper regime flow. Also, the vegetation density method of Petryk and Bosmajian (1975) is presented for the vegetation component n_v . Although the work was published in the mid-1970's, it has not received widespread attention in the profession. It has considerable appeal as a design procedure, however, and deserves additional evaluation.

a. Example. Figure 5-1 is the proposed design for a levee project in which the sponsor proposes vegetation along the project. The hydraulic roughness values for this section are estimated from several different handbook sources in Tables 5-1 and 5-2. Note that handbooks divide n values into two categories: channel bed and bank and flood plains.

b. Sensitivity of calculations to n values. The calculated water depth is shown in Table 5-3 using the mean values of both channel and overbank roughness. The mean values are considered to be the best estimate, statistically.

Both n values were increased by adding their standard deviation. The resulting water surface elevation increased about 0.7 ft, from 9.4 ft to 10.1 ft. This standard deviation in n values is really quite small. However, it demonstrates how sensitive water depth is to n value.

5-5. Hydraulic Roughness by Analytical Methods

Investigators continue to explore physically based hydraulic roughness equations. These are the methods in which hydraulic roughness is calculated from the effective surface roughness k_s . The new Hydraulic Design Package (SAM), under development at the U.S. Army Engineer Waterways Experiment Station (WES) (Thomas et al., in preparation), offers nine analytical methods for n values (Table 5-4). None of the n value equations account for momentum or bend losses. Presently, the only technique for bend losses is to increase the n values by a factor. Cowan (Chow 1959) proposed a multiplier in Equation 5-1, and both Chow and the USDT report suggest

values to use. Scobey (Chow 1959) proposed increasing the n value by 0.001 for each 20 degrees of curvature. Chow suggested that should not exceed a total of 0.002 even in flumes having pronounced curvature.

a. Effective surface roughness height k_s . For the design of concrete channels, Corps of Engineers values for k_s are shown in Chapter 2 (Table 2-1). Chow (1959) gives a table of k_s values (Table 8-1) for other boundary materials such as k_s for natural rivers. Please note that, at this point in time, the profession has not adopted tables of k_s values as they have Manning's n values. Moreover, there is no generally accepted technique for measuring this property geometrically. Therefore, the use of Table 8-1 is discouraged. Instead, use the Strickler or the Keulegan equations and calculate k_s from available sources of Manning's n value. (Note: These equations do not necessarily give the same results.)

b. Relative roughness. Relative roughness refers to the ratio of the effective surface roughness height, k_s to the hydraulic radius R . The relative roughness parameter is R/k_s .

c. Strickler equation, rigid bed. The Strickler function (Chow 1959) is shown in Figure 5-2. Notice that the effective surface roughness height k_s is correlated with the D_{50} of the bed sediment in this figure. However, k_s can be correlated with other measures of the surface roughness depending on what is representative of the surface roughness height of the boundary materials. For example, riprap research at WES has shown that the Strickler equation (Equation 5-2) will give satisfactory n values when k_s is taken to be the D_{90} of the stone.

$$n = C k_s^{1/6} \quad (5-2)$$

where

$$\begin{aligned} C &= 0.034 \text{ for riprap size calculations where } k_s = D_{90} \\ &= 0.038 \text{ for discharge capacity of riprapped channels where } k_s = D_{90} \\ &= 0.034 \text{ for natural sediment where } k_s = D_{50} \text{ (Chow 1959)} \end{aligned}$$

*

*

Table 5-1
Hydraulic Roughness, Channel Bed and Banks

Reference	m	n_b	n_1	n_2	n_3	n_4	n
USDT (Arcement and Schneider 1989), pp 4 & 7	1.0	0.024	0.002	0.002	0.001	0.005	0.034
Barnes (1967), p 78	-	0.037	-	-	-	-	0.034
Chow (1959), p 109, Table 5-5, Fine Gravel	1.0	0.024	0.005	0.0	0.0	0.00	0.034
Chow (1959), p 112, Table 5-6, D-1a3	-	0.040	-	-	-	-	0.040
Chow (1959), p 120, Figure 5-5(14)	-	0.030	-	-	-	-	0.030
Brater and King (1976), p 7-17, Natural	-	0.035	-	-	-	-	0.035
Mean							0.035
Standard deviation							0.003

Note:

$$n = (n_b + n_1 + n_2 + n_3 + n_4)m$$

where

n_b = base n-value

n_1 = addition for surface irregularities

n_2 = addition for variation in channel cross section

n_3 = addition for obstructions

n_4 = addition for vegetation

m = ratio for meandering

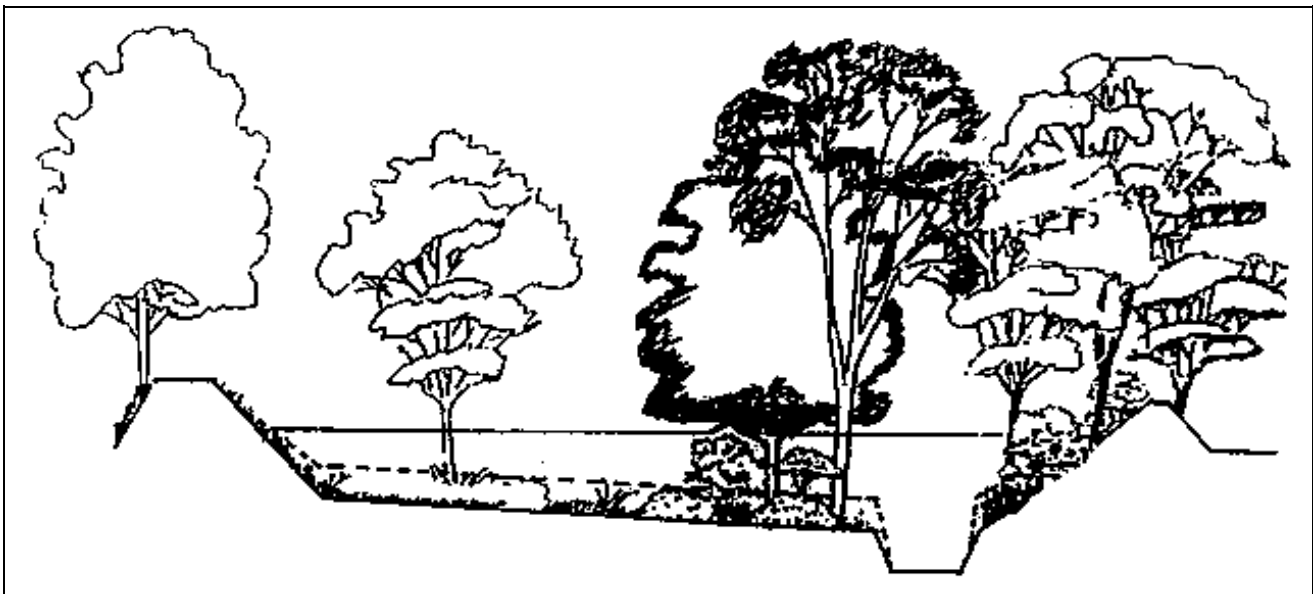


Figure 5-1. Design cross section

*

*

Table 5-2
Hydraulic Roughness, Floodplain

Reference	n_b	n_1	n_2	n_3	n_4	n
USDT (Arcement and Schneider 1989), pp 4 & 9	0.028	0.010	-	0.012	0.050	0.100
Barnes (1967), None Given	-	-	-	-	-	-
Chow (1959), p 113, Table 5-6, D-2c5	0.100	-	-	-	-	0.100
Chow (1959), p 123, Figure 5-5(23)	0.125	-	-	-	-	0.125
Brater and King (1976), None Given	-	-	-	-	-	-
Mean						0.108
Standard deviation						0.012

Note: Same n value equation as channel bed and banks.

Table 5-3
Sensitivity of Depth to n Value

Case	Channel	n Value	
		Flood-plain	Water Surface
Mean	0.035	0.108	9.4
+1 Standard Deviation	0.038	0.120	10.1

Table 5-4
 n Value Equations and Compositing Methods in SAM

n Value Equations	Methods for Compositing
Manning's n	Alpha Method
Keulegan	Equal Velocity Method
Strickler	Total Force Method
Limerinos	Total Discharge Method
Brownlie	
Grass E ¹	
Grass D ¹	
Grass C ¹	
Grass B ¹	
Grass A ¹	

Note: ¹ Grass type described in Table 5-7.

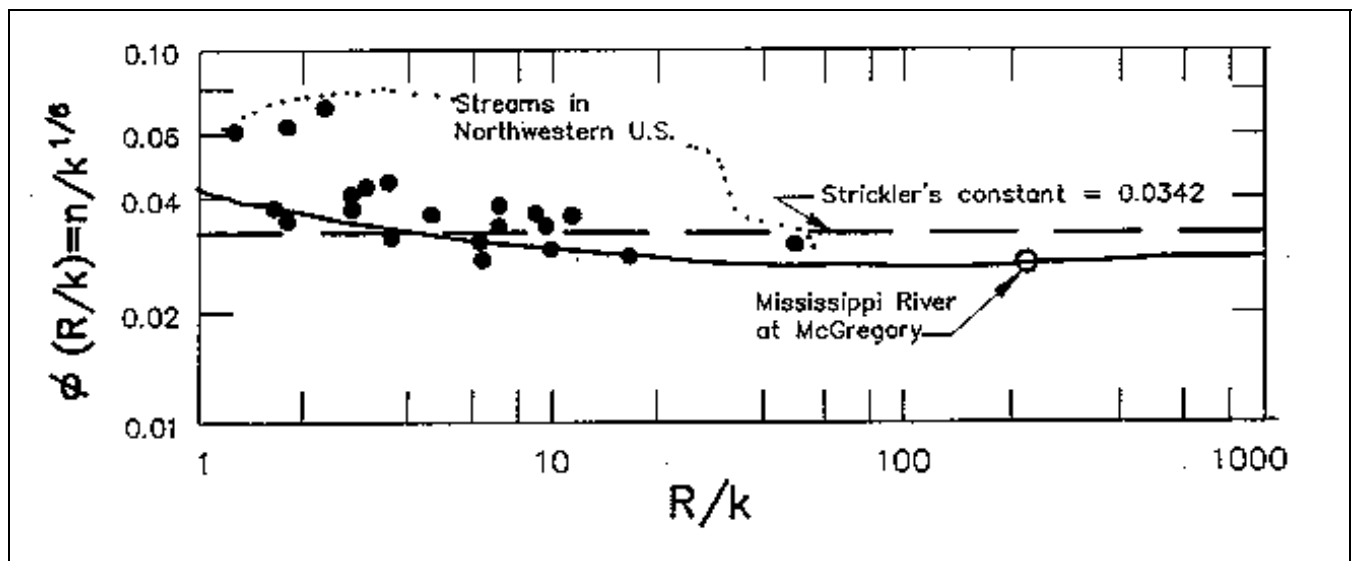


Figure 5-2. The Strickler function (Chow 1959) (courtesy of McGraw-Hill Book Company, Inc.)

*

* *d. Keulegan equations, rigid bed.* The procedure in Chapter 2 is still the state of the art in n values for rigid boundary channel design. It is a relative roughness approach based on the Keulegan equations for velocity distribution (Chow 1959). Keulegan classified flow types as hydraulically smooth flow, hydraulically rough flow, and a transition zone. His equations, presented in Chapter 2 and repeated as follows, are written in terms of the Chezy coefficient because of the simpler powers involved. The conversion to Manning's n value follows.

(1) The equation for fully rough flow is

$$C = 32.6 \log_{10} \left(\frac{12.2 R}{k} \right) \quad (2-6 \text{ bis})$$

(2) For smooth flow the equation is

$$C = 32.6 \log_{10} \left(\frac{5.2 R_n}{C} \right) \quad (2-5 \text{ bis})$$

(3) The equation showing the relationship of n value and Chezy C is (see Equation 2-4)

$$n = \frac{1.486}{C} R^{1/6} \quad (5-3)$$

where

$$R_n = \text{Reynolds number} \\ = 4RV/\nu$$

where

$$V = \text{average flow velocity} \\ \nu = \text{kinematic viscosity of water}$$

and 32.6, 12.2 and 5.2 are empirical coefficients determined from laboratory experiments. These equations, when graphed, produce a Moody-type diagram for open channel flow (Plate 3).

e. The Iwagaki relationship.

(1) Chow presents Keulegan's equation for the average flow velocity V in the following form

$$V = U_* \left[6.25 + 5.75 \log_{10} \left(\frac{R}{k_s} \right) \right] \quad (5-4)$$

where

$$U_* = \text{boundary shear velocity} = \sqrt{gRS}$$

g = acceleration of gravity

S = slope

6.25 = coefficient for fully rough flow

(2) Substituting a variable, A_r , for the constant, 6.25, substituting the Chezy equation for velocity, and substituting \sqrt{gRS} for U_* gives

$$\frac{V}{U_*} = \frac{C}{\sqrt{g}} = A_r + 5.75 \log_{10} \left(\frac{R}{k_s} \right) \quad (5-5)$$

$$C = \sqrt{g} \left[A_r + 5.75 \log_{10} \left(\frac{R}{k_s} \right) \right] \quad (5-6)$$

The form shown in Chapter 2 can be written as follows:

$$C = 32.6 \log_{10} \left[10^{\frac{A_r \sqrt{g}}{32.6}} \left(\frac{R}{k_s} \right) \right] \quad (5-7)$$

where A_r is the Iwagaki coefficient for rough flow.

From Keulegan's study of Bazin's data, the value of A_r was found to have a wide range, varying from 3.23 to 16.92. Thus, a mean value of 6.25 for A_r may be used.

*

* "A further study was made by Iwagaki on experimental data obtained from many sources. The results of the study have disclosed that resistance to turbulent flow in open channels becomes obviously larger than that in pipes with increase in the Froude number. Iwagaki reasoned that this is due to the increased instability of the free surface at high Froude numbers" (Chow 1959, p 204).

(3) The Iwagaki relationship is shown in Figure 5-3.

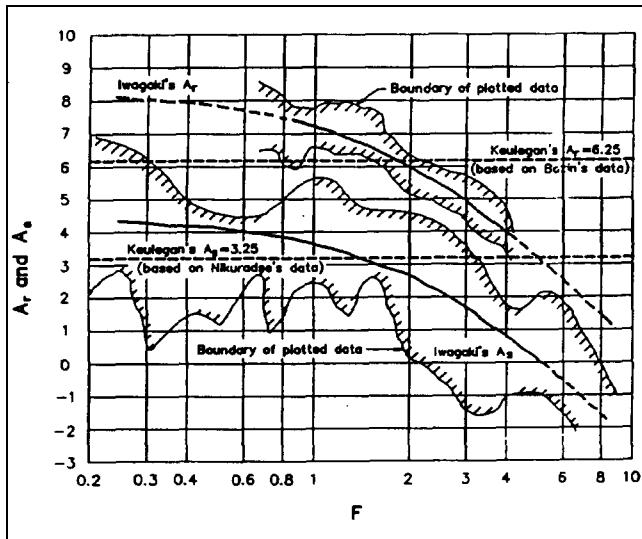


Figure 5-3. The Iwagaki relationship (Chow 1959) (courtesy of McGraw-Hill Book Company, Inc.)

(4) The comparable form of the equation for smooth flow is

$$C = 32.6 \log_{10} \left[10^{\frac{A_s \sqrt{g}}{32.6}} \left(\frac{\sqrt{g} R_n}{4C} \right) \right] \quad (5-8)$$

where A_s is the Iwagaki coefficient for smooth flow.

f. A_r and A_s coefficients.

(1) The A_r and A_s coefficients are shown graphically in Figure 5-3, but the equations for the curves were not provided. It can be shown that the equation for A_r is of the form

$$A_r = -27.058 \log_{10} (F + 9) + 34.289 \quad (5-9)$$

where F is the Froude number. Data ranged from $0.2 < F < 8.0$.

(2) Using an equation of the same form, the relationship for A_s is

$$A_s = -24.739 \log_{10} (F + 10) + 29.349 \quad (5-10)$$

(3) When the values of A_r and A_s are 6.2411 and 3.25, the coefficients in the roughness equations are 12.2 and 5.2, respectively. These are the values shown in Equations 2-5 and 2-6. Using Equations 5-9 and 5-10, those values correspond to Froude numbers of 1.88 and 1.35, respectively.

g. Transition zone. The limit of the fully rough zone is

$$\frac{R_n / C}{R / k_s} > 50 \quad (5-11)$$

The roughness equation in the transition zone is a combination of the equations for smooth and fully rough flow as follows:

$$C = -32.6 \log_{10} \left(\frac{4C}{\sqrt{g} R_n 10^{\frac{A_s \sqrt{g}}{32.6}}} + \frac{k_s}{R 10^{\frac{A_s \sqrt{g}}{32.6}}} \right) \quad (5-12)$$

h. Comparison of n -values, from Strickler and Keulegan equations. Table 5-5 is a comparison of n values calculated by the Strickler and Keulegan equations. Flow is fully rough. Notice the Strickler equation uses the effective surface roughness height k_s , and not relative roughness. Therefore, the n value does not vary with hydraulic radius R . On the other hand, the Keulegan equation uses relative roughness, and that requires both k_s and R . The constant in the Strickler equation, 0.034, is that recommended by Chow (1959). The resulting n values match the Keulegan results adequately. For example, the k_s for concrete is 0.007. That converts to an n value of 0.015 using Strickler and to 0.014-0.018 using Keulegan.

*

*

Table 5-5
n Values Calculated by Strickler and Keulegan Equations

Effective Roughness		Strickler $n = 0.034 \cdot k_s^{1/6}$	F	Keulegan Equation R, ft				
k_s , mm	k_s , ft			1	5	10	20	50
0.10	0.0003281	0.009	8	0.012	0.013	0.014	0.015	0.016
			1.88	0.010	0.011	0.012	0.013	0.014
			0.2	0.009	0.011	0.011	0.012	0.013
1.00	0.003281	0.013	8	0.017	0.017	0.018	0.019	0.020
			1.88	0.013	0.014	0.015	0.015	0.017
			0.2	0.012	0.013	0.014	0.015	0.016
2.13	0.007	0.015	8	0.019	0.019	0.020	0.020	0.021
			1.88	0.014	0.015	0.016	0.017	0.018
			0.2	0.013	0.015	0.015	0.015	0.018
10	0.03281	0.019	8	0.026	0.025	0.025	0.025	0.026
			1.88	0.018	0.018	0.019	0.019	0.020
			0.2	0.016	0.017	0.017	0.018	0.019
64	0.20997	0.026	8	0.049	0.037	0.035	0.034	0.033
			1.88	0.026	0.024	0.024	0.025	0.025
			0.2	0.022	0.022	0.022	0.022	0.023
100	0.3281	0.028	8	0.060	0.042	0.039	0.037	0.036
			1.88	0.029	0.026	0.026	0.026	0.027
			0.2	0.024	0.023	0.023	0.024	0.024
152.4	0.500	0.030	8	0.084	0.048	0.043	0.041	0.039
			1.88	0.033	0.029	0.028	0.028	0.028
			0.2	0.027	0.025	0.025	0.025	0.026
1,000	3.2808	0.041	8	—	—	0.092	0.073	0.061
			1.88	—	—	0.043	0.040	0.039
			0.2	—	—	0.036	0.034	0.034

Note:

$$C = 32.6 \log_{10} (Coef_2 \cdot R/k_s)$$

$$Coef_2 = 10^{(\sqrt{g} \cdot A/32.6)}$$

$$A_r = 27.058 \cdot \log_{10} (F + 9) + 34.289$$

*

* *i. Bed roughness in mobile boundary streams.*

(1) In mobile boundary channels the bed roughness is composed of grain roughness and form roughness. The grain roughness refers to the effective surface roughness height of the mixture of sediment particles on the stream-bed. Form roughness refers to bed features described as ripples, dunes, transition, plain bed, standing waves, and antidunes. These bed features, called bed forms, are grouped into the general categories of lower regime, transitional, and upper regime.

(2) Regime, in this usage of the term, does not refer to whether the flow is sub- or supercritical. The Froude number may remain less than 1, and the bed regime may still shift from lower to upper and back. Neither does it refer to channel dimensions, flow velocity, nor slope. It is simply the category of bed forms that are contributing to the hydraulic roughness. However, the amount of hydraulic loss produced by bed form roughness may exceed that produced by grain roughness. Therefore, it cannot be ignored.

(3) The significant difference between mobile boundary streams and rigid boundary streams is in the requirement to predict when the bed forms change from one regime to another. It seems to be related to flow velocity, flow depth, water temperature, and effective sediment particle size.

(4) Two functions are presented in this chapter for calculating n values in mobile boundary channels: Limerinos (1970) and Brownlie (1983). However, only the Brownlie method includes predicting the change from one bed regime to the other. These relationships are described in more detail in the following paragraphs.

(5) It is important to establish which portion of the channel cross section is bed and which is bank because the bed roughness predictors apply only to the channel bed. That is, typically the vegetation roughness and bank angle do not permit the bed load to move along the face of the banks. Therefore, the Limerinos and Brownlie n value equations should not be used to forecast bank roughness.

(6) On the other hand, the point bar is a natural source-sink zone for sediment transport. Consequently, it is a location at which the Limerinos and Brownlie equations apply.

j. Limerinos n-value predictor, mobile bed.

(1) Limerinos developed an empirical relative roughness equation for coarse, mobile bed streams using field data (Limerinos 1970). He correlated n values with hydraulic radius and bed sediment size. The following equation resulted:

$$n = \frac{0.0926 R^{1/6}}{1.16 + 2.0 \log_{10} \left(\frac{R}{d_{84}} \right)} \quad (5-13)$$

where

n = Manning's n value. Data ranged from 0.02 to 0.10.

R = hydraulic radius, ft. Data ranged from 1 to 6 ft.

d_{84} = the particle size, ft, for which 84 percent of the sediment mixture is finer. Data ranged from 1.5 to 250 mm.

(2) Data were from relatively wide, straight streams having a simple trapezoidal shape and no overbank flow. There was very little increase in width with depth, and the banks were stable. Irregularity was minimal. The amount of vegetation on the bed and banks was negligible.

(3) Grain sizes in Limerinos's data ranged from very coarse sand to large cobbles. The objective was to select field sites at which the bed forms would not change with flow hydraulics during the measurement. Consequently, it follows that this equation is applicable to gravel/cobble bed streams and to bed regimes similar to those found in such streams.

(4) N values predicted with the Limerinos equation are sufficiently larger than those predicted by the Strickler equation to indicate that some loss other than grain roughness must have been present. However, the Limerinos equation is not applicable to lower regime flow nor does it forecast the transition between upper and lower regimes.

(5) Burkham and Dawdy (1976) showed the Limerinos equation could be used in sand bed streams provided the regime was plain bed. In that analysis they

*

* extended the range of the relative roughness parameter as follows:

$$600 < \frac{R}{d_{84}} < 10,000$$

k. *Comparison of Strickler and Limerinos n values.*

(1) Table 5-6 shows n values calculated by the Strickler and the Limerinos equations. For a hydraulic radius of 1 ft, the Limerinos values are higher than Strickler's by 15 to 57 percent.

(2) Furthermore, for k_s up to about 10 mm the Limerinos n values increase with depth, which is the same trend as seen in the Keulegan n values in Table 5-5. However, the Limerinos n values are larger than Keulegan's by 7 to 52 percent. These consistent differences lead one to suspect some bed irregularities in Limerinos' field data in addition to grain roughness.

(3) Arcement and Schneider (1989, p 6) state, "If a measured d_{84} is available or can be estimated, [Limerinos] may be used to obtain a base n for sand channels in lieu of using Table 1." However, n values calculated by Limerinos, shown in Table 5-6 herein, are considerably smaller than the values shown in Table 1 of Arcement and Schneider even though they state their Table 1 is for upper regime flow.

l. *The Brownlie bed-roughness predictor, mobile bed.*

(1) In sediment transport calculations it is important to link n values to the bed regime. This is particularly true when hydraulic conditions shift between upper regime and lower regime flow. There are several methods in Vanoni (1975) that express n value in terms of sediment parameters, but Brownlie (1983) is the only method that calculates the transition. This method post-dates Vanoni (1975).

(2) Brownlie sought to reconstitute the most fundamental process--the discontinuity in the graph of hydraulic radius versus velocity (Figure 5-4). In the process of this research, he collected the known sediment data sets--77 in all, containing 7,027 data points. Of the total, 75 percent were from flume studies and 25 percent from field tests. He used 22 of these data sets and demonstrated a significant agreement with both field and laboratory data.

(3) Brownlie's basic equations were modified for SAM to display bed roughness as a coefficient times the grain roughness.

$$n = [\text{BED FORM ROUGHNESS}] \times [\text{STRICKLER GRAIN ROUGHNESS}] \quad (5-14)$$

Table 5-6
n Values Calculated by Strickler and Limerinos Equations

Effective Roughness		Strickler $n = 0.034 \cdot k_s^{1/6}$	Limerinos Equation R, ft				
k_s , mm	k_s , ft		1	5	10	20	50
0.10	0.0003281	0.009	0.011	0.013	0.013	0.014	0.015
1.00	0.003281	0.013	0.015	0.016	0.017	0.017	0.019
2.13	0.007	0.015	0.017	0.018	0.018	0.019	0.020
10	0.03281	0.019	0.022	0.022	0.022	0.023	0.024
64	0.20997	0.026	0.037	0.031	0.030	0.030	0.030
100	0.3281	0.028	0.044	0.034	0.033	0.032	0.032
152.4	0.5	0.030	0.053	0.038	0.036	0.035	0.034

Note:

$$\text{Limerinos Equation: } n = \frac{0.0926 R^{1/6}}{1.16 + 2 \cdot \log(R/k)}$$

*

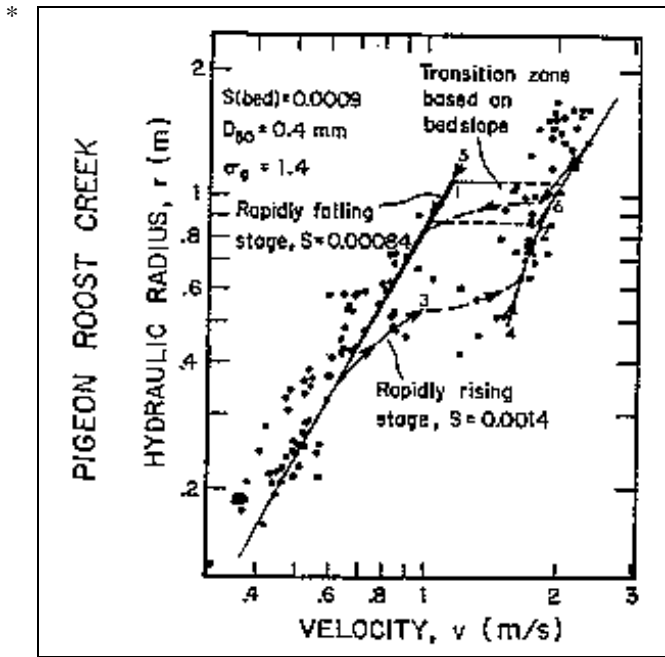


Figure 5-4. Velocity versus hydraulic radius in a mobile bed stream (courtesy of W. M. Keck Laboratories of Hydraulics and Water Resources (Brownlie 1981))

This makes it easy to compare the results with the skin friction for fixed bed systems as presented in Plate 3. The resulting forms of the equations for lower and upper regimes are as follows:

(a) Lower regime flow:

$$n = \left[1.6940 \left(\frac{R}{d_{50}} \right)^{0.1374} S^{0.1112} \sigma^{0.1605} \right] 0.034 (d_{50})^{0.167} \quad (5-15)$$

(b) Upper regime flow:

$$n = \left[1.0213 \left(\frac{R}{d_{50}} \right)^{0.0662} S^{0.0395} \sigma^{0.1282} \right] 0.034 (d_{50})^{0.167} \quad (5-16)$$

where

R = hydraulic radius, ft, of the bed portion of the cross section

d_{50} = the particle size, ft, for which 50 percent of the sediment mixture is finer

S = bed slope. Probably the energy slope will be more representative if flow is nonuniform.

σ = the geometric standard deviation of the sediment mixture (is shown as σ_g in Figure 5-4)

$$\sigma = 0.5 \left(\frac{d_{84}}{d_{50}} + \frac{d_{50}}{d_{16}} \right) \quad (5-17)$$

(c) Transition function: If the slope is greater than 0.006, flow is always upper regime. Otherwise, the transition is correlated with the grain Froude number as follows:

$$F_g = \frac{V}{\sqrt{(s_s - 1) g d_{50}}} \quad (5-18)$$

$$F'_g = \frac{1.74}{S^{1/3}} \quad (5-19)$$

If $F_g \leq F'_g$, then lower regime flow

If $F_g > F'_g$, then upper regime flow

where

F_g = grain Froude number

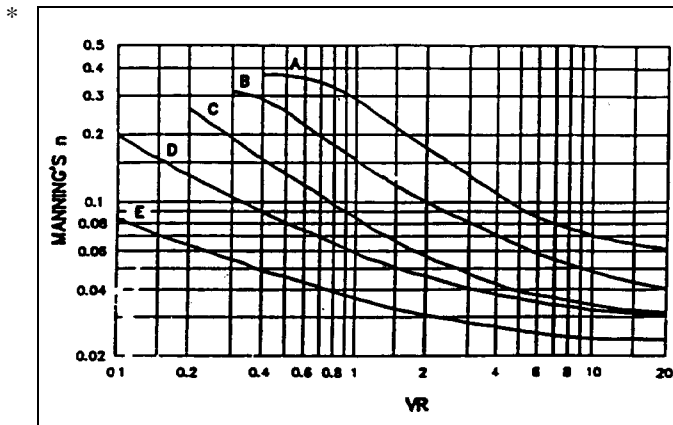
V = velocity of flow

s_s = specific gravity of sediment particles

The transition occurs over a range of hydraulic radii and not at a point. Over this range, then, it is a double-valued function, and the transition test will give different regimes depending on which equation is being solved for roughness at that iteration. That is realistic since one expects the rising side of a hydrograph to trigger the transition at a different discharge than does the falling side.

m. Soil Conservation Service (SCS) n values, grass cover. Hydraulic roughness curves for five types of grass cover were published by SCS (US Department of Agriculture 1947) (Figure 5-5). Each curve type, A

*

Figure 5-5. *n* value relationships for grass cover

through E, refers to grass conditions described in Table 5-7.

n. Example. To use analytical methods, the engineer is faced with assigning physically based parameters, like surface roughness or material type, to each subdivided area in a cross section. The subdivided areas are bounded by vertical lines between successive coordinate points on the boundary and the water surface. Table 5-8 illustrates the development of *n* values for the cross section in Figure 5-1 by the application of analytical equations. The analytical methods are in the Hydraulic Design Package SAM. The cross section is coded as station and elevation starting at the levee on the left, Area 1.

Table 5-7
Characteristics of Grass Cover

Type	Cover	Condition
A	Weeping love grass Yellow bluestem (<i>Andropogon ischaemum</i>)	Excellent stand, tall (average 30 in.) Excellent stand, tall (average 36 in.)
B	Kudzu Bermuda grass Native grass mixture (little bluestem, blue grama, other long and short midwest grasses) Weeping love grass Lespedeza sericea Alfalfa Weeping love grass Kudzu Blue grama	Very dense growth, uncut Good stand, tall (average 12 in.) Good stand, unmowed Good stand, tall (average 24 in.) Good stand, not woody, tall (average 19 in.) Good stand, uncut (average 11 in.) Good stand, mowed (average 13 in.) Dense growth, uncut Good stand, uncut (average 13 in.)
C	Crabgrass Bermuda grass Common lespedeza Grass-legume mixture--summer (orchard grass, redtop, Italian ryegrass, and common lespedeza) Centipede grass Kentucky bluegrass	Fair stand, uncut (10 to 48 in.) Good stand, mowed Good stand, uncut (average 11 in.) Good stand, uncut (6 to 8 in.) Very dense cover (average 6 in.) Good stand, headed (6 to 12 in.)
D	Bermuda grass Common lespedeza Buffalo grass Grass-legume mixture--fall, spring (orchard grass, redtop, Italian ryegrass, and common lespedeza) Lespedeza sericea	Good stand, cut to 2.5-in. height Excellent stand, uncut (average 4.5 in.) Good stand, uncut (3 to 6 in.) Good stand, uncut (4 to 5 in.) After cutting to 2-in. height; very good stand before cutting
E	Bermuda grass Bermuda grass	Good stand, cut to 1.5-in. height Burned stubble

*

*

Table 5-8
Hydraulic Roughness from Surface Properties

Area No.	Station	Elevation	n Value	k_s , ft	Comment
1	0.0	18.00			Grass D: Bermuda grass cut to 2.5 in. From Soil Conservation Service (Chow 1959, pp 179-184)
2	50.0	5.50	0.100		Left Floodplain, (USDT (Arcement and Schneider 1989), Table 3) $n = (n_0 + n_1 + n_2 + n_3 + n_4)$ $= (0.028 + 0.010 + 0.012 + 0.050)$
3	125.0	2.00		1	Strickler k_s -ft; Assumed (Chow, p 206)
4	129.0	0.00			Brownlie bed roughness equations (Brownlie 1983) $D_{84} = 6.5$ mm, $D_{50} = 1.7$ mm, $D_{16} = 0.4$ mm
5	154.0	0.00		1	Same as left bank (Area 3)
6	158.0	2.00	0.125		Right Floodplain, (USDT (Arcement and Schneider 1989), Table 3) $n = (0.028 + 0.010 + 0.012 + 0.075)$
7	168.0	5.50			Same as left levee (Area 1)
	218.0	18.00			

(1) Area 1 is designed to be a mowed grass surface. The n value will depend on the flow depth and velocity over the panel.

(2) Area 2 is the left floodplain. The best source for n values in large, woody vegetation is the USDT procedure, referenced in Table 5-2. Therefore, that n value will be coded directly.

(3) Area 3 is the left bank of the channel. Roughness will be calculated by estimating a surface irregularity k_s for the bank line to be 1 ft.

(4) For Area 4, the channel bed roughness will be calculated from the bed sediment gradation using the Brownlie bed roughness equations. That method predicts whether the roughness is lower or upper regime. It uses the d_{84} , d_{50} , and d_{16} grain sizes of the bed surface.

(5) Area 5 is the right bank. It will be the same as the left bank.

(6) Area 6 is expected to have a more dense stand of vegetation than on the left side.

(7) Area 7, the right levee, will be the same as the left levee.

5-6. Composite n Values and Hydraulic Radius

The calculations that transform the complex geometry and roughness into representative one-dimensional hydraulic parameters for flow depth calculations are called compositing hydraulic parameters. That is, in a complex cross section the composite hydraulic radius includes, in addition to the usual geometric element property, the variation of both depth and n values. There are several methods in the literature for compositing. The Alpha method, described in Appendix C, was selected as the default for SAM. Two other methods are provided as options: equal velocity and sum of forces.

a. Equal velocity method. Cox (1973) tested three methods for determining the equivalent roughness in a rectangular channel: the equal velocity method, which is sometimes called the Horton or the Einstein method after the developers; the Los Angeles District method; and the Colbatch method.

*

- * (1) Perhaps a more rational method for vertical walls is the equal velocity method. It was proposed independently by Horton and by Einstein (Chow 1959), and is one which prevents dividing by zero.

$$\bar{n} = \frac{(p_1 n_1^{1.5} + p_2 n_2^{1.5} + \dots + p_N n_N^{1.5})^{2/3}}{P^{2/3}} \quad (5-20)$$

where

\bar{n} = the composite n value for the section

p_N = wetted perimeter in subdivided area n

n_N = n value in subdivided area n

N = the last subdivided area in the cross section

P = total wetted perimeter in the cross section

Since only wetted perimeter, and not hydraulic radius, appears in this equation, it is always well behaved.

(2) The equations for the Los Angeles District (Equation 5-21) and Colbatch (Equation 5-22) methods (Figure 5-6) are as follows:

$$\bar{n} = \frac{(a_1 n_1 + a_2 n_2 + \dots + a_N n_N)}{A} \quad (5-21)$$

$$\bar{n} = \frac{(a_1 n_1^{1.5} + a_2 n_2^{1.5} + \dots + a_N n_N^{1.5})^{2/3}}{A^{2/3}} \quad (5-22)$$

where

a_N = end area associated with subdivided area n

A = total area in cross section

As a result of these experiments, Cox concluded that Horton's method was not as accurate as the Los Angeles District method or the Colbatch method. Based on one of Cox's figures, the Horton method gave a composite n value as much as 8 percent higher than measured for the combination of rough walls and a smooth bed. One test, a combination of smooth walls and a rough bed, gave an effective n value about 4 percent lower than measured.

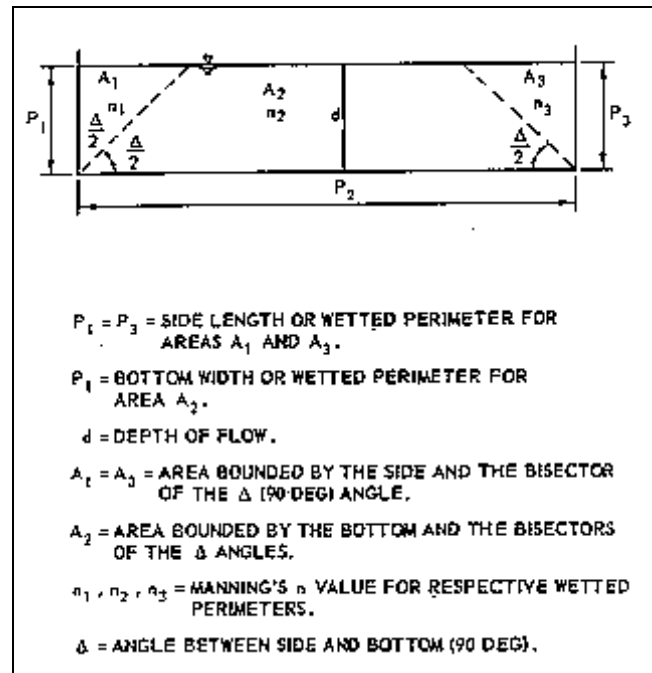


Figure 5-6. Definition sketch for Los Angeles District and Colbatch methods

(3) Horton's method is retained here because of its simplicity. It is adequate for the simple cross-section shapes, and it is programmable for the complex cross-section shapes. The other methods that Cox tested would be very difficult to program for automatic computations in complex cross sections.

b. Alpha method.

(1) The Chezy equation forms the basis for this method. The cross section is subdivided into areas between coordinate points.

(2) Calculations always begin at the first area in the cross section, and the geometric properties are calculated and saved for each wet area across the section. The hydraulic radius and Chezy C are then calculated and the compositing parameters summed. Computations move area by area to the end of the cross section.

(3) The alpha method fails when there is a vertical wall.

(4) James and Brown reported that the "Manning or Chezy equations do not accurately predict the stage-discharge relation in a channel-floodplain configuration for shallow depths on the floodplain ($1.0 < Y/D < 1.4$;

*

* where Y = main channel depth and D = main channel bank full depth) without adjustments to either the resistance coefficient or the hydraulic radius.... the effects of geometry seem to disappear at the higher stages, i.e., for Y/D > 1.4, it no longer became necessary to make any correction to the basic equations” (James and Brown 1977, p 24).

c. *Sum of forces method.* This method was proposed by Pavlovskii, by Muhlhofer, and by Einstein and Banks (Chow 1959). It is based on the hypothesis that the total force resisting the flow is equal to the sum of the forces resisting the flow in each area. The resulting composite n value is

$$\bar{n} = \frac{\sqrt{P_1 n_1^2 + P_2 n_2^2 + \dots + P_N n_N^2}}{P^{1/2}} \quad (5-23)$$

d. *Conveyance method.* The traditional approach to compositing by the conveyance method requires the cross section to be subdivided into subsections between channel and overbanks. Conveyance is calculated for each subsection as follows:

$$K_i = \frac{1.486 A_i R_i^{2/3}}{n_i} \quad (5-24)$$

where

K_i = conveyance in subsection i

A_i = end area of subsection i

R_i = hydraulic radius in subsection i

n_i = n value in subsection i

The composite n value is calculated from the total conveyance and the hydraulic radius as follows:

$$\bar{n} = \frac{1.486 AR^{2/3}}{K} \quad (5-25)$$

where

A = total end area of cross section

R = hydraulic radius for the entire cross section

$$= A/P$$

$$K = \text{total conveyance of cross section} = K_1 + K_2 + \dots + K_n$$

e. *Example.* Flow depth calculations using n values calculated by the analytical methods are shown in Tables 5-9 through 5-11. Note the column headed “ n_i value” in Table 5-10. The value for each area is shown, and at the bottom of that column the composited value for the entire cross section is 0.062. Table 5-11 shows the equivalent n value for the conveyance method to be 0.051. It is important not to mix n values determined by different compositing methods.

5-7. Expansion and Contraction in a 1-D Model

If the handbook approach is used, the expansion and contraction losses are included in the n_2 term. That is the contribution from variation in cross sections. Therefore, if contraction and expansion coefficients are being used, leave that term out.

If the analytical methods are used, no terms for expansion or contraction will be included. They would have to be added separately--perhaps by increasing the k_s value. Values from the n_2 component in the handbook method would be appropriate. They would have to be included in k_s .

5-8. Unforeseen Factors

a. *Seasonality.* This affects water temperature and vegetation. Both can cause significant changes in n value.

b. *Tubeworms and barnacles.* The Corps built a concrete channel in Corte Madera Creek only to find that marine creatures called tubeworms were attracted to it. They create a substantial increase in the surface roughness in the zone below sea level. Rather than the usual k_s of 0.007 ft, WES estimated the zone with the tubeworms had a k_s of 0.08 ft (Copeland and Thomas 1989).

c. *Roughness from gravel moving in a concrete channel.* In recent experiments at WES, gravel movement was modeled along a hard bottom flume to determine how much the n value would increase (Stonestreet, Copeland, and McVan 1991). As long as it moved, the increase was only about 10 percent. That was the case for concentrations up to about 3,000 ppm. When the concentration exceeded that, bed deposits began to form. That effect on

*

*

Table 5-9
Water Surface Elevations Using the Alpha Method
Normal Depth Using Composite Properties by Alpha Method

****	N	Discharge cfs	Water Surface Elevation ft	Top Width ft	Composite R ft	Slope ft/ft	Composite n Value	Velocity fps	Froude Number	Boundary Shear Stress psf
****	1	2,300.00	9.58	150.6	7.77	0.000800	0.0621	2.64	0.17	0.39

Table 5-10
Water Surface Elevations Using the Alpha Method
Flow Distribution by Alpha Method, Discharge = 2,300.00 cfs

Station	Percentage Increase Discharge	Area A_i sq ft	Wetted Perimeter p_i ft	$R_i =$ A_i/p_i	k_s ft	n_i Value	Velocity fps
0.0	3.06	33.2	16.8	1.98	1.179	0.0312	2.11
50.0	25.74	437.0	75.1	5.82	624.9	0.1000	1.35
125.0	7.10	34.3	4.5	7.67	1.000	0.0342	4.76
129.0	51.31	239.4	25.0	9.58	4.563	0.0383	4.93
154.0	7.10	34.3	4.5	7.67	1.000	0.0342	4.76
158.0	2.64	58.3	10.6	5.50	2,384.0	0.1250	1.04
168.0	3.06	33.2	16.8	1.98	1.179	0.0312	2.11
218.0							
	100.00	869.9	153.2	7.77	18.59	0.0621	2.64

Table 5-11
Water Surface Elevations Using the Alpha Method
Equivalent Hydraulic Properties using Conveyance Method

Hydraulic Radius Velocity ft	Manning's n Value	Discharge cfs	Subsection Area sq ft	Velocity fps
5.68	0.0506	2300.00	869.86	2.64

*

* n value is very significant and requires a sedimentation investigation.

d. Bed form roughness in concrete channels. After the Corte Madera Creek channel went into operation, sediment deposited over the smooth concrete bed in the downstream portion. A sedimentation study was conducted, after the fact, using HEC-6 (Copeland and Thomas 1989). They determined the channel n value to be 0.028 using high-water marks and the known water discharge. The calculated depth and gradation of bed deposits matched prototype values very nicely. This n value is not suggested as a design value. It is presented to illustrate surprises that can come from a fixed-bed hydraulic approach.

e. Large woody debris. Large woody debris refers to downed trees and log jams. This is a condition that exists, but its effect on the hydraulic roughness during large floods is not well documented.

f. Wetlands. Measurements by the South Florida Water Management District in connection with the restoration of the Kissimmee River produced n values of 1.011. That coincided with flow depths below the top of the marsh vegetation. They chose to use an n value of 0.3 for the levee design calculations because the flow depth was considerably above the top of the dense marsh vegetation. However, that was judgment rather than experiment. (Once flow depth exceeds the top of vegetation, it seems reasonable to reduce n values.)

g. Marsh. Studies for a flood at Kawanui Marsh, Hawaii, resulted in an n value of 0.95. That is attributed to a dense vine that was growing on the water surface. It was attached to the bed from place to place, but when the flood occurred, it piled the vine into accordion-like folds. Subsequent measurements, on smaller floods, were used to develop the n value.

*

Appendix A References

A-1. Required Publications

National Environmental Policy Act
National Environmental Policy Act (NEPA), PL 9-190,
Section 102(2)(c), 1 Jan 1970, 83 Stat 853.

ER 1110-1-8100

Laboratory Investigations and Materials Testing

ER 1110-2-1150

Engineering After Feasibility Studies, Ch 1

ER 1110-2-1402

Hydrologic Investigation Requirements for Water Quality
Control

ER 1110-2-1405

Hydraulic Design for Local Flood Protection Projects

ER 1110-2-2901

Construction Cofferdams

EM 1110-2-1205

Environmental Engineering for Local Flood Control
Channels

EM 1110-2-1409

Backwater Curves in River Channels, Ch 1

EM 1110-2-1602

Hydraulic Design of Reservoir Outlet Works

EM 1110-2-1603

Hydraulic Design of Spillways

EM 1110-2-1612

Ice Engineering, Ch 1

EM 1110-2-1901

Seepage Analysis and Control for Dams

EM 1110-2-2302

Construction with Large Stone

EM 1110-2-4000

Sedimentation Investigations of Rivers and Reservoirs

Hydraulic Design Criteria (HDC) sheets and charts avail-
able from US Army Engineer Waterways Experiment

Station, ATTN: CEWES-IM-MI-S, 3909 Halls Ferry
Road, Vicksburg, MS 39180-6199. A fee of \$10 is
charged non-Government requestors.

- * Conversationally Oriented Real-Time Programming Sys-
tem (CORPS) computer programs available from
US Army Engineer Waterways Experiment Station,
ATTN: CEWES-IM-DS, 3909 Halls Ferry Road,
Vicksburg, MS 39180-6199, for several US Army Corps
of Engineers computer systems.

A-2. Related Publications

Note: References used in this EM are available on
interlibrary loan from the Research Library, ATTN:
CEWES-IM-MI-R, US Army Engineer Waterways Exper-
iment Station, 3909 Halls Ferry Road, Vicksburg, MS
39180-6199.

Abt et al. 1988

Abt, S. R., Wittler, R. J., Ruff, J. F., LaGrone, D. L.,
Khattak, M. S., Nelson, J. D., Hinkle, N. E., and Lee, D.
W. 1988 (Sep). "Development of Riprap Design Criteria
by Riprap Testing in Flumes: Phase II; Followup Investi-
gations," Vol 2, NUREG/CR-4651, ORNL/TM-10100/V2,
prepared for US Nuclear Regulatory Commission,
Washington, DC.

American Society of Civil Engineers 1942

American Society of Civil Engineers. 1942. "Hydraulic
Models," Manuals of Engineering Practice No. 25,
New York.

American Society of Mechanical Engineers 1958

American Society of Mechanical Engineers. 1958.
"American Standard Letter Symbols for Hydraulics," ASA
Y10.2-1958, New York.

Apmann 1972

Apmann, R. P. 1972 (May). "Flow Processes in Open
Channel Bends," *Journal of the Hydraulics Division,
American Society of Civil Engineers*, Vol 98, HY5, Pro-
ceedings Paper 8886, pp 795-810.

- * **Arcement and Schneider 1989**

Arcement, George J., Jr., and Schneider, Verne R. 1989.
"Guide for Selecting Manning's Roughness Coefficients
for Natural Channels and Flood Plains," US Geological
Survey, Water-Supply Paper 2339, Department of the
Interior, US Geological Survey, prepared in cooperation
with US Department of Transportation, Federal Highway
Administration, for sale by Books and Open-File Reports
Section, Federal Center, Box 25425, Denver, CO 80225. *

Bagnold 1960

Bagnold, Ralph A. 1960. "Some Aspects of the Shape of River Meanders," Geological Survey Professional Paper 282-E, US Government Printing Office, Washington, DC.

Bakhmeteff and Matzke 1936

Bakhmeteff, Boris A., and Matzke, Arthur E. 1936. "The Hydraulic Jump in Terms of Dynamic Similarity," *Transactions, American Society of Civil Engineers*, Vol 101, Paper No. 1935, pp 630-680.

* **Barnes 1967**

Barnes, Harry H., Jr. 1967. "Roughness Characteristics of Natural Channels," US Geological Survey Water-Supply Paper 1849, US Government Printing Office, Washington, DC. *

Behlke and Pritchett 1966

Behlke, Charles E., and Pritchett, Harold D. 1966. "The Design of Supercritical Flow Channel Junctions," Highway Research Record No. 123, Highway Research Board, National Research Council, Washington, DC. *

* **Bernard 1993**

Bernard, Robert S. 1993. "STREMR; Numerical Model for Depth-Averaged Incompressible Flow," Technical Report REMR-HY-11, US Army Engineer Waterways Experiment Station, Vicksburg, MS. *

Blue and Shulits (1964)

Blue, F. L., and Shulits, Sam. 1964 (Dec). "Open-Channel Transitions in Supercritical Flow," Hydraulic Laboratory Bulletin, Department of Civil Engineering, Pennsylvania State University, University Park, PA. (See also Blue, F. L., Jr., and Rajagopal, H. Y. 1969 (Apr). "Open-Channel Transitions in Supercritical Flow," Engineering Research Bulletin B-98, Pennsylvania State University, University Park, PA.)

Bowers 1950

Bowers, Charles E. 1950 (Jan). "Hydraulic Model Studies for Whiting Field Naval Air Station, Part V: Studies of Open-Channel Junctions," Project Report No. 24, St. Anthony Falls Hydraulic Laboratory, Minneapolis, MN.

Bradley 1978

Bradley, Joseph N. 1978. "Hydraulics of Bridge Waterways," Hydraulic Design Series No. 1, 2d ed., US Department of Transportation, Federal Highway Administration, Washington, DC.

Bradley and Peterka 1957

Bradley, J. N., and Peterka, A. J. 1957 (Oct). "The Hydraulic Design of Stilling Basins: Hydraulic Jumps on a Horizontal Apron (Basin I)," *Journal of the Hydraulics Division, American Society of Civil Engineers*, Vol 83, Paper No. 1401, HY5, pp 1401-1 through 1401-24.

Brater and King 1976

Brater, Ernest F., and King, Horace William. 1976. *Handbook of Hydraulics for the Solution of Hydraulic Engineering Problems*, 6th ed., McGraw-Hill, New York.

* **Brownlie 1981**

Brownlie, William R. 1981. "Prediction of Flow Depth and Sediment Discharge in Open Channels," Report No. KH-R-43A, California Institute of Technology, W. M. Keck Laboratories of Hydraulics and Water Resources, Pasadena, CA. *

* **Brownlie 1983**

Brownlie, William R. 1983 (Jul). "Flow Depth in Sand-Bed Channels," *Journal of Hydraulic Engineering, American Society of Civil Engineers*, Vol 109, No. 7, pp 959-990. *

* **Burkham and Dawdy 1976**

Burkham, Durl E., and Dawdy, David R. 1976 (Oct). "Resistance Equation for Alluvial Channel Flow," *Journal of the Hydraulics Division, American Society of Civil Engineers*, pp 1479-1489. *

Carlson and Miller 1956

Carlson, Enos J., and Miller, Carl R. 1956 (Apr). "Research Needs in Sediment Hydraulics," *Journal of the Hydraulics Division, American Society of Civil Engineers*, Vol 82, Paper No. 953, HY2, pp 953-1 through 953-33.

Carter, Carlson, and Lane 1953

Carter, A. C., Carlson, E. J., and Lane, E. W. 1953. "Critical Tractive Forces on Channel Side Slopes in Coarse, Non-Cohesive Material," Hydraulic Laboratory Report No. HYD-366, US Bureau of Reclamation, Denver, CO.

Chow 1959

Chow, Ven Te. 1959. *Open Channel Hydraulics*, McGraw-Hill, New York.

Chien 1956

Chien, Ning. 1956. "The Present Status of Research on Sediment Transport," *Transactions, American Society of Civil Engineers*, Vol 121, Paper No. 2824, pp 833-868.

Colby 1964a

Colby, Bruce R. 1964a. "Discharge of Sands and Mean-Velocity Relationships in Sand-Bed Streams: Sediment Transport in Alluvial Channels," Geological Survey Professional Paper 462-A, US Department of Interior, US Government Printing Office, Washington, DC.

Colby 1964b

Colby, Bruce R. 1964b (Mar). "Practical Computations of Bed-Material Discharge," *Journal of the Hydraulics Division, American Society of Civil Engineers*, Vol 90, Paper No. 3843, pp 217-246.

* **Copeland and Thomas 1989**

Copeland, Ronald R., and Thomas, William A. 1989 (Apr). "Corte Madera Creek Numerical Sedimentation Study," Technical Report HL-89-6, US Army Engineer Waterways Experiment Station, Vicksburg, MS. *

* **Cox 1973**

Cox, R. G. 1973 (Feb). "Effective Hydraulic Roughness for Channels Having Bed Roughness Different from Bank Roughness," Miscellaneous Paper H-73-2, US Army Engineer Waterways Experiment Station, Vicksburg, MS. *

Davis and Sorenson 1969

Davis, Calvin Victor, and Sorenson, Kenneth E., eds. 1969. *Handbook of Applied Hydraulics*, 3d ed., McGraw-Hill, New York.

Dodge 1948

Dodge, B. H. 1948 (Jan). "Design and Operation of Debris Basins," *Proceedings, Federal Inter-Agency Sedimentation Conference*, Denver, CO, 6-8 May 1947, US Department of the Interior, Bureau of Reclamation, Washington, DC, pp 274-301.

Escoffier and Boyd 1962

Escoffier, Francis F., and Boyd, Marden B. 1962 (Nov). "Stability Aspects of Flow in Open Channels," *Journal of the Hydraulics Division, American Society of Civil Engineers*, Vol 88, Paper No. 3331, HY6, pp 145-166. (See also "Types of Flow in Open Channels," Miscellaneous Paper No. 2-498, June 1962, US Army Engineer Waterways Experiment Station. Essentially the same paper except design graphs are included to a larger scale.)

Ferrell and Barr 1963

Ferrell, W. R., and Barr, W. R. 1963 (Jan). "Criteria and Methods for Use of Check Dams in Stabilizing Channel Banks and Beds," *Proceedings, Federal Inter-Agency*

Sedimentation Conference, Jackson, MS, 28 January-1 February 1963, US Department of Agriculture, Agriculture Research Service Miscellaneous Publication No. 970, Paper No. 44, pp 376-386.

Fortier and Scobey 1926

Fortier, Samuel, and Scobey, Fred C. 1926. "Permissible Canal Velocities," *Transactions, American Society of Civil Engineers*, Vol 89, Paper No. 1588, pp 940-984.

Galay, Yaremko, and Quazi 1987

Galay, V. J., Yaremko, E. K., and Quazi, M. E. 1987. "River Bed Scour and Construction of Stone Riprap Protection," *Sediment Transport in Gravel-bed Rivers*, edited by Thorne, Bathurst, and Hey, Wiley, New York, pp 353-383.

Gildea 1963

Gildea, A. P. 1963 (Jan). "Design Practice for Levee Revetment on West Coast Intermittent Streams," *Proceedings, Federal Inter-Agency Sedimentation Conference*, Jackson, MS, 28 January-1 February 1963, US Department of Agriculture, Agriculture Research Service Miscellaneous Publication No. 970, Paper No. 57, 492-507.

Gildea and Wong 1967

Gildea, Albert P., and Wong, Ralph F. 1967. "Flood Control Channel Hydraulics," *Proceedings, Twelfth Congress of the International Association for Hydraulic Research*, 11-14 September 1967, Fort Collins, CO, Vol 1, pp 330-337.

Gumensky 1949

Gumensky, D. B. 1949 (Dec). "Air Entrained in Fast Water Affects Design of Training Walls and Stilling Basins," *Civil Engineering*, Vol 19, No. 12, pp 35-37, 93.

Hall 1943

Hall, L. Standish. 1943. "Open Channel Flow at High Velocities," *Transactions, American Society of Civil Engineers*, Vol 108, Paper No. 2205, pp 1394-1434.

Ippen 1950

Ippen, A. T. 1950. "Channel Transitions and Controls," *Engineering Hydraulics, Proceedings of the Fourth Hydraulics Conference*, Iowa Institute of Hydraulic Research, 12-15 June 1949, edited by H. Rouse, Wiley, New York, Chapter VIII, pp 496-588.

Ippen 1951

Ippen, Arthur T. 1951. "Mechanics of Supercritical Flow," *Transactions, American Society of Civil Engineers*, Vol 116, pp 268-295.

* **Ippen and Dawson 1951**

Ippen, Arthur T., and Dawson, John H. 1951. "Design of Channel Contractions," *Transactions, American Society of Civil Engineers*, Vol 116, pp 326-346.

Ippen and Harleman 1956

Ippen, Arthur T., and Harleman, Donald R. F. 1956. "Verification of Theory for Oblique Standing Waves," *Transactions, American Society of Civil Engineers*, Vol 121, Paper No. 2815, pp 678-694.

Isbash 1936

Isbash, S. V. 1936. "Construction of Dams by Depositing Rock in Running Water," *Transaction, Second Congress on Large Dams*, Vol 5, pp 123-126.

Jaeger 1957

Jaeger, Charles. 1957. *Engineering Fluid Mechanics*, St. Martin's Press, Inc., New York, (translated from the German by P. O. Wolf).

* **James and Brown 1977**

James, Maurice, and Brown, Bobby J. 1977 (Jun). "Geometric Parameters that Influence Floodplain Flow," Research Report H-77-1, US Army Engineer Waterways Experiment Station, Vicksburg, MS. *

Jones 1964

Jones, Llewellyn Edward. 1964 (May). "Some Observations on the Undular Jump," *Journal of the Hydraulics Division, American Society of Civil Engineers*, Vol 90, Paper No. 3901, HY3, pp 69-82.

Keulegan and Patterson 1940

Keulegan, Garbis H., and Patterson, George W. 1940 (Jan). "Mathematical Theory of Irrotational Translation Waves," *Journal of Research of the National Bureau of Standards*, Research Paper RP1272, Vol 24, No. 1, pp 47-101.

Koch 1926

Koch, A. 1926. *Von der Bewegung des Wassers und den dabei auftretenden Kräften*, M. Carstanjen, ed., Julius Springer, Berlin. *

Komura 1960

Komura, Saburo. 1960 (Mar). "Some Studies on the Hydraulic Jump and the Submerged Efflux," *Translation of the Japan Society of Civil Engineers*, No. 67, 27-34. English translation by the author available at the US Army Engineer Waterways Experiment Station, ATTN: Research Library, CEWES-IM-MI-R, 3909 Halls Ferry Road, Vicksburg, MS 39180-6199.

Lane 1955

Lane, Emory W. 1955. "Design of Stable Channels," *Transactions, American Society of Civil Engineers*, Vol 120, Paper No. 2776, pp 1234-1279.

Lane and Carlson 1953

Lane, E. W., and Carlson, E. J. 1953. "Some Factors Affecting the Stability of Canals Constructed in Coarse Granular Materials," *Proceedings, Minnesota International Hydraulics Convention*, Minneapolis, MN, 1-4 September 1953, pp 37-48.

Leliavsky 1955

Leliavsky, Serge. 1955. *An Introduction to Fluvial Hydraulics*, Constable and Company, London.

* **Limerinos 1970**

Limerinos, J. T. 1970. "Determination of the Manning Coefficient from Measured Bed Roughness in Natural Channels," Geological Survey Water-Supply Paper 1898-B, Prepared in cooperation with the California Department of Water Resources, US Government Printing Office, Washington, DC. *

Linder 1963

Linder, Walter M. 1963 (Jan). "Stabilization of Stream Beds with Sheet Piling and Rock Sills," *Proceedings, Federal Inter-Agency Sedimentation Conference*, Jackson, MS, 28 January-1 February 1963, US Department of Agriculture, Agriculture Research Service Miscellaneous Publication No. 970, Paper No. 55, pp 470-484.

Maynard 1988

Maynard, S. T. 1988 (Mar). "Stable Riprap Size for Open Channel Flows," Technical Report HL-88-4, US Army Engineer Waterways Experiment Station, Vicksburg, MS.

* **Maynard 1992**

Maynard, S. T. 1992. "Riprap Stability: Studies in Near-Prototype Size Laboratory Channel," Technical Report

HL-92-5, US Army Engineer Waterways Experiment Station, Vicksburg, Ms. *

* **Maynard 1993**

Maynard, S. T. 1993. "Flow Impingement, Snake River, Wyoming," Technical Report HL-93-9, US Army Engineer Waterways Experiment Station, Vicksburg, MS. *

McCormick 1948

McCormick, Charles W. B. 1948 (Jun). "Modified Spiral Curve Tables," US Army Engineer District, Los Angeles, Los Angeles, CA.

Moore, Wood, and Renfro 1960

Moore, Charles M., Wood, Walter J., and Renfro, Graham W. 1960 (Feb). "Trap Efficiency of Reservoirs, Debris Basins, and Debris Dams," *Journal of the Hydraulics Division, American Society of Civil Engineers*, Vol 86, Paper No. 2374, HY2, pp 69-87.

Neill 1973

Neill, C. R. 1973. "Guide to Bridge Hydraulics," Roads and Transportation Association of Canada, University of Toronto Press, Toronto, ON.

* **Petryk and Bosmajian 1975**

Petryk, Sylvester, and Bosmajian, George, III. 1975. "Analysis of Flow Through Vegetation," *Journal of the Hydraulics Division, American Society of Civil Engineers*, HY7, pp 871-884. *

Posey and Hsing 1938

Posey, C. J., and Hsing, P. S. 1938 (22 Dec). "Hydraulic Jump in Trapezoidal Channels," *Engineering News-Record*, Vol 121, No. 25, pp 797-798.

Raju 1937

Raju, S. P. 1937 (Nov). "Resistance to Flow in Curved Open Channels," *Abridged Translations of Hydraulic Papers, Proceedings, American Society of Civil Engineers*, Vol 63, No. 9, pp 49-55.

Rouse 1950

Rouse, Hunter, ed. 1950. *Engineering Hydraulics, Proceedings of the Fourth Hydraulics Conference*, Iowa Institute of Hydraulic Research, 12-15 June 1949, Wiley, New York. *

Rouse 1965

Rouse, Hunter. 1965 (Jul). "Critical Analysis of Open-Channel Resistance," *Journal of the Hydraulics Division, American Society of Civil Engineers*, Vol 91, Paper No. 4387, HY4, pp 1-25.

Rouse, Bhoota, and Hsu 1951

Rouse, Hunter, Bhoota, B. V., and Hsu, En-Yun. 1951. "Design of Channel Expansions," *Transactions, American Society of Civil Engineers*, Vol 116, pp 347-363.

Sandover and Zienkiewicz 1957

Sandover, J. A., and Zienkiewicz, O. C. 1957 (Nov). "Experiments on Surge Waves," *Water Power*, Vol 9, No. 11, pp 418-424.

Scobey 1933

Scobey, Fred C. 1933. "The Flow of Water in Flumes," Technical Bulletin No. 393, US Department of Agriculture, US Government Printing Office, Washington, DC.

Scobey 1939

Scobey, Fred C. 1939. "The Flow of Water in Irrigation and Similar Canals," Technical Bulletin No. 652, Washington, DC.

Shukry 1950

Shukry, Ahmed. 1950. "Flow Around Bends in an Open Flume," *Transactions, American Society of Civil Engineers*, Vol 115, pp 751-788.

Simons 1957

Simons, Daryl B. 1957 (Reprinted 1960). "Theory and Design of Stable Channels in Alluvial Materials," Report CER. No. 57DBS17, Colorado State University, Fort Collins, CO.

* **Simons and Richardson 1966**

Simons, D. B., and Richardson, E. V. 1966. "Resistance to Flow in Alluvial Channels," US Geological Survey Professional Paper 422-J, US Government Printing Office, Washington, DC. *

Soil Conservation Service 1954

Soil Conservation Service. 1954 (Jun). "Handbook of Channel Design for Soil and Water Conservation," SCS-TP-61, March 1947, revised June 1954, Stillwater Outdoor Hydraulic Laboratory, Stillwater, OK, US Department of Agriculture, Washington, DC.

Stonestreet, Copeland, and McVan 1991

Stonestreet, Scott E., Copeland, Ronald R., and McVan, Darla C. 1991 (Aug). "Bed Load Roughness in Supercritical Flow," *Hydraulic Engineering, Proceedings of the 1991 National Conference*, American Society of Civil Engineers, Nashville, TN, July 29-August 2, Richard M. Shane, ed., New York, pp 61-66. *

Straub and Anderson 1960

Straub, Lorenz C., and Anderson, Alvin G. 1960. "Self-Aerated Flow in Open Channels," *Transactions, American Society of Civil Engineers*, Vol 125, Paper No. 3029, pp 456-486.

Task Committee on Preparation of Sedimentation Manual 1966

Task Committee on Preparation of Sedimentation Manual. 1966 (Mar). "Sediment Transportation Mechanics: Initiation of Motion," *Journal of the Hydraulics Division, American Society of Civil Engineers*, Vol 92, Paper No. 4738, HY2, pp 291-314.

Tatum 1963

Tatum, F. E. 1963 (Jan). "A New Method of Estimating Debris-Storage Requirements for Debris Basins," *Proceedings, Federal Inter-Agency Sedimentation Conference*, Jackson, MS, 28 January-1 February 1963, US Department of Agriculture, Agriculture Research Service Miscellaneous Publication No. 970, Paper No. 89, pp 886-898.

Taylor 1944

Taylor, Edward H. 1944. "Flow Characteristics at Rectangular Open-Channel Junctions," *Transactions, American Society of Civil Engineers*, Vol 109, Paper No. 2223, pp 893-912.

Terrell and Borland 1958

Terrell, Pete W., and Borland, Whitney M. 1958. "Design of Stable Canals and Channels in Erodible Material," *Transactions, American Society of Civil Engineers*, Vol 123, Paper No. 2913, pp 101-115.

* **Thomas, Copeland, Raphael, and McComas (in preparation)**

Thomas, William A., Copeland, Ronald R., Raphael, Nolan K., and McComas, Dinah N. "Hydraulic Design Package for Channels (SAM), User Manual" (in preparation), US Army Engineer Waterways Experiment Station, Vicksburg, MS. *

Thorne 1989

Thorne, Colin R. 1989 (May). "Bank Processes on the Red River Between Index, Arkansas and Shreveport, Louisiana; Final Technical Report," European Research Office of the US Army, London, England.

Tilp and Scrivner 1964

Tilp, Paul J., and Scrivner, Mansil W. 1964 (Apr). "Analysis and Descriptions of Capacity Tests in Large

Concrete Lined Canals," Technical Memorandum No. - 661, US Department of Interior, Bureau of Reclamation, Denver, CO.

US Army Corps of Engineers 1981

US Army Corps of Engineers. 1981 (Dec). "Final Report to Congress, The Streambank Erosion Control Evaluation and Demonstration Act of 1974," Section 32, Public Law 93-251, Washington, DC.

US Army Engineer District, Los Angeles 1939

US Army Engineer District, Los Angeles. 1939 (May). "Report on Engineering Aspects, Flood of March, 1938; Appendix I, Theoretical and Observed Bridge Pier Losses," Los Angeles, CA.

US Army Engineer District, Los Angeles 1943

US Army Engineer District, Los Angeles. 1943 (Dec). "Hydraulic Model Study, Los Angeles River Channel Improvement, Dayton Avenue to Fourth Street, Los Angeles, California," Los Angeles, CA.

US Army Engineer District, Los Angeles 1947

US Army Engineer District, Los Angeles. 1947 (Jun). "Hydraulic Model Study, Los Angeles River Channel Improvement, Stewart and Gray Road to Pacific Electric Railway," Los Angeles, CA.

US Army Engineer District, Los Angeles 1949

US Army Engineer District, Los Angeles. 1949 (Jul). "Hydraulic Model Study, Los Angeles River Improvement, Whitsett Avenue to Tujunga Wash," Los Angeles, CA.

US Army Engineer District, Los Angeles 1950

US Army Engineer District, Los Angeles. 1950 (May). "Analysis of Design on Tujunga Wash Channel Improvement, Los Angeles River to Hansen Dam, Vanowen Street to Beachy Avenue," Los Angeles, CA.

US Army Engineer District, Los Angeles 1958

US Army Engineer District, Los Angeles. 1958 (May). "Transition Structure for North Diversion Channel, Albuquerque, New Mexico; Hydraulic Model Investigation," Report No. 1-102, Los Angeles, CA.

US Army Engineer District, Los Angeles 1960a

US Army Engineer District, Los Angeles. 1960a (Aug). "Inlet and Outlet Channels for Upper Rio Hondo Spreading Basin; Hydraulic Model Investigation," Report No. 1-103, Los Angeles, CA.

US Army Engineer District, Los Angeles 1960b

US Army Engineer District, Los Angeles. 1960b (Mar). "Typical Side Drains; Hydraulic Model Investigation," Report No. 2-101, Los Angeles, CA.

US Army Engineer District, Los Angeles 1961

US Army Engineer District, Los Angeles. 1961 (May). "Walnut Creek Inlet Channel; Hydraulic Model Investigation," Report No. 1-104, Los Angeles, CA.

US Army Engineer District, Los Angeles 1962

US Army Engineer District, Los Angeles. 1962 (Oct). "Transition for Chino Creek Channel; Hydraulic Model Investigation," Report No. 1-106, Los Angeles, CA.

US Army Engineer District, Los Angeles 1963

US Army Engineer District, Los Angeles. 1963 (Jun). "General Design for San Gabriel River, Whittier Narrows Dam to Coyote Creek," Design Memorandum No. 3, Los Angeles, CA.

US Army Engineer District, Los Angeles 1964

US Army Engineer District, Los Angeles. 1964 (Feb). "Walnut Creek Channel and Side Drains; Hydraulic Model Investigation," Report No. 2-104, Los Angeles, CA.

US Army Engineer District, Los Angeles 1972

US Army Engineer District, Los Angeles. 1972 (Mar). "Supercritical Flow in Curved Channels; Hydraulic Model Investigation," Report No. 1-109, Los Angeles, CA.

US Army Engineer District, Walla Walla 1960

US Army Engineer District, Walla Walla. 1960 (24 Jun). "Flood Control Improvement, Colfax, Washington, Palouse River and Tributaries, Washington," Design Memorandum No. 1, Walla Walla, WA.

* **US Army Engineer Hydrologic Engineering Center 1986**

US Army Engineer Hydrologic Engineering Center 1986 (Dec). "Accuracy of Computed Water Surface Profiles," Research Document 26, Prepared for the Federal Highway Administration by the Hydrologic Engineering Center, Davis, CA. *

* **US Army Engineer Hydrologic Engineering Center 1990**

US Army Engineer Hydrologic Engineering Center. 1990 (Sep). "HEC-2, Water Surface Profiles; Users Manual," Davis, CA. *

US Army Engineer Waterways Experiment Station 1949a

US Army Engineer Waterways Experiment Station. 1949a (Nov). "Flood-Control Project for Johnstown, Pennsylvania; Model Investigation," Technical Memorandum No. 2-303, Vicksburg, MS.

US Army Engineer Waterways Experiment Station 1949b

US Army Engineer Waterways Experiment Station. 1949b (Mar). "Flood Protection Plans for Brady, Texas; Model Investigation," Technical Memorandum No. 2-270, Vicksburg, MS.

US Army Engineer Waterways Experiment Station 1953

US Army Engineer Waterways Experiment Station. 1953 (Dec). "Flood-Control Project for Allentown, Pennsylvania; Hydraulic Model Investigation," Technical Memorandum No. 2-376, Vicksburg, MS.

US Army Engineer Waterways Experiment Station 1957

US Army Engineer Waterways Experiment Station. 1957 (Jan). "Flood Protection Plans for Cumberland, Maryland & Ridgeley, West Virginia; Hydraulic Model Investigation," Technical Report No. 2-448, Vicksburg, MS.

US Army Engineer Waterways Experiment Station 1962

US Army Engineer Waterways Experiment Station. 1962 (Jun). "Flood-Control Project, Hoosic River, North Adams, Massachusetts; Hydraulic Model Investigation," Technical Memorandum No. 2-338, Report 2, Vicksburg, MS.

US Bureau of Reclamation 1948

US Bureau of Reclamation. 1948. "Studies of Crests for Overfall Dams," Boulder Canyon Project Final Reports, Part VI, Hydraulic Investigations Bulletin 3, US Department of the Interior, Denver, CO.

US Bureau of Reclamation 1967

US Bureau of Reclamation. 1967. "General Design Information for Structures," Chapter 2, *Canals and Related Structures*, Design Standards No. 3, US Department of the Interior, Denver, CO.

US Department of Agriculture 1947

US Department of Agriculture. 1947 (Revised June 1954). "Handbook of Channel Design for Soil and Water

EM 1110-2-1601

Change 1

30 Jun 94

Conservation,” SCS-TP-61, prepared by Stillwater Outdoor Hydraulic Laboratory, Stillwater, OK, for Soil Conservation Service, Washington, DC. *

* **Vanoni 1975**

Vanoni, V. A., ed. (1975). “Sedimentation Engineering,” Manuals and Reports on Engineering Practice--No. 54, American Society of Civil Engineers, New York. *

Vanoni, Brooks, and Kennedy 1961

Vanoni, V. A., Brooks, N. H., and Kennedy, J. F. 1961 (Jan). “Lecture Notes on Sediment Transportation and Channel Stability,” Report No. KH-R-1, W. M. Keck Laboratory of Hydraulics and Water Resources, California Institute of Technology, Pasadena, CA.

Webber and Greated 1966

Webber, Norman Bruton, and Greated, Clive Alan. 1966 (Jul). “An Investigation of Flow Behaviour at the Junction of Rectangular Channels,” *Proceedings, The Institution of Civil Engineers*, Vol 34, Paper No. 6901, pp 321-334.

Winkel 1951

Winkel, Richard. 1951 (Dec). “Technical Possibilities of Guiding a Swift Current into Slowly Flowing Water with

a Minimum of Losses” (“Bautechnische Möglichkeiten, einen schnell fließenden Wasserstrom möglichst verlustfrei in langsam fließendes Wasser überzuleiten”), *Die Bautechnik*, Vol 28, No. 12, pp 309-310. Translation No. 53-2, March 1953, US Army Engineer Waterways Experiment Station, Vicksburg, MS.

Woodward 1920

Woodward, Sherman M. 1920. “Hydraulics of the Miami Flood Control Project,” Technical Reports, Part VII, The Miami Conservancy District, State of Ohio, Dayton, OH.

Woodward and Posey 1941

Woodward, Sherman M., and Posey, Chesley J. 1941. *Hydraulics of Steady Flow in Open Channels*, Wiley, New York.

Woolhiser and Lenz 1965

Woolhiser, David A., and Lenz, Arno T. 1965 (May). “Channel Gradients Above Gully-Control Structures,” *Journal of the Hydraulics Division, American Society of Civil Engineers*, Vol 91, Paper No. 4333, HY3, pp 165-187. *

Appendix B Plates

Plate No.	Title	Plate No.	Title
B-1	Cost Computations, Rectangular Concrete Channel	B-17	Rectangular Section, Energy Method, Class B Flow
B-2	Special Concrete Channel Cross Sections	B-18	Design for Bridge Pier Extension
B-3	Open Channel Flow, Resistance Coefficients	B-19	Transition Types
B-4	Open Channels, C-n-R-k Relation, $0.008 < n < 0.04$	B-20	Wedge-Type Transition Geometry
B-5	Open Channels, C-n-R-k Relation, $0.03 < n < 0.15$	B-21	Transitions, Rectangular Channels
B-6	Depth vs Specific Energy	B-22	Transition Design Curves, Rectangular Channels
B-7	Flow Stability vs Froude Number	B-23	Rectangular Transitions, Example of Design Computation
B-8	Varied Flow Profile, Standard Step Method, Sample Computation Using Manning's n	B-24	Expanding Transition, Rectangular Channel, Rapid Flow
B-9	Varied Flow Profile, Standard Step Method, Sample Computation Using k and Chezy C	B-25	Stilling Basin Transition
B-10	Classification of Flow Through Bridges	B-26	Roughness Control Transition
B-11	Classification of Flow Through Bridges, Rectangular Section	B-27	Bed-Load Discharge
B-12	Trapezoidal Section, Momentum Method, Example Curves	B-28	Gradation and Permissible Velocity
B-13	Momentum Method, Example Computations, Trapezoidal Section	B-29	Stone Stability, Velocity vs Stone Diameter
B-14	Rectangular Section, Energy Method, Class A Flow	B-30	Stone Stability, Velocity vs Stone Diameter
B-15	Rectangular Section, Energy Method, Sample Computation	B-31	Stone Weight vs Spherical Diameter
B-16	Rectangular Section, Momentum Method, Class B Flow	B-32	Riprap Gradation Curves
		B-33	Riprap Design Velocities
		B-34	Parameters Used in Stone Size Calculation

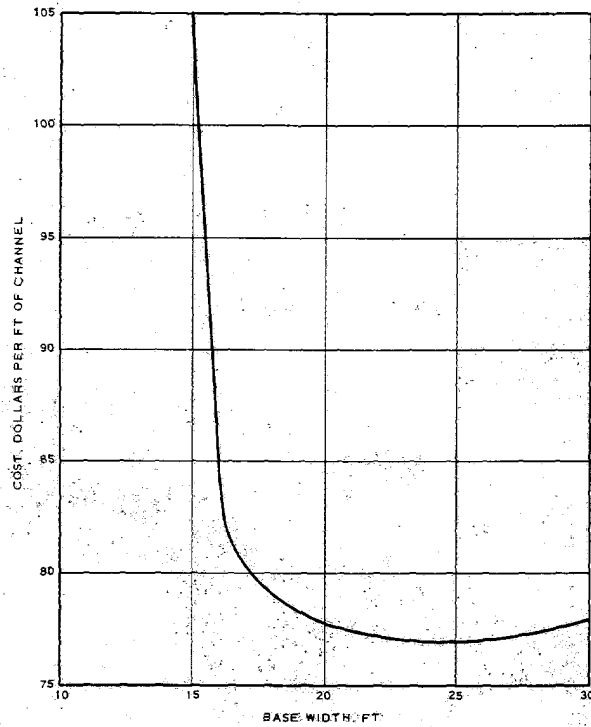
EM 1110-2-1601
1 Jul 91

<u>Plate No.</u>	<u>Title</u>	<u>Plate No.</u>	<u>Title</u>
B-35	Velocity Distribution in Trapezoidal Channel; Discharge 6.75 cfs, Depth 0.455 ft, 1V:2H Side Slopes	B-47	Sheet Piling Stabilizer, Energy Loss
B-36	Side Slope Velocity Distribution in Channel Bends	B-48	Details and Design Chart for Typical Drop Structure
B-37	Depth Averaged Velocity versus D_{30} and Depth	B-49	Debris Basin, Typical Design
B-38	Correction for Unit Stone Weight	B-50	Air Entrainment
B-39	Correction for Side Slope Angle	B-51	Hydraulic Jump Characteristics, Rectangular Channel
B-40	Correction for Vertical Velocity Distribution in Bend and Riprap Thickness	B-52	Undular Jump, Rectangular Channel
B-41	Riprap End Protection	B-53	Open Channel Confluence, Standing Waves-Rapid Flow
B-42	Scour Depth in Bends	B-54	Maximum Wave Height, Channel Junction
B-43	Revetment Toe Protection	B-55	Tapered Junction Walls
B-44	Rock Stabilizer	B-56	Typical Confluence Layouts, Rectangular Channels
B-45	Sheet Pile Stabilizer	B-57	Confluence Design Chart
B-46	Sheet Pile Stabilizer, Derrick Stone Size	B-58	Side Channel Spillway Inlet

WIDTH FT	d _n FT	AREA SQ FT	V _n FPS	Δy FT	AIR %	TOTAL FREE- WALL			COST PER FOOT, DOLLARS					
						DEPTH FT	BOARD FT	HEIGHT FT	EXCAVATION	CONCRETE	1/W BRIDGES	TOTAL		
REACH 1: STA 1098+00 TO STA 860+00; Q = 8000 CFS; n = 0.014; S = 0.03900; r _c = 6000														
10	15.6	156	51.3	0.14	10	17.3	2.0	19.3				1.00		
15	9.7	146	54.8	0.23	10	10.9	2.0	12.9	18.50	81.00	1.50	3.00	104.00	
20	7.3	146	54.8	0.31	10	8.4	2.0	10.4	14.50	57.00	2.00	4.50	78.00	
25	6.0	150	53.3	0.37	10	7.0	2.0	9.0	14.50	54.50	2.50	5.50	77.00	
30	5.2	156	51.3	0.41	10	6.2	2.0	8.2	14.00	54.50	3.00	6.50	78.00	

UNIFORM AIR ENTRAINMENT ASSUMED FOR PURPOSE OF COMPUTATION DEMONSTRATION OF BULKING. SEE PARAGRAPH 4-2 FOR METHOD OF ESTIMATING AIR ENTRAINMENT.

a. COMPUTATION FOR COST CURVE



b. COST CURVE

COST COMPUTATIONS
RECTANGULAR CONCRETE CHANNEL

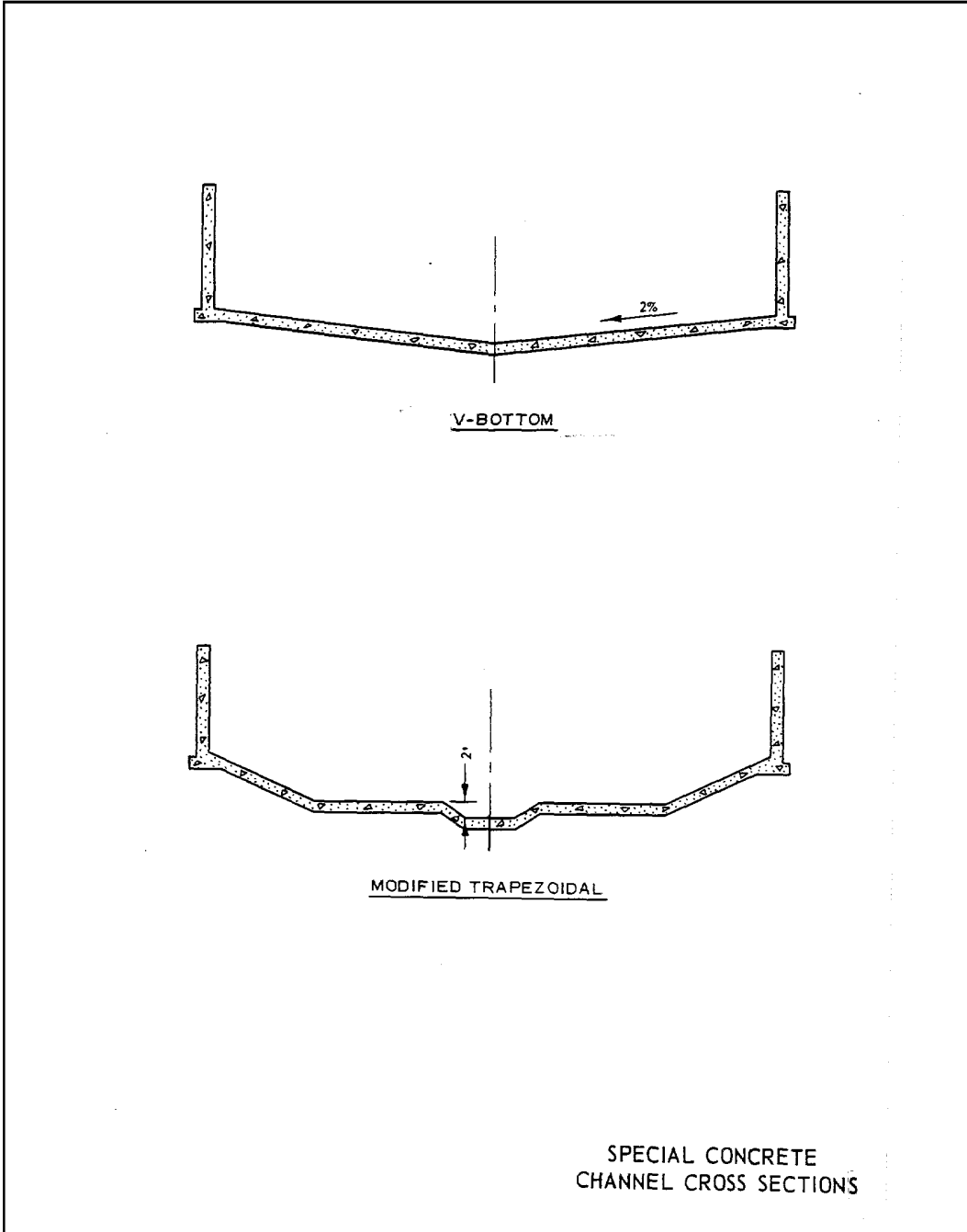
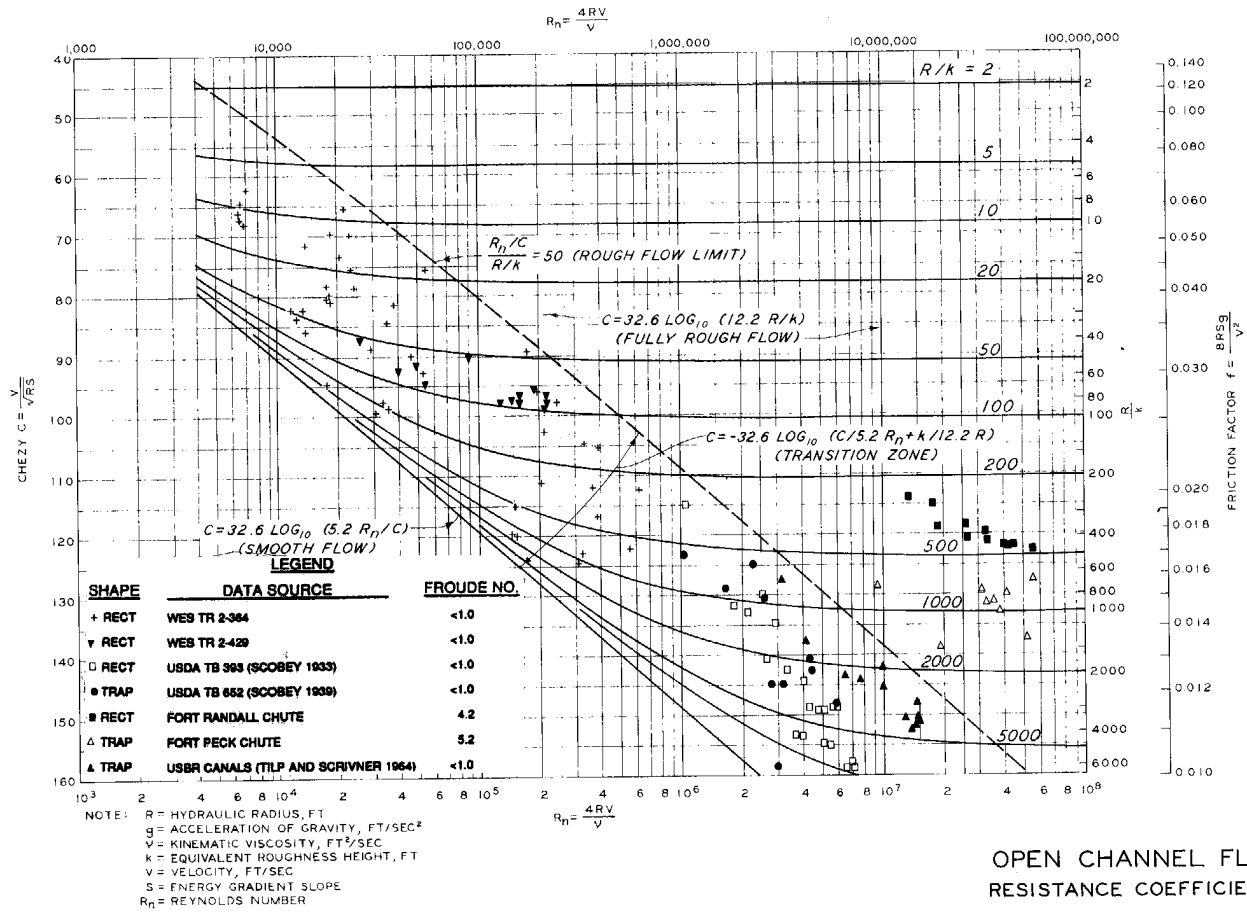


PLATE B-2



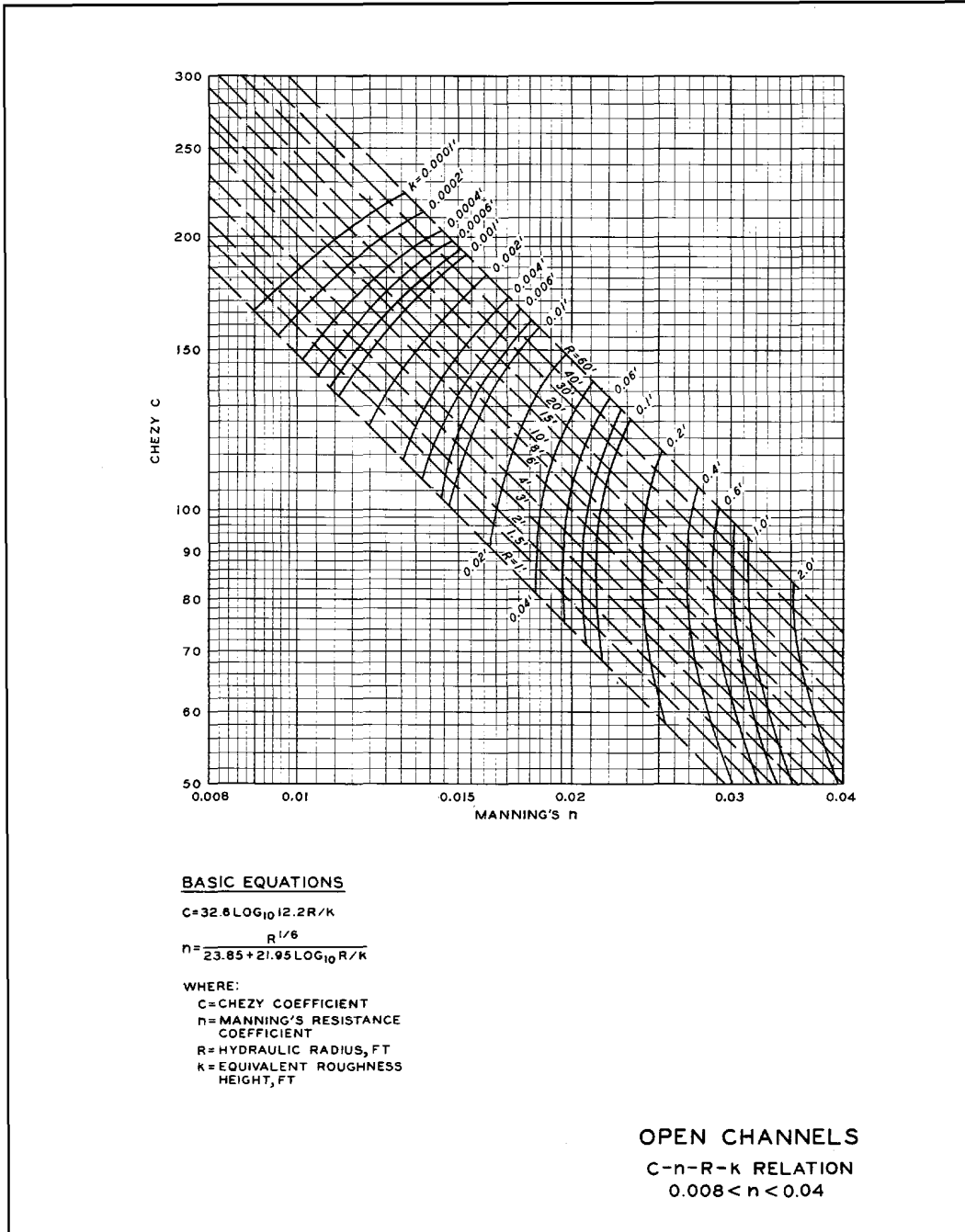


PLATE B-4

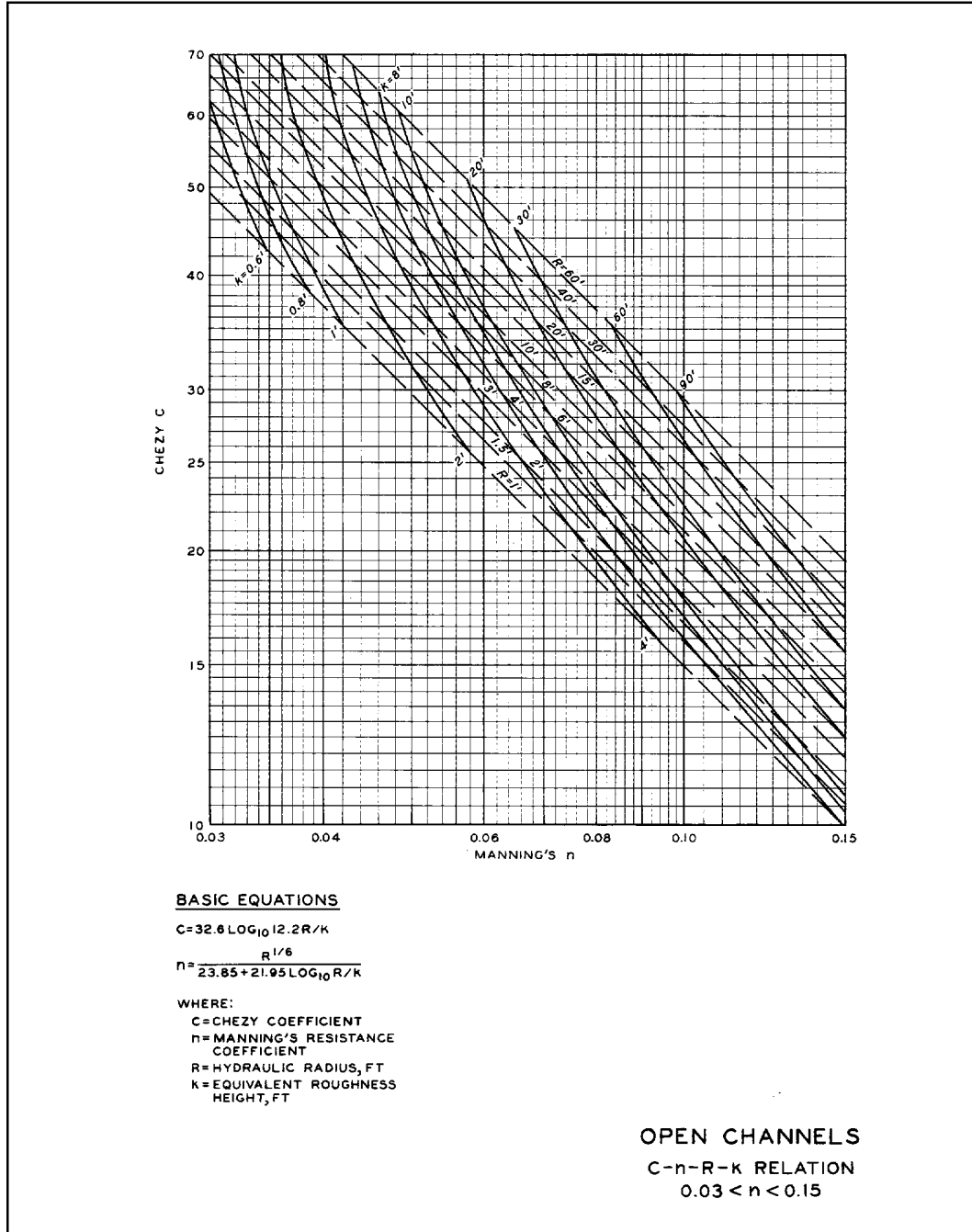


PLATE B-5

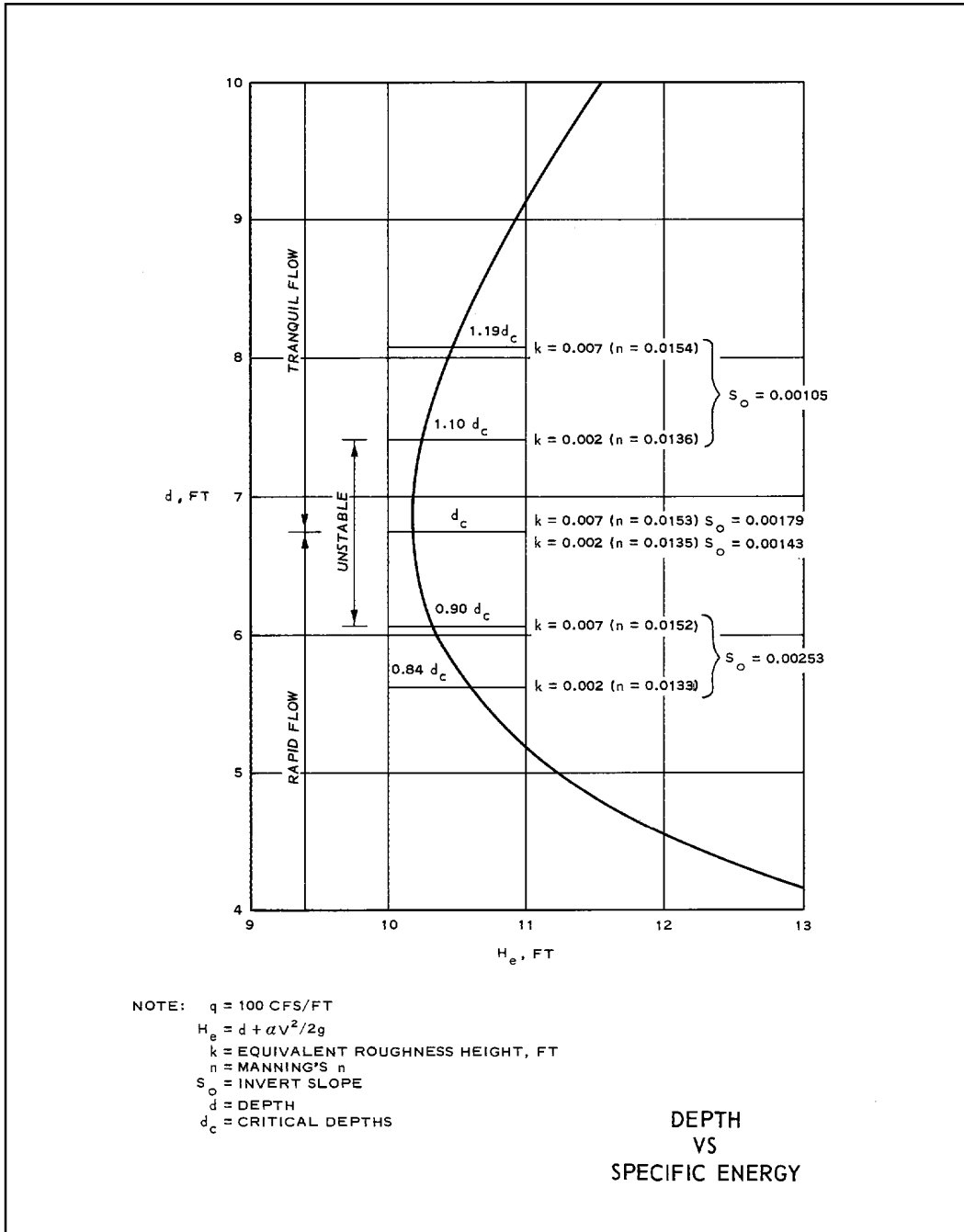


PLATE B-6

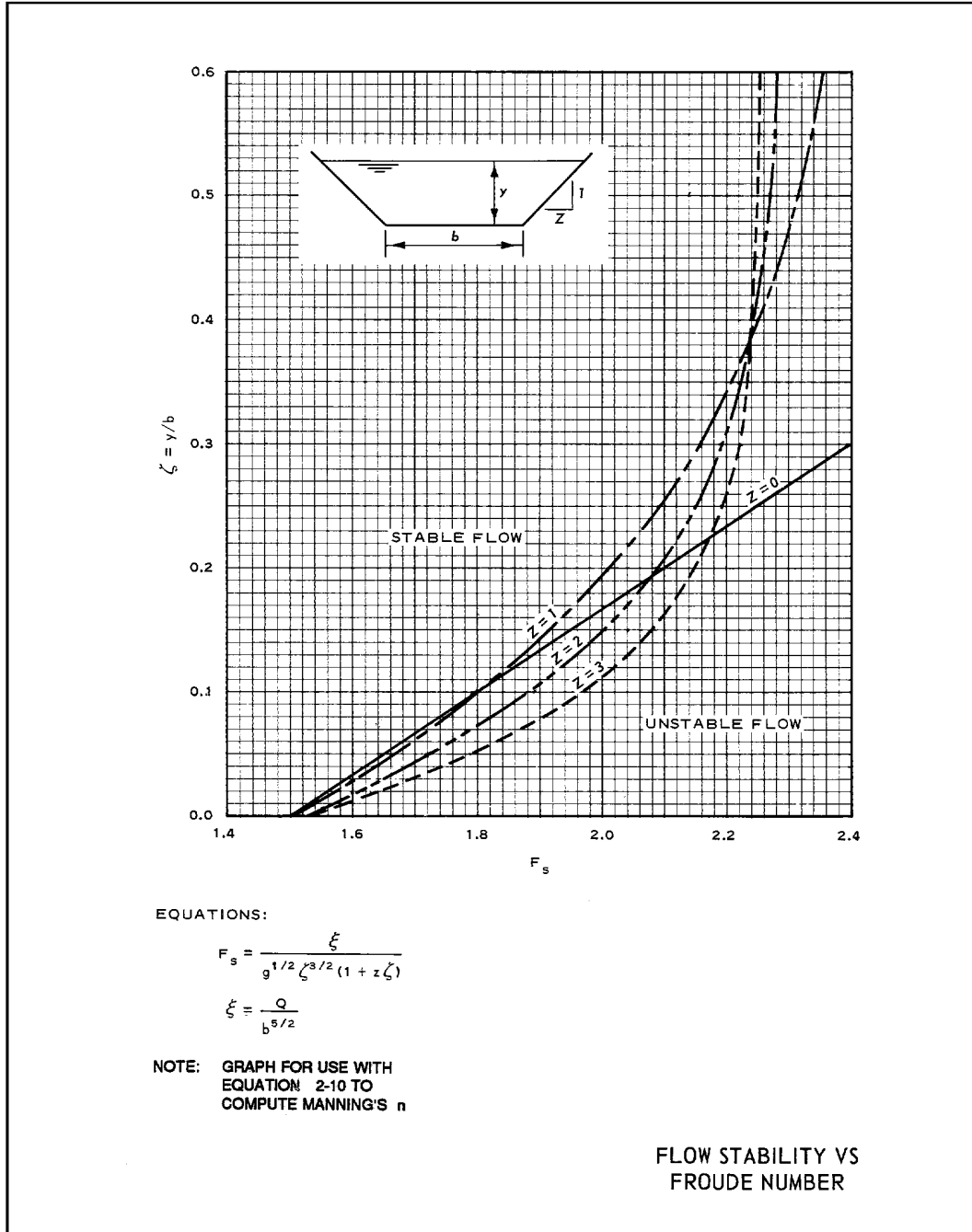
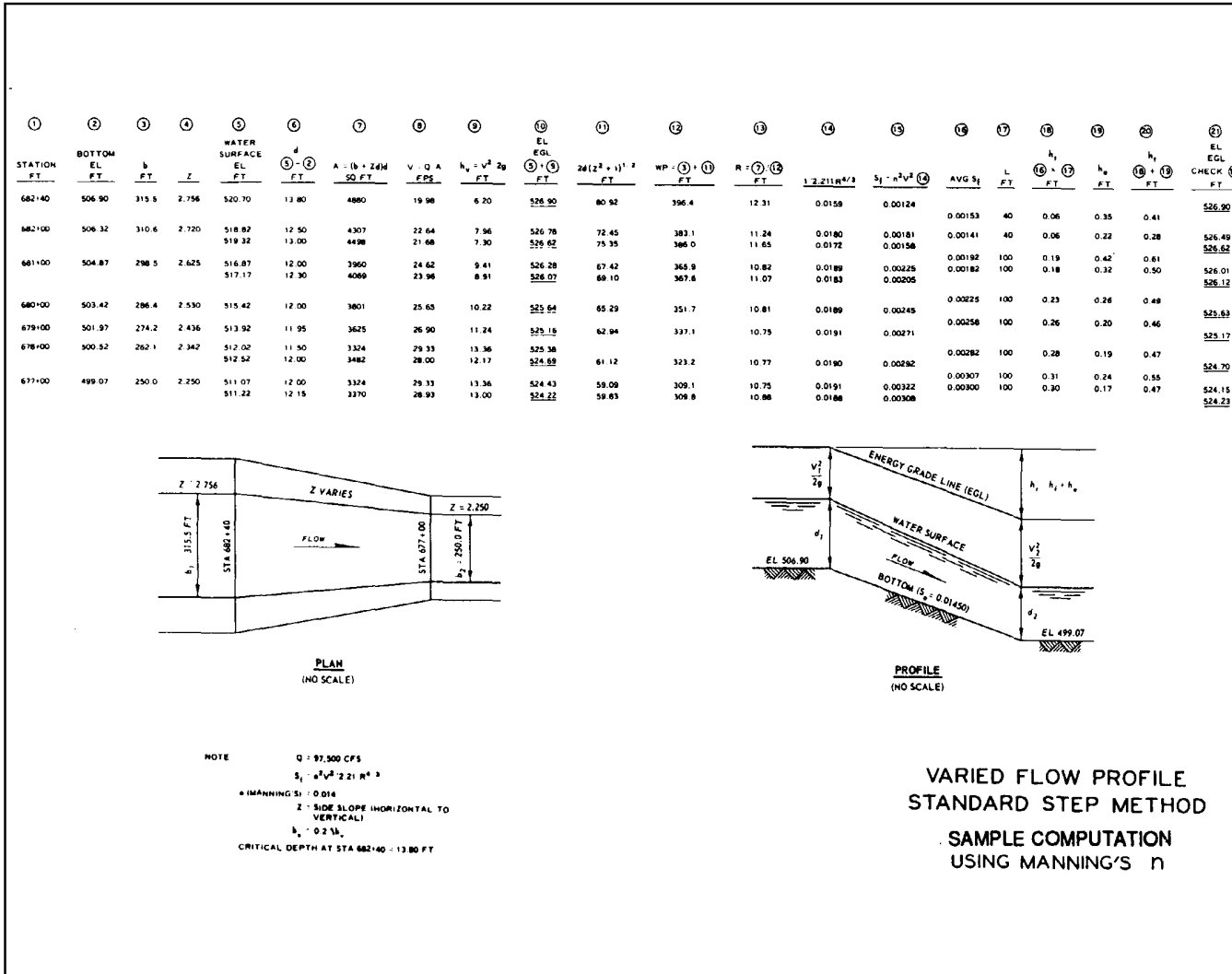


PLATE B-7

PLATE B-8



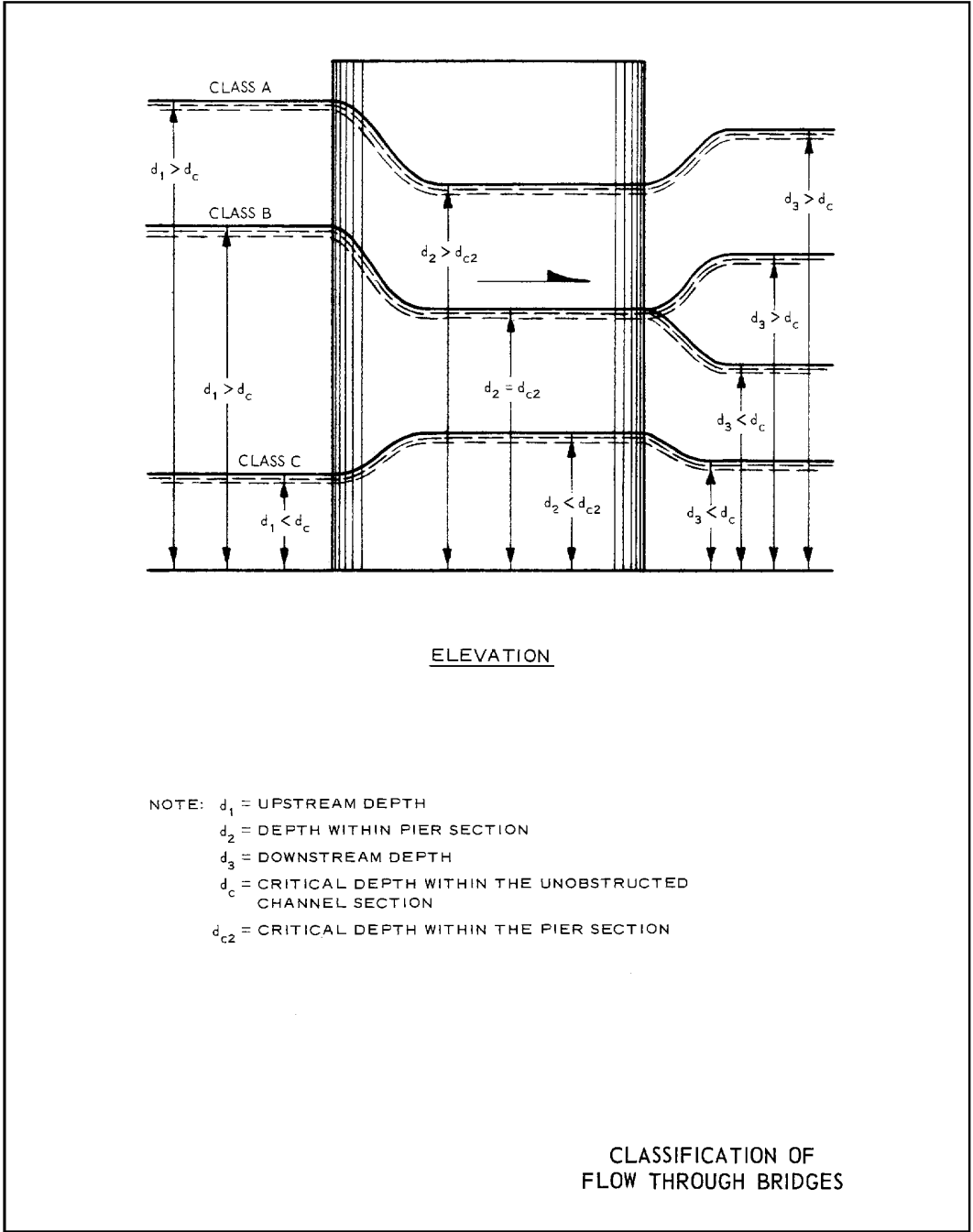


PLATE B-10

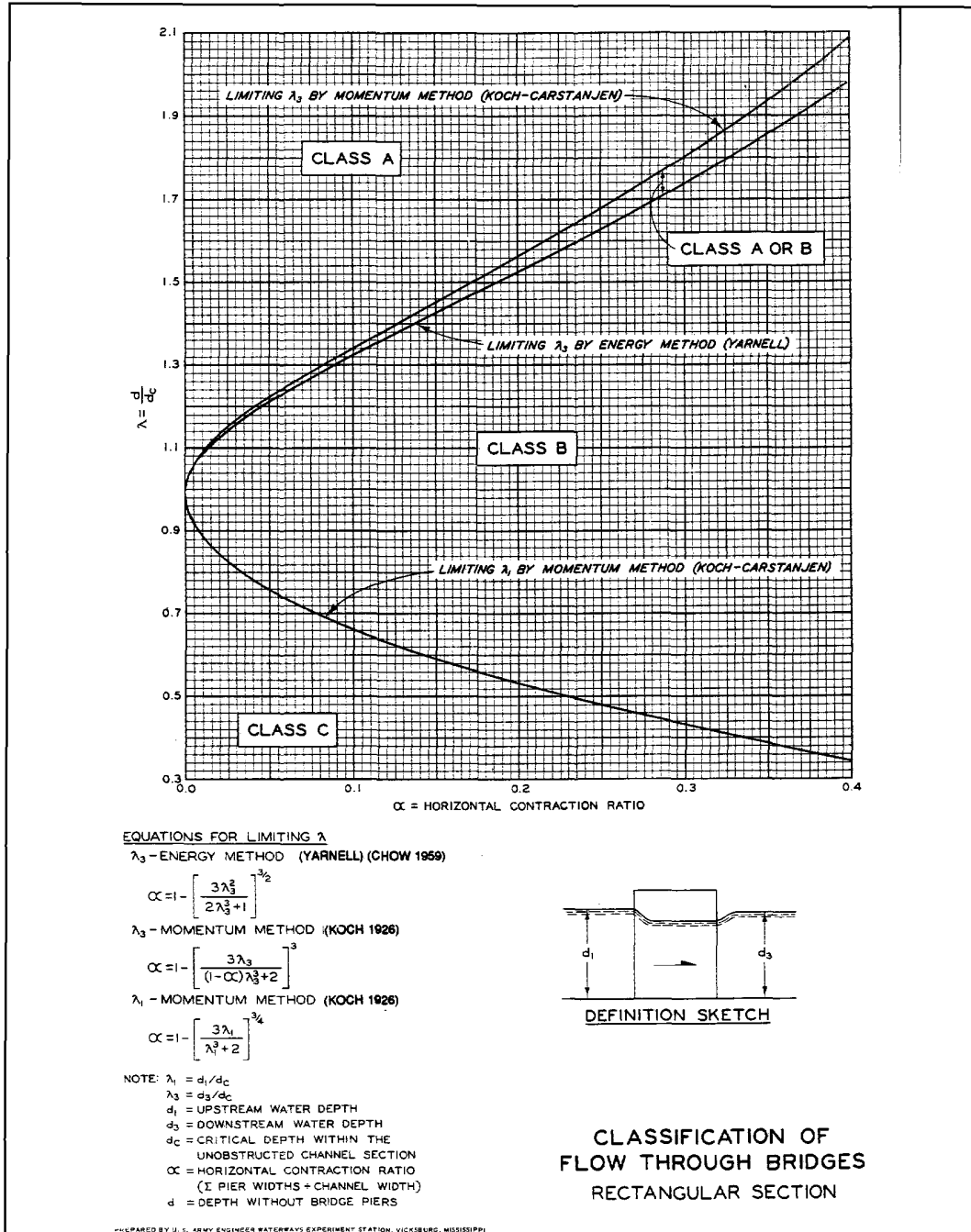
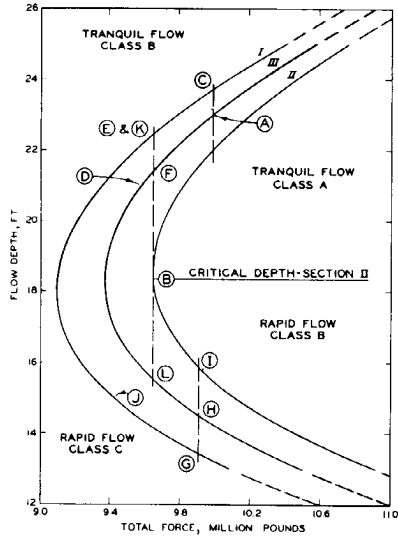


PLATE B-11



d. FORCE CURVES FOR CHANNEL SECTIONS I, II, AND III

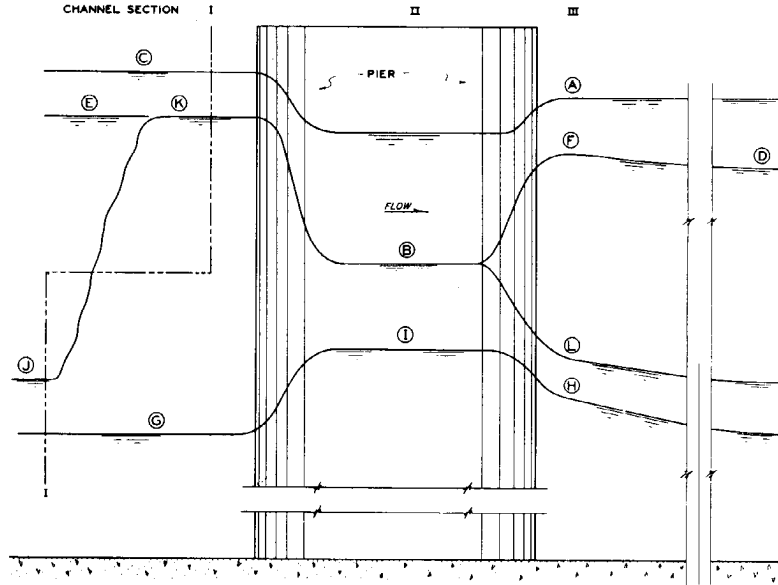
$$I = m_1 - m_{P_1} + \frac{v Q^2}{g A_1^2} (A_1 - A_{P_1})$$

$$II = m_2 + \frac{v Q^2}{g A_2}$$

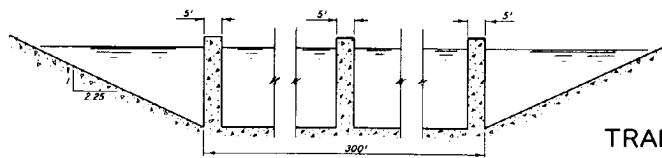
$$III = m_3 - m_{P_3} + \frac{v Q^2}{g A_3}$$

$\frac{v Q^2}{g A} = \text{MOMENTUM FORCE}$
 $m = v \bar{q} A$

c. FORCE EQUATIONS FOR CHANNEL SECTIONS I, II, AND III



b. FLOW PROFILES



d. CHANNEL SECTION II
Q = 140,000 CFS

TRAPEZOIDAL SECTION
MOMENTUM METHOD
EXAMPLE CURVES

GIVEN

Q = 140,000 CFS
CHANNEL WIDTH B = 300 FT
SIDE SLOPE = 1:2.25
PIER WIDTH = 5 FT
NO. OF PIERS = 3

SPECIFIC FORCE EQUATIONS

$$I = m_1 - m_{p1} + \frac{yQ^2}{gA_1^2} (A_1 - A_{p1})$$

$$II = m_2 + \frac{yQ^2}{gA_2}$$

$$III = m_3 - m_{p3} + \frac{yQ^2}{gA_3}$$

SOLVE FORCE EQUATIONS FOR ASSUMED VALUES OF FLOW DEPTH d

FOR d = CONSTANT: $m_1 = m_3$, $m_{p1} = m_{p3}$, $m_1 - m_{p1} = m_2$.

$A_1 = A_3$, $A_{p1} = A_{p3}$, $A_1 - A_{p1} = A_3 - A_{p3} = A_2$

①	②	③	④	⑤	⑥	⑦
d	$A_1 = A_3$	$m_1 = m_3$	$A_{p1} = A_{p3}$	$m_{p1} = m_{p3}$	$A_1 - A_{p1}$	$m_1 - m_{p1}$
UNITS	UNITS	MILLIONS	UNITS	MILLIONS	UNITS	MILLIONS
(FT)	(FT ²)	(LB)	(LB)	(LB)	(FT ²)	(LB)
13	4280	1.687	195	0.079	4085	1.608
14	4641	1.966	210	0.092	4431	1.874
15	5006	2.267	225	0.105	4781	2.162
16	5376	2.592	240	0.120	5136	2.472
17	5750	2.940	255	0.135	5495	2.804
18	6129	3.311	270	0.152	5859	3.159
19	6512	3.706	285	0.169	6227	3.537
20	6900	4.125	300	0.188	6600	3.937
21	7292	4.568	315	0.207	6977	4.361
22	7689	5.037	330	0.227	7359	4.810
23	8090	5.530	345	0.248	7745	5.282
24	8496	6.048	360	0.270	8136	5.778
25	8906	6.592	375	0.293	8531	6.299

⑧	⑨	⑩	⑪	⑫	⑬
$\frac{yQ^2}{g(A_1 - A_{p1})}$	$\frac{yQ^2}{gA_3}$	$\frac{yQ^2(A_1 - A_{p1})}{gA_1^2}$	I	II	III
MILLIONS	MILLIONS	MILLIONS	⑦ + ⑩	⑦ + ⑧	⑦ + ⑨
(LB)	(LB)	(LB)	(LB)	(LB)	(LB)
9.313	8.889	8.484	10.092	10.921	10.497
8.586	8.197	7.826	9.700	10.460	10.071
7.957	7.600	7.258	9.420	10.119	9.762
7.407	7.077	6.761	9.232	9.879	9.549
6.923	6.616	6.323	9.126	9.727	9.420
6.493	6.207	5.934	9.093	9.652	9.366
6.109	5.842	5.586	9.123	9.646	9.379
5.764	5.514	5.274	9.211	9.701	9.451
5.458	5.217	4.992	9.353	9.819	9.578
5.170	4.948	4.735	9.545	9.980	9.758
4.912	4.703	4.502	9.784	10.194	9.984
4.676	4.478	4.288	10.066	10.454	10.256
4.459	4.272	4.092	10.391	10.758	10.571

NOTE: m = HYDROSTATIC FORCE = $y\bar{y}A$, LB
y = SPECIFIC WEIGHT OF WATER, LB
 \bar{y} = DISTANCE FROM WATER SURFACE TO CENTER OF GRAVITY, FT
A = CROSS-SECTION AREA, SQ FT
 $\frac{yQ^2}{gA}$ = MOMENTUM FORCE, LB
g = ACCELERATION OF GRAVITY, FT/SEC²

**MOMENTUM METHOD
EXAMPLE COMPUTATIONS
TRAPEZOIDAL SECTION**

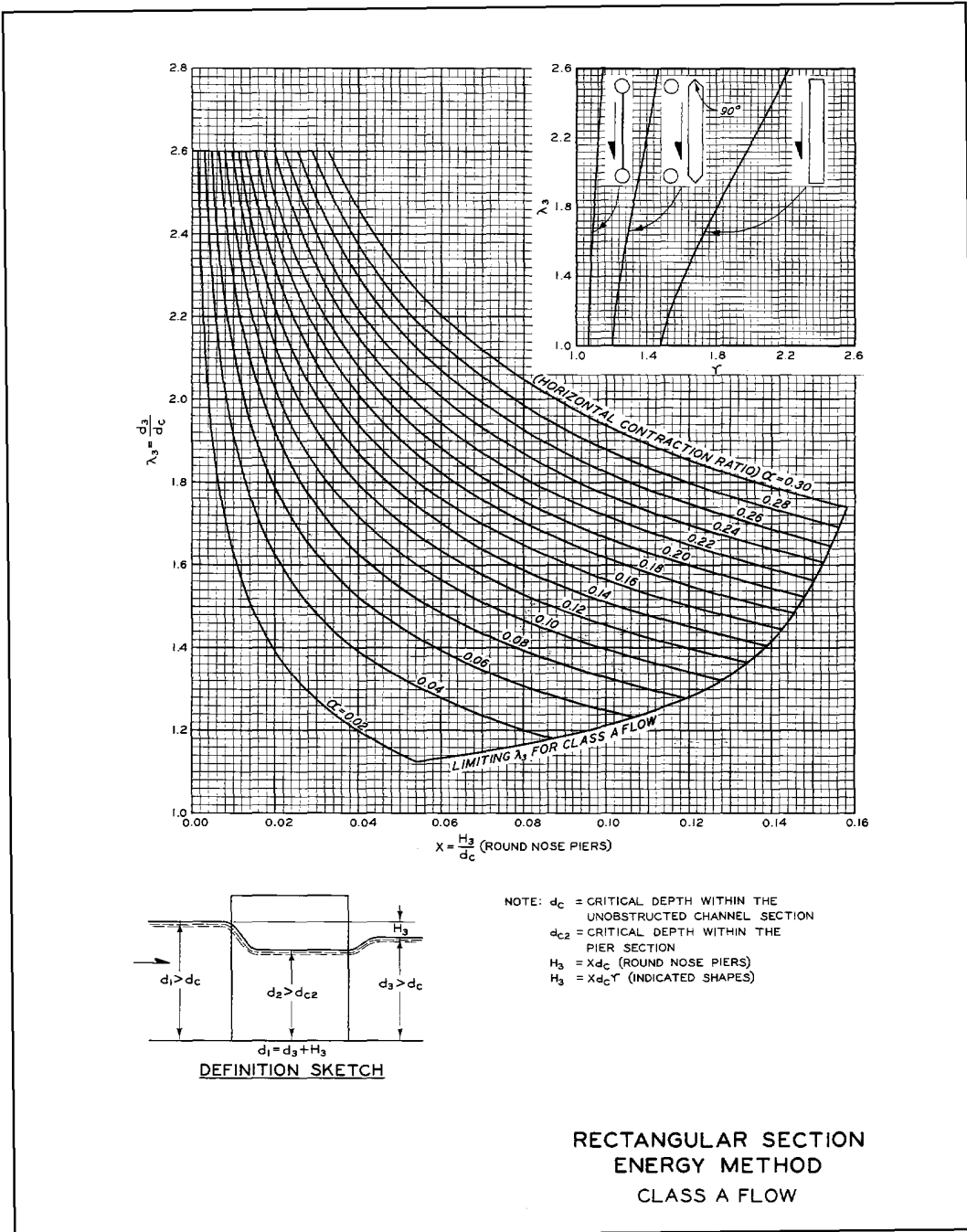
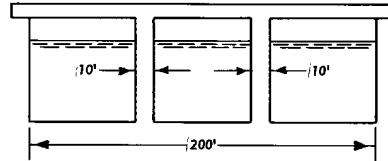


PLATE B-14

GIVEN:

Rectangular channel section
 Round nose piers
 Channel discharge (Q) = 40,000 cfs
 Channel width (W_c) = 200 ft
 Total pier width (W_p) = 20 ft
 Depth without bridge piers (d) = 14.3 ft



COMPUTE:

1. Horizontal contraction ratio (α)

$$\alpha = \frac{W_p}{W_c} = \frac{20}{200} = 0.10$$

2. Discharge (q) per ft of channel width

$$q = \frac{Q}{W_c} = \frac{40,000}{200} = 200 \text{ cfs}$$

3. Critical depth (d_c) in unobstructed channel

From Chart 610-8, d_c = 10.8 ft
 for q = 200 cfs.

4. $\lambda = d/d_c = 14.3/10.8$
 = 1.324

5. Flow classification

On Plate 11, intersection
 of $\alpha = 0.10$ and $\lambda = 1.324$ is
 in zone marked Class A or B.

6. Upstream depth (d₁)

- a. Class A flow - Energy Method

$$d_1 = d_3 + H_3 \text{ (Plate 14)}$$

$$H_3 = X d_c$$

$$X = 0.127 \text{ for } \alpha = 0.10$$

$$\text{and } \lambda_3 = \lambda = 1.324$$

$$H_3 = 0.127 \times 10.8 = 1.37$$

$$d_1 = 14.3 + 1.37 = 15.67 \text{ ft}$$

- b. Class B flow - Momentum Method

$$d_1 = \lambda_1 d_c \text{ (Plate 16)}$$

$$\lambda_1 = 1.435 \text{ for } \alpha = 0.10$$

$$d_1 = 1.435 \times 10.8 = 15.50 \text{ ft}$$

- c. Class B flow - Energy Method

$$d_1 = \lambda_1 d_c \text{ (Plate 17)}$$

$$\lambda_1 = 1.460 \text{ for } \alpha = 0.10$$

$$d_1 = 1.460 \times 10.8 = 15.77 \text{ ft}$$

RECTANGULAR SECTION
 ENERGY METHOD
 SAMPLE COMPUTATION

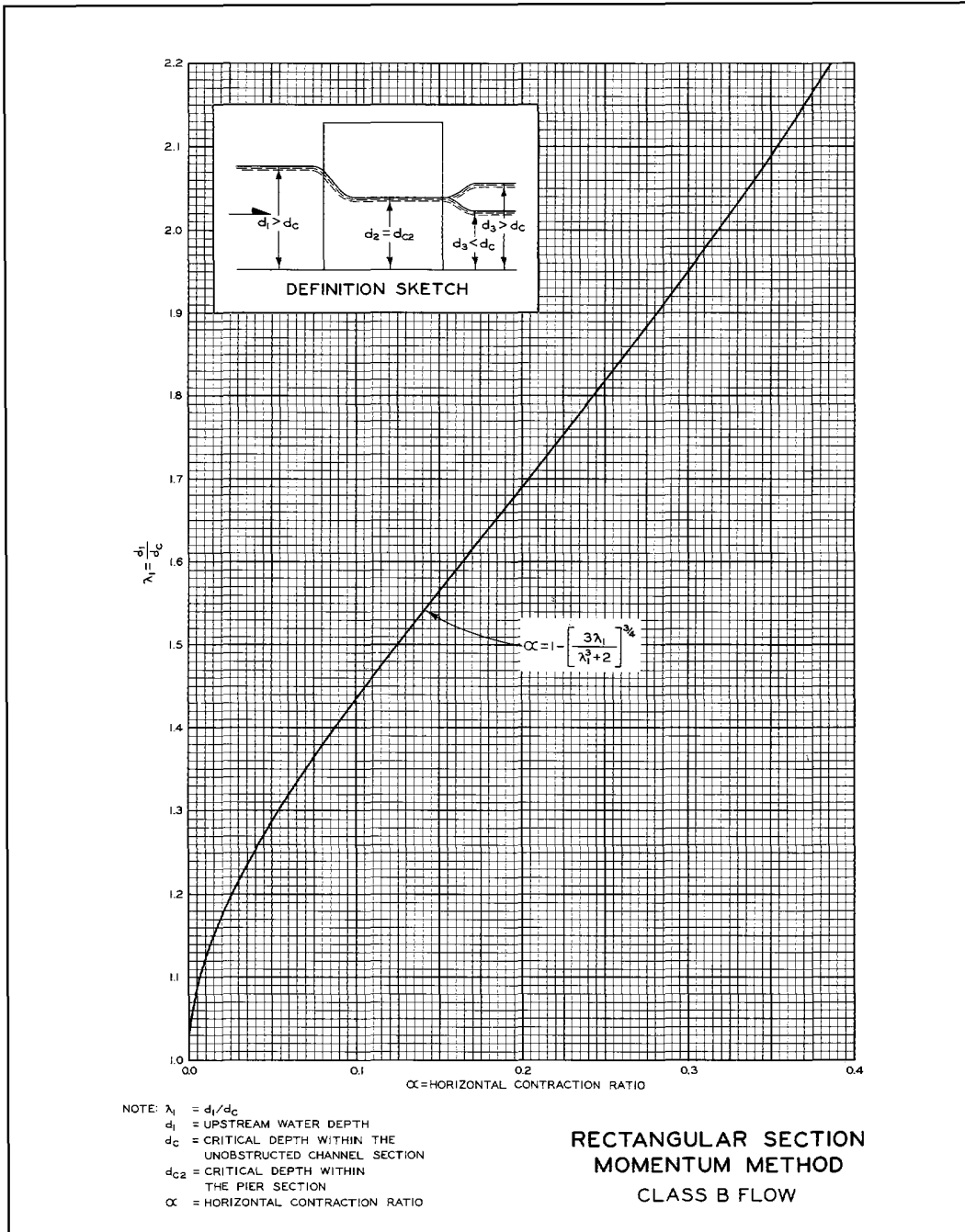
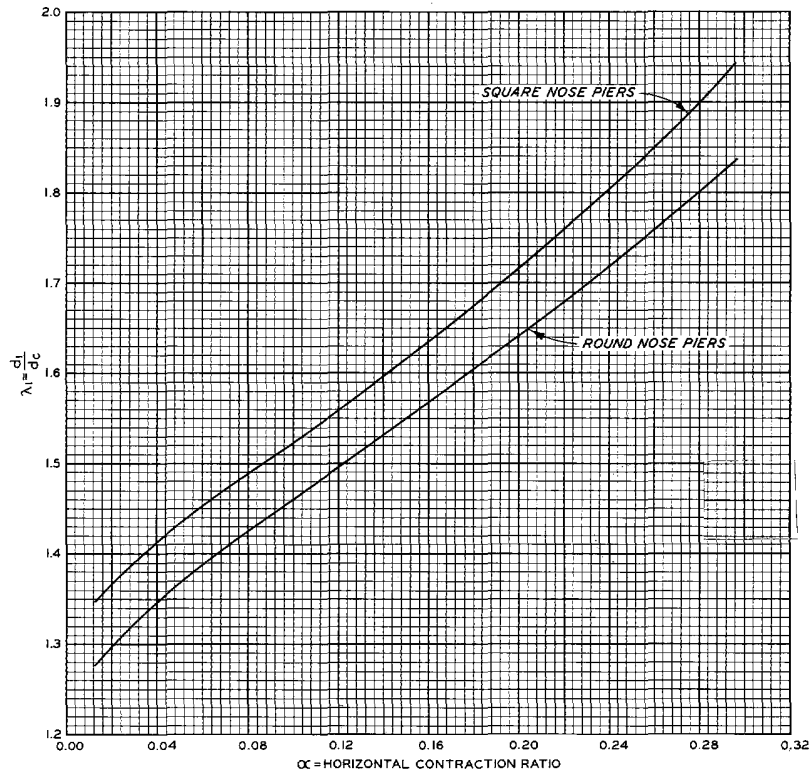


PLATE B-16

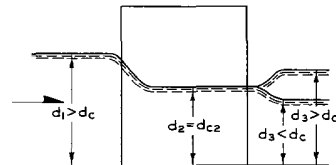


EQUATIONS

$$\frac{1}{(1-\alpha)^{2/3}} = \frac{1}{3\lambda_L^2} + \frac{2\lambda_L}{3}$$

$$\lambda_L = \lambda_L + \frac{0.5 + K_B(5.5\alpha^3 + 0.08)}{2\lambda_L^2}$$

- NOTE: $\lambda_1 = d_1/d_c$
 $\lambda_3 = d_3/d_c$
 λ_L = LIMITING λ_3 BY ENERGY METHOD
 d_1 = UPSTREAM WATER DEPTH
 d_3 = DOWNSTREAM WATER DEPTH
 d_c = CRITICAL DEPTH WITHIN THE UNOBSTRUCTED CHANNEL SECTION
 d_{c2} = CRITICAL DEPTH WITHIN THE PIER SECTION
 α = HORIZONTAL CONTRACTION RATIO
 K_B = YARNELL PIER-SHAPE COEFFICIENT
 (1.0 FOR ROUND NOSE)
 (5.0 FOR SQUARE NOSE)



DEFINITION SKETCH

**RECTANGULAR SECTION
ENERGY METHOD
CLASS B FLOW**

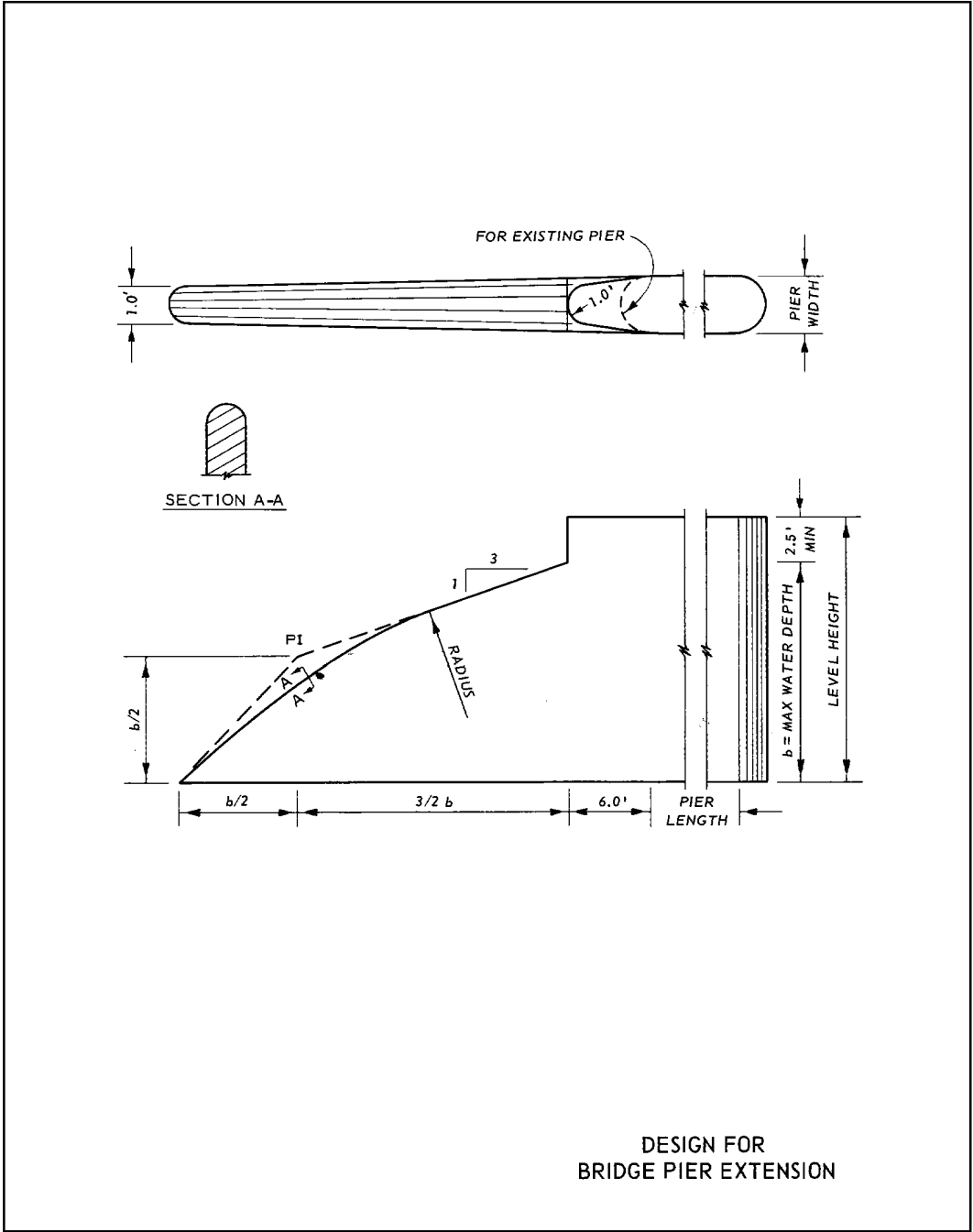


PLATE B-18

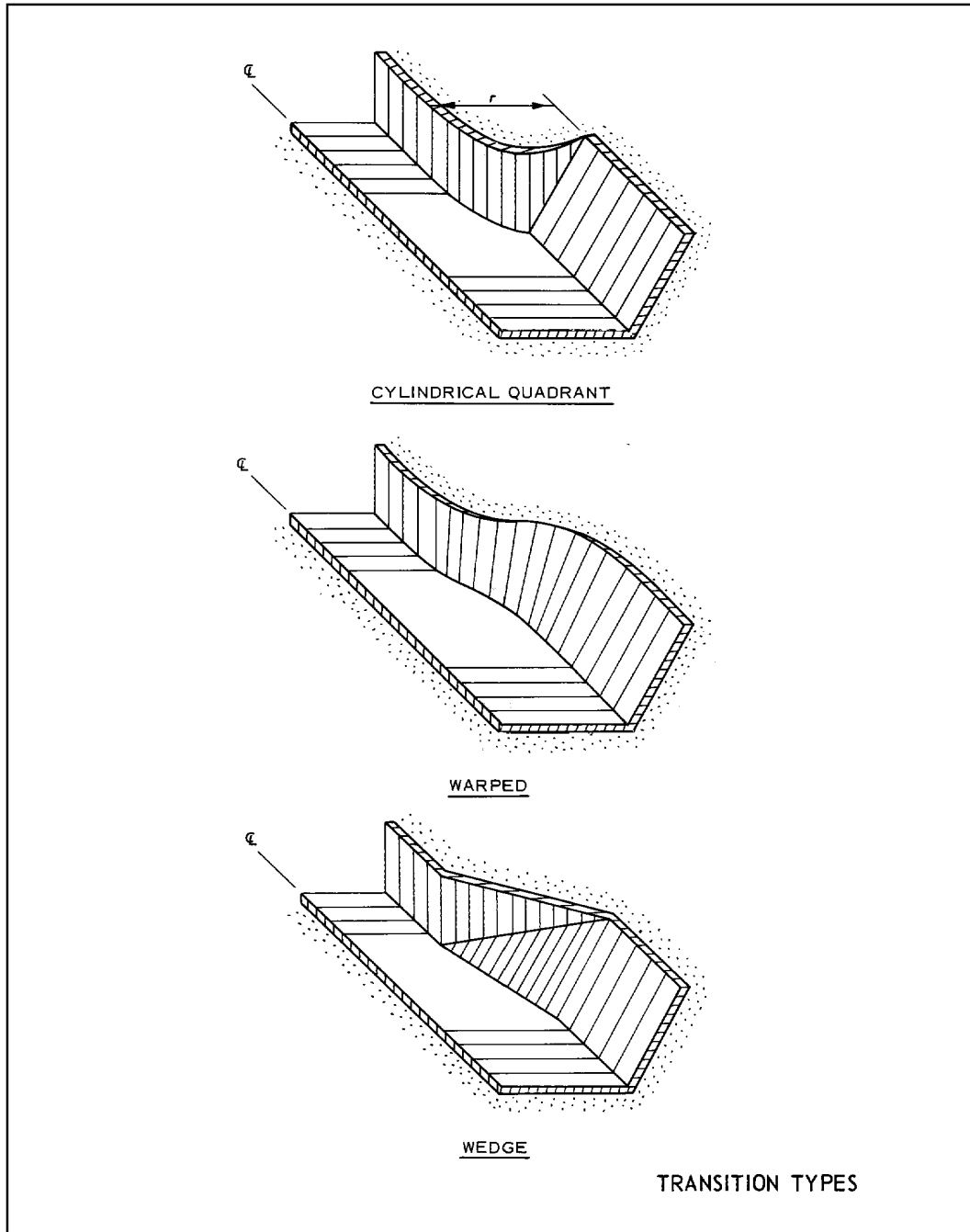


PLATE B-19

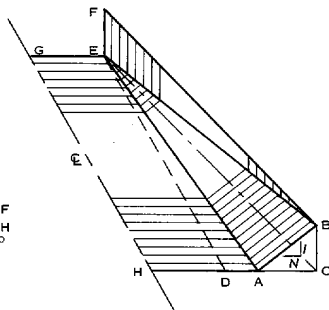
TABLE OF GEOMETRIC VALUES

N	AD/BC	DE/BC	AE/BC	CE/BC	BE/BC	ANG AEC ^a	ANG BEC ^a
2.0	0.4000	22.8344	22.8379	22.9602	22.9820	4.9964	2.4939
2.0	0.6000	24.7373	24.7446	24.8735	24.8936	4.6106	2.3022
2.0	0.8000	26.6402	26.6522	26.7869	26.8056	4.2799	2.1380
2.0	1.0000	28.5438	28.5605	28.7002	28.7177	3.9935	1.9955
2.0	1.2000	30.4459	30.4695	30.6136	30.6299	3.7429	1.8709
2.0	1.4000	32.3488	32.3790	32.5269	32.5423	3.5219	1.7609
2.0	1.6000	34.2516	34.2890	34.4403	34.4548	3.3255	1.6632
2.5	0.4000	27.5916	27.5945	27.7436	27.7616	5.1694	2.0643
2.5	0.6000	29.4945	29.5006	29.6569	29.6738	4.8346	1.9312
2.5	0.8000	31.3973	31.4075	31.5703	31.5861	4.5404	1.8143
2.5	1.0000	33.3002	33.3152	33.4836	33.4986	4.2799	1.7106
2.5	1.2000	35.2031	35.2235	35.3970	35.4111	4.0477	1.6182
2.5	1.4000	37.1059	37.1323	37.3103	37.3237	3.8393	1.5353
2.5	1.6000	39.0088	39.0416	39.2237	39.2364	3.6513	1.4604
3.0	0.4000	32.3488	32.3512	32.5269	32.5423	5.2916	1.7609
3.0	0.6000	34.2516	34.2569	34.4403	34.4548	4.9964	1.6632
3.0	0.8000	36.1545	36.1633	36.3536	36.3674	4.7324	1.5757
3.0	1.0000	38.0574	38.0705	38.2670	38.2801	4.4948	1.4969
3.0	1.2000	39.9602	39.9783	40.1803	40.1928	4.2799	1.4257
3.0	1.4000	41.8631	41.8865	42.0937	42.1056	4.0846	1.3609
3.0	1.6000	43.7660	43.7952	44.0070	44.0184	3.9063	1.3017

^a DEGREES

NOTE:

- BC = EF
- EG = DH
- ∠CED = 6°



DEFINITION SKETCH

WEDGE-TYPE TRANSITION
GEOMETRY

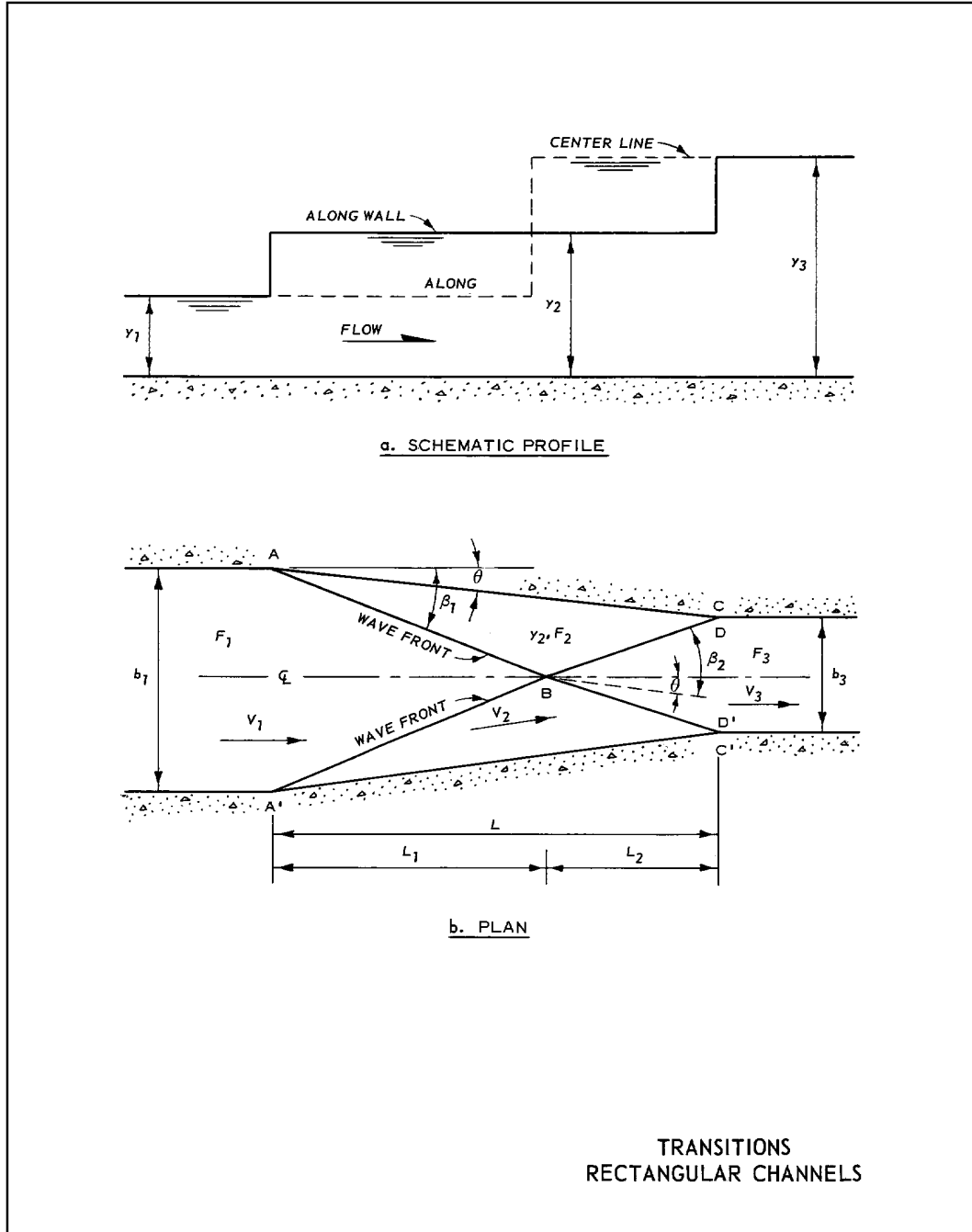


PLATE B-21

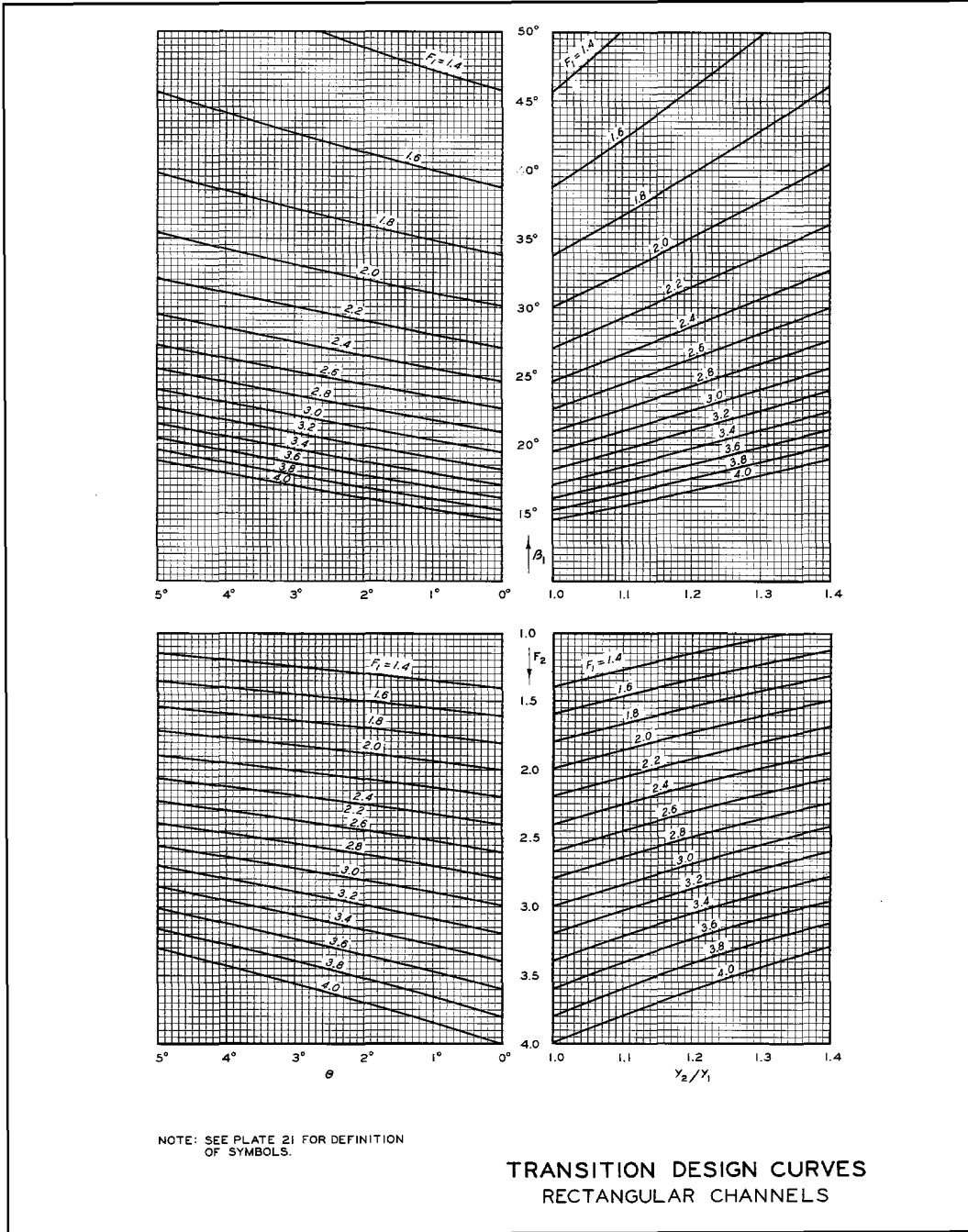


PLATE B-22

GIVEN

FROUDE NO. $F_1 = 3.5$
 FLOW DEPTH $y_1 = 5$ FT
 CHANNEL WIDTH $b_1 = 160$ FT
 CHANNEL WIDTH $b_3 = 140$ FT

REQUIRED

CONVERGENCE ANGLE θ
 FROUDE NO. F_3
 FLOW DEPTH y_3
 TRANSITION LENGTH $L = L_1 + L_2$

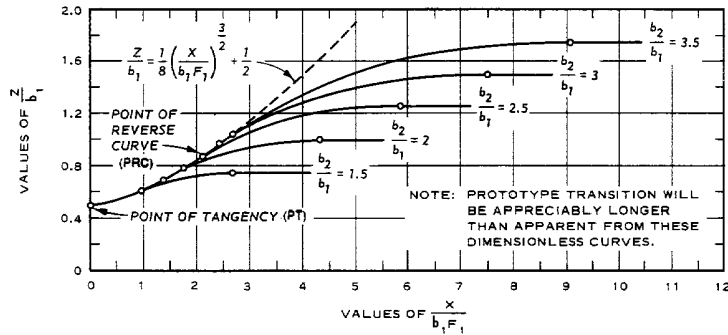
PROCEDURE

ASSUME VALUES OF θ AND BY REPETITIVE USE OF PLATE 22 SOLVE EQUATIONS 2-25, 2-26, AND 2-27 UNTIL $L = L_1 + L_2$. IF COL 6 IS GREATER THAN COL 9, CONTINUE COMPUTATION USING VALUE OF θ WITH F_2 IN SAME MANNER AS WAS DONE WITH F_1 . TO COMPUTE COL 11 THROUGH 18, EACH SUBSCRIPT IN PLATE 22 IS ASSUMED TO BE INCREASED BY ONE UNIT.

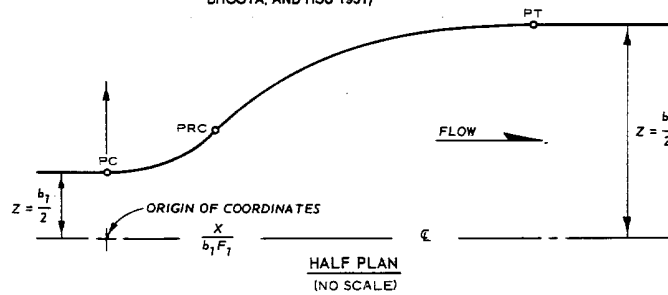
COMPUTATION

(1)	(2)	(3)	(4)	(5)	(6)
θ	$\frac{y_2}{y_1}$	y_2 , FT	β_1 , DEG	TAN θ	L , FT = $\frac{(b_1 - b_3) \div 2}{\text{TAN } \theta}$
3.0	1.20	6.00	19.2	0.0524	191
2.0	1.12	5.60	18.3	0.0349	287
1.3	1.07	5.35	17.6	0.0227	441
1.2	1.06	5.30	17.5	0.0209	478
(7)	(8)	(9)	(10)	(11)	(12)
TAN β	$\frac{b_1}{2}$, FT	L_1 , FT = (8) \div (7)	F_2	$\frac{y_3}{y_2}$	y_3 , FT
0.348	80	230	($L_1 > L$; ASSUME SMALLER θ)		
0.331	80	242	3.25	1.12	6.27
0.319	80	251	3.34	1.08	5.78
0.315	80	254	3.35	1.08	5.72
(13)	(14)	(15)	(16)	(17)	(18)
β_2	F_3	$\frac{b_3}{2}$	TAN ($\beta_2 - \theta$)	L_2 , FT = (15) \div (16)	$L_1 + L_2$, FT
---	---	---	---	---	---
19.7	3.05	70	0.319	219	461 > L
18.5	3.20	70	0.310	226	477 > L
18.2	3.22	70	0.306	229	483 \approx L

RECTANGULAR TRANSITIONS
EXAMPLE OF DESIGN COMPUTATION



a. GENERALIZED DESIGN CURVES
(REPRODUCED FROM FIG. 59, ROUSE, BHOOTA, AND HSU 1951)



POINTS	$\frac{Z}{b_1}$	$\frac{X}{b_1 F_1}$
PC	$\frac{1}{2}$	0
PRC	$\frac{11}{60} \left(\frac{b_2}{b_1} \right) + \frac{19}{60}$	$\left[\frac{22}{15} \left(\frac{b_2}{b_1} - 1 \right) \right]^{2/3}$
PT	$\frac{1}{2} \frac{b_2}{b_1}$	$\frac{13}{4} \left(\frac{b_2}{b_1} \right) - \frac{9}{4}$
PC TO PRC	$\frac{1}{8} \left(\frac{X}{b_1 F_1} \right)^{3/2} + \frac{1}{2}$	0 TO $\left(\frac{X}{b_1 F_1} \right)_{PRC}$
PRC TO PT	$\frac{b_2}{2b_1} - q \left[\left(\frac{X}{b_1 F_1} \right)_{PT} - \left(\frac{X}{b_1 F_1} \right)_{PRC} \right]^r$	$\left(\frac{X}{b_1 F_1} \right)_{PRC}$ TO $\left(\frac{X}{b_1 F_1} \right)_{PT}$

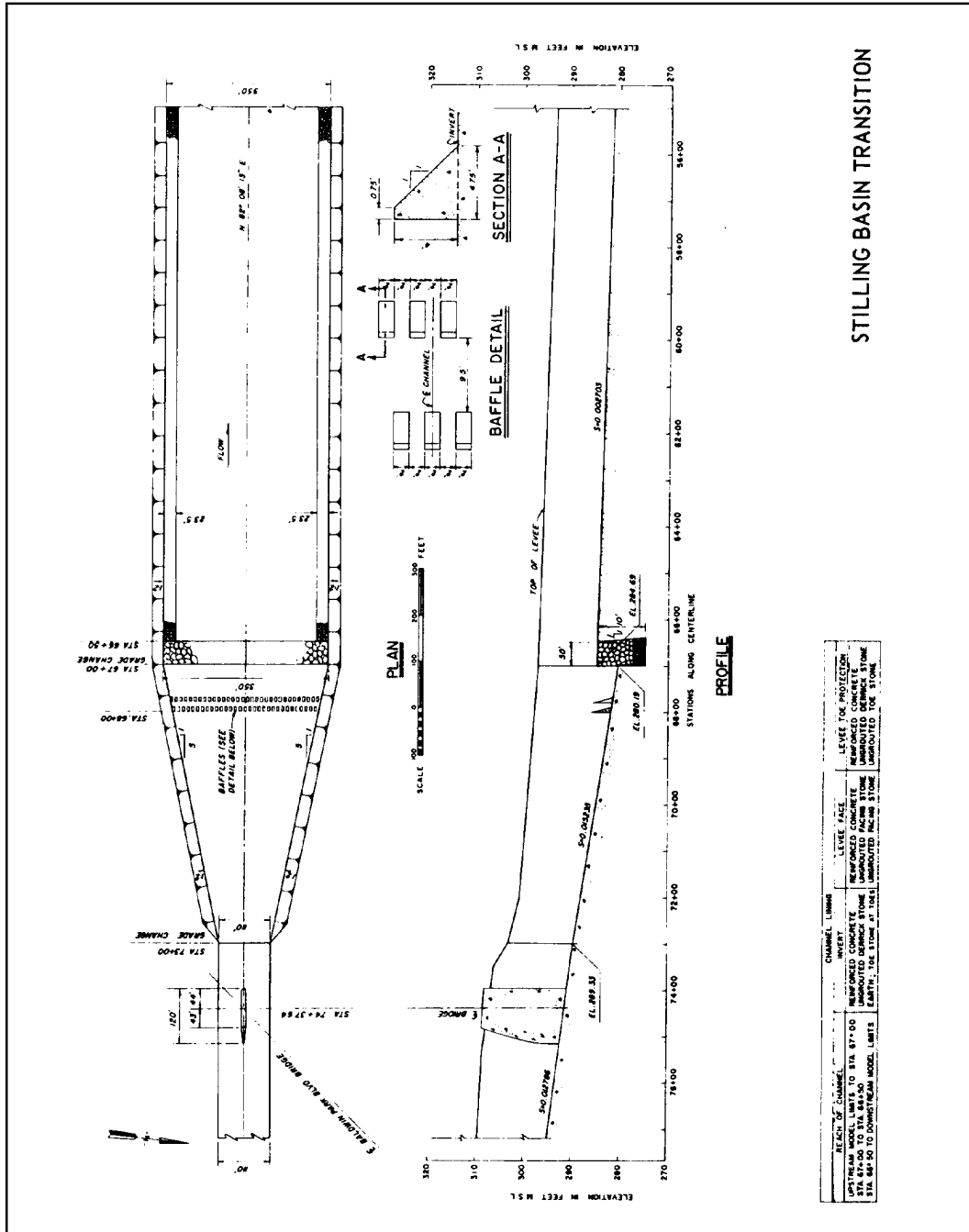
WHERE

$$q = \frac{\frac{b_2}{2b_1} - \left(\frac{Z}{b_1} \right)_{PRC}}{\left[\left(\frac{X}{b_1 F_1} \right)_{PT} - \left(\frac{X}{b_1 F_1} \right)_{PRC} \right]^r} \quad \text{AND} \quad r = \frac{\left(\frac{X}{b_1 F_1} \right)_{PT} - \left(\frac{X}{b_1 F_1} \right)_{PRC}}{\frac{b_2}{2b_1} - \left(\frac{Z}{b_1} \right)_{PRC}} \left(\frac{3}{16} \right) \left(\frac{X}{b_1 F_1} \right)_{PRC}^{1/2}$$

b. EQUATIONS APPROXIMATING CURVES

NOTE: TRANSITION COORDINATES CAN BE SCALED FROM CURVES OR COMPUTED FROM EQUATIONS USING b_1 , b_2 , AND F_1 .

**EXPANDING TRANSITION
RECTANGULAR CHANNEL
RAPID FLOW**



STILLING BASIN TRANSITION

PLATE B-25

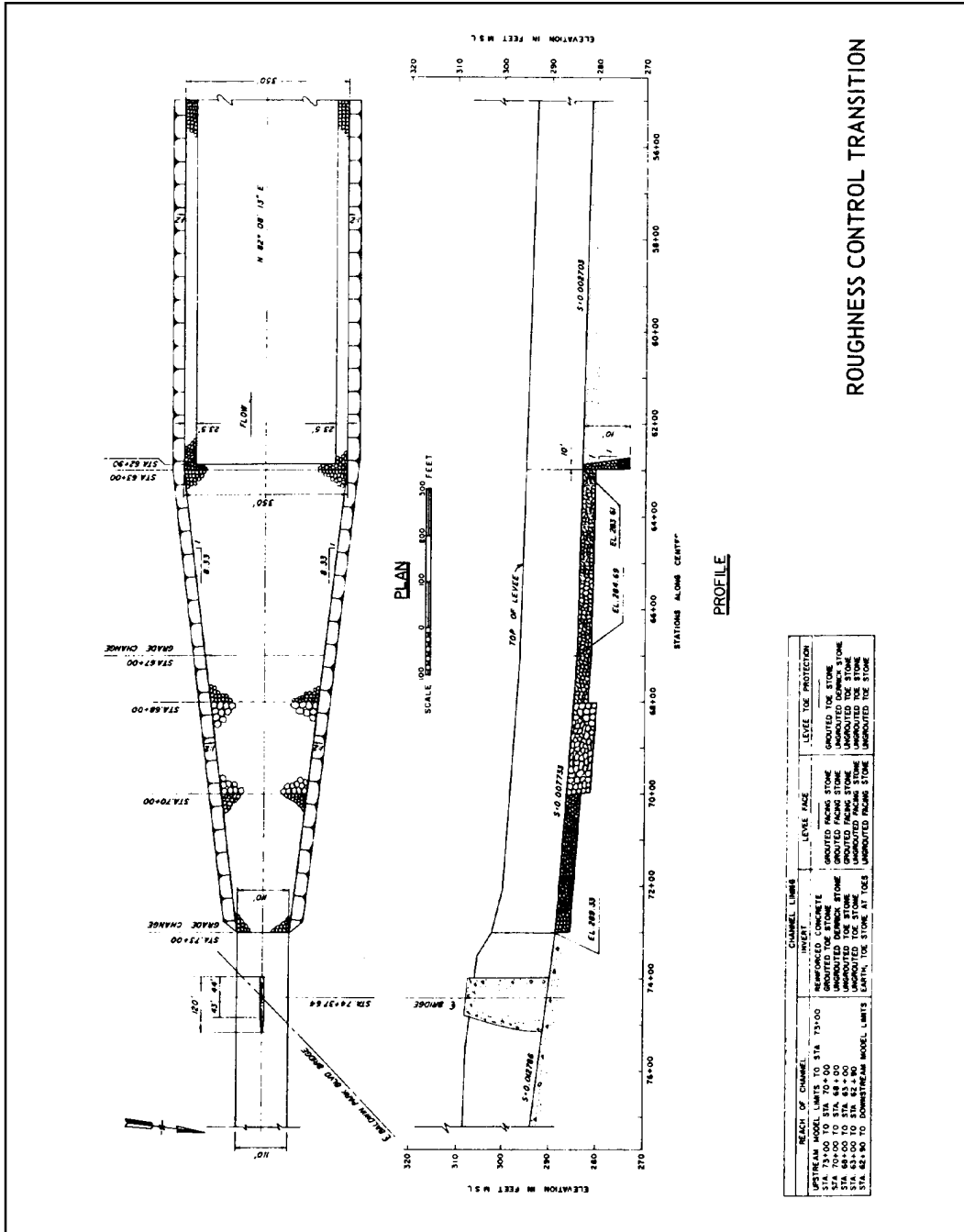
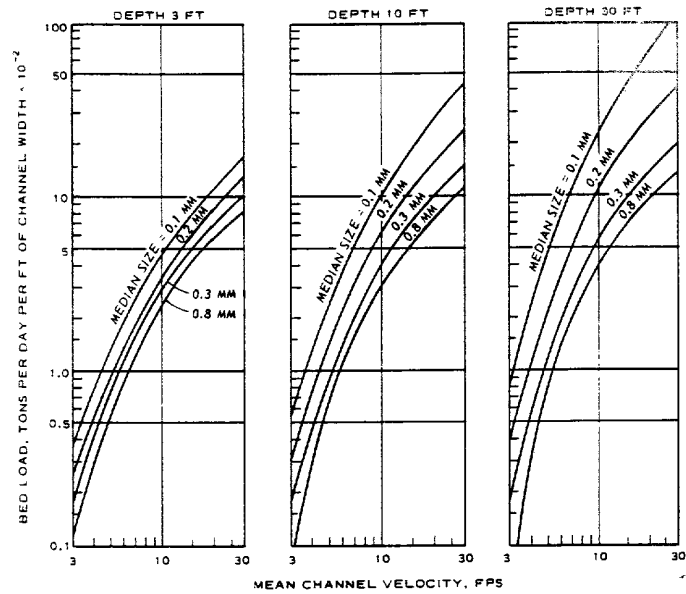


PLATE B-26



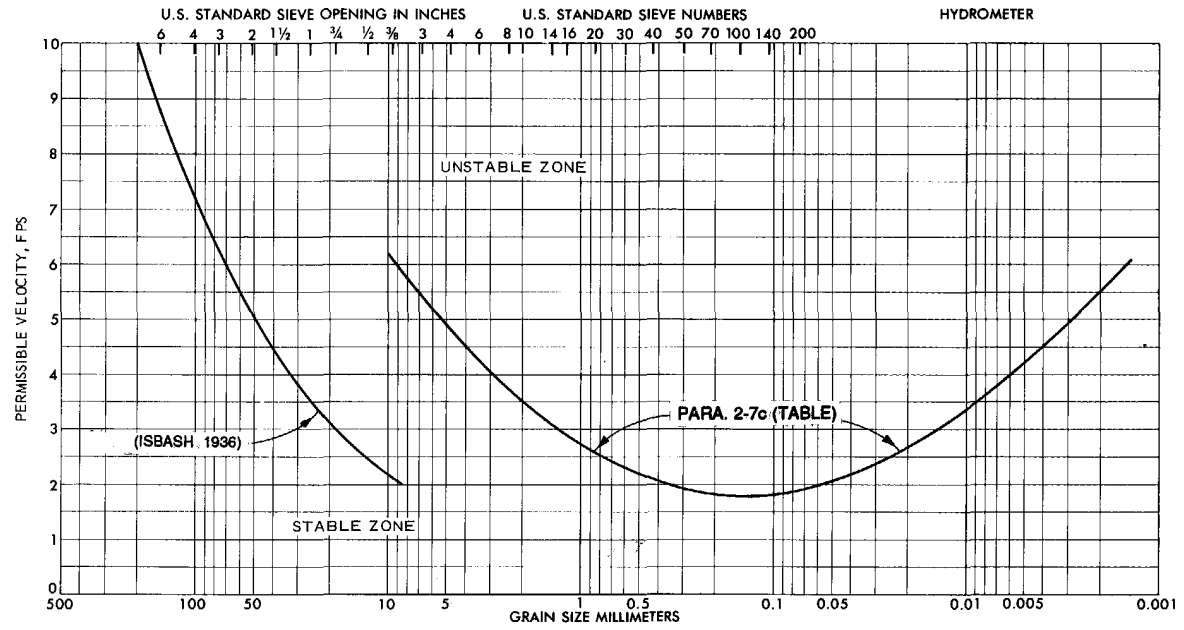
BASIC DATA SOURCES

FIELD DATA		FLUME DATA	
RIVER	LOCATION	INVESTIGATOR	DATE OF TESTS
MIDDLE LOOP ^a	DUNNING, NEBRASKA	GILBERT	1914
NIORARA ^a	CODY, NEBRASKA	BARTON AND LIN	1955
ELKHORN	WATERLOO, NEBRASKA	SIMONS, ET AL.	1961
LOWER COLORADO	---	BROOKS	1958
PIGEON ROOST CK.	NORTHERN MISSISSIPPI		
MISSISSIPPI	ST. LOUIS, MO.		
CEDAR	NEBRASKA		
LITTLE BLUE	NEBRASKA		
NORTH LOOP	NEBRASKA		
SOUTH LOOP	NEBRASKA		
RIO GRANDE	NEW MEXICO		
RIO PUERCO	NEW MEXICO		

NOTE: SOURCES OF PUBLISHED FLUME AND FIELD DATA ARE GIVEN IN COLBY (1964A); SOME FIELD DATA HAVE NOT BEEN PUBLISHED. CURVES ARE FOR WATER TEMPERATURE OF 60 F AND NO SUSPENDED FINE SEDIMENT LOAD AND ARE EXTRAPOLATED FROM A PLOT IN THE REFERENCE.

^a TOTAL LOAD MEASURED FOR THESE TWO STREAMS; SUSPENDED LOAD MEASURED AND BED LOAD COMPUTED FOR OTHER FIELD DATA.

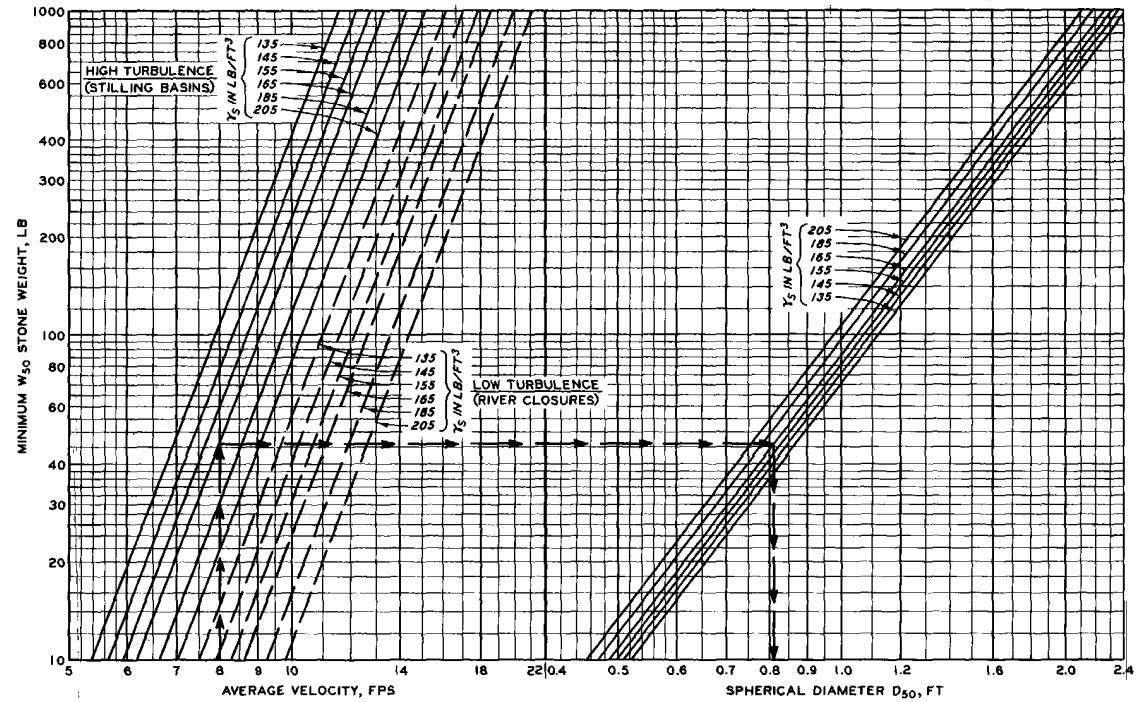
BED-LOAD DISCHARGE



COBBLES	GRAVEL		SAND			SILT OR CLAY
	COARSE	FINE	COARSE	MEDIUM	FINE	
"SELF ARMORING" RIPRAP SIZES			SCOUR AND DEPOSITION BED-LOAD SIZES			SCOUR ONLY WASH-LOAD SIZES

**NONCOHESIVE SEDIMENT GRADATION
AND PERMISSIBLE VELOCITY**

PREPARED BY U. S. ARMY ENGINEER WATERWAYS EXPERIMENT STATION, WASHINGTON, DISTRICT OF COLUMBIA



BASIC EQUATIONS

$$V = C \left[2g \left(\frac{\gamma_s - \gamma_w}{\gamma_w} \right) \right]^{1/2} (D_{50})^{1/2}$$

$$D_{50} = \left(\frac{6W_{50}}{\pi \gamma_s} \right)^{1/3}$$

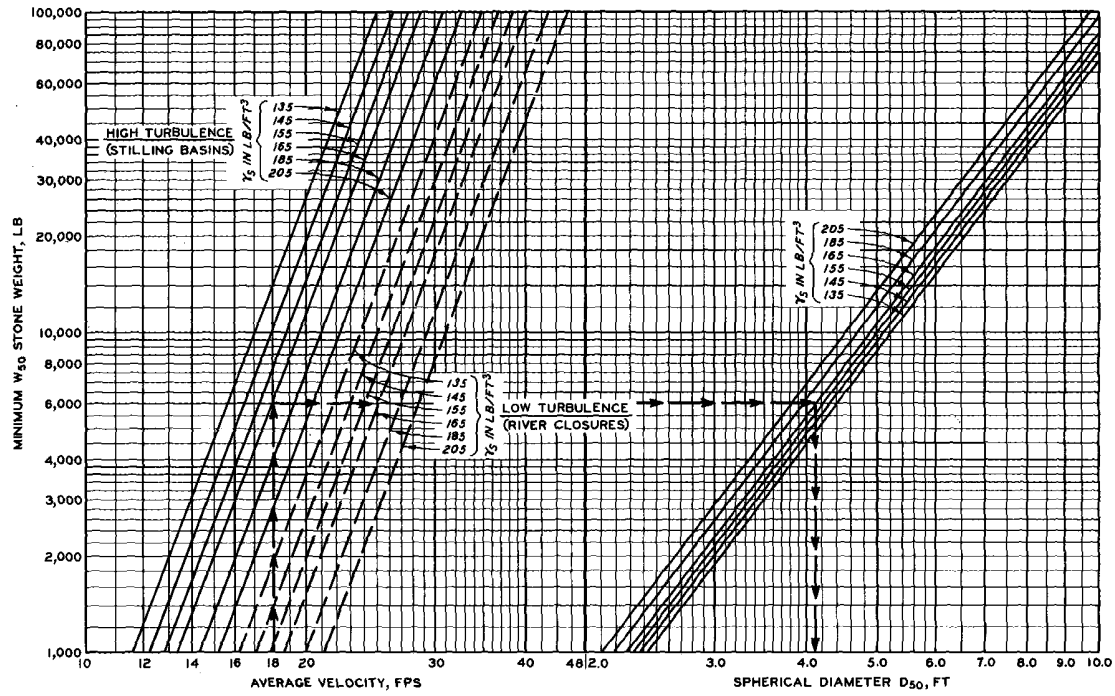
- WHERE: V = VELOCITY, FPS
 γ_s = SPECIFIC STONE WEIGHT, LB/FT³
 γ_w = SPECIFIC WEIGHT OF WATER, 62.5 LB/FT³
 W_{50} = WEIGHT OF STONE. SUBSCRIPT DENOTES PERCENT OF TOTAL WEIGHT OF MATERIAL CONTAINING STONE OF LESS WEIGHT.
 D_{50} = SPHERICAL DIAMETER OF STONE HAVING THE SAME WEIGHT AS W_{50}
 C = ISBASH CONSTANT (0.86 FOR HIGH TURBULENCE LEVEL FLOW AND 1.20 FOR LOW TURBULENCE LEVEL FLOW)
 g = ACCELERATION OF GRAVITY, FT/SEC²

STONE STABILITY VELOCITY VS STONE DIAMETER

HYDRAULIC DESIGN CHART 712-1
 (SHEET 1 OF 2)
 REV 8-56, 9-70 WES 6-57

PLATE B-29

PREPARED BY U. S. ARMY ENGINEER ASSISTANT CHIEF OF STAFF, WASHINGTON, DISTRICT OF COLUMBIA



BASIC EQUATIONS

$$V = C \left[2g \left(\frac{\gamma_s - \gamma_w}{\gamma_w} \right) \right]^{1/2} (D_{50})^{1/2}$$

$$D_{50} = \left(\frac{6W_{50}}{\pi \gamma_s} \right)^{1/3}$$

- WHERE:
- V = VELOCITY, FPS
 - γ_s = SPECIFIC STONE WEIGHT, LB/FT³
 - γ_w = SPECIFIC WEIGHT OF WATER, 62.5 LB/FT³
 - W_{50} = WEIGHT OF STONE, SUBSCRIPT DENOTES PERCENT OF TOTAL WEIGHT OF MATERIAL CONTAINING STONE OF LESS WEIGHT.
 - D_{50} = SPHERICAL DIAMETER OF STONE HAVING THE SAME WEIGHT AS W_{50}
 - C = ISBASH CONSTANT (0.86 FOR HIGH TURBULENCE, LEVEL FLOW AND 1.20 FOR LOW TURBULENCE, LEVEL FLOW)
 - g = ACCELERATION OF GRAVITY, FT/SEC²

**STONE STABILITY
VELOCITY VS STONE DIAMETER**

HYDRAULIC DESIGN CHART 712-1
(SHEET 2 OF 2)

REV 8-56, 9-70

WES 6-57

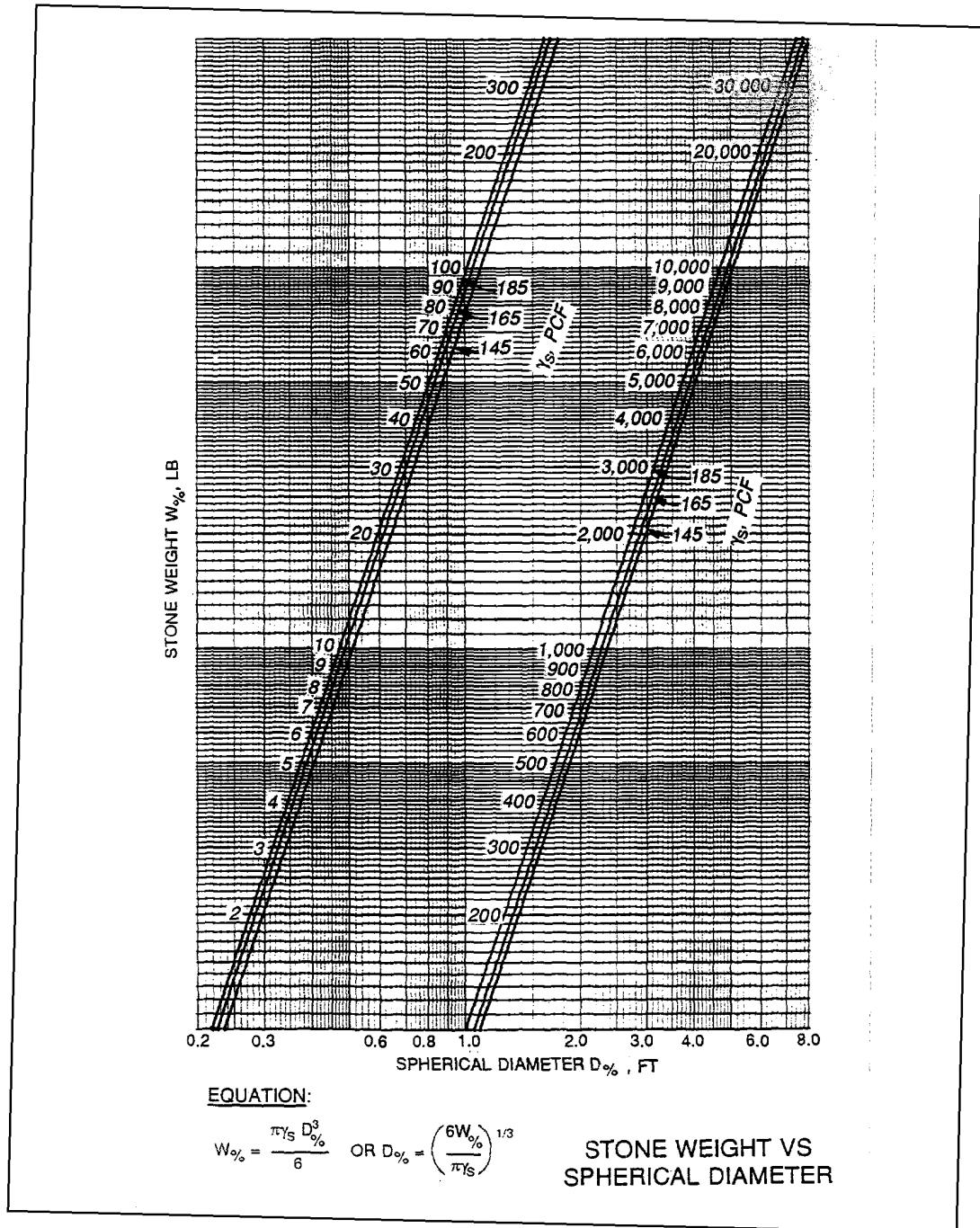


PLATE B-31

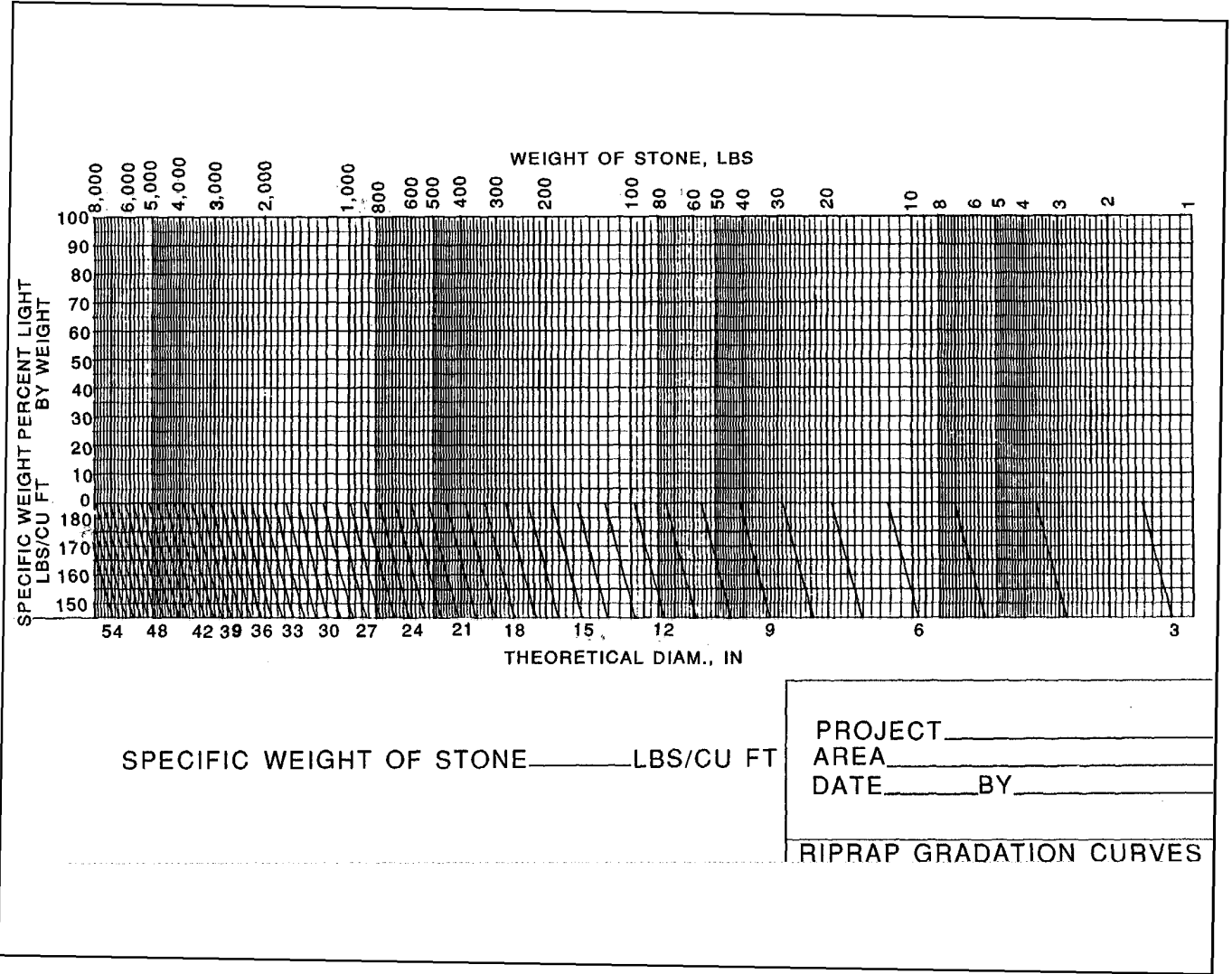
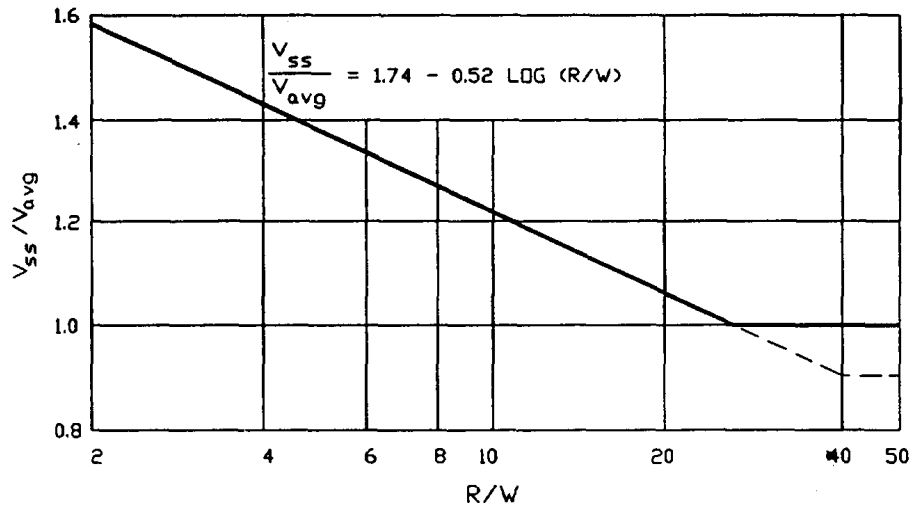


PLATE B-32

*



NOTE: V_{ss} IS DEPTH-AVERAGED VELOCITY AT 20 PERCENT
OF SLOPE LENGTH UP FROM TOE

RIPRAP DESIGN VELOCITIES
NATURAL CHANNEL

Plate B-33
(Sheet 1 of 2)

*

*

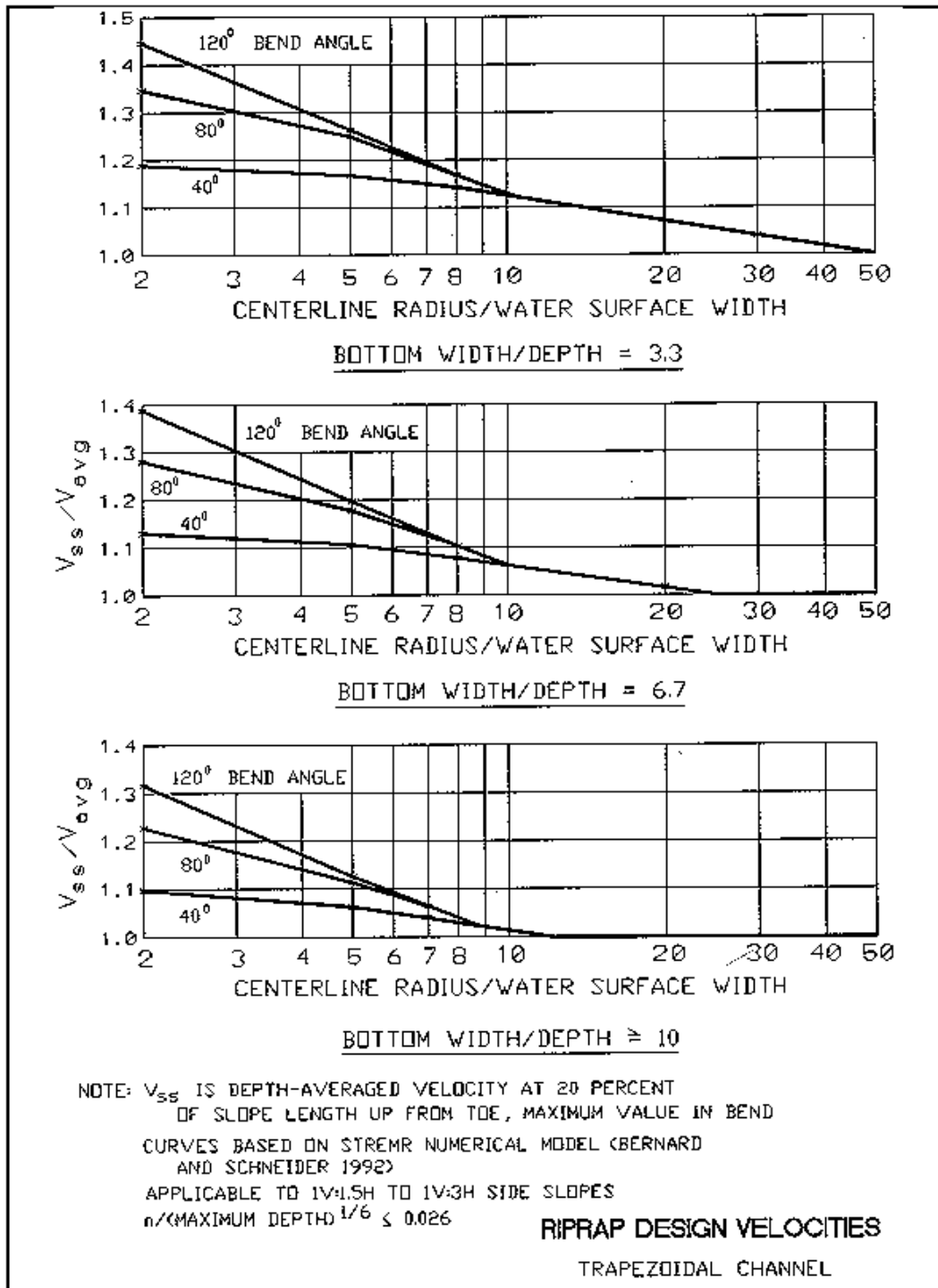


Plate B-33
 (Sheet 2 of 2)

*

*

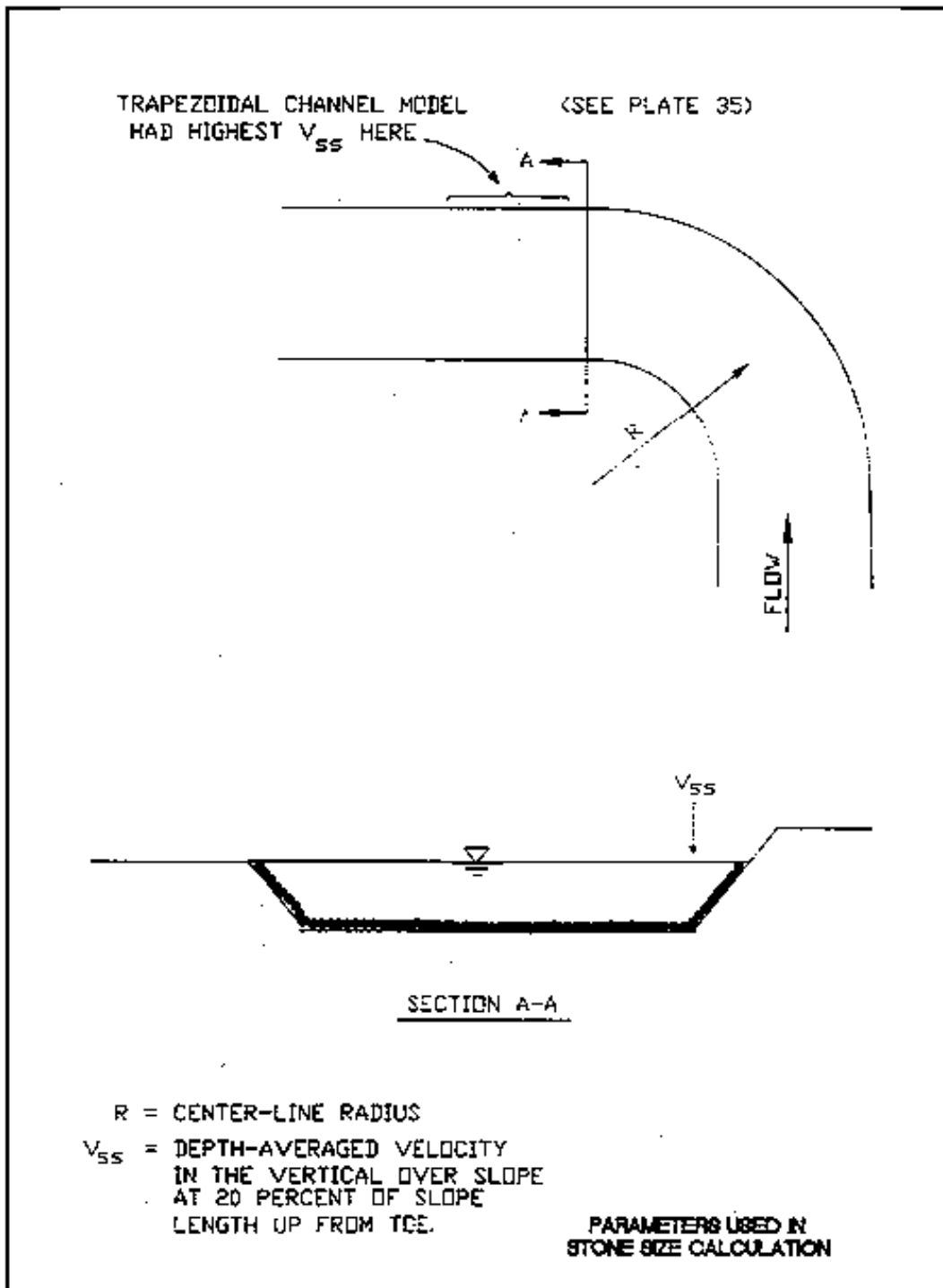


Plate B-34

*

*

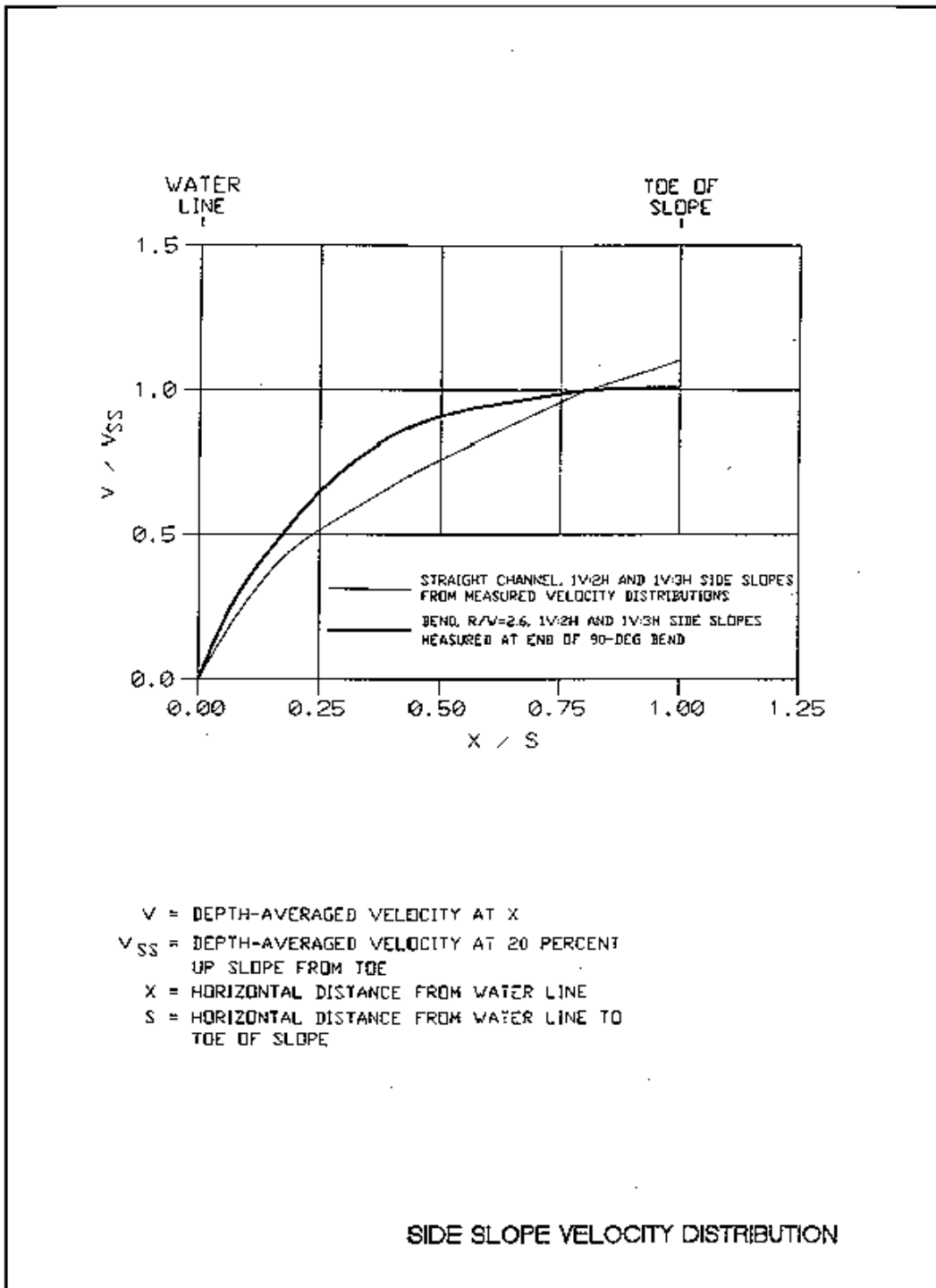
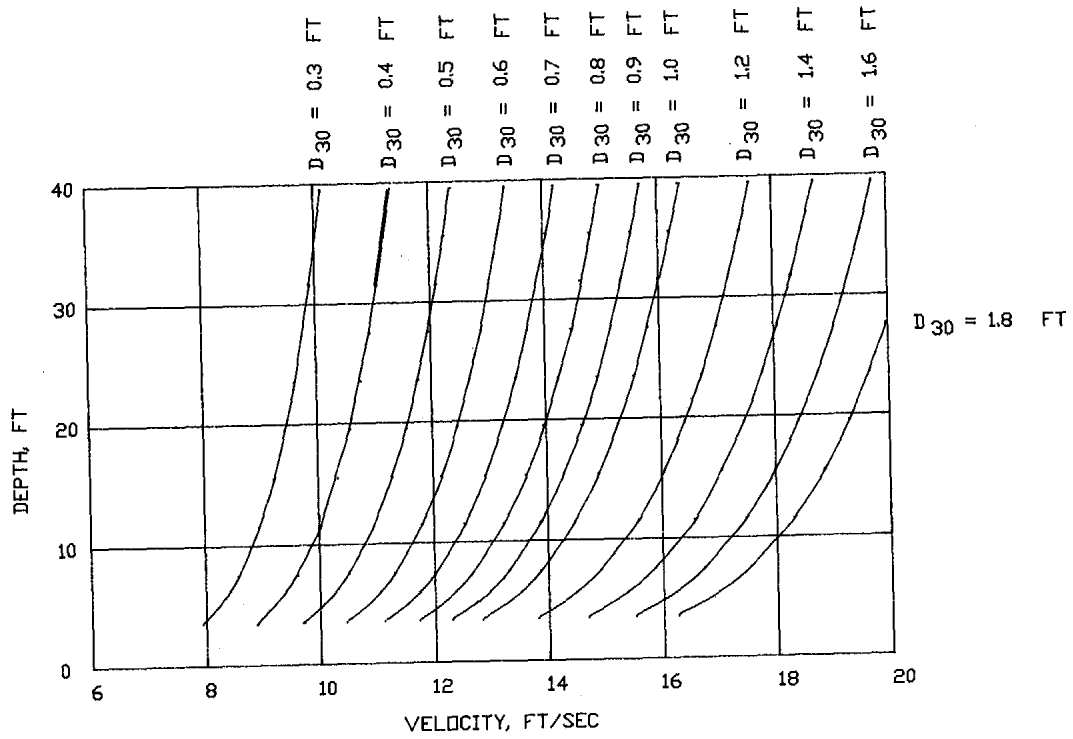


Plate B-36

*

Plate B-37



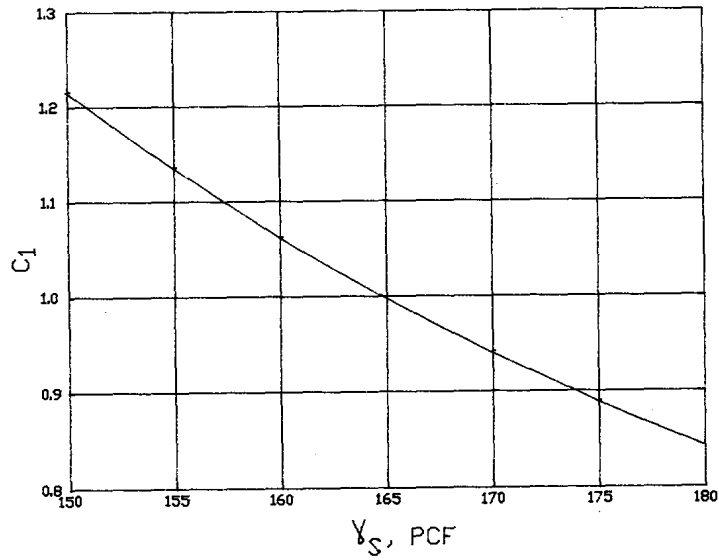
NOTE: APPLICABLE TO THICKNESS $1D_{100}$ (max)
 AND CHANNEL BOTTOMS OR SIDE SLOPES
 FLATTER THAN OR EQUAL TO 1V ON 4H.
 STONE WEIGHT 165 pcf, $C_s = 0.30$, $C_v = C_T = 1.0$
 $S_f = 1.1$ BASED ON EQUATION 3-3.

DEPTH-AVERAGED VELOCITY
 VS D_{30}
 AND DEPTH

*

*

*



$$D_{30} = C_1 * (D_{30} \text{ FROM PLATE 37})$$

WHERE C_1 = CORRECTION FOR UNIT STONE WEIGHT

NOTE: DO NOT MAKE THIS CORRECTION IF
 D_{30} COMPUTED FROM EQUATION 3-3

CORRECTION FOR UNIT STONE WEIGHT

Plate B-38

*

*

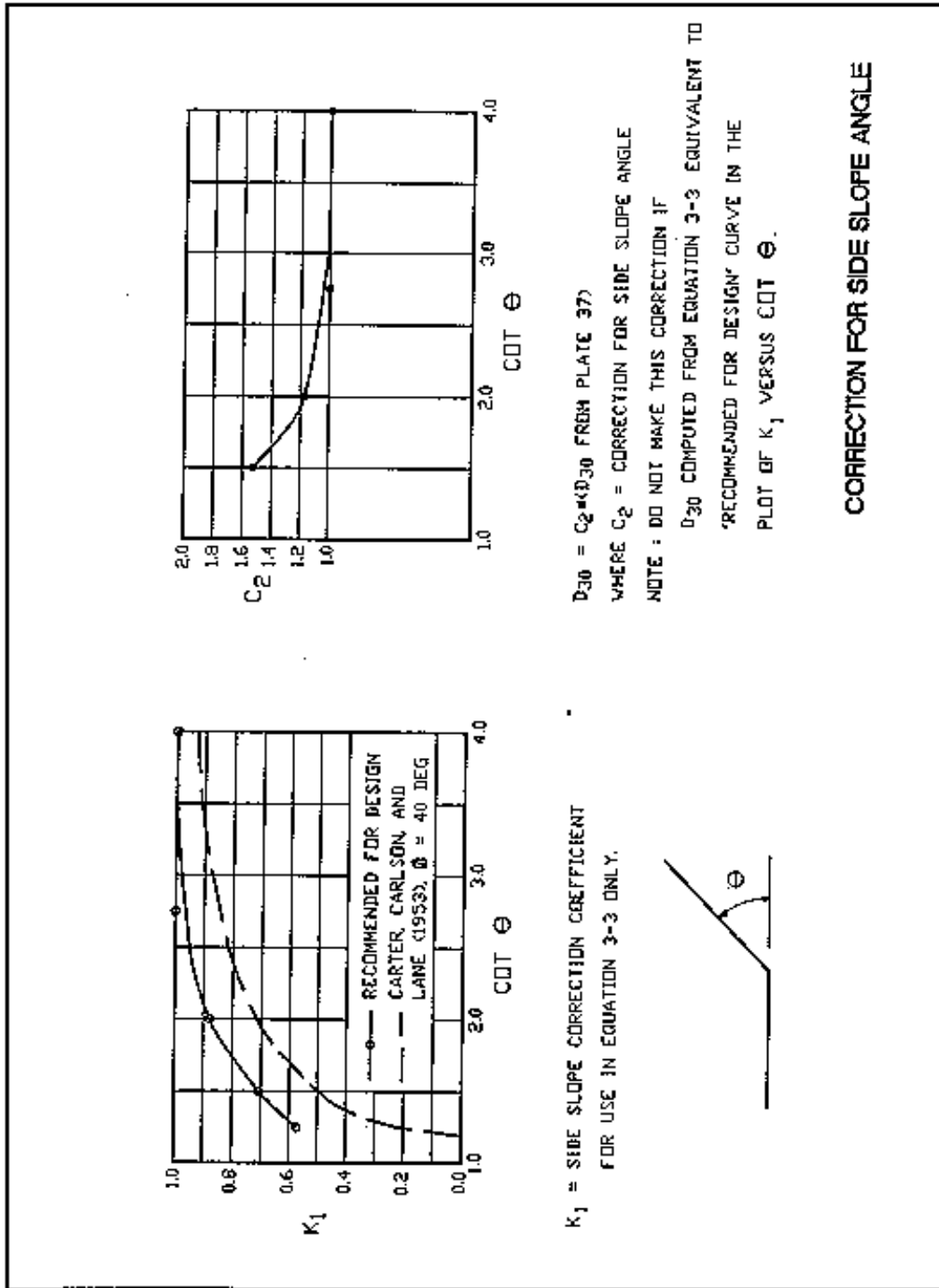
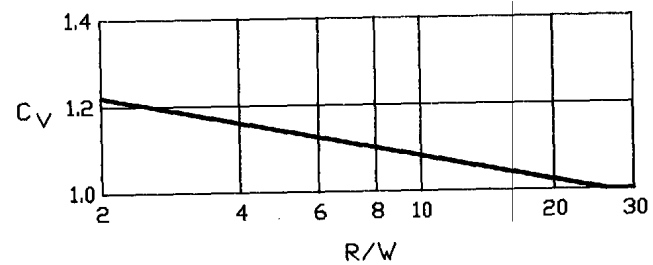
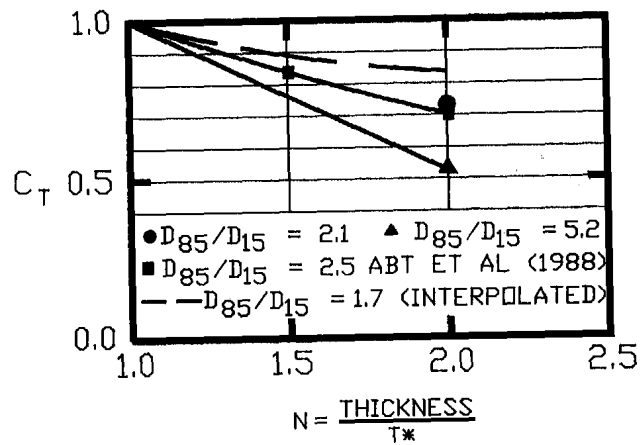


Plate B-39

*



WHERE C_T = CORRECTION FOR THICKNESS

$$= \frac{D_{30} \text{ FOR THICKNESS OF } NT^*}{D_{30} \text{ FOR THICKNESS OF } T^*}$$

$T^* = 1D_{100}$ OR $1.5D_{50}$, WHICHEVER IS GREATER

$$D_{30} = C_V * (D_{30} \text{ FROM PLATE 37})$$

WHERE C_V = CORRECTION FOR VERTICAL VELOCITY DISTRIBUTION

CORRECTION FOR VERTICAL VELOCITY DISTRIBUTION IN BEND AND RIPRAP THICKNESS

Plate B-40

*

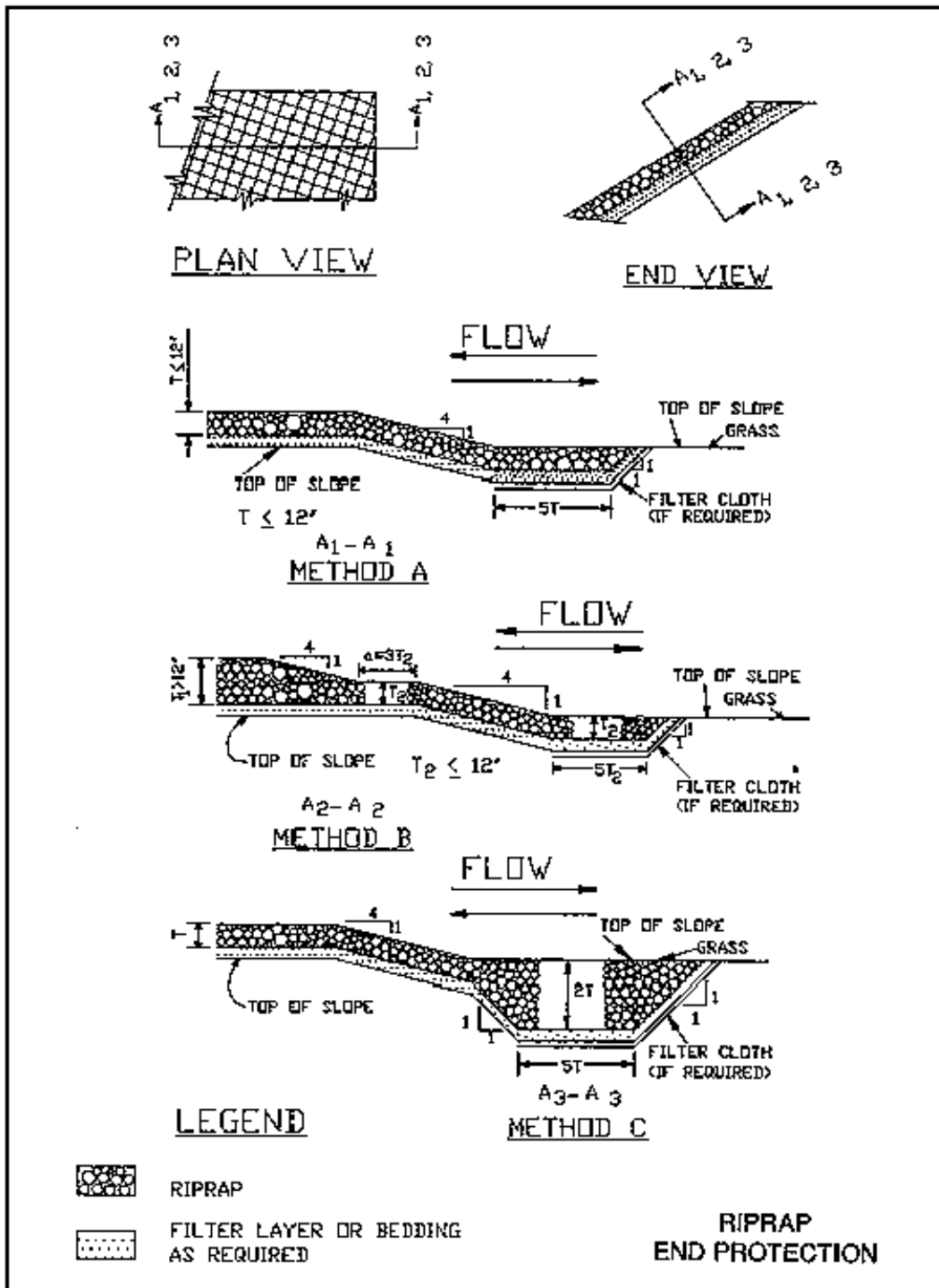


Plate B-41

*

*

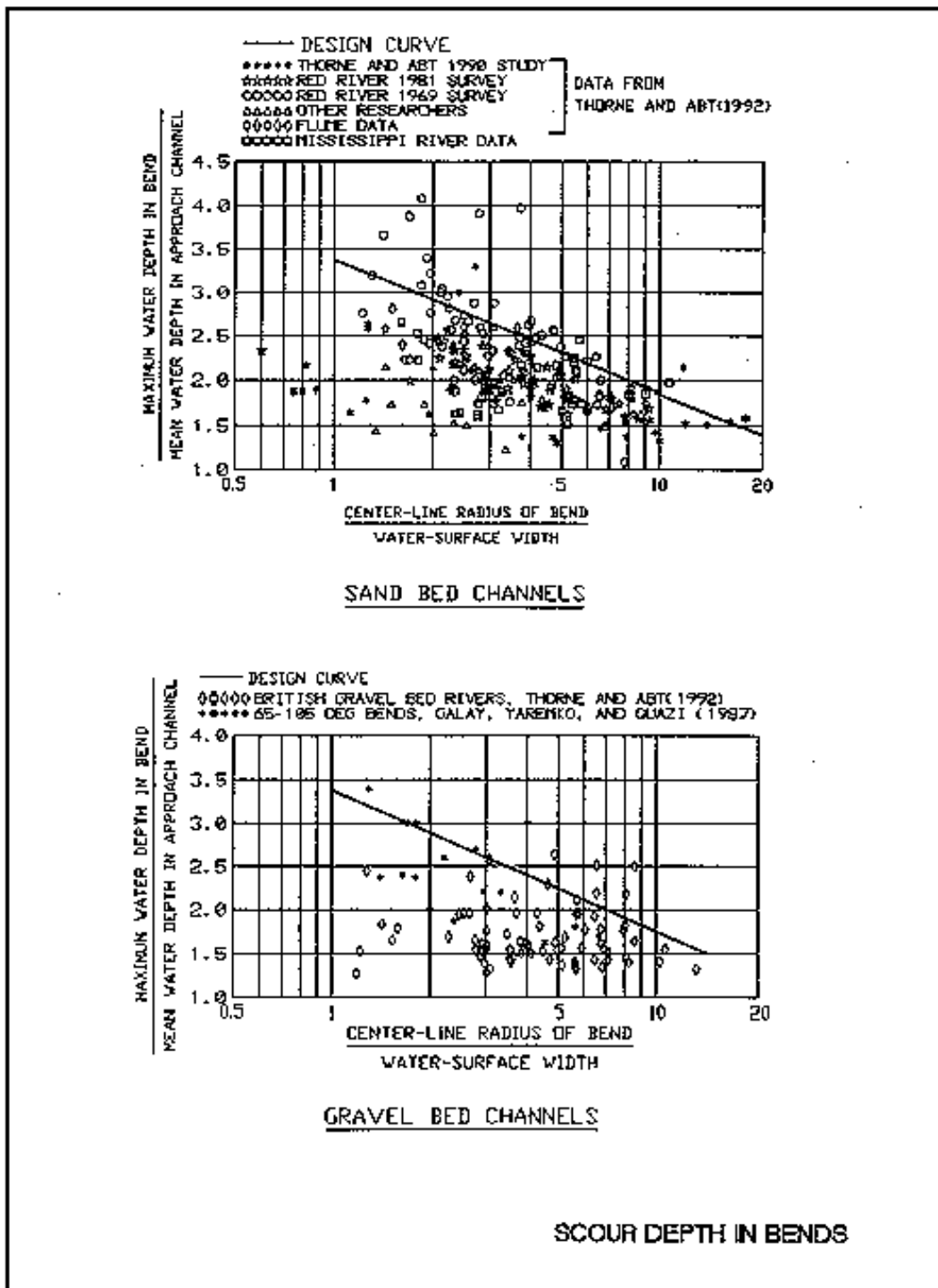


Plate B-41

*

*

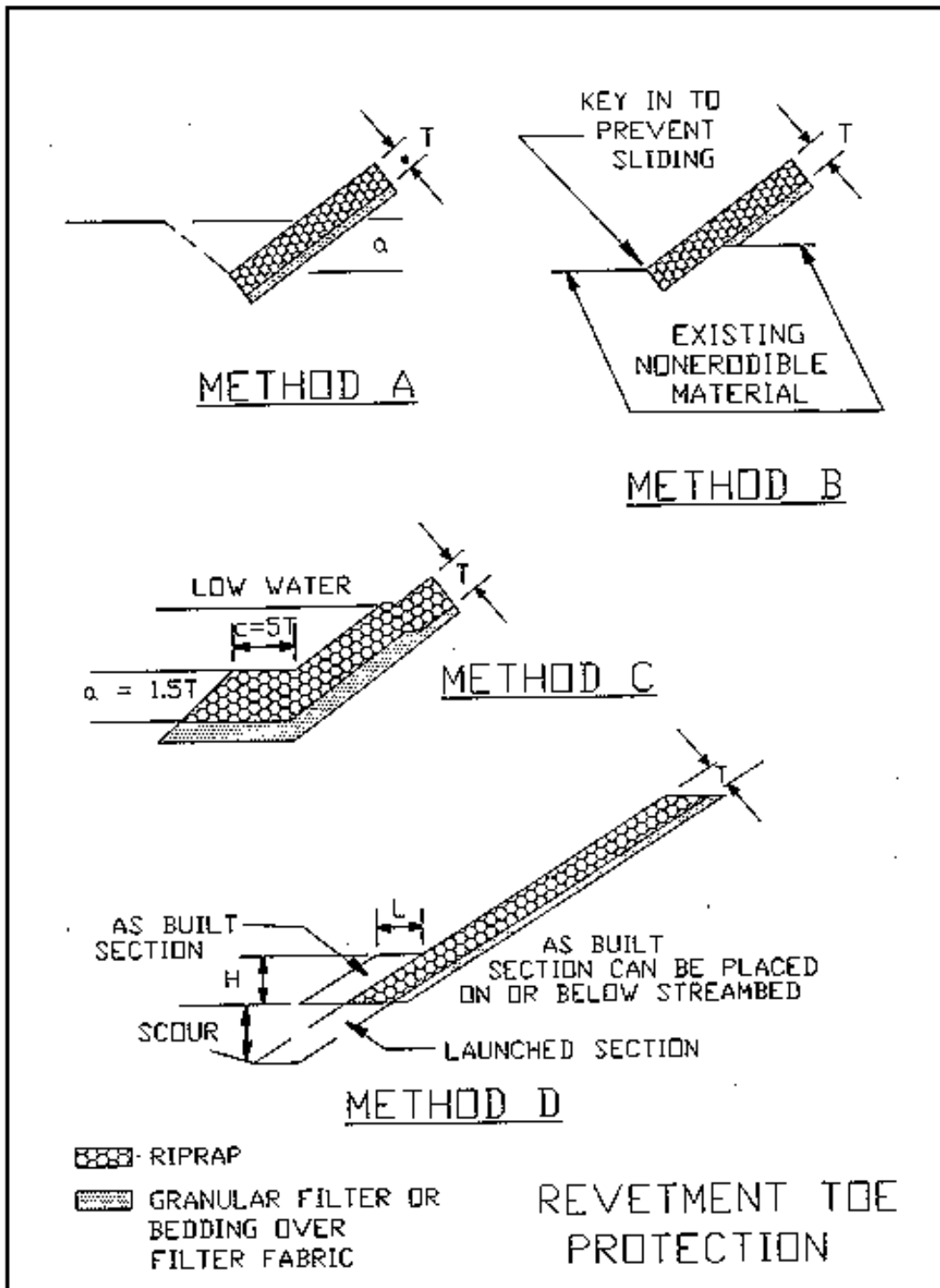
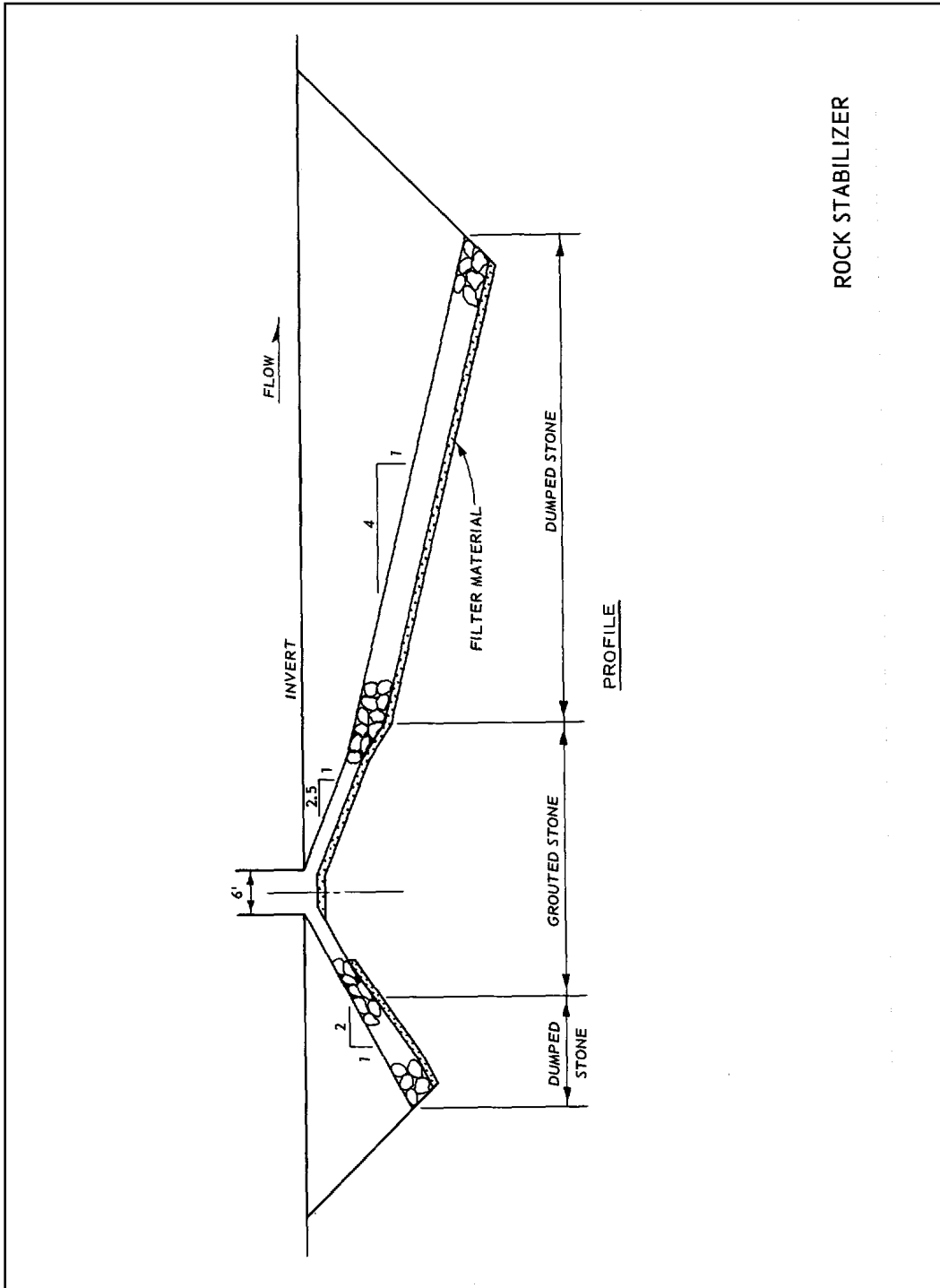


Plate B-43

*

*



ROCK STABILIZER

Plate B-44

*

*

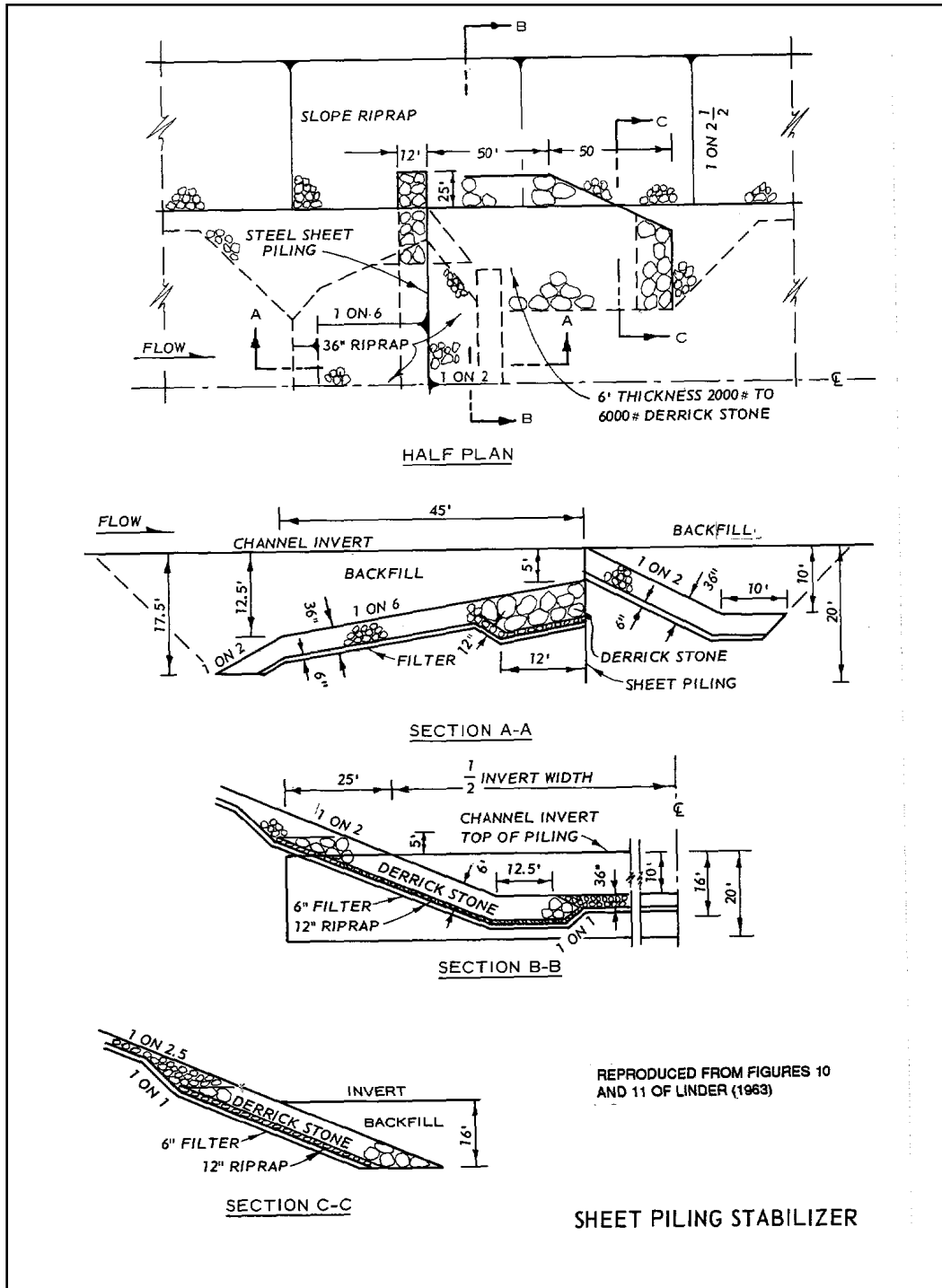
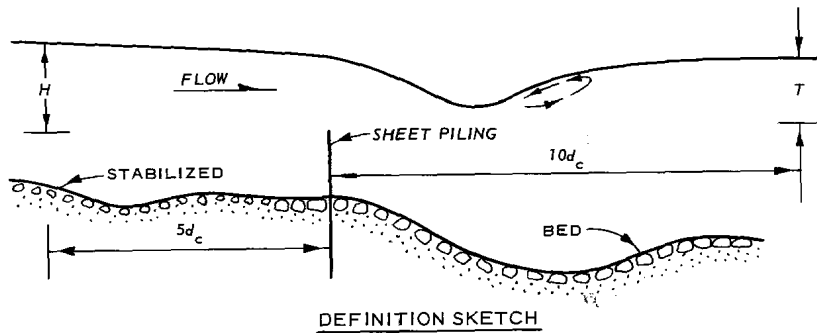
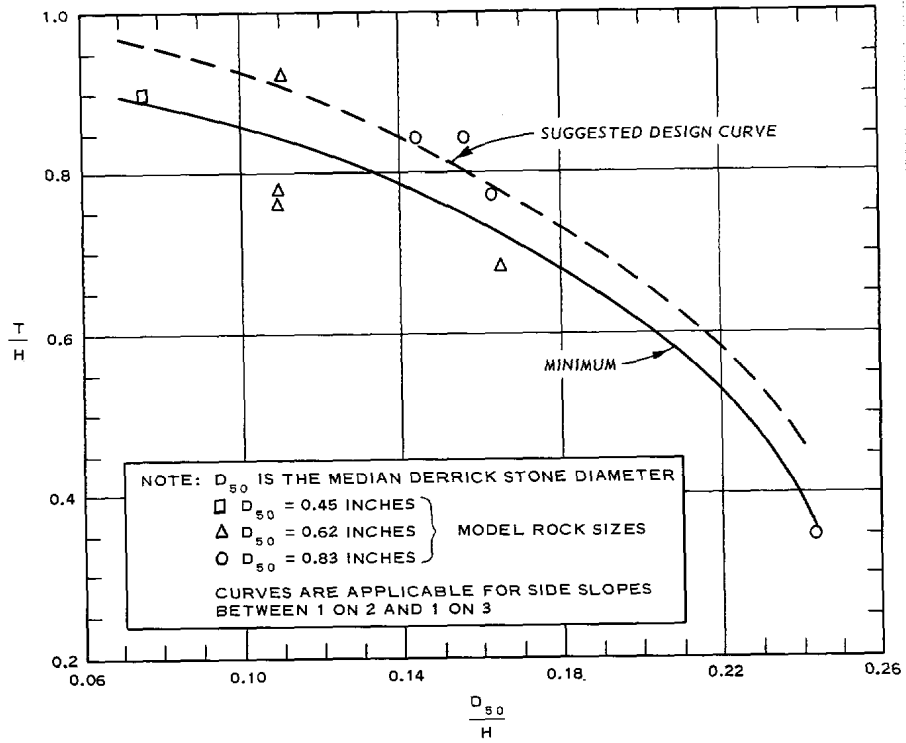


Plate B-45

*

*



GRAPH LIMITED TO

$$\frac{T}{d_c} \geq 0.8$$

d_c = CRITICAL DEPTH

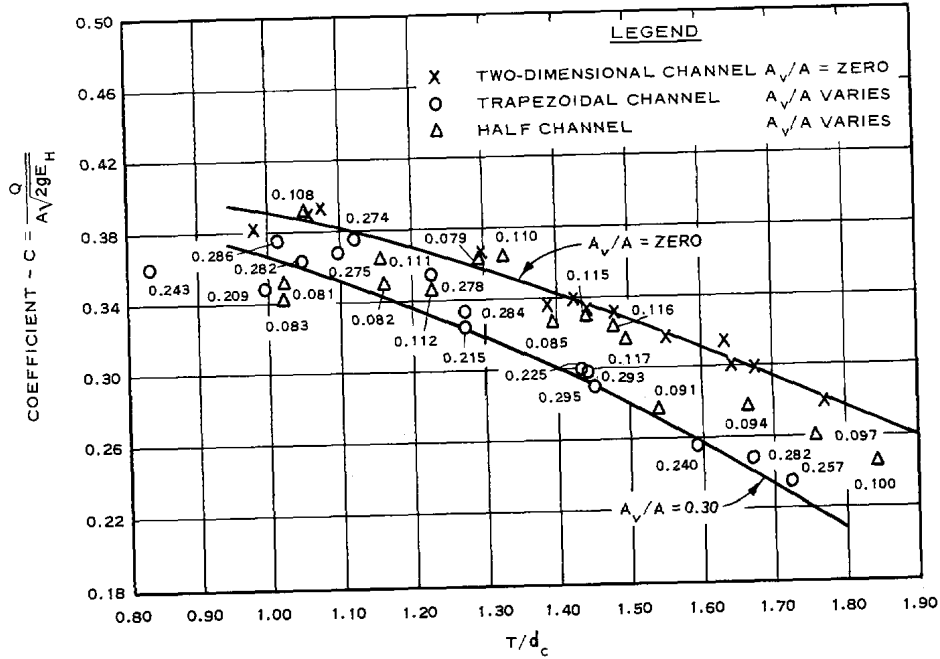
REPRODUCED FROM FIGURE 17, LINDER (1963)

SHEET PILING STABILIZER
DERRICK STONE SIZE

Plate B-46

*

*



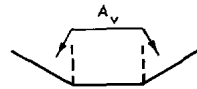
NOTE: $E_H = \frac{Q^2}{2A^2 C^2 g}$

Q = TOTAL DISCHARGE

$E_M = \text{ENERGY} \left(\text{TOTAL HEAD, } H + \frac{V^2}{2g} \right)$
ABOVE THE CREST $5d_c$ UPSTREAM
OF THE CREST

T = TAILWATER DEPTH ABOVE THE
CREST $10d_c$ DOWNSTREAM OF
THE CREST

d_c = CRITICAL DEPTH FOR THE
TRAPEZOIDAL CREST SECTION
CURVE IS APPLICABLE FOR SIDE
SLOPES FROM VERTICAL TO 1 ON 3



A = TOTAL AREA ABOVE THE CREST
AT $5d_c$ UPSTREAM OF THE CREST
 A_v = AREA IN THE END SECTIONS OF
CREST $5d_c$ UPSTREAM OF THE
CREST

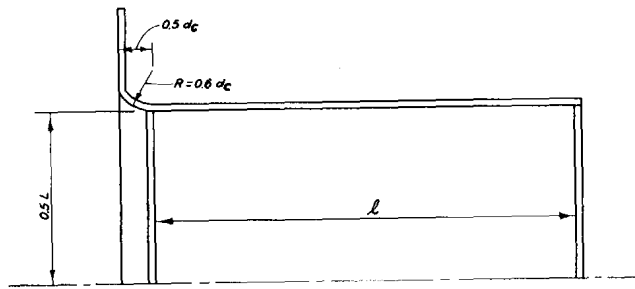
NUMBERS BESIDE THE PLOTTED
POINTS REPRESENT VALUES
OF A_v/A

REPRODUCED FROM FIGURE 16, LINDEF (1963)

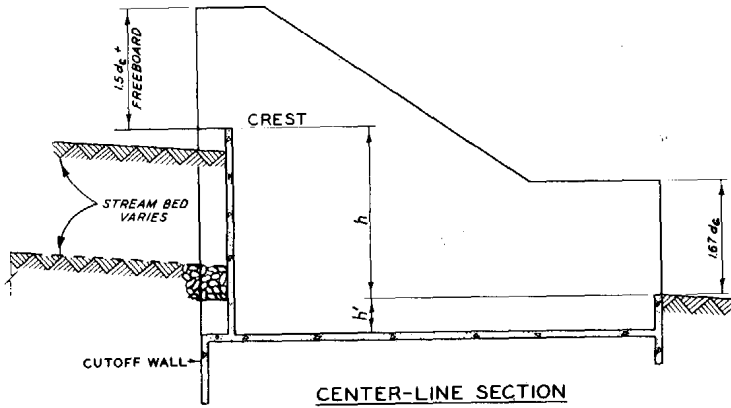
SHEET PILING STABILIZER
ENERGY LOSS

Plate B-47

*

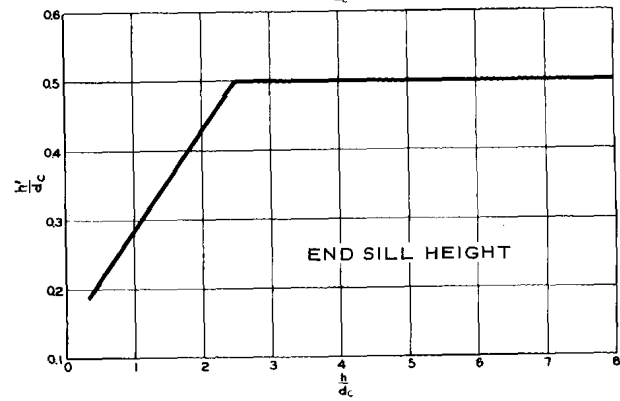
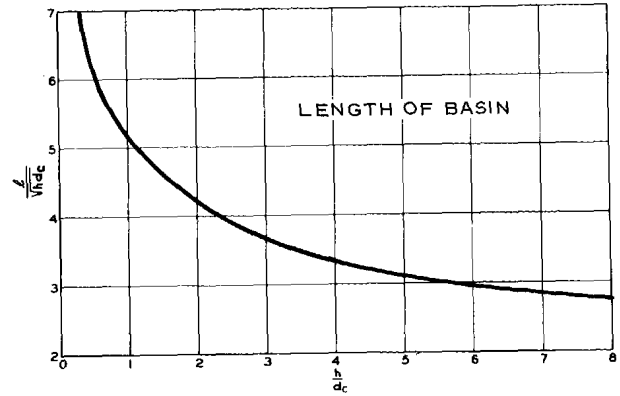


HALF PLAN



CENTER-LINE SECTION

- $c =$ WEIR DISCHARGE = 3.0
- $d_c =$ CRITICAL DEPTH OVER CREST
- $h =$ HEIGHT OF DROP
- $h_1 =$ HEIGHT OF END SILL
- $H =$ HEAD ON WEIR = $3/2(d_c)$
- $l =$ LENGTH OF BASIN
- $L =$ LENGTH OF WEIR CREST
- $Q =$ DISCHARGE, $CLH^{3/2}$



DETAILS AND DESIGN CHART FOR TYPICAL DROP STRUCTURE

*

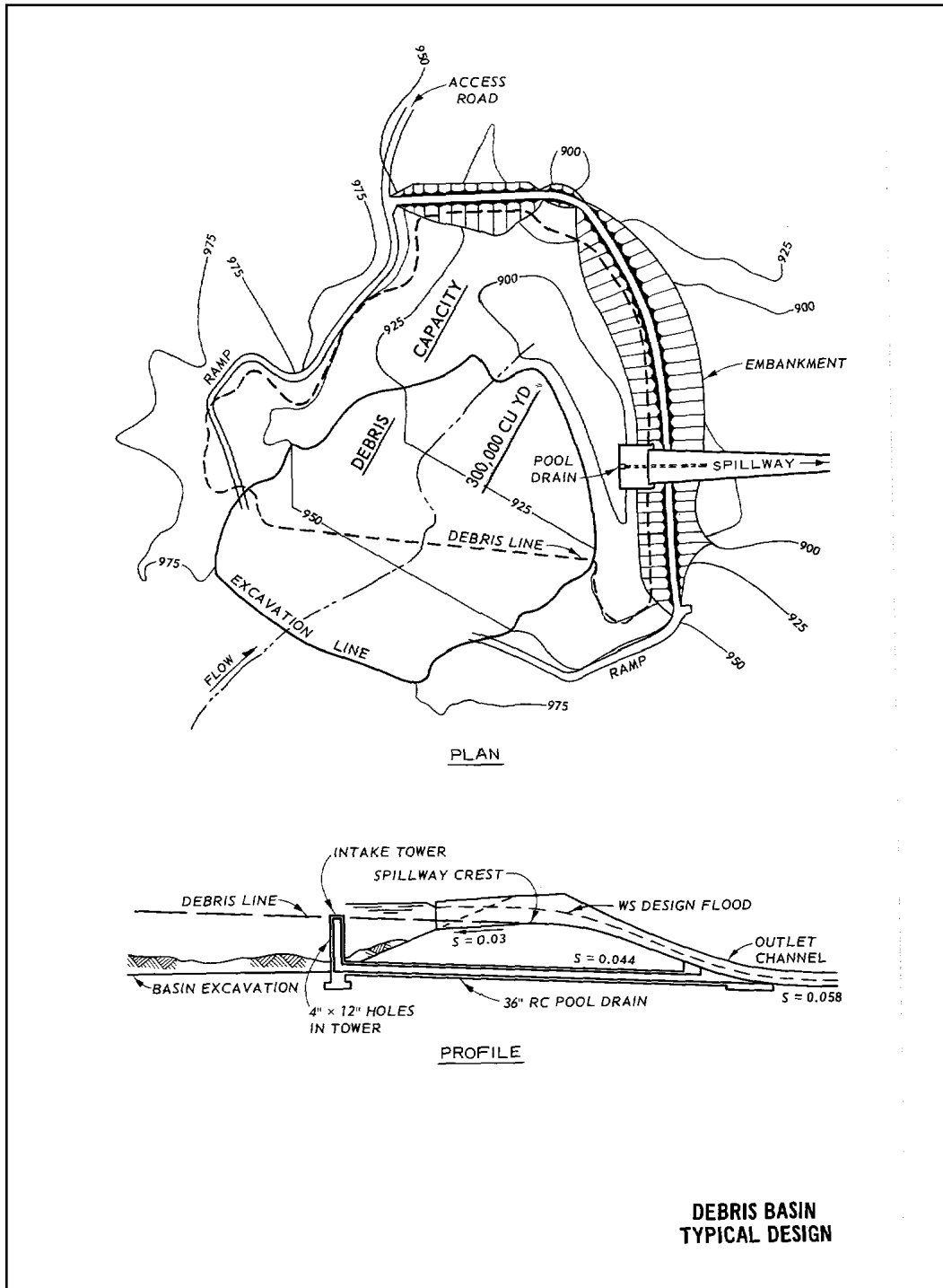
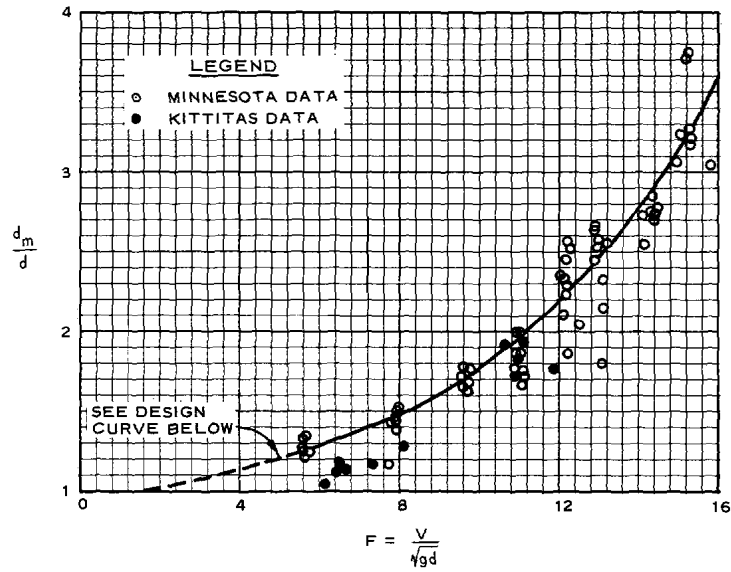


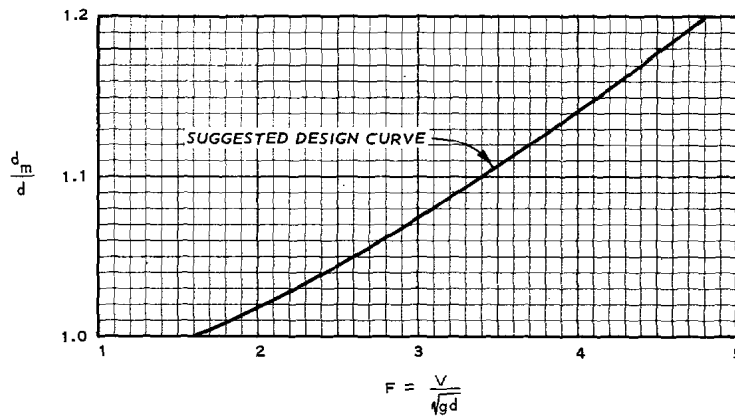
Plate B-49

*

*



a. EXPERIMENTAL DATA



b. DESIGN CURVE

NOTE: d_m = DEPTH OF WATER AND AIR MIXTURE
 d = COMPUTED DEPTH FOR NON-AERATED FLOW
 V = COMPUTED VELOCITY FOR NON-AERATED FLOW
 g = GRAVITATIONAL ACCELERATION
 F = FROUDE NUMBER FOR NONAERATED FLOW

AIR ENTRAINMENT

Plate B-50

*

*

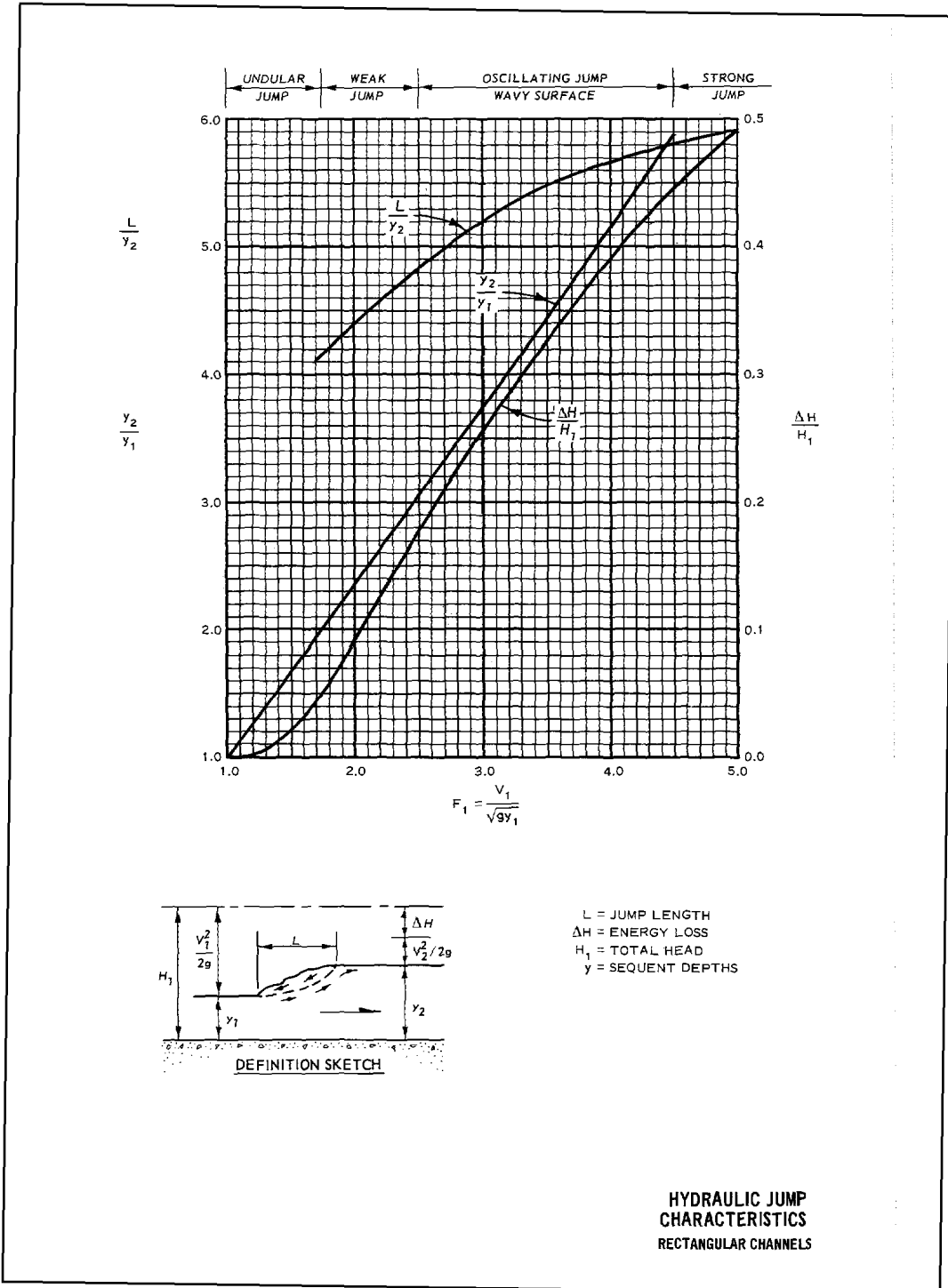
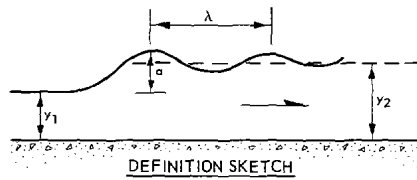
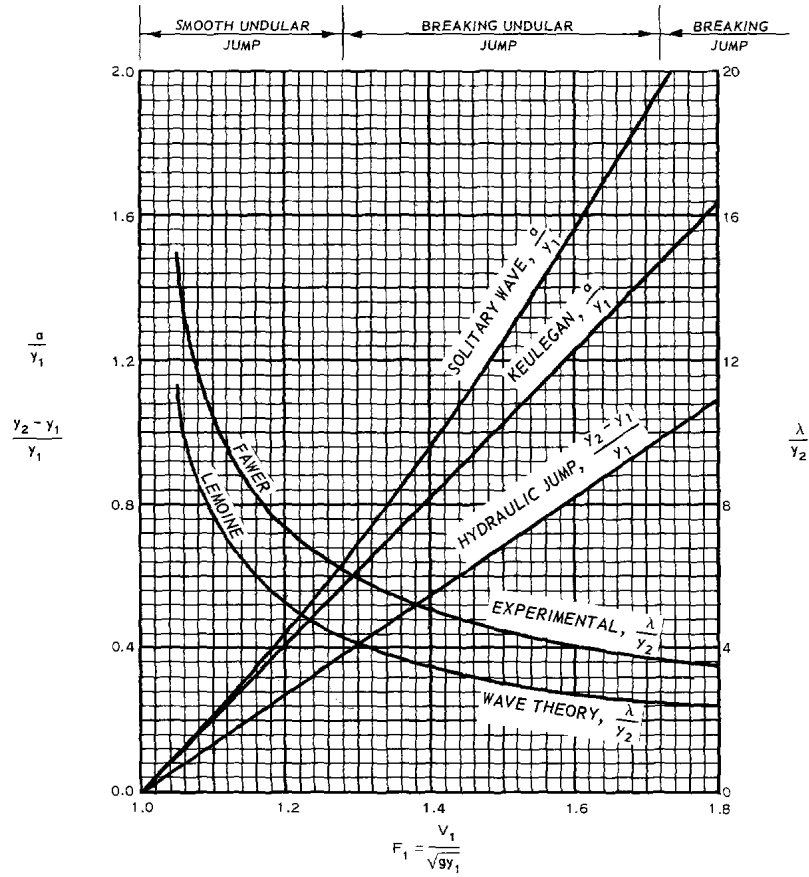


Plate B-51

*

*



λ - WAVE LENGTH
 a - WAVE HEIGHT
 y - FLOW DEPTH

NOTE: FAWER AND LEMOINE CURVES FROM JAEGER (1957).
KEULEGAN CURVE FROM KEULEGAN AND PATTERSON (1940).

UNDULAR JUMP
RECTANGULAR CHANNEL

*

*

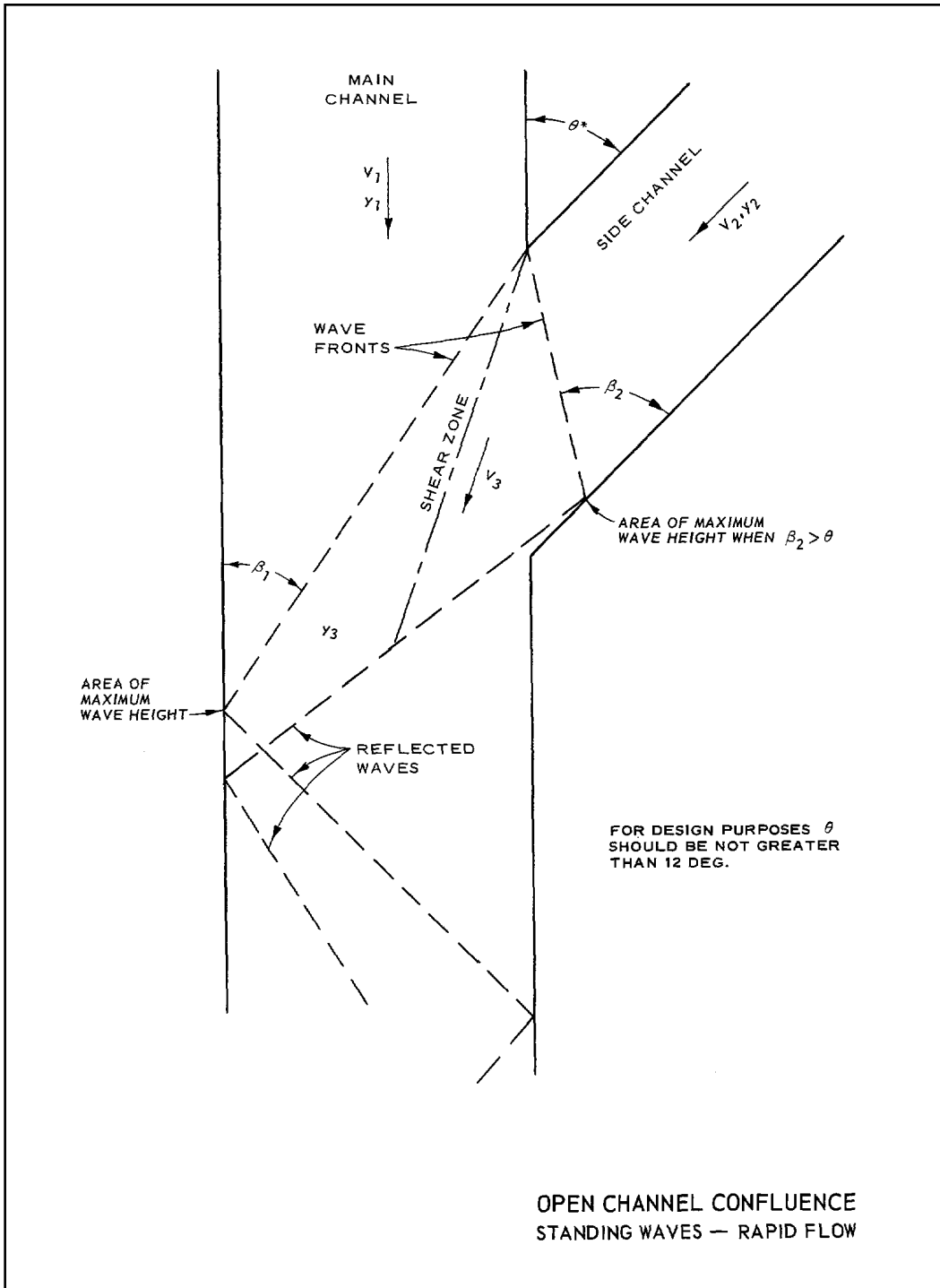
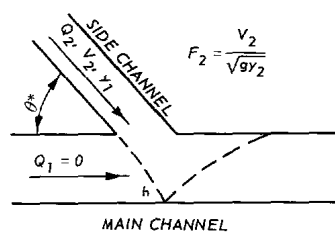
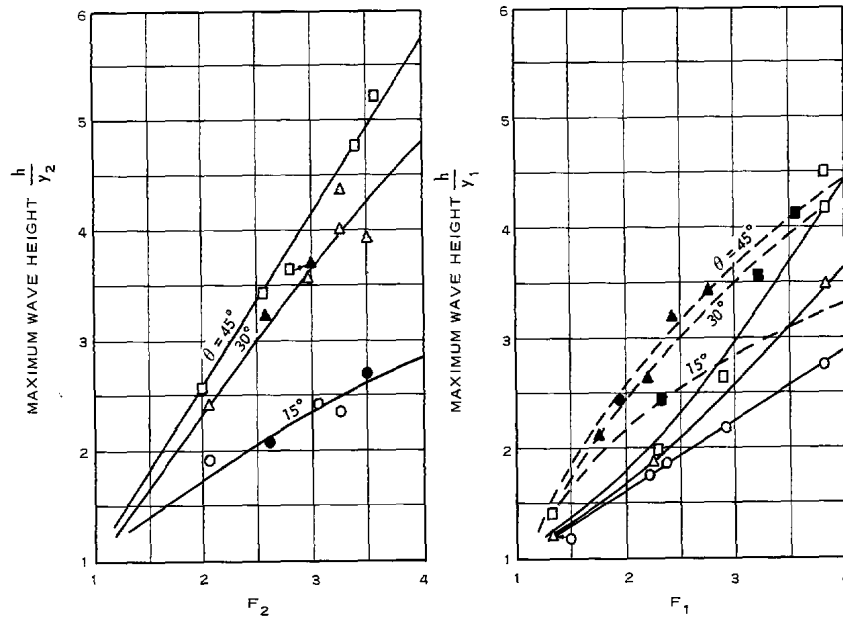


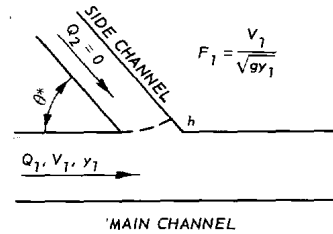
Plate B-53

*

*



a. SIDE CHANNEL FLOW ONLY



b. MAIN CHANNEL FLOW ONLY

FOR DESIGN PURPOSES θ SHOULD NOT
BE GREATER THAN 12 DEG

NOTE: 1. DATA AND CURVES BASED ON
FIGURES 10-12, BEHLKE AND PRITCHETT (1966).

2. \square \circ \triangle TRAPEZOIDAL CHANNELS
 \blacksquare \bullet \blacktriangle RECTANGULAR CHANNELS

MAXIMUM WAVE HEIGHT
CHANNEL JUNCTION

Plate B-54

*

*

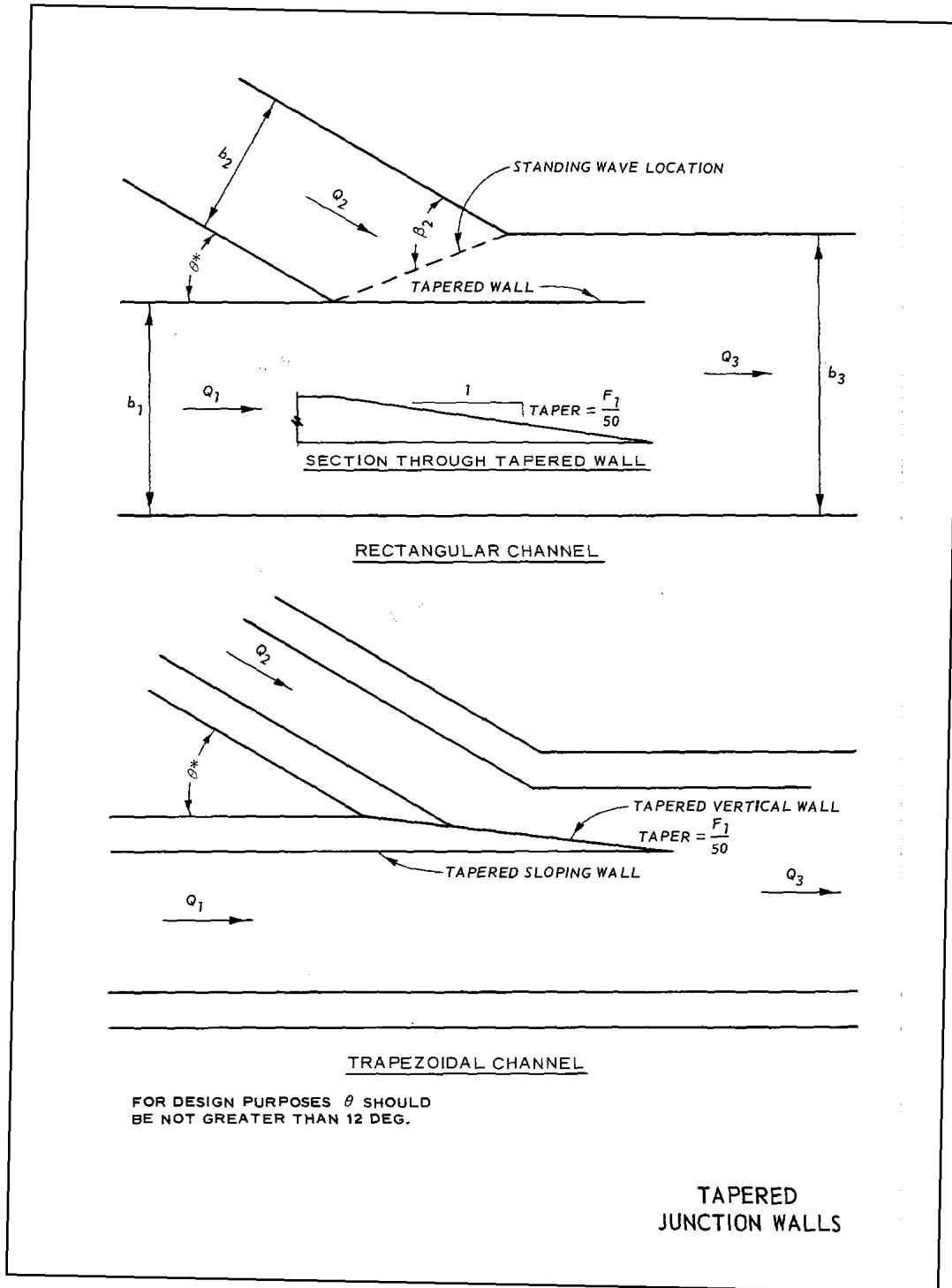


Plate B-55

*

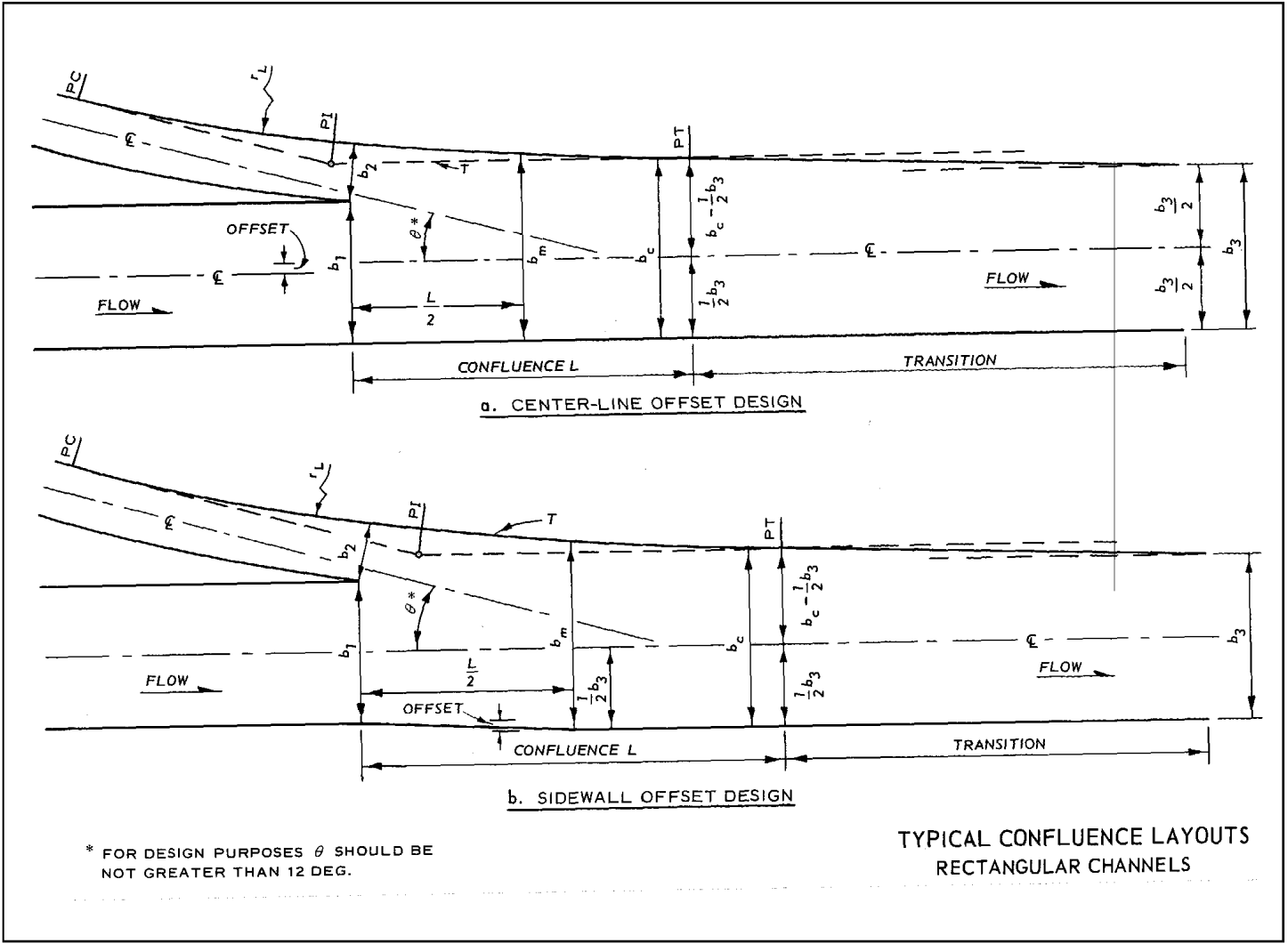


Plate B-56

*

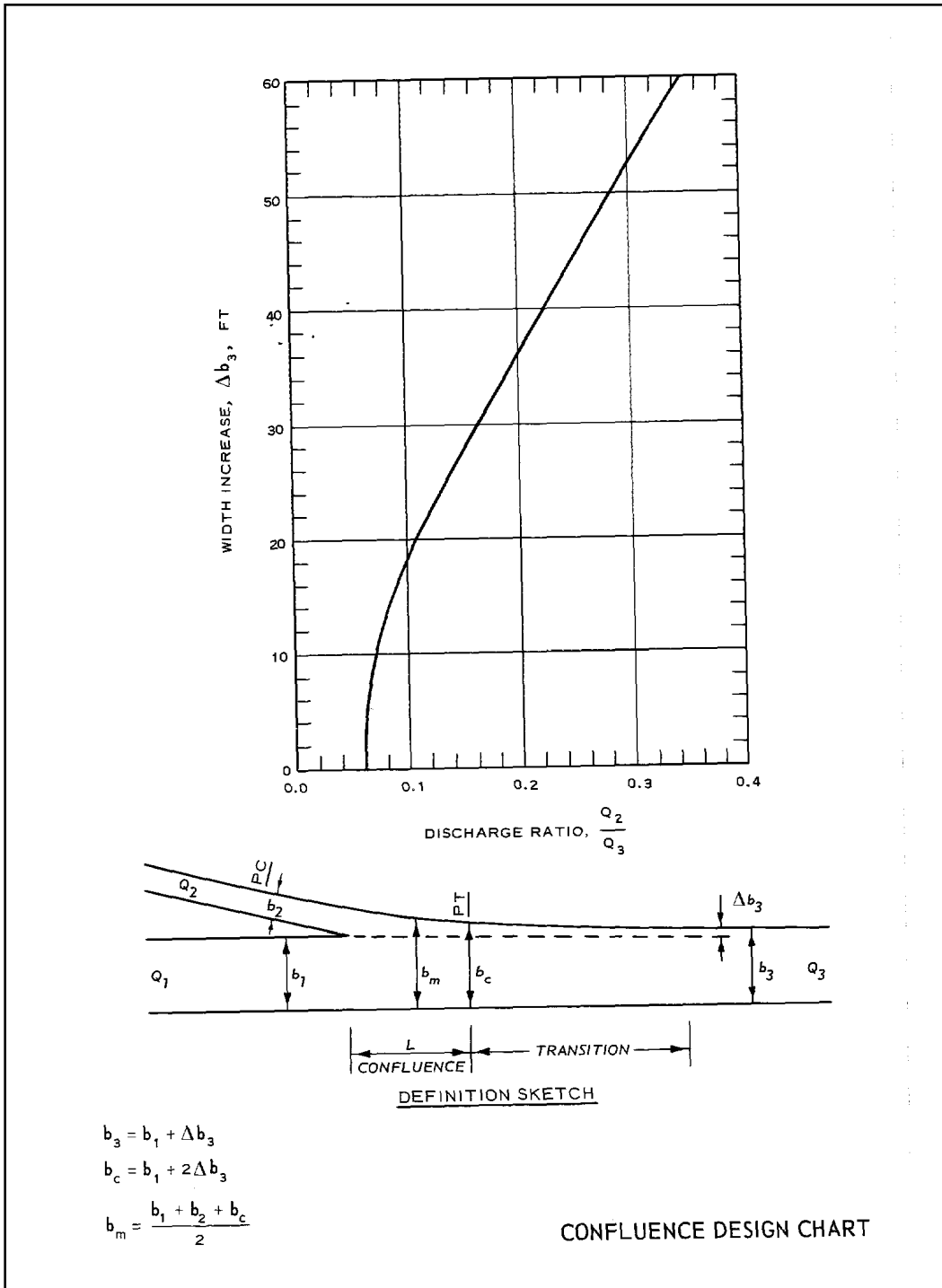
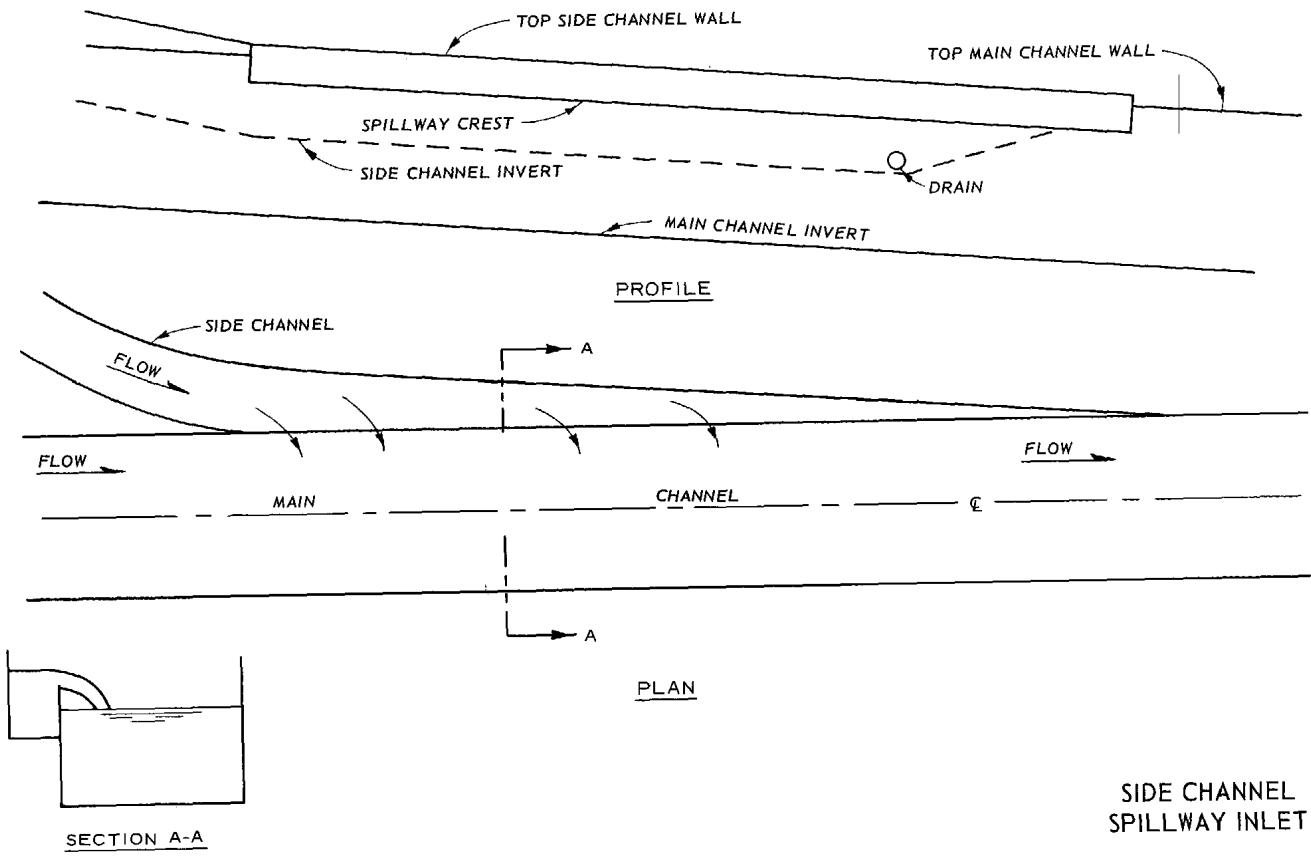


Plate B-57

*



SIDE CHANNEL SPILLWAY INLET

Appendix C Notes on Derivation and Use of Hydraulic Properties by the Alpha Method

C-1. General

The Alpha method for determining the local boundary shear and composite roughness is applicable to uniform and gradually varied flow problems. Computations for effective average channel roughness k with and without considering the energy correction factor are included as well as computations for Manning's n . The necessary basic equations and a computation procedure are given in the paragraphs that follow. Illustrations of the Alpha method applied to the effective channel roughness problem are given in Plates C-1 through C-4.

C-2. Basic Procedure and Equations

a. The cross section (Plate C-1) is divided into subsections bounded by vertical lines extending from water surface to the wetted perimeter. The mean velocity in the vertical of the subsection is given by V_n and the subsection discharge by $V_n A_n$. The integer subscript n defines the channel subsection. As explained in paragraph 6-5 of Chow (1959),¹ a simplifying assumption becomes necessary. It is assumed that the energy grade line has the same slope across the entire cross section, that S in the familiar Chezy equation ($V = C(RS)^{1/2}$) is constant at each subsection, and that the following proportion may be written

$$V_n \propto (CR^{1/2})_n \quad (C-1)$$

where C is Chezy's coefficient and R is the hydraulic radius.

b. The resistance equation for hydraulically rough channels (paragraph 2-2(c)) is

$$C = 32.6 \log_{10} \frac{12.2R}{k} \quad (C-2)$$

where

C = Chezy's coefficient

R = hydraulic radius, ft

k = equivalent roughness dimension, ft

This equation is plotted in Plate C-2.

c. As $(CR^{1/2})_n$ is proportional to V_n , then $(CR^{1/2})_n A_n$ is proportional to Q_n .² From this the following equations are derived

$$Q_n = \frac{Q_T (CR^{1/2})_n A_n}{\sum [(CR^{1/2})_i A_i]} \quad (C-3)$$

$$V_n = \frac{Q_T (CR^{1/2})_n}{\sum [(CR^{1/2})_i A_i]} \quad \text{or} \quad \frac{Q_n}{A_n} \quad (C-4)$$

$$(CR^{1/2})_{\text{mean}} = \frac{\sum [(CR^{1/2})_i A_i]}{\sum A_i} \quad (C-5)$$

$$S = \frac{\bar{V}^2}{[(CR^{1/2})_{\text{mean}}]^2} \quad (C-6)$$

$$\bar{R} = \frac{\sum [R_i (CR^{1/2})_i A_i]}{\sum [(VR^{1/2})_i A_i]} \quad (C-7)$$

where

Q_n = discharge in subsection, cfs

Q_T = total discharge, cfs

¹ References cited in this appendix are listed in Appendix A.

² The subscript i assumes all values of n .

1 Jul 91

A = cross-sectional area, ft^2

\bar{V} = flow velocity in subsection, fps

\bar{R} = hydraulic radius of subsection

C-3. Backwater Computation

a. All the cross-section hydraulic parameters necessary for backwater computations are computed in Plates C-2 and C-3. Computing the same parameters at several water-surface elevations and plotting the results permits ready interpolation for intermediate values. The method is programmed for digital computer use if manual computations for a particular project are too time consuming.

b. The boundary and hydraulic characteristics of a channel reach are assumed to be those obtained by averaging the conditions existing at each end of the reach. This procedure implies that the roughness dimensions k assigned to the upstream and downstream sections extend to the midsection of the reach. Therefore, it is important that the reach limits be carefully selected. Two different sets of subsection roughness values should be assigned in cases where the boundary condition changes abruptly such as at the beginning or end of an improved reach. One set of values would apply in the improved reach and the other in the natural channel.

C-4. Roughness Relation

The roughness dimension k may be taken as equivalent spherical diameter of the average size bed material when the hydraulic losses in the flow regime are attributable to friction alone. In a flow regime where hydraulic losses in addition to friction are present, k may still be used if the losses result in a reasonably uniform slope of the energy grade line. In this case, k will be larger dimensionally than the equivalent spherical diameter of the average size bed material. As Chezy C and Manning's n are equatable ($C/1.486 = R^{1/6}/n$), k may be determined from a knowledge of Manning's coefficient n . While k remains fairly constant with changing R , n varies with the onesixth power of R . Therefore, it is better to extrapolate from known conditions to unknown by the use of k rather than n . The k must be evaluated for each subsection. Subsections should be chosen with this in mind so that differing bed materials or bed conditions producing frictionlike losses, such as ripples, dunes, or other irregularities will appear in separate subsections.

Hydraulic losses tending to cause breaks in the energy grade line, such as expansion and contraction, should be evaluated separately. Computations are presented in Plate C-4 showing the use of the Alpha computation results for determining an effective channel k value and the relation between k and n .

C-5. Energy Correction Factor

The velocity head correction factor (Brater and King 1976) is expressed as

$$\alpha = \frac{1}{AV^3} \int_0^A V_x^3 dA \quad (\text{C-8})$$

where

α = velocity head correction factor

V = mean velocity of the section

V_x = mean velocity in the vertical at horizontal location x throughout the cross section

The mean velocity may be expressed

$$V = \frac{\int_0^A V_x dA}{A} \quad (\text{C-9})$$

Substituting Equation C-9 in C-8 yields

$$\alpha = \frac{A^2 \int_0^A V_x^3 dA}{\left(\int_0^A V_x dA \right)^3} \quad (\text{C-10})$$

Substituting the relation given by Equation C-1 into Equation C-10 yields

$$\alpha = \frac{A^2 \int_o^A (CR^{1/2})_x^3 dA}{\left[\int_o^A (CR^{1/2})_x dA \right]^3} \quad (C-11)$$

$$\alpha = \frac{A^2 \sum [(CR^{1/2})_n^3 A_n]}{\left[\sum (CR^{1/2})_i A_i \right]^3} \quad (C-12)$$

or

Computations illustrating the application of the Alpha method for determining the energy correction factor α are given in Plate C-4. In addition, the effect of the energy correction factor on the apparent average channel roughness value is shown.

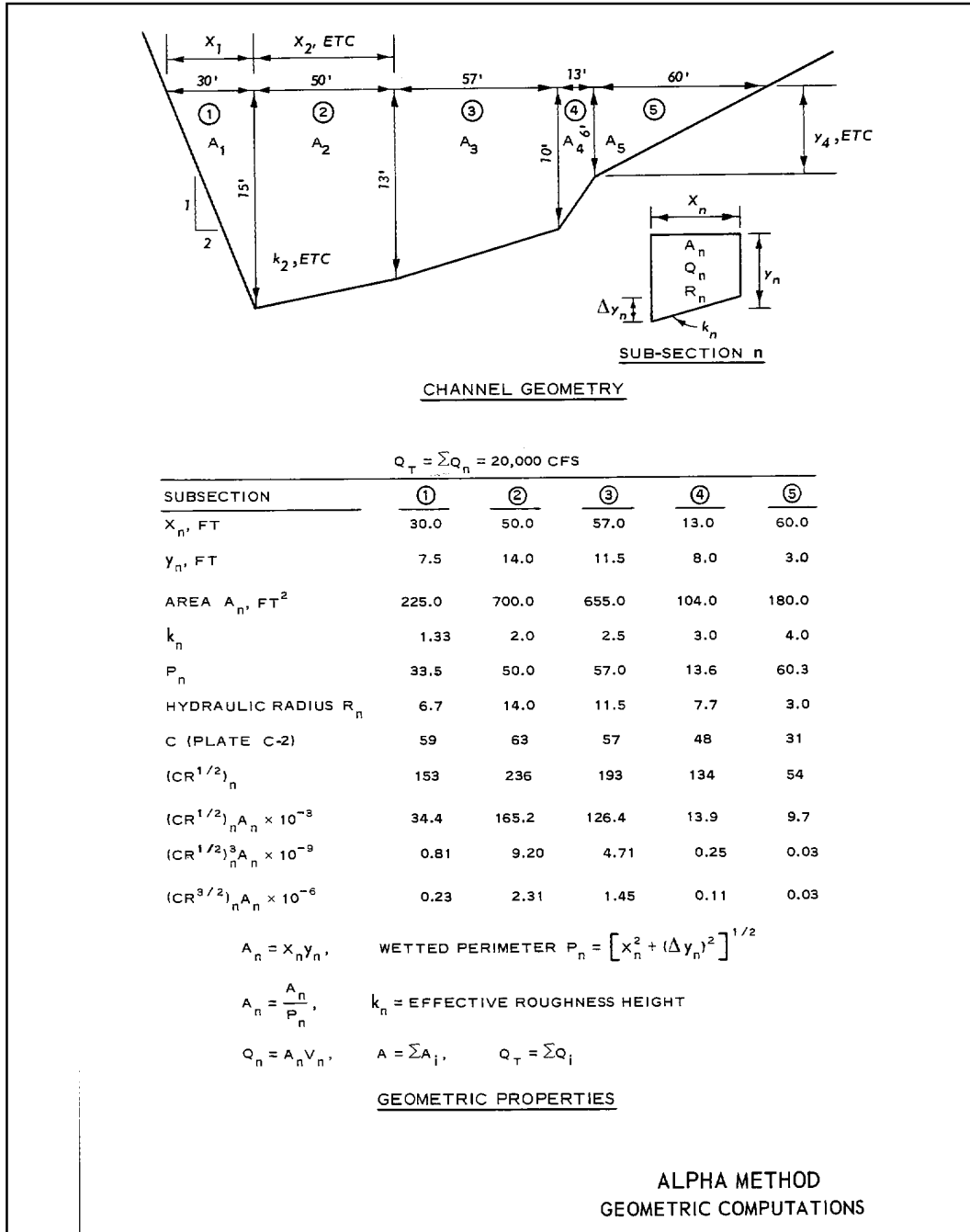
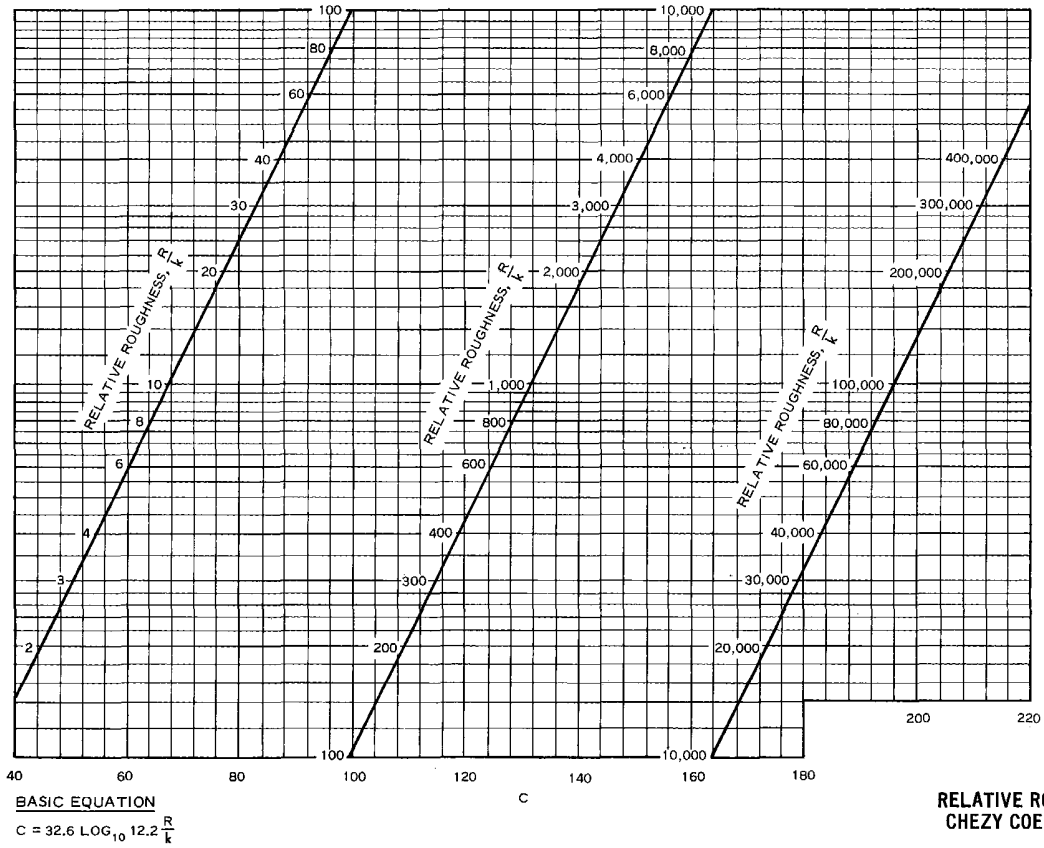


PLATE C-1

PLATE C-2



1. CALCULATE THE AVERAGE VELOCITY, \bar{V} .

$$\bar{V} = Q_T / A$$

$$\bar{V} = (20,000) / (1864.0) = 10.7 \text{ FPS}$$

2. CALCULATE THE DISCHARGE THROUGH EACH SUB-SECTION, Q_n .

$$Q_n = \frac{Q_T (CR^{1/2})_n A_n}{\sum [(CR^{1/2})_i A_i]} = \frac{20,000 (CR^{1/2})_n A_n}{349,600}$$

$$Q_1 = 0.0572(34400) = 1968 \text{ CFS}$$

$$Q_2 = 0.0572(165200) = 9449$$

$$Q_3 = 0.0572(126400) = 7230$$

$$Q_4 = 0.0572(13900) = 795$$

$$Q_5 = 0.0572(9700) = 555$$

$$\sum Q_n = 19,997$$

3. CALCULATE THE VELOCITY THROUGH EACH SUB-SECTION

$$V_n = \frac{Q_n}{A_n}$$

$$V_1 = (1968) / (225.0) = 8.7 \text{ FPS}$$

$$V_2 = (9449) / (700.0) = 13.5$$

$$V_3 = (7230) / (655.0) = 11.0$$

$$V_4 = (795) / (104.0) = 7.6$$

$$V_5 = (555) / (180.0) = 3.1$$

4. CALCULATE THE MEAN SLOPE OF ENERGY GRADE LINE, S .

$$S = \frac{(\bar{V})^2}{(CR^{1/2})_{\text{MEAN}}^2}$$

$$(CR^{1/2})_{\text{MEAN}} = \frac{\sum [(CR^{1/2})_i A_i]}{A} = \frac{349,600}{1864.0} = 188$$

$$S = (10.7)^2 / (188)^2 = 0.00324$$

5. CALCULATE THE MEAN HYDRAULIC RADIUS, \bar{R} .

$$\bar{R} = \frac{\sum [(CR^{3/2})_i A_i]}{\sum [(CR^{1/2})_i A_i]}$$

$$\bar{R} = (4.13 \times 10^6) / (0.3496 \times 10^6) = 11.8 \text{ FT}$$

6. CALCULATE THE AVERAGE SHEAR FORCE $\bar{\tau}_0$

$$\bar{\tau}_0 = \gamma \bar{R} S$$

$$= (62.5)(11.8)(0.00324) = 2.39 \text{ LB/FT}^2$$

ALPHA METHOD
HYDRAULIC PROPERTIES

PLATE C-3

1. CALCULATE ENERGY CORRECTION FACTOR

$$\alpha = \frac{A^2 \sum [(CR^{1/2})_i^3 A_i]}{[\sum (CR^{1/2})_i^3 A_i]}$$

FROM PLATE C-1

$$A^2 = (\sum A_i)^2 = (1864.0)^2 = 3.47 \times 10^6$$

$$\sum [(CR^{1/2})_i^3 A_i] = 15.00 \times 10^9$$

$$[\sum (CR^{1/2})_i^3 A_i]^3 = (349.6 \times 10^3)^3 = 42.7 \times 10^{15}$$

$$\alpha = \frac{(3.474 \times 10^6)(15.00 \times 10^9)}{42.7 \times 10^{15}} = 1.22$$

2. EFFECTIVE k (α NEGLECTED)

$$C^2 = 32.6 \log_{10} 12.2 \frac{R}{k} = \frac{V\bar{V}^2}{\bar{V}_0}$$

FOR $\bar{V} = 10.7$ AND $\bar{V}_0 = 2.39$ (PLATE C-3)

$$C = \frac{(62.5 \times 10.7^2)^{1/2}}{2.39} = 54.7$$

FOR $C = 54.7$, $\frac{R}{k} = 3.9$ (PLATE C-2)

FOR $\bar{R} = 11.8$ (PLATE C-3)

$$k = 3.03 \text{ FT}$$

3. EFFECTIVE k (α CONSIDERED)

$$\alpha \frac{\bar{V}^2}{2g} = \frac{(1.22)(10.7)^2}{64.4} = 2.17 \text{ FT}$$

$$V^1 = (64.4 \times 2.17)^{1/2} = 11.8 \text{ FPS}$$

$$C = \frac{[(62.5)(11.8)^2]^{1/2}}{2.39} = 60.3$$

$$\frac{R}{k} = 5.8 \quad (\text{PLATE C-2})$$

$$k = 2.03 \text{ FT FOR } \bar{R} = 11.8 \text{ FT}$$

4. CALCULATE MANNING'S n (α NEGLECTED)

$$n = \frac{1.486 \bar{R}^{-2/3} S^{1/2}}{\bar{V}} = \frac{(1.486)(11.8)^{-2/3}(0.00324)^{1/2}}{10.7}$$

$$= 0.041$$

ALPHA METHOD
BACKWATER COMPUTATION DATA

PLATE C-4

Appendix D Computer Program for Designing Banked Curves for Supercritical Flow in Rectangular Channels

D-1. Introduction

a. General. The design of curves for supercritical flow may include several alternatives which produce curves that perform satisfactorily for the design flow and that are compatible with existing field conditions. The solution for any one alternative is time consuming, requiring trial-and-error computations. The alternative designs described in this appendix include basic limiting design criteria developed by the US Army Engineer District (USAED), Los Angeles. Combining the results of two or more of these alternatives should produce a satisfactory design for nearly any condition. A list of symbols used in the program (Plate D-1), a program listing (Plate D-2), a program flow chart (Plate D-3), subroutine flow charts (Plates D-4 and D-5), an example input sheet (Plate D-6), and an example output listing (Plate D-7) are included herein. The computer program is written in FORTRAN IV and has been tested on a GE-425 computer through a remote teletype terminal.

b. Hydraulic elements. The hydraulic elements are computed using an equation for open channel flow adapted from the Colebrook-White equation for pipe flow (HDC 224-1). The equivalent open channel flow equation in terms of Chezy C is

$$C = -32.6 \log_{10} \left(\frac{C}{5.2R_n} + \frac{k}{12.2R} \right) \quad (D-1)$$

where

R_n = Reynolds number = $4RV/v$

R = hydraulic radius

V = velocity

v = kinematic viscosity of water at
given temperature

k = assigned equivalent roughness
height

Equation D-1 is graphically presented in Plate 3,

Appendix B. Its derivation is described in HDC 631 to 631-2. The equation has been used in the program subroutine because it is equally applicable to all flow zones and eliminates the need of advanced prediction of the channel flow type.

c. Spiral transition. The modified spiral (McCormick 1948) is used for the transition between the tangent and fully banked sections of the curved channel.¹ This type of curve permits location of the channel interior and exterior walls by means of a simple coordinate system based upon a series of circular arcs of uniform length compounded to approximate a conventional spiral. The initial arc has a large radius, and the radius of each succeeding arc is decreased in a prescribed manner until the desired channel curve radius is attained. The advantage of the modified spiral over a conventional spiral is realized during field layout of the short chord lengths required for the concrete wall forms.

d. Tables of spiral transition. Tables have been prepared for 22 different spirals (McCormick 1948) to facilitate design layout and field location. The curve numbers in the tables correspond to the number of seconds in the central angle of the first arc of the spiral. This designation is followed in the computer program. However, the curve and corresponding number computed by the program may not be listed in the modified spiral tables because the program selects the exact curve for the specified radius and spiral length.

D-2. Description of Problem

The basic criteria for the design of spiral-banked curves for rectangular channels are given by Equations 2-33, 2-34, and 2-36 of the main text. A review of these equations reveals that the designer has several alternatives at his disposal to satisfy the design criteria. For example, if the minimum radius of curvature is selected from Equation 2-34, i.e.,

$$r_{\min} = \frac{4WV^2}{gy} = 4WF^2 \quad (2-34, D-2)$$

then the maximum allowable amount of banking (difference between inside and outside invert elevations in the circular curve) is required. The amount of banking (e ,

¹ References cited in this appendix are included in Appendix A.

Plate D-8) is equal to twice the superelevation given by Equation 2-36. For $C = 0.5$,

$$e = 2\Delta y = (2)(0.5) \frac{V^2 W}{gr} = \frac{V^2 W}{gr} \quad (2-36, D-3)$$

Where $r = r_{\min}$, e is therefore a maximum, or

$$e_{\max} = \frac{V^2 W}{gr_{\min}} = \frac{y}{4} \quad (D-4)$$

Also, the minimum recommended spiral length for banked curves (Equation 2-33) is

$$L_s = 30\Delta y \quad (2-33, D-5)$$

The choice of minimum radius of curvature in Equation 2-34 (D-2), maximum banking (Equation D-3), and the corresponding spiral lengths (Equation D-5) results in the shortest total curve length. If radii greater than minimum are selected, then according to Equation 2-36 (D-3), the amount of banking would be less than that expressed by Equation D-4. Moreover, both the radius of curvature and the spiral lengths may be arbitrarily selected to satisfy field conditions so long as they exceed the minimum criteria as expressed by Equations 2-33 (D-5) and 2-34 (D-2). Also, the entering and exit spiral lengths do not have to be equal as long as each exceeds the value determined by Equation 2-33 (D-5). It should be noted that with banked inverts, an upper limit on the radius of curvature exists at which the banking ($2\Delta y$) is less than 0.5ft. In this case banking and spiral transitions may not be necessary (paragraph 2-5b). Substituting this limiting (0.5 ft) value for e into Equation D-3 and solving for r , the limits for the radius of curvature where banking is required can be expressed as

$$4WF^2 \leq r \leq 2WyF^2 \quad (D-6)$$

Lastly, the transverse slope $2\Delta y/W$ of the water surface should not exceed 0.18 which corresponds to a slope angle ϕ of 10 deg (Equation 2-36, D-3).

a. Free drainage. Another criterion that must be

satisfied in some cases is that the channel be free draining. Banking is introduced by rotation of the bottom about the channel invert center line. Therefore, to provide free drainage along the inside wall, the product of the exit spiral length and centerline invert slope must be greater than the superelevation (Δy), i.e.

$$L_s S > \Delta y \quad (D-7)$$

Generally, the curves designed for minimum radii (Equations D-2, D-4, and D-5) will not be free draining unless the channel center-line invert slope is extremely steep. There are several ways of accomplishing free drainage by varying independently or dependently the spiral length and channel invert slope. However, the most common method is illustrated in Plate D-8. In this plate the length of the exit spiral is increased to satisfy Equation D-7 while the channel invert slope is held constant. The unequal spiral lengths generated by increasing the exit spiral should perform satisfactorily, but if symmetry is desired, the entering spiral may be equally increased.

b. Alternatives. The following list of design alternatives is based on the previously discussed criteria.

(1) Minimum radius of curvature (Equation D-2), maximum banking (Equation D-4), and corresponding spiral length (Equation D-5). Shortest total length. Not free draining. Equal spiral lengths.

(2) Minimum radius of curvature (Equation D-2), maximum banking (Equation D-4), and arbitrary spiral length greater than value given by Equation D-5. Not free draining. Equal spiral lengths.

(3) Arbitrary radius of curvature greater than Equation D-2, banking in accordance with Equation D-3, and corresponding spiral length (Equation D-5). Not free draining. Equal spiral lengths.

(4) Arbitrary radius of curvature and spiral length both greater than value given by Equations D-2 and D-5, respectively. Banking per Equation D-3. Not free draining. Equal spiral lengths.

(5) Arbitrary radius of curvature greater than value given by Equation D-2. Arbitrary entering and exit spiral lengths (unequal) but both greater than value given by Equation D-5. Banking computed using Equation D-3. Not free draining. Unequal spiral lengths.

(6) Same as (1) above except free drainage provided by increasing exit spiral length. Entering spiral remains per Equation D-5. Unequal spiral lengths.

(7) Same as (1) above except free drainage provided by increasing length of both spirals. Equal spiral lengths.

(8) Same as (3) above except free drainage provided by increasing exit spiral length; entering spiral remains per Equation D-5. Unequal spiral lengths.

(9) Same as (3) above except free drainage provided by increasing length of both spirals. Equal spiral lengths.

(10) Same as (4) above except free drainage provided by increasing exit spiral length. Entering spiral length retains arbitrary assigned value. Unequal spiral lengths.

(11) Same as (4) above except free drainage provided by increasing lengths of both spirals. Equal spiral lengths.

(12) Same as (5) above except free drainage provided by increasing exit spiral length. Unequal spiral lengths.

The various characteristics of these alternatives are compared in Plate D-9.

D-3. Description of Program

The program herein described is comprehensive in that any of the above-listed alternatives can be solved. The program is written for remote terminal use because of the increasing use of remote terminals and the definite advantages gained through this mode of operation provided the volume of input-output data is moderate. The main advantage of the remote terminal is that the program can be written so that it is user oriented. The user is guided by typewritten messages throughout the program execution, and the program is controlled by the user's response to these typed questions. Communication between the user and the computer during program solutions results in advantages in problems having alternative solutions. Conversion to batch processing is relatively simple and only requires modification of the READ statements in the program. A complete description of each input variable is given prior to its respective READ statement in the program listing (Plate D-2).

D-4. Input Data

a. Hydraulic parameters. Plate D-6 shows sample input data format. The first line of input represents the given design data, which include the discharge (cfs), channel center-line invert slope (ft/ft), channel width (ft), equivalent roughness height (ft), water temperature (°F), and the deflection angle (deg) between the curve tangents. Since the hydraulic elements are solved by trial and error using Equation D-1, the roughness parameter is the equivalent roughness height k . The curve design should be based on the maximum average channel velocity, for which the recommended minimum value of k for concrete-lined channels is 0.002 ft (paragraph 2-2c). The k value should always be the lowest value of the expected equivalent roughness height range if the minimum of that range is less than 0.002 ft. However, the wall heights in the curve, as in the case of the straight channel, should be designed for capacity based on $k = 0.007$ ft (paragraph 2-2c) or a higher value if anticipated.

b. Circular curve data. The second line of input is the design radius for the circular curve. The recommended minimum radius as calculated from the given flow conditions (Equation D-2) is stated in the typed request for this variable. If the minimum radius is desired, then 0.0 is assigned, otherwise, the desired value is typed in. The third and fourth lines of input are for the entering and exit spiral lengths, respectively. Similar to the request for the radius, the minimum spiral length based on Equation 2-33 (D-5) is stated. Either 0.0 or the desired value for each spiral length is assigned.

c. Radius of curvature. Occasionally, field conditions will limit the radius of curvature such that it must be less than the recommended minimum. The program can design a curve for values of radius and spiral length that are less than the recommended minimums, but the amount of banking will exceed the value given by Equation D-4. Furthermore, the cross-slope angle of the water surface will be greater than that which would occur with the recommended minimum radius. Should it exceed 10 deg, a message will be generated to advise the user that this criterion has been violated. Model testing of curves that violate any of these criteria should be considered.

d. Free drainage. The fifth line of input is for providing free drainage. The question is typed on the keyboard, and the user replies "yes" or "no." If yes, the

program computes the length of spiral necessary to provide free drainage and compares it with the exit spiral length as per input line 4. If the value supplied by input line 4 is less than the length required for free drainage, the exit spiral length is increased accordingly. Input line 6 affords the user the option to make both spirals equal length for symmetry and appears only if the reply of "yes" is made to input line 5.

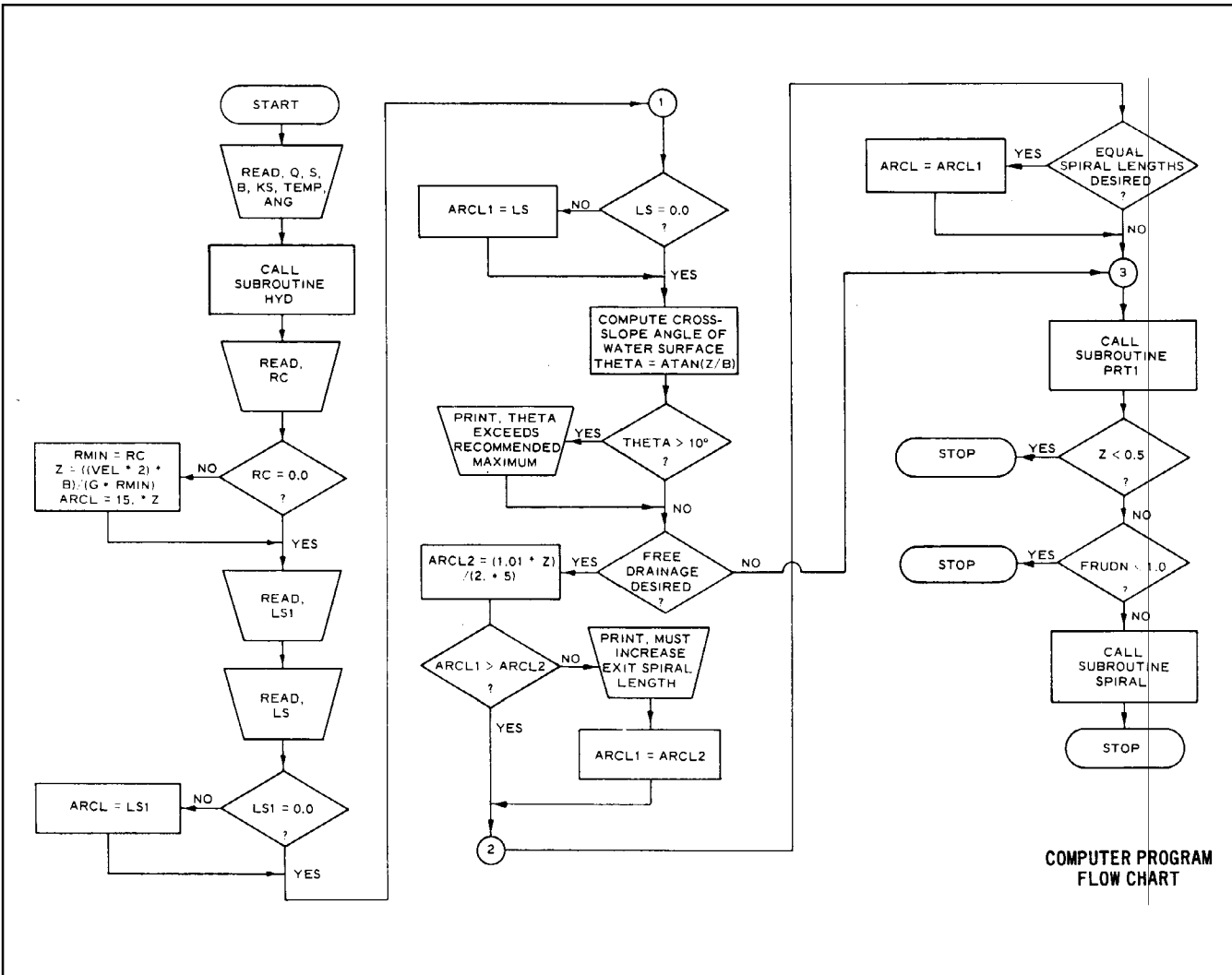
D-5. Program Output

The program output (Plate D-7) consists of the hydraulic and geometric design of the channel curve. The hydraulic elements include a listing of all the given design data and the pertinent computed hydraulic parameters. The channel curve elements are presented in two parts. The first part

gives the information required to prepare contract drawings. The second part gives the detailed data for field layout of the channel center line. The field book format is set up under the assumption that the entering spiral is first surveyed from TS; then the transit is moved to the end of the curve (ST) and the exit spiral backed in; finally, the transit is moved to the downstream end of the entering spiral (SC) and the circular curve surveyed. This is the recommended procedure for field layout found in most route survey textbooks. Curve stations are established using 12.5-ft chords around the spiral and 100-ft chords around the circular curve rather than the actual curve lengths. Shorter chord lengths may be required at the beginning and end of the circular curve, but these can be easily computed during the actual field layout.

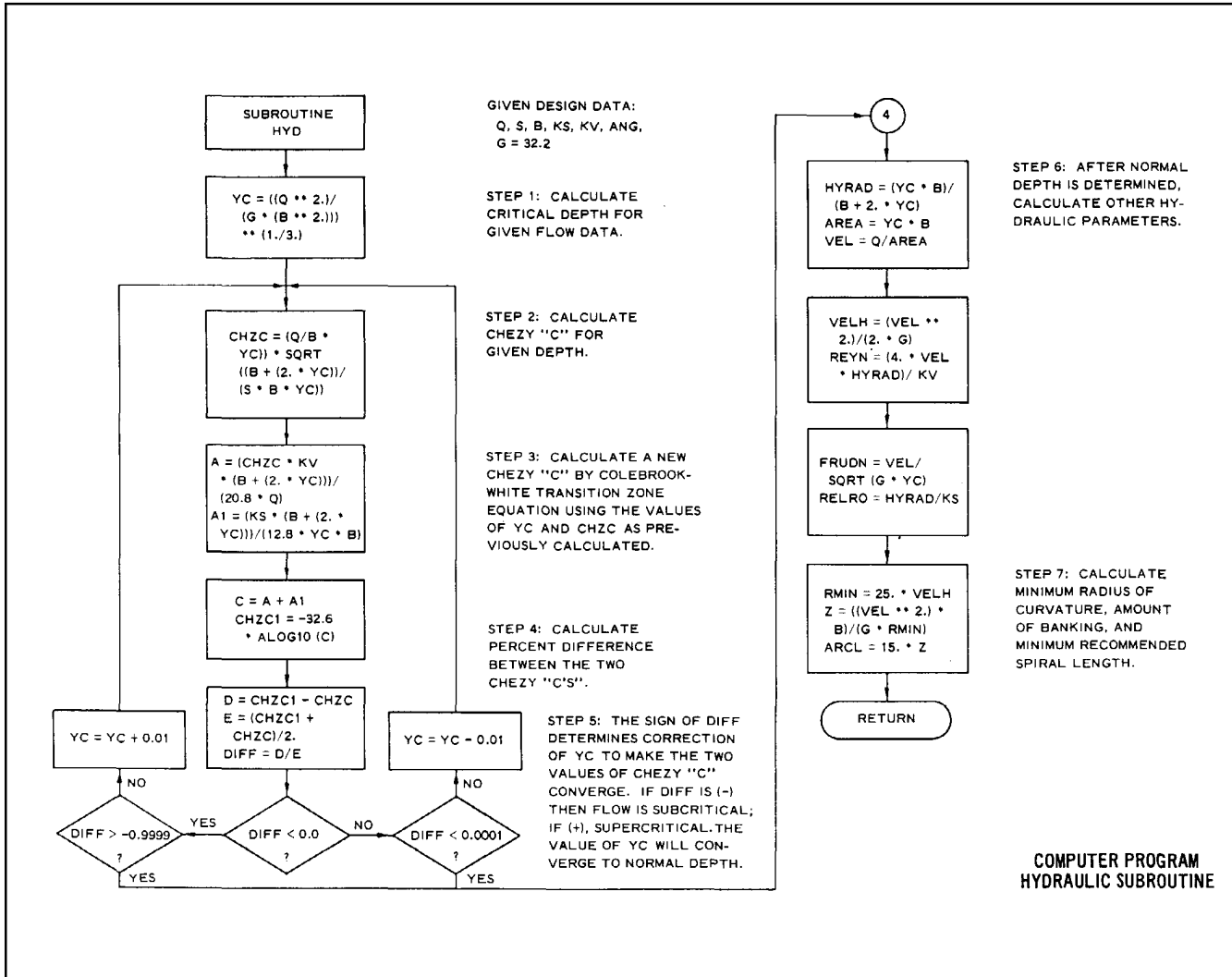
A:	DEFLECTION ANGLE FOR POINTS ALONG SPIRAL, DEG	DIFF:	PERCENT DIFFERENCE BETWEEN CHZC AND CHZCI	RC:	DESIGN RADIUS OF CURVATURE, FT
ANG:	DEFLECTION ANGLE BETWEEN INITIAL AND FINAL TANGENTS; TOTAL CENTRAL ANGLE OF CIRCULAR CURVE AND SPIRALS, DEG	FRUON:	FROUDE NUMBER	RELRO:	RATIO OF HYDRAULIC RADIUS TO EQUIVALENT ROUGHNESS HEIGHT (RELATIVE ROUGHNESS)
ARC(1):	LENGTH OF ENTERING SPIRAL, FT	G:	ACCELERATION DUE TO GRAVITY, FT/SEC ²	REYN:	REYNOLDS NUMBER
ARC(2):	LENGTH OF EXIT SPIRAL, FT	IARC:	NUMBER OF HUNDRED DIGITS IN ENTERING SPIRAL LENGTH, I.E., THE LENGTH OF SPIRAL IS BROKEN DOWN INTO THE FORM 00+00.00. THE HUNDRED DIGITS ARE THOSE TO THE LEFT OF THE + SIGN, FT	RMIN:	MINIMUM RADIUS OF CURVATURE OF CIRCULAR CURVE, FT
ARCF:	DIGITS TO RIGHT OF PLUS SIGN IN STATION NUMBER CORRESPONDING TO LENGTH OF ENTERING SPIRAL, I.E. 00+00.00	IARC1:	SAME AS IARC EXCEPT THAT IT DESIGNATES EXIT SPIRAL LENGTH, FT	S:	CHANNEL CENTER-LINE INVERT SLOPE, FT/FT
ARCF1:	DIGITS TO RIGHT OF PLUS SIGN IN STATION NUMBER CORRESPONDING TO LENGTH OF EXIT SPIRAL, I.E. 00+00.00	ICSS:	DIGITS TO LEFT OF PLUS SIGN IN STATION NUMBER OF C.S., I.E. 00+00.00	SCC:	POINT OF CHANGE FROM SPIRAL TO CIRCULAR CURVE MEASURED FROM BEGINNING OF CURVE (S.S.), FT
ARCL:	LENGTH OF ENTERING SPIRAL, FT	ISCC:	SAME AS ICSS EXCEPT THAT IT DESIGNATES THE STATION NUMBER OF THE S.C.	SCCF1:	DIGITS TO RIGHT OF PLUS SIGN IN STATION NUMBER OF THE S.C., I.E. 00+00.00
ARCL1:	LENGTH OF EXIT SPIRAL, FT	ICLGT:	SAME AS IARC EXCEPT THAT IT DESIGNATES THE LENGTH OF THE CIRCULAR CURVE	STA:	STATION NUMBERS OF POINTS ALONG CIRCULAR CURVE
ARCL2:	MINIMUM LENGTH OF EXIT SPIRAL TO PROVIDE FREE DRAINAGE, FT	ISTA:	DIGITS TO LEFT OF PLUS SIGN IN STATION NUMBERS OF CIRCULAR CURVE	STAF:	DIGITS TO RIGHT OF PLUS SIGN IN CIRCULAR CURVE STATION NUMBERS, I.E. 00+00.00
AREA:	CROSS-SECTION AREA OF FLOW IN CHANNEL, FT ²	ISTT:	DIGITS TO LEFT OF PLUS SIGN IN STATION NUMBER OF S.T., I.E. 00+00.00	STAS:	STATION NUMBERS OF 12.5-FT-CHORD SPIRAL POINTS
B:	CHANNEL WIDTH, FT	ISTAS:	DIGITS TO LEFT OF PLUS SIGN FOR ANY STATION NUMBER ON EXIT OR ENTERING SPIRAL	STASF:	DIGITS TO RIGHT OF PLUS SIGN IN STATION NUMBERS OF SPIRAL POINTS, I.E. 00+00.00
C:	CHORD LENGTH OF INDIVIDUAL ARCS ALONG THE SPIRAL, FT	KS:	EQUIVALENT ROUGHNESS HEIGHT OF CHANNEL BOUNDARY, FT	STT:	POINT OF CHANGE FROM SPIRAL TO TANGENT OR S.T., FT
CHORDC:	CHORD LENGTH USED IN STAKING OUT CIRCULAR CURVE, IN THIS CASE 100 FT	KV:	KINEMATIC VISCOSITY OF WATER, FT ² /SEC	STTF:	DIGITS TO RIGHT OF PLUS SIGN IN STATION NUMBER OF S.T.
CHZC:	CHEZY C AS CALCULATED BY CHEZY'S EQUATION	LS:	DESIGN EXIT SPIRAL LENGTH; MUST BE GREATER THAN 30 TIMES THE SUPER-ELEVATION, FT	TEMP:	WATER TEMPERATURE, °F
CHZCI:	CHEZY C AS CALCULATED BY COLEBROOK-WHITE TRANSITIONAL ZONE EQUATION	LS1:	DESIGN ENTERING SPIRAL LENGTH; MUST BE GREATER THAN 30 TIMES THE SUPER-ELEVATION, FT	TL:	TANGENT DISTANCE OF SPIRALED CURVE: DISTANCE FROM T.S. OR S.T. TO POINT OF INTERSECTION OF TANGENTS (PI), FT
CLGT:	DIGITS TO RIGHT OF PLUS SIGN IN STATION NUMBER CORRESPONDING TO LENGTH OF CIRCULAR CURVE, I.E. 00+00.00	MDG:	NUMBER OF DEGREES, MINUTES, AND SECONDS, RESPECTIVELY, IN DEFLECTION ANGLE TO ANY POINT ON SPIRAL	VEL:	MEAN CHANNEL VELOCITY, FPS
CSS:	POINT OF CHANGE FROM CIRCULAR CURVE TO SPIRAL	MSEC:	NUMBER OF DEGREES, MINUTES, AND SECONDS, RESPECTIVELY, IN BACK DEFLECTION ANGLE TO T.S. WITH TRANSIT AT S.C.	VELH:	VELOCITY HEAD OF FLOW IN CHANNEL, FT
CSSF:	DIGITS TO RIGHT OF PLUS SIGN IN STATION NUMBER CORRESPONDING TO THIS POINT (C.S.), I.E. 00+00.00	MGDB:	NUMBER OF DEGREES, MINUTES, AND SECONDS, RESPECTIVELY, IN DEFLECTION ANGLE TO ANY POINT ON CIRCULAR CURVE WITH TRANSIT AT S.C.	X:	CENTER-LINE COORDINATE OF POINTS ALONG SPIRAL ALONG PRIMARY TANGENT, FT
DEFC:	DEFLECTION ANGLES FOR POINTS ALONG CIRCULAR CURVE, MIN	MDGC:	NUMBER OF DEGREES, MINUTES, AND SECONDS, RESPECTIVELY, IN DEFLECTION ANGLE TO ANY POINT ON CIRCULAR CURVE WITH TRANSIT AT S.C.	YC:	DEPTH OF FLOW IN CHANNEL, FT
DEGC:	DEGREE OF CURVATURE OF CIRCULAR CURVE, DEG	MSECC:	ANGLE TO ANY POINT ON CIRCULAR CURVE WITH TRANSIT AT S.C.	Y:	ORDINATE OR TANGENT OFFSET OF POINTS ALONG SPIRAL, FT
DELTA:	CENTRAL ANGLE OF INDIVIDUAL ARCS, SEC	Q:	DESIGN CHANNEL DISCHARGE, CFS	Z:	AMOUNT OF BANKING, OR DIFFERENCE IN ELEVATION BETWEEN OUTSIDE AND INSIDE INVERT OF CHANNEL, FT
DELTA1:	MEDIAN ANGLE OF INDIVIDUAL ARCS, SEC	R:	RADIUS OF CURVATURE OF INDIVIDUAL ARCS ALONG SPIRAL, FT		
DELTA1A:	CENTRAL ANGLE OF WHOLE SPIRAL, DEG				
DELTA2:	CENTRAL ANGLE OF CIRCULAR CURVE, DEG				

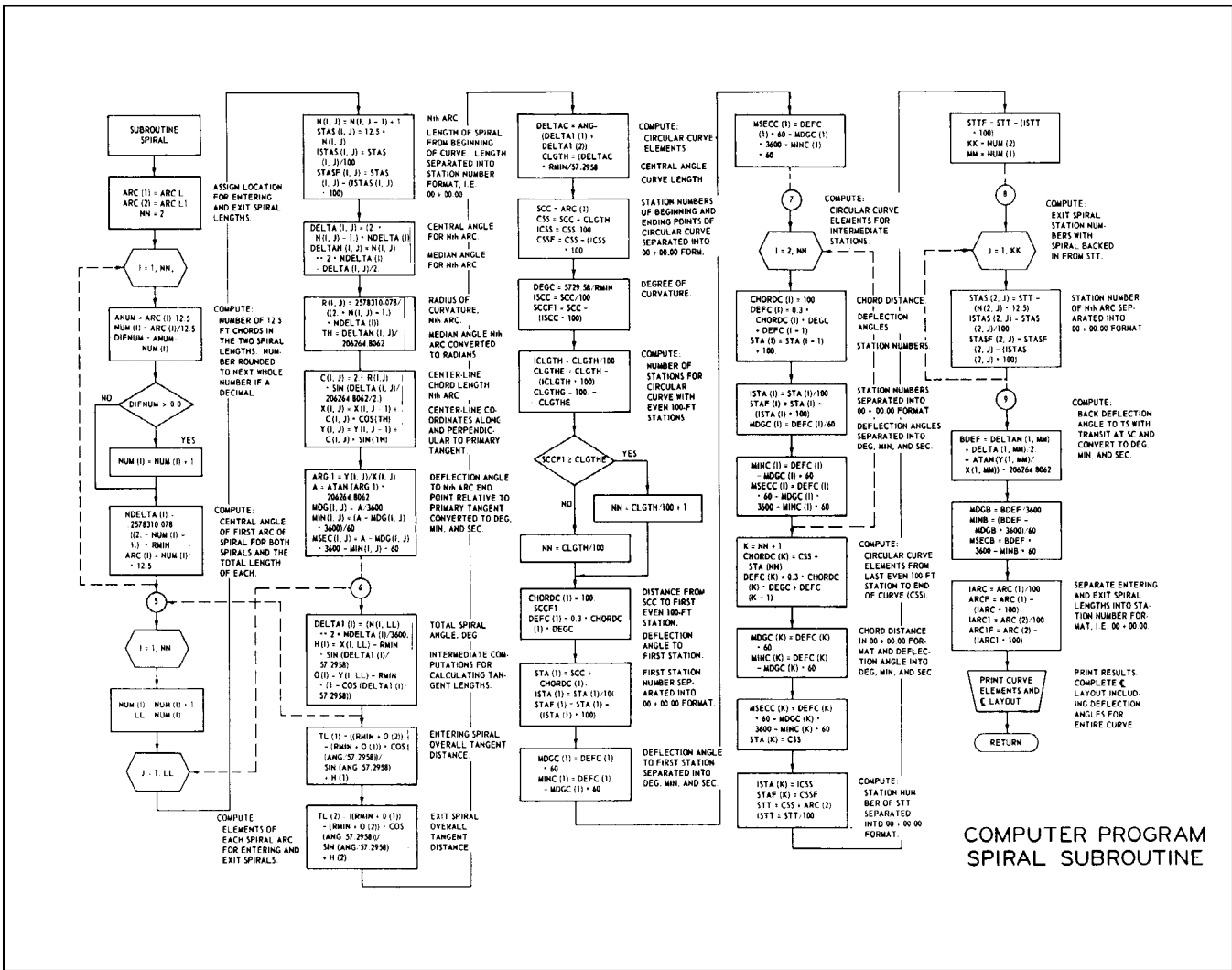
COMPUTER PROGRAM
SYMBOLS



COMPUTER PROGRAM FLOW CHART

PLATE D-4





COMPUTER PROGRAM SPIRAL SUBROUTINE

EXAMPLE PROBLEM:

GIVEN: Q = 15,000 CFS S = 0.01 FT/FT B = 50.0 FT
KS = 0.002 FT WATER TEMP = 60° F
ANG = 45°

FIND: SHORTEST CURVE FOR GIVEN CONDITIONS AND PROVIDE
FREE DRAINAGE.

READ DESIGN DATA - Q,S,B,KS,TEMP,ANG
INPUT:00250
?15000.,.01,50.,.002,60.,45.

READ THE DESIGN RADIUS OF CURVATURE. THE MINIMUM RECOMMENDED
RADIUS = 1049.44FT. IF MINIMUM RADIUS IS DESIRED, ASSIGN A VALUE
OF 0.0 TO THIS VARIABLE.
INPUT:00320
?0.0

READ DESIGN ENTERING SPIRAL LENGTH. THE MINIMUM RECOMMENDED
SPIRAL LENGTH = 30.40FT. IF MINIMUM LENGTH DESIRED, ASSIGN A VALUE
OF 0.0 TO THIS VARIABLE.
INPUT:00410
?0.0

READ DESIGN EXIT SPIRAL LENGTH. THE MINIMUM RECOMMENDED
SPIRAL LENGTH = 30.40FT. IF MINIMUM LENGTH DESIRED, ASSIGN A VALUE
OF 0.0 TO THIS VARIABLE.
INPUT:00460
?0.0

IS FREE DRAINAGE DESIRED? TYPE YES OR NO
INPUT:00550
?YES

MUST INCREASE EXIT SPIRAL LENGTH TO 102.34FT. TO PROVIDE FREE DRAINAGE.

ARE EQUAL SPIRAL LENGTHS DESIRED? TYPE YES OR NO!
INPUT:00660
?NO

PROGRAM INPUT
EXAMPLE

HYDRAULIC ELEMENTS OF DESIGN						CENTERLINE CURVE LAYOUT				
GIVEN DESIGN DATA						DEFLECTION ANGLES FOR ENTERING SPIRAL WITH TRANSIT AT T.S.				
Q.CFS	SLOPE	WIDTH	KS	WATER TEMP.	DEF.ANGLE	DEFLECTION ANGLE	STATION	CHORD LENGTH	COORDINATES	
						DEG MIN SEC		(FT)	X(FT) Y(FT)	
15000.	.0100	50.00	.0020	60.0	45.000	TRANSIT AT T.S. = 00 + 00.00	00.000	00.000	00.000	
						0 4 5	0 + 12.50	12.500	12.500 0.015	
						0 12 16	0 + 25.00	12.500	25.000 0.069	
						0 25 54	0 + 37.50	12.500	37.498 0.283	
COMPUTED HYDRAULIC PARAMETERS						DEFLECTION ANGLES FOR CIRCULAR CURVE WITH TRANSIT AT THE S.C.				
DEPTH	HYD RAD	CHEZY C	VEL	FR.#	REY.#	R/KS	BACK DEFLECTION TO T.S. = 0(DEG) 47(MIN) 44(SEC)			
8.11	6.12	149.52	37.01	2.29	0.7527E+08	3060.70	DEFLECTION ANGLE STATION			
							DEG MIN SEC	TRANSIT AT S.C. = 0 + 37.50		
							1 42 22	1 + 0.00		
							4 26 9	2 + 0.00		
							7 9 56	3 + 0.00		
							9 53 44	4 + 0.00		
							12 37 31	5 + 0.00		
							15 21 19	6 + 0.00		
							18 5 6	7 + 0.00		
							20 15 58	7 + 79.90		
CHANNEL CURVE ELEMENTS						DEFLECTION ANGLES FOR EXIT SPIRAL WITH TRANSIT AT S.T.				
RADIUS OF CURVATURE(FT) = 1049.436						(SPIRAL RUN BACKWARDS)				
BANKING (FT) = 2.027						DEFLECTION ANGLE	STATION	CHORD LENGTH	COORDINATES	
T.S. = STA 00 + 00.00						DEG MIN SEC		(FT)	X(FT) Y(FT)	
0 + 37.50 = LENGTH OF ENTERING SPIRAL # 491						TRANSIT AT T.S. = 8 + 92.40	00.000	00.000	00.000	
S.C. = STA 0 + 37.50						0 1 12	8 + 79.90	12.500	12.500 0.004	
7 + 42.40 = LENGTH OF CIRCULAR CURVE						0 3 35	8 + 67.40	12.500	25.000 0.026	
C.S. = STA 7 + 79.90						0 7 35	8 + 54.90	12.500	37.500 0.063	
1 + 12.50 = LENGTH OF EXIT SPIRAL # 144						0 13 11	8 + 42.40	12.500	49.999 0.152	
S.T. = STA 8 + 92.40 = TOTAL LENGTH OF CURVE						0 20 23	8 + 29.90	12.500	62.498 0.371	
CENTRAL ANGLE OF ENTERING SPIRAL(DEG) = 1.2275						0 29 11	8 + 17.40	12.500	74.995 0.637	
CENTRAL ANGLE OF EXIT SPIRAL(DEG) = 3.2400						0 39 35	8 + 4.90	12.500	87.490 1.008	
TOTAL ENTERING TANGENT LENGTH(FT) = 450.31						0 51 35	7 + 92.40	12.500	99.980 1.501	
TOTAL EXIT TANGENT LENGTH = 487.45						1 5 11	7 + 79.90	12.500	112.464 2.133	
TANGENT OFFSET COORDINATES OF S.C. FROM T.S.						STOP				
X(FT) Y(FT)						RUNNING TIME: 13.9 SECS 1/0 TIME : 06.1 SECS				
37.50 0.28										
TANGENT OFFSET COORDINATES OF C.S. FROM S.T.										
X(FT) Y(FT)										
112.46 2.13										

PROGRAM OUTPUT EXAMPLE

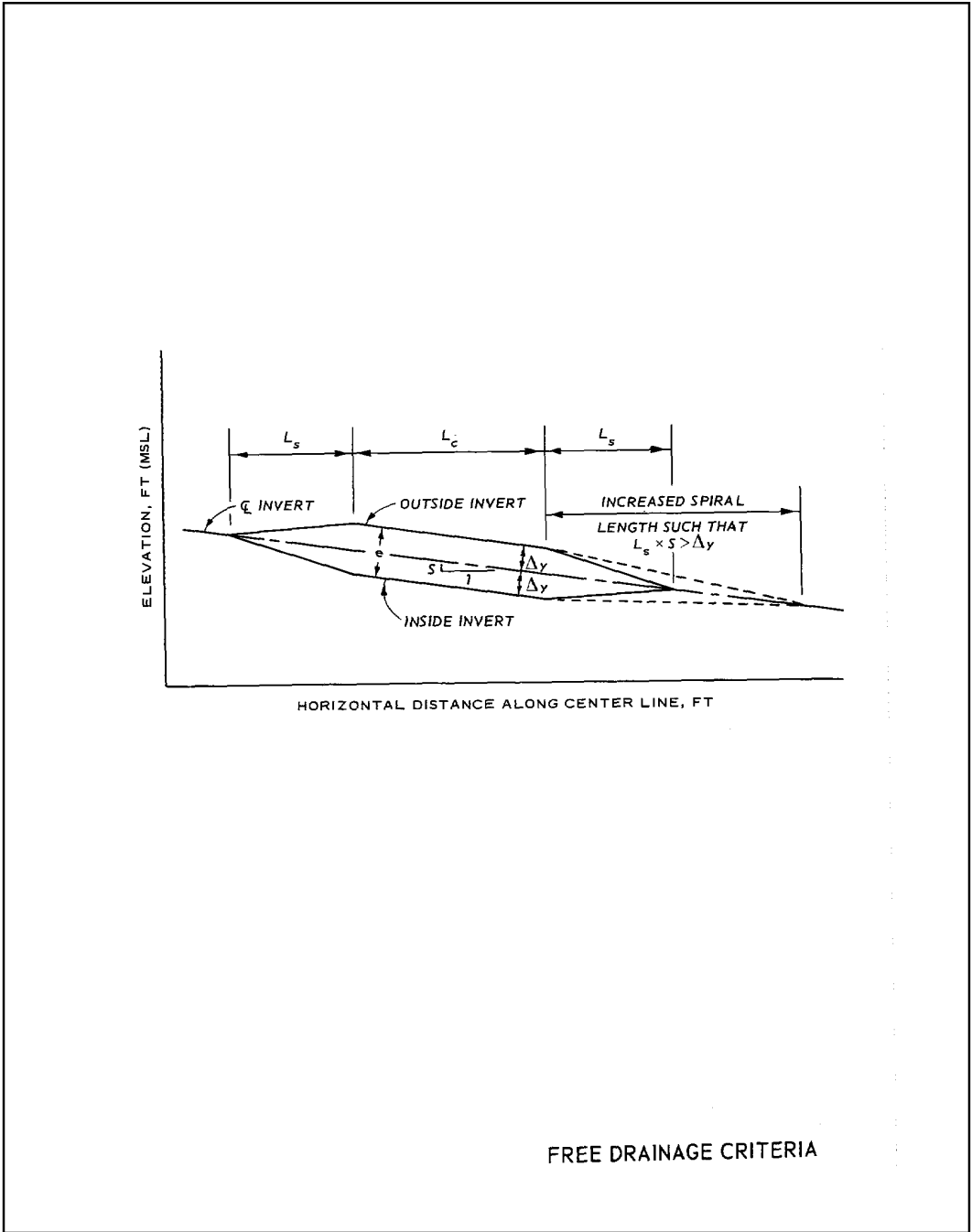


PLATE D-8

<u>ALTERNATIVE</u>	<u>RADIUS CURVE</u>	<u>CURVE BANKING</u>	<u>BOTH SPIRALS</u>	<u>SPIRAL LENGTH</u>	<u>FREE DRAINAGE</u>	<u>REMARKS</u>
(1)	MIN EQ D-2	MAX EQ D-4	EQUAL	MIN EQ D-5	NO	SHORTEST TOTAL LENGTH
(2)	MIN EQ D-2	MAX EQ D-4	EQUAL	ARBITRARY > EQ D-5	NO	
(3)	ARBITRARY > EQ D-2	CORRESPONDING EQ D-3	EQUAL	CORRESPONDING EQ D-5	NO	
(4)	ARBITRARY > EQ D-2	CORRESPONDING EQ D-3	EQUAL	ARBITRARY > EQ D-5	NO	
(5)	ARBITRARY > EQ D-2	CORRESPONDING EQ D-3	UNEQUAL	ARBITRARY > EQ D-5	NO	
(6)	MIN EQ D-2	MAX EQ D-4	UNEQUAL	ENTERING = MIN EQ D-5 EXIT TO DRAIN > EQ D-5	YES	SIMILAR TO (1)
(7)	MIN EQ D-2	MAX EQ D-4	EQUAL	ENTER = TO EXIT EXIT TO DRAIN > EQ D-5	YES	SIMILAR TO (1)
(8)	ARBITRARY > EQ D-2	CORRESPONDING EQ D-3	UNEQUAL	ENTER = CORRESPONDING EQ D-5 EXIT TO DRAIN > EQ D-5	YES	SIMILAR TO (3)
(9)	ARBITRARY > EQ D-2	CORRESPONDING EQ D-3	EQUAL	ENTER = EXIT EXIT TO DRAIN > EQ D-5	YES	SIMILAR TO (3)
(10)	ARBITRARY > EQ D-2	CORRESPONDING EQ D-3	UNEQUAL	ENTER = ARBITRARY > EQ D-5 EXIT TO DRAIN > EQ D-5	YES	SIMILAR TO (4)
(11)	ARBITRARY > EQ D-2	CORRESPONDING EQ D-3	EQUAL	ENTER = EXIT EXIT TO DRAIN > EQ D-5	YES	SIMILAR TO (4)
(12)	ARBITRARY > EQ D-2	CORRESPONDING EQ D-3	UNEQUAL	ENTER = ARBITRARY > EQ D-5 EXIT TO DRAIN > EQ D-5	YES	SIMILAR TO (5)
SPIRAL ALTERNATIVES COMPARISONS						

PLATE D-9

Appendix E Theory of Combining Flow at Open Channel Junctions (Confluences)

E-1. General

In the design of flood-control channels, one of the more important hydraulic problems is the analysis of the flow conditions at open channel junctions. The junction problem is common in flood-control channel design as flows from the smaller drainage basins generally combine with those in larger main channels. The momentum equation design approach has been verified for small angles by Taylor (1944) and Webber and Greated (1966).¹ The US Army Engineer District (USAED), Los Angeles (1947), developed equations, based on the momentum principle, for the analysis of several types of open channel junctions commonly used in flood-control channel systems. Model tests of several confluence structures with various conditions of flow have been made, and the experimental results substantiated those calculated theoretically by the equations. This appendix is a presentation of the detailed derivation of the momentum equation.

E-2. Theory and Assumptions, Tranquil Flow

a. Plate E-1 gives a definition sketch of a junction. The following assumptions are made for combining tranquil flows:

(1) The side channel cross section is the same shape as the main channel cross section.

(2) The bottom slopes are equal for the main channel and the side channel.

(3) Flows are parallel to the channel walls immediately above and below the junction.

(4) The depths are equal immediately above the junction in both the side and main channels.

(5) The velocity is uniform over the cross sections immediately above and below the junction.

Assumption (3) implies that hydrostatic pressure distributions can be assumed, and assumption (5) suggests that the momentum correction factors are equal to each other at the reference sections.

b. The use of the momentum equation in the analysis of flow problems is discussed in detail on page 49 of Chow (1959). Plate E-1c shows the forces acting on the control volume through the junction. The net force acting in the direction of the main channel is given by

$$F_{1-3} = P_1 + P_2 \cos \theta + W \sin \alpha - P_f - P_3 - U \quad (E-1)$$

where

P_1, P_2, P_3 = hydrostatic pressure forces acting on the control volume at the reference sections

$P = \gamma b y^2 / 2$ for rectangular section

γ = specific weight of water (62.5 pcf)

b = width

y = depth

θ = angle of intersection of the junction

W = weight of the water in the control volume

α = angle of the channel slope ($\tan \alpha$ = channel slope)

P_f = total external force of frictional resistance along the wetted surface

U = unknown reaction force exerted by the walls of the lateral in the upstream direction

The change in momentum per unit of time in the control volume is equal to the net force acting on the control volume (Newton's Second Law of Motion). The change in momentum in the direction of the main channel is

¹ References cited in this appendix are included in Appendix A.

$$F_{1-3} = \frac{\gamma}{g} Q_3 V_3 - \frac{\gamma}{g} Q_1 V_1 - \frac{\gamma}{g} Q_2 V_2 \cos \theta \quad (\text{E-2})$$

where

$$g = \text{acceleration due to gravity} = 32.2 \text{ ft/sec}^2$$

V_1, V_2, V_3 = average channel velocity at the reference sections

Q_1, Q_2, Q_3 = discharge of the appropriate channels

When Equations E-1 and E-2 are equated, the basic momentum equation for the flow through the junction is obtained.

E-3. Simplification of General Equation, Rectangular Channels

a. If the slope is appreciable, the evaluation of the hydrostatic pressure distributions will involve a correction factor $\cos^2 \alpha$ (Chow 1959). However, for slopes normally employed for flood-control channels, this correction factor will be negligible. For slopes less than 10 percent ($\alpha \approx 6$ deg) the $\cos \alpha$ and $\cos^2 \alpha$ terms can be neglected in the momentum equation and the result will be accurate to within 1 percent.

b. The unknown reaction force U has been assumed by Taylor (1944) and Webber and Greated (1966) to be equal and opposite to the pressure term from the lateral; that is,

$$U + P_2 \cos \theta \quad (\text{E-3})$$

and the pressure term from the lateral is balanced by the pressure force on the curve wall BC in Plate E-1a. This assumption is reasonable as long as the depth in the region of the curved wall (area ABC in Plate E-1a) is basically uniform and the curvature of the streamlines is not appreciable.

c. The component weight of fluid acting along the main channel is equal to the frictional resistance for both uniform flow and gradually varied flow; that is,

$$P_f = W \sin \alpha \quad (\text{E-4})$$

can be assumed as long as the flow is not rapidly varying. This is the basic assumption of uniform flow; i.e., the total force of resistance is equal to the gravitational force component causing the flow. Introducing those three simplifications, the momentum equation reduces to

$$P_1 - P_3 = \frac{\gamma}{g} Q_3 V_3 - \frac{\gamma}{g} Q_1 V_1 - \frac{\gamma}{g} Q_2 V_2 \cos \theta \quad (\text{E-5})$$

d. Introduction of the hydrostatic pressure distribution in Equation E-5 leads to the following:

$$\frac{\gamma b y_1^2}{2} - \frac{\gamma b y_3^2}{2} - \frac{\gamma}{g} (Q_3 V_3 - Q_1 V_1 - Q_2 V_2 \cos \theta) \quad (\text{E-6})$$

By the use of the continuity equation at each reference section

$$Q_1 = A_1 V_1; Q_2 = A_2 V_2; Q_3 = A_3 V_3 \quad (\text{E-7})$$

where A is the area. Dividing by the unit weight of water, the equation can be simplified to

$$\frac{Q_3^2}{g A_3} + \frac{b y_3^2}{2} = \frac{Q_1^2}{g A_1} + \frac{Q_2^2}{g A_2} \cos \theta + \frac{b y_1^2}{2} \quad (\text{E-8})$$

If a further assumption is made that the side channel width is equal to the main channel width, this equation can be generalized. The papers by Taylor (1944) and Webber and Greated (1966) contain the details of the derivation including graphs of the equation and experimental data.

E-4. Unequal Width of Main Channels

The derivation of the momentum equation for a rectangular channel with unequal widths follows very closely that outlined in the preceding paragraphs. Plate E-1b gives a definition sketch for this type of junction. The only additional force is that pressure force not balanced by the curved wall *DC*. The pressure ΔP_1 is the component in the main channel direction of the hydrostatic pressure acting over the width *EF* at reference section 2. The effective width for computing ΔP_1 is $(b_3 - b_1)$ and the pressure is

$$\Delta P_1 = \gamma \left(\frac{b_3 - b_1}{2} \right) y^2 \quad (E-9)$$

By adding appropriate subscripts and omitting γ for simplicity, the momentum equation then becomes:

$$\frac{Q_3^2}{gA_3} + \frac{b_3 y_3^2}{2} = \frac{Q_1^2}{gA_1} + \frac{Q_2^2}{gA_2} \cos \theta + \frac{b_1 y_1^2}{2} + \frac{(b_3 - b_1)}{2} y_1^2 \quad (E-10)$$

This can be further simplified to

$$\frac{Q_3^2}{gA_3} + \frac{b_3 y_3^2}{2} = \frac{Q_1^2}{gA_1} + \frac{Q_2^2}{gA_2} \cos \theta + \frac{b_3 y_1^2}{2} \quad (E-11)$$

E-5. Trapezoidal Channels

a. The hydrostatic pressure distribution in a trapezoidal cross section is given by

$$P = A\bar{y} = y^2 \left(\frac{b}{2} + \frac{Zy}{3} \right) \quad (E-12)$$

where

\bar{y} = distance of the centroid of the water area below the surface of the flow

y = flow depth

b = bottom width of the trapezoidal cross section

Z = side slope, horizontal to vertical

Introduction of this term with the proper subscripts in the basic momentum equation will give the following:

$$\frac{Q_3^2}{gA_3} + \left(\frac{b_3}{2} + \frac{Zy_3}{3} \right) y_3^2 = \frac{Q_1^2}{gA_1} + \frac{Q_2^2}{gA_2} \cos \theta + \left(\frac{b_1}{2} + \frac{Zy_1}{3} \right) y_1^2 \quad (E-13)$$

b. The equation for unequal widths of trapezoidal channels is derived in much the same manner as for unequal width of rectangular channels given in paragraph E-4. The inclusion of the hydrostatic pressure distribution terms for a trapezoidal cross section in that equation will result in

$$\frac{Q_3^2}{gA_3} + \left(\frac{b_3}{2} + \frac{Zy_3}{3} \right) y_3^2 = \frac{Q_1^2}{gA_1} + \frac{Q_2^2}{gA_2} \cos \theta + \left(\frac{b_3}{2} + \frac{Zy_1}{3} \right) y_1^2 \quad (E-14)$$

E-6. Energy Loss

The energy loss at a junction H_L can be obtained by writing an energy balance equation between the entering and exiting flow from the junction.

$$H_L = E_1 + E_2 - E_3 \quad (E-15)$$

The momentum and continuity equations could be used to obtain depths and velocities for evaluating the specific energy at the sections. However, it is not desirable to generalize the energy equation because of the many types of junctions.

E-7. Rapid Flow

In contrast with tranquil flows at junctions, rapid flows with changes in boundary alignments are generally complicated by standing waves (Ippen 1951). In tranquil flow, backwater effects are propagated upstream, thereby tending to equalize the flow depths in the main and side channels. However, backwater cannot be propagated upstream in rapid flow, and flow depths in the main and

side channels cannot generally be expected to be equal. Junctions for rapid flows and very small junction angles are designed assuming equal water-surface elevations in the side and main channels (paragraph 4-4d(1)(a)). Model tests by the USAED, Los Angeles (1949), on rapid-flow junctions have verified the use of the momentum equation developed in this appendix for this purpose.

E-8. Sample Computation

Typical momentum computations for a confluence are given in Plate E-2. The computation conditions are for the type of junction developed by the USAED, Los Angeles, to minimize standing wave effects.

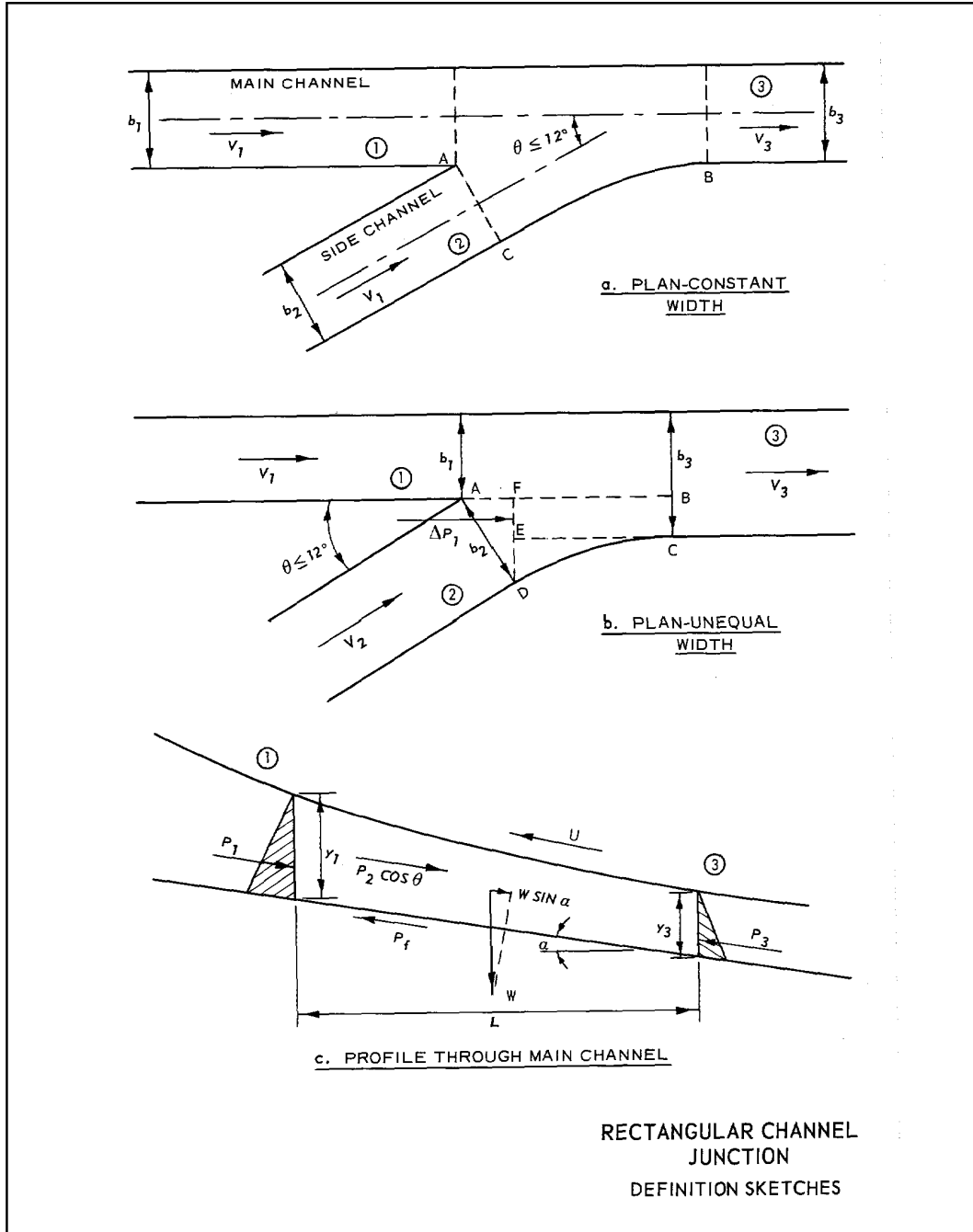
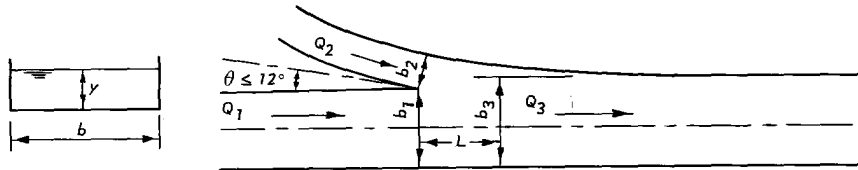


PLATE E-1



GIVEN DATA

DISCHARGES	CHANNEL WIDTHS	FLOW DEPTHS	FROUDE NO.	ANGLE & LENGTH
Q ₁ 37,000 CFS	b ₁ 110 FT	y ₁ 12.29 FT	F ₁ 1.39	θ = 0°
Q ₂ 5,000 CFS	b ₂ 36 FT	y ₂ 12.29 FT	F ₂ 0.57	COS θ = 1
Q ₃ 42,000 CFS	b ₃ 145 FT	y ₃ 10.40 FT	F ₃ 1.52	L = 100.0 FT

MOMENTUM EQUATION *

$$\frac{Q_1^2}{gA_1} + \frac{Q_2^2}{gA_2} \cos \theta + \frac{b_1 y_1^2}{2} + \frac{(b_3 - b_1)}{2} y_1^2 = \frac{Q_3^2}{gA_3} + \frac{b_3 y_3^2}{2} \quad (VI-4)$$

$$y_{c_3} = 13.80 \quad 0.85 y_{c_3} = 11.73$$

MOMENTUM UPSTREAM*	FT ³	MOMENTUM DOWNSTREAM	FT ³
$\frac{Q_1^2}{gA_1} = \frac{(37,000)^2}{32.2 \times 1,351.9}$	= 31,449	y ₃ ESTIMATE = 10.40	
$\frac{Q_2^2 \cos \theta}{gA_2} = \frac{(5,000)^2 \times 1}{32.2 \times 442.44}$	= 1,755	$\frac{Q_3^2}{gA_3} = \frac{(42,000)^2}{32.2 \times 1,508.0}$	= 36,328
$\frac{b_1 y_1^2}{2} = \frac{110 \times (12.29)^2}{2}$	= 8,307	$\frac{b_3 y_3^2}{2} = \frac{145 \times (10.40)^2}{2}$	= 7,842
$\frac{(b_3 - b_1)}{2} y_1^2 = \frac{(145 - 110) \times (12.29)^2}{2}$	= 2,643		
ΣM ₁₋₂	= 44,154	ΣM ₃	= 44,170

* THE TERM γ (SPECIFIC WEIGHT OF WATER) HAS BEEN OMITTED FROM ALL TERMS OF THIS EQUATION AND THE FOLLOWING COMPUTATIONS.

RECTANGULAR CHANNEL
JUNCTION
COMPUTATIONS

U.S. ARMY CORPS OF ENGINEERS
LOWER MISSISSIPPI VALLEY DIVISION

REPORT
ON
STANDARDIZATION OF RIPRAP GRADATIONS

NOVEMBER 1981
REVISED MARCH 1989

TABLE OF CONTENTS

	<u>Page</u>
Purpose	1
Scope	1
Background	1
Field Investigations	1
Riprap Design Analysis	3
Standardization of Riprap Gradations	5
Summary and Actions	8
References	9
Inclosures 1-6	

REPORT ON STANDARDIZATION OF RIPRAP GRADATIONS

1. Purpose. This report on standardization of riprap gradations is prepared in response to comments made by the Associated General Contractors (AGC) meeting on specifications held in Biloxi, Mississippi, on 29 January 1981 (Inclosure 1). The Lower Mississippi Valley Division (LMVD) concurred with AGC that it was desirable to develop standard gradations for riprap at and adjacent to structures, and agreed to make a study to determine the cost effectiveness within the design criteria for such special riprap.

2. Scope. The report addresses the capability of the quarries to produce various riprap gradations, and the sensitivity of changing gradations during a production cycle. It also provides a review of the design guidance and background information on their development. The economic solutions to all the problems associated with producing the riprap gradations, transporting the riprap, and meeting in-place gradation requirements are quite complex and beyond the scope of this study. However, several of these problems are discussed from the standpoint of the contractor, the quarry operator, and the designer in an effort to properly evaluate the impact of riprap standardization. Finally, areas where standardization can be accomplished are identified and actions to be taken for implementation are outlined. Design and gradation of riprap for wave-wash protection on earth embankments and construction of river dikes are beyond the scope of the study; therefore, this report does not address the gradation of graded stone A, B, or C or "stone bank paving," all of which are used extensively in the Channel Improvement Program on the main stem Mississippi River.

3. Background. General guidance for the design of riprap to be used at U. S. Army Corps of Engineers (Corps) structures and channels is provided in Engineer Technical Letter (ETL) 1110-2-120¹, Engineer Manual (EM) 1110-2-1601², and Hydraulic Design Criteria (HDC) 712-1³. These criteria specify methods that are to be used in establishing the minimum 50 percent lighter by weight (W_{50}) of a stable layer of graded stone riprap for the hydrodynamic forces to which it will be subjected. From this mean weight, the stone gradation and layer thickness are established through specified relationships, depending on the specific gravity of the stone and the degree of flow turbulence expected at the job site. Rather than specifying a single gradation, a gradation band is established that is intended to provide some latitude in the gradation of stone produced in the quarry and delivered to the job site.

4. Field Investigations.

a. During the course of this study six quarries that produce riprap were visited and one other was contacted by telephone to gain first-hand knowledge on quarry operations and discuss the various aspects of riprap production. Quarry managers were queried with respect to production capabilities, costs of changing machinery to produce different gradations, and problems related to producing the gradation bands presently being used. The visits also allowed the quarry managers the opportunity to ask about the different gradation curves and the reason for the curves overlapping in some cases. The following paragraphs summarize these discussions as they relate to riprap gradations specified for Corps projects.

b. A major concern of the rock quarry managers during the past few years has been the increasing number of different gradation curves specified for riprap production. Those interviewed all felt that the number of different gradations being requested was increasing. One quarry manager stated that he had received a set of specifications which called for two separate riprap gradations, with the two gradation curves having the same maximum and minimum 100 percent lighter by weight (W_{100}); and minimum 15 percent lighter by weight (W_{15}) size. The quarry manager further stated that the two gradations would have required two separate sets of screens to produce, however, the final product would have looked the same. The two sets of curves as originally specified are shown on Inclosure 2. The District requesting the stone did change the specifications to one common gradation.

c. Production rates of graded stone were found to vary considerably between the quarries visited, with the production rate being a function of the shot pattern, type of stone being produced, type of machinery being used to grade stone, and the gradation of the stone being produced. Most of the quarries have their operation set up to produce the graded stone first after it passes through the grizzly and over the lower size screen. Stone falling outside the gradation band is then used to produce other crushed stone and aggregate. Normally, this means that when the grizzly and screens are changed to produce a different gradation of stone, the total production has to shut down. Managers of the larger quarries generally agreed that total stone production would usually average about 1,200 tons per hour and of the total, the production of graded stone could vary from 100 tons to 500 tons per hour depending on the variables stated above. They generally agreed that making a change in the machinery required a shutdown of 6 to 10 hours. Some of the managers stated that in order for it to be cost effective to change their machinery to produce a special riprap gradation, an order of at least 1 week's production would be required. This would mean that small orders of graded stone would receive little or no interest from some of the quarries unless they had the stone stockpiled or expected another order of the same gradation in the immediate future. Quarry managers were asked if production costs varied with a change from smaller to larger stone gradations. There was no consensus of opinion, but most stated their total production rate would increase if they were producing the coarser gradations, however this required more screens to remove the greater amount of fines.

d. Selected sets of gradation curves covering the spectrum of gradations commonly used in LMVD was prepared and shown the quarry managers (Inclosures 3 and 4). They all stated this full range of gradation bands could be produced, however, they indicated that production cost would be increased due to the need for additional screens. While all managers were not in agreement, the consensus of opinion was that the gradation bands were too tight at the 50 percent lighter by weight point for the set of gradation curves shown them. Most also agreed they would prefer the band be opened on the coarser side rather than the finer side since there is a tendency for certain types of stone to break up and segregate during transit, resulting in a different gradation from that produced at the quarry. Since some gradation tests are run at the job site rather than at the quarry, they stated that some relaxation of the band width and amount of fines allowed would assist in meeting gradation requirements. There appeared to be some confusion among the quarry managers on the amount and size of fines allowed below the minimum 15 percent lighter by weight point (W_{15}) of the specified gradation curves. Several of the quarry managers expressed concern over the lack of fines allowed below the minimum W_{15} , while at least one manager asked

specifically that 5 to 10 percent be allowed for fines below the minimum point. By definition, up to 15 percent of the total sample weight can weigh below the minimum W_{15} stone weight. However, guidance furnished in EM 1110-2-1601 for establishing the allowed volume of fines states that, "the bulk volume of stone lighter than the W_{15} stone should not exceed the volume of voids in revetment without this lighter stone." Therefore, the amount of fines should be kept to the minimum practical to be consistent with good riprap production practices and handling procedures. Quarry producers, as well as Corps inspectors, should be aware that small amounts of fines are acceptable.

5. Riprap Design Analysis.

a. A review of the design criteria presently being used in LMVD to size riprap and specify gradation and layer thickness was made during this study in order to determine if any standardization in design could be accomplished. The basic riprap design criteria being used to size riprap compare favorably to preliminary results of recent Waterways Experiment Station (WES) hydraulic model studies⁴ on riprap stability. The gradation curves furnished in ETL 1110-2-120 allow for some relaxation in the maximum 50 and 15 percent lighter by weight points, which would result in a wider band as requested by quarry managers. The resistance of riprap layers to tractive forces would not be affected by this change. The following is a summary of the design guidance presently being used.

(1) Since 1970 the Corps has used riprap design guidance based on Isbach's equation for movement of stone in flowing water. This guidance was published in HDC 712-1 and has been used to design riprap sizes for channel bottoms and side slopes downstream from stilling basins, river closures, and flood control channels. The Isbach coefficient of 0.86 recommended for sizing riprap for use in high-turbulence flow areas downstream of stilling basins and a coefficient of 1.20 was recommended for use in sizing riprap for low-turbulence flow areas such as flood control channels. Guidance furnished in the above referenced publication stated that the lower limit of the W_{50} stone should not be less than the weight of stone determined using the Isbach equation.

$$V = C \left\{ 2g \frac{\gamma_s - \gamma_w}{\gamma_w} \right\}^{\frac{1}{2}} (D_{50})^{\frac{1}{2}}$$

where:

V = Velocity (Average)

C = Isbach coefficient

g = Acceleration of gravity ft/sec²

γ_s = Specified weight of stone, lb/ft³

γ_w = Specified weight of water: lb/ft³

D = Stone diameter, ft, where the diameter of a spherical stone in terms of its weight W is:

$$D = \left(\frac{6W_{50}C}{\pi \gamma_s} \right)^{1/3}$$

(2) The thickness of the riprap blanket and the gradation are interrelated. Depending on where the riprap will be placed, the thickness of the riprap layer specified will vary from 1.0 to 1.5 times the maximum D_{100} stone size in the gradation. Miscellaneous Paper No. 2-777⁵ discusses this

relationship and points out that with a broad size span of riprap gradation, isolated pieces of large rock could protrude into the flow unless sufficient layer thickness is provided. The flow will accelerate around the large stone and remove smaller pieces, creating pockets where turbulence is intensified. Therefore, the layer thickness should be increased to 1.5 times the maximum D_{100} stone size in high-turbulence areas, such as around stilling basins, in order to ensure the larger pieces are inbedded properly. In low-turbulence flow areas the layer thickness can be reduced to the diameter of the largest stone in the gradation band. A nominal increase (50 percent) in layer thickness for underwater placement is normal to assure minimum layer thickness. Guidance furnished in EM 1110-2-1601 is used to compute the shear forces on riprap layers on both channel bottom and side slopes. The following is a summary of the guidance furnished in EM 1110-2-1601 and ETL 1110-2-120 for determining riprap gradation and thickness.

(a) Stone Gradation. The gradation of stones in riprap revetment affects the riprap's resistance to erosion. The stone should be reasonably well graded throughout the in-place layer thickness. Specifications should provide for two limiting gradation curves, and any stone gradation as determined from a field test sample, that lies within these limits should be acceptable. The gradation limits should not be so restrictive that stone production costs would be excessive. The choice of limits also depends on the underlying filter requirements if a graded stone filter is used. The following criteria provide guidelines for establishing gradation limits.

The lower limit of W_{50} stone should not be less than the weight of stone required to withstand the design shear forces as determined by the procedure given in EM 1110-2-1601 and HDC 712-1.

The lower limit of W_{50} stone should not exceed: five times the lower limit of W_{50} stone, that size which can be obtained economically from the quarry, or that size which will satisfy layer thickness requirements specified in paragraph 5a(2)(b) below.

The lower limit of W_{100} stone should not be less than two times the lower limit of W_{50} stone.

The upper limit of W_{100} stone should not exceed: five times the lower limit of W_{50} stone, that size which can be obtained economically from the quarry, or that size which will satisfy layer thickness requirements specified in paragraph 5a(2)(b) below.

The lower limit of W_{15} stone should not be less than one-sixteenth the upper limit of W_{100} stone.

The upper limit of W_{15} stone should be less than the upper limit of the filter as determined using guidance in EM 1110-2-1601.

The bulk volume of stone lighter than the W_{15} stone should not exceed the volume of voids in revetment without this lighter stone.

W_0 to W_{25} stone limits may be used instead of W_{15} stone limits determined by the above criteria if desirable to better utilize available stone sizes.

(b) Riprap Layer Thickness. All stones should be contained reasonably well within the riprap layer thickness to provide maximum resistance against erosive forces. Oversize stones, even in isolated spots, may cause riprap failure by precluding mutual support between individual stones, providing large voids that expose filter and bedding materials, and creating excessive local turbulence that removes smaller stones. Small amounts of oversize stone should be removed individually and replaced with proper size stones. When a quarry produces a large amount of oversize stone, consideration should be given to changing the quarrying method, using a grizzly to remove the oversize stone, obtaining the stone from another source, or increasing the riprap layer thickness to contain the larger stone. The following criteria apply to the riprap layer thickness:

It should not be less than the spherical diameter of the upper limit W_{100} stone or less than 1.5 times the spherical diameter of the upper limit W_{50} stone, whichever results in the greater thickness.

It should not be less than 12 inches for practical placement.

The thickness determined by either method above should be increased by 50 percent when the riprap is placed underwater to provide for uncertainties associated with this type of placement.

An increase in thickness of 6 to 12 inches, accompanied by appropriate increase in stone size, should be provided where riprap revetment will be subject to attack by large floating debris or by waves from boat wakes, wind, and bed ripples or dunes.

b. The placement of riprap is also an important part of riprap design since the effectiveness of riprap layer can be decreased significantly if excessive segregation and breakage occur. This concern is addressed in EM 1110-2-1601 and is summarized as follows:

The common methods used to place riprap are hand placing; machine placing, such as from a slip, dragline, or some other form of bucket; and dumping from trucks and spreading by bulldozer. Hand placement produces the best riprap revetment, but it is the most expensive method except when stone is usually costly and/or labor unusually cheap. Hand placed riprap can be used on steeper side slopes than with other placing methods. This reduces the required volume of rock. However, the greater cost of hand placement usually makes machine or dump placement methods and flatter slopes more economical. Hand placement on steeper slopes should be considered when channel widths are constricted by existing bridge openings or other structures and when rights-of-way are costly, provided the steeper slopes satisfy the appropriate slope stability guidance. In the machine placement method, sufficiently small increments of stone should be released as close to their final positions as practical. Rehandling or dragging operations to smooth the revetment surface tend to result in segregation and breakage of stone and rough revetment surface. Stone should not be dropped from an excessive height as this may result in the same undesirable conditions. Riprap placement by dumping and spreading is the least desirable method as a large amount of segregation and breakage can occur. In some cases, it may be economical to increase the layer thickness and stone size somewhat to offset the shortcomings of this placement method.

1 July 91

6. Standardization of Riprap Gradations.

a. There are several areas in which the criteria can be modified to reduce the number of different gradations currently being used within the Corps. The most obvious is to establish a set of gradation limits for given design conditions and layer thickness, to avoid arbitrary differences resulting from "rounding" preferences. This action can and will be implemented within LMVD. Other actions that would result in a reduced number of gradations are:

(1) Increasing the incremental step between theoretical layer thicknesses from the 3- and 6-inch increments currently used.

(2) Reducing the number of different riprap designs by using oversized riprap in some areas to be protected rather than specifying different gradations and layer thicknesses for two or more areas to be protected.

(3) Selecting a single design value of specific weight for stone that is representative of quarries in the region, and still ensure the stone meets minimum standards.

(4) Eliminating the option of using a slightly open or closed gradation band at the upper limits of the D_{50} and D_{15} points and adopting only one set of gradation bands for given design conditions.

(5) Combining design gradations for low-turbulence and high-turbulence areas; i.e., gradations established that will meet low-turbulence design guidance with a set of layer thicknesses, and also meet high-turbulence design guidance with a correspondingly different set of layer thickness. Each of these actions is discussed in the following paragraphs.

b. Action 1. Constrained by the fact that the riprap must meet minimum guidance, "standardizing" gradations becomes primarily an economic consideration. Increasing the interval between layer thickness for a set of standard gradations would result in an oversized riprap with increased reliability, but would also require an increased volume of stone on some jobs. In these cases, added cost would result due to the increased volume of riprap to be produced at the quarry, and in transporting and placing the additional riprap at the construction site. The trade-off in production savings that may be obtained by not having to change the machinery to produce a smaller gradation may be offset by the added cost of the increased volume and layer thickness required for an oversized gradation. The design and materials engineer would be required to determine the trade-off for each job. The cost effectiveness of increasing the interval between gradation layer thickness versus using non-standard layers is difficult to analyze without knowing the quarry that will be used to supply the stone and the mode of transportation for moving the riprap from the quarry to the job site. If the quantity of stone is sufficiently large, increasing the thickness of the riprap layer in order to use a standard gradation would probably be more expensive than paying the extra unit production cost at the quarry necessary to produce the non-standard gradation riprap. Information provided by quarry managers which indicates that 1 week's production is normally required for an economical change in gradation should be helpful in making this

gradations. However, it is concluded that the 27-inch and 33-inch thick layers be deleted because the gradations have a high degree of overlap with adjacent layers, and they are not as commonly used as the 24-, 30-, and 36-inch layers.

c. Action (2). There are many examples where small quantities of several different riprap gradations are specified in a single contract. A good example would be where scour protection is required at several bridges, and each design indicates a different gradation. Good engineering practice requires the designer to consolidate the minimum number of different designs and accept an oversized job on some of the bridges in order to avoid the added cost of producing, transporting, stockpiling, and placing several different gradations of stone in small quantities.

d. Action (3). A study of practices within LMVD Districts indicates that several different specific weight values are being used in riprap design, resulting in different gradations being specified to meet the same design conditions. Since in the design stage the quarry that will supply the stone is unknown, this procedure has little merit. A more logical procedure would be to use the minimum specific weight for stone that normally meets other specified requirements such as abrasion, hardness, absorption, etc., and does not eliminate quarries from competition which are approved as supply sources. This weight has been determined to be a specific weight of 155 pounds per cubic foot.

e. Action (4). Design guidance now allows some latitude in establishing the upper weight limits for the gradation band at the W_{50} and W_{15} Points as discussed previously in paragraph 5 and shown on Inclosure 5 for a typical gradation. This was intended to provide the designer with flexibility in establishing the gradation band in order that varying degrees of control would be exercised depending on design conditions, anticipated problems in production; etc., as previously discussed. Based on the field visits and discussions with quarry managers, establishing standards at these points which specify the open gradation band is highly desirable. Since this is also acceptable from a design standpoint, it is concluded that the gradation bands be standardized to use only the open bands.

f. Action (5). As discussed in paragraph 5, the design of riprap for low-turbulence and high-turbulence flow areas differ only slightly, however, the layer thickness is increased in the latter case. An analysis of different design cases reveals that there are gradation bands that are essentially identical, although they represent entirely different design conditions. Slight adjustments in the gradation bands and an accompanying slight shift in layer thicknesses for the low-turbulence design would result in standardization of these bands and essentially eliminate half the possible number of gradations previously used. The table on Inclosure 6 shows the resulting standard gradations and layer thicknesses for both high- and low-turbulence designs that are to be used. Gradations shown are the slightly opened bands as discussed in paragraph e above.

7. Summary and Actions.

a. This report has addressed several steps that can and will be taken to standardize riprap gradations and reduce the number of gradations currently in use. The report also reviewed design criteria and quarry operations in relation to the production of this riprap. The investigation revealed that there was some misunderstanding of gradation bands, particularly with regard to the smaller

stone. Mutual understanding of the gradation bands is needed among quarry managers, contractors, and Government inspectors. It was also found that quarries capable of producing graded riprap could produce almost any gradation specified. However, there are inherent cost savings and increased efficiency associated with using standard gradations that quarries have experience in producing, and keeping the number of gradations to the minimum practical. An analysis of cost versus production indicates that this is not necessarily an overriding factor, but does lend merit to establishing a set of standardized gradations. It is concluded that the almost unlimited number of gradations currently in use should be reduced to eight machine produced gradations. This will provide economy in construction and still retain sufficient flexibility for design.

b. The conclusions summarized below, which ensure safety and economy in design, will be implemented by the LMVD Districts.

(1) Use the standardized gradations shown on Inclosure 6 for specifying riprap at hydraulic structures and in channels adjacent thereto. Both low- and high-turbulence design gradations are included. There may be isolated cases where the use of a non-standard gradation is appropriate and can be justified as cost effective.

(2) Use oversized stone when cost effective, in order to reduce the number of gradations required in a contract involving several small placements.

(3) Use a specific weight of 155 pounds per cubic foot for all riprap design in order to prevent small gradation differences for the same design conditions.

(4) Use the increased maximum W_{50} and W_{15} points on the gradation curve (open hand) as shown in Inclosure 6 for both low- and high-turbulence flow conditions.

References

¹Engineering Technical Letter No. 1110-2-120, dated 14 May 1971

²Engineering Manual 1110-2-1601, dated 1 July 1970

³Hydraulic Design Criteria, sheet 712-1, dated September 1970

⁴Ongoing WES Research and Development Program, 31028, Title: Effects of Water Flow on Riprap in Flood Channels.

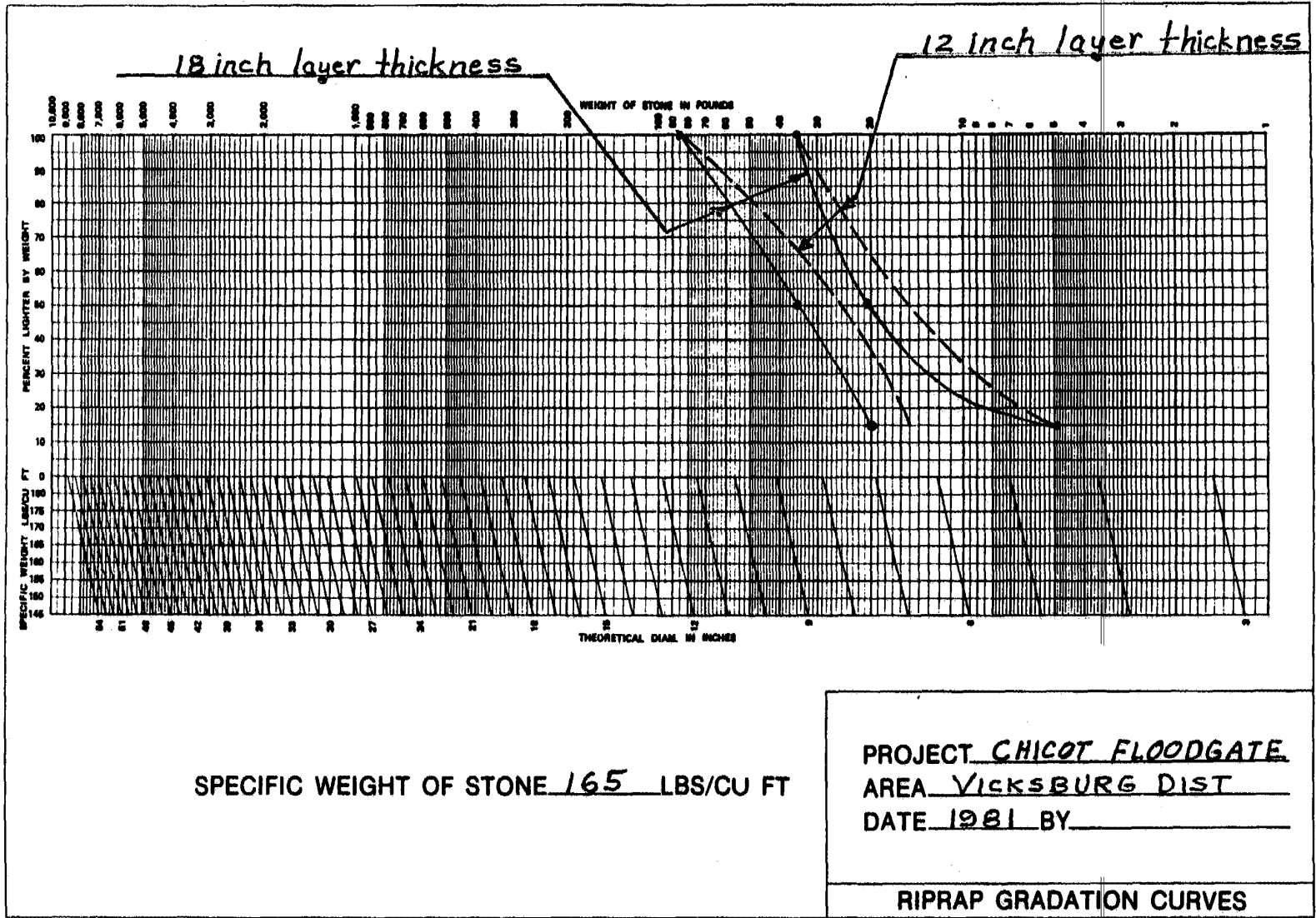
⁵Hydraulic Design of Rock Riprap, Miscellaneous Paper No. 2-777, dated February 1966

⁶Engineering Manual 1110-2-1602, dated 15 October 1980

AGC We know that design requirements on some special structures require different and special stone gradation from the normal A, B, and C. We have noticed an increase in the number of special gradations in the past year and believe that in some instances, one of the standard gradations would adequately serve. We request that special gradations be held to the minimum practicable and that standard gradation be used to the maximum extent possible.

LMVD As you may recall, several years ago we preformed a study of stone sizes for use on the Mississippi River and navigable tributaries to help standardize stone gradations and facilitate procurement of stone. The resulting gradations are called graded stone A, B, and C and are primarily used in trenchfill revetments, protecting river banks, and for rock dikes. For protection at major flood control and navigation structures, the use of A, B, or C stones is not cost effective because these gradations allow too wide a range of stone sizes and allow a high percentage of fines which do not provide proper protection in areas of high velocity and turbulence which leads to riprap failure. Also, these gradations do not meet the Corps of Engineers criteria for stone gradation in such areas where high turbulence exists. At such structures a more uniformly graded stone is required. For example, the ratio of the weight of the largest size piece to that of the smaller pieces is in the neighborhood of 6, whereas that same ratio for Graded Stones A, B, and C is in the range of 70 to 200.

We recognize the desirability of developing standard gradations for riprap which can be used at structures, and we will undertake a study to do this. In this regard, it will be necessary for us to check with some quarries to determine the availability of stone sizes in the desired range in attempting to develop these new standard gradations. The cost effectiveness of using standard gradations will be evaluated. We will keep you informed of progress on this study.



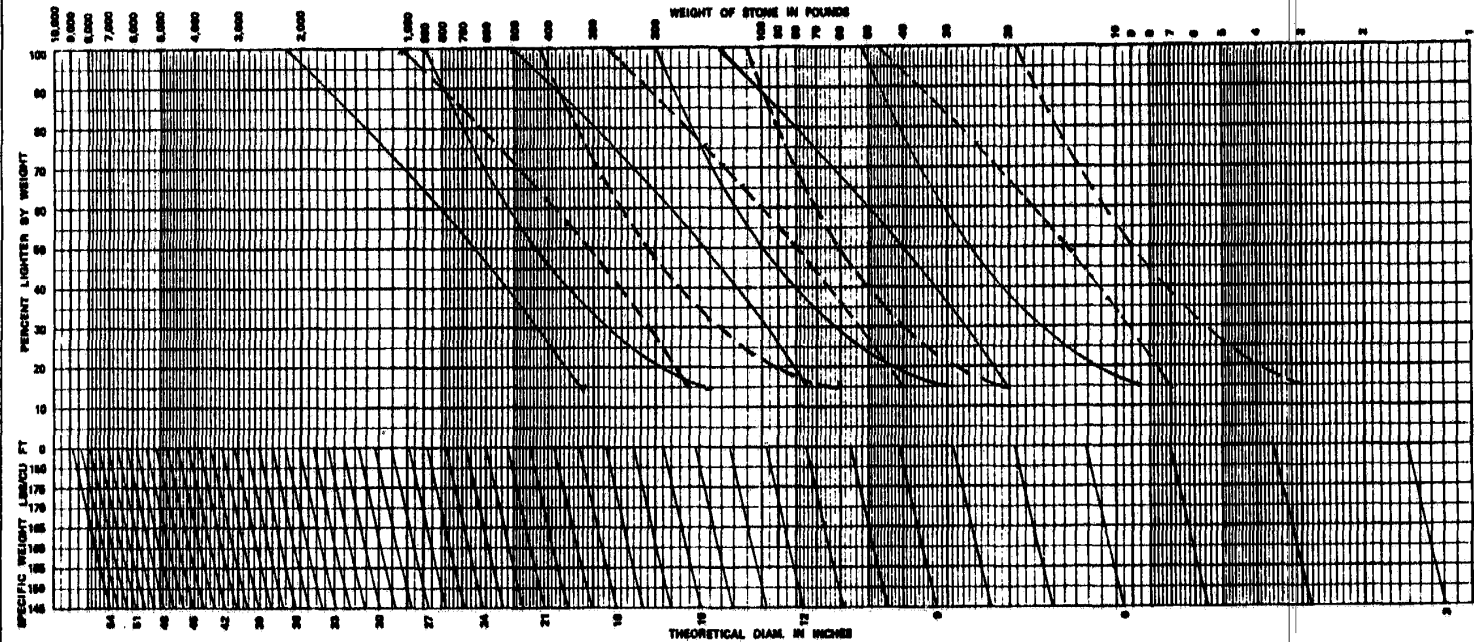
ENG FORM 4794-R, Sep 82

(EM 1110-2-1601)

(Proponent: DAEN-CWE-HD)

set of gradation curves shown to Quarry Managers

Layer thickness = 54, 42, 33, 27, 21, 15 inches



SPECIFIC WEIGHT OF STONE 155 LBS/CU FT

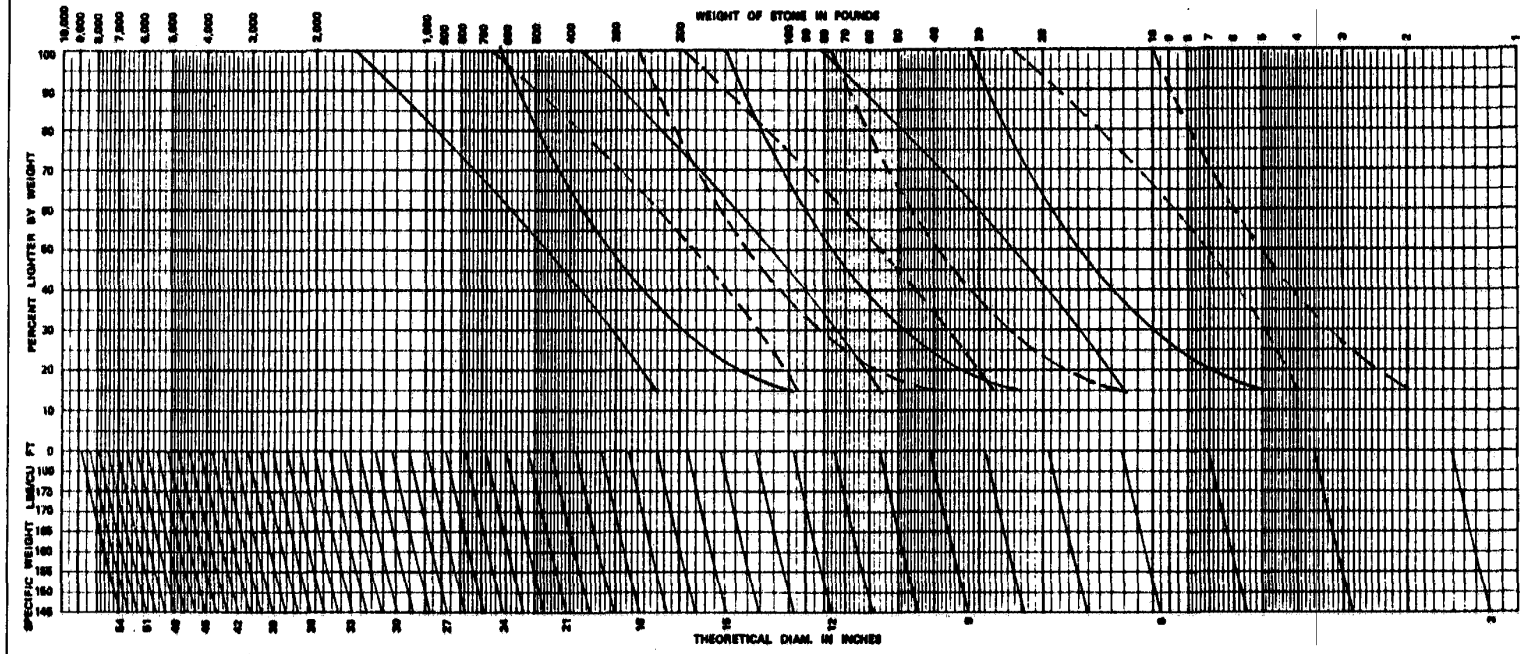
$T = 1.5 D_{(100)} \text{ Max}; 2.25 D_{(50)} \text{ Max}$

PROJECT STANDARD GRADATIONS
 AREA LMVD
 DATE Oct 82 BY Malcolm Dove

RIPRAP GRADATION CURVES

Set of gradation curves shown to Quarry Managers

Layer thickness = 48 , 36 , 30 , 24 , 18 , 12 inches

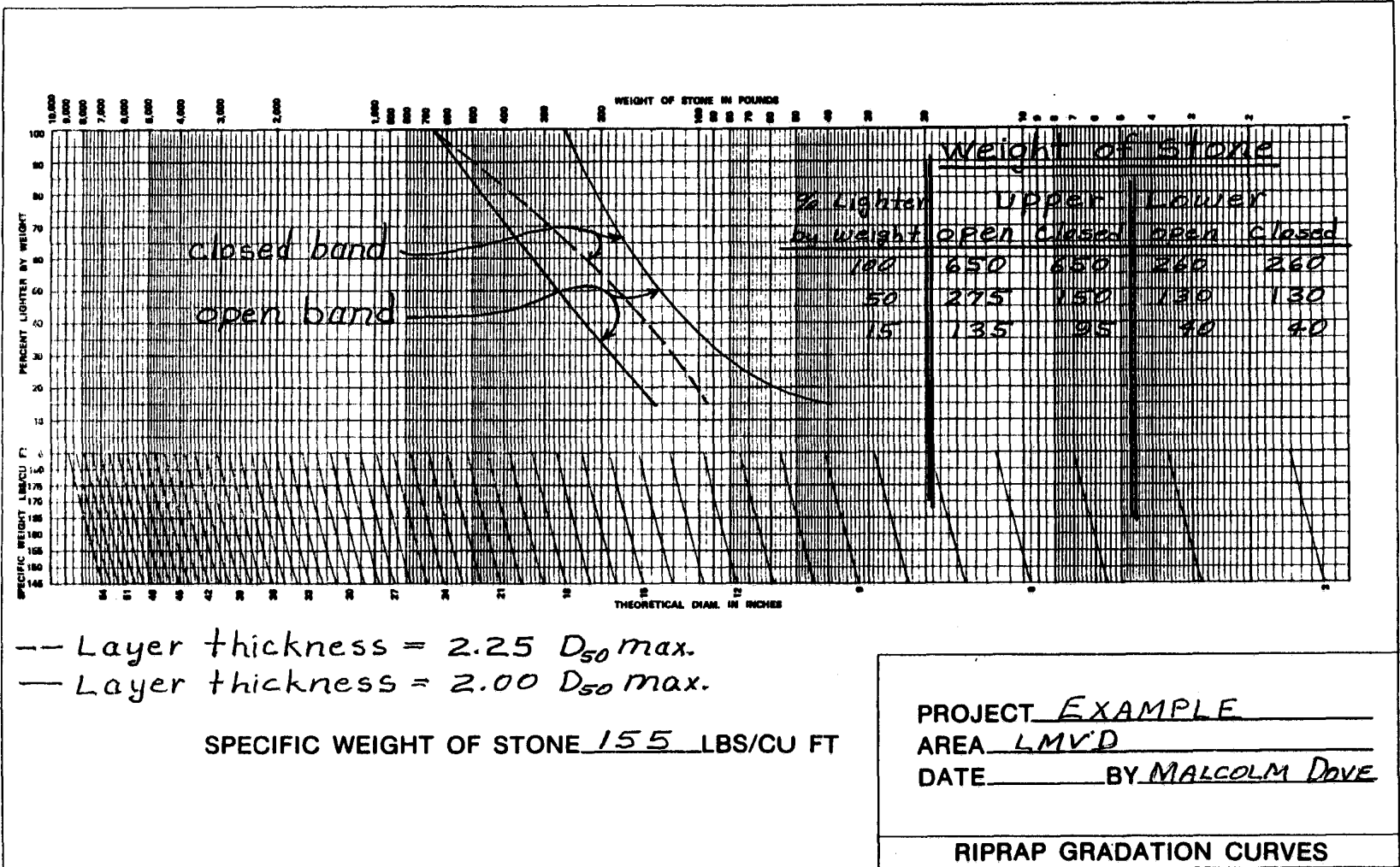


SPECIFIC WEIGHT OF STONE 155 LBS/CU FT

$T = 1.5 D(100) \text{ Max} ; 2.25 D(50) \text{ Max}$

PROJECT STANDARD GRADATIONS
 AREA LMVD
 DATE Oct 82 BY Malcolm Dove

RIPRAP GRADATION CURVES



ENG FORM 4794-R, Sep 82

(EM 1110-2-1601)

(Proponent: DAEN-CWE-HD)

U.S. Government Printing Office : 1982 - 522-097/536

EM 1110-2-1601
1 Jul 91

*

LMVD
 12 November 81
 STANDARD RIPRAP GRADATIONS
 (Design Specific Weight 155 pounds per cubic feet)

	GRADATION NORMALLY PRODUCED MECHANICALLY								GRADATIONS NORMALLY REQUIRING SPECIAL HANDLING				
Layer Thickness in Inches High Turbulent Flow	12	15	18	21	24	30	36	42	48	54	63	72	81
Layer Thickness in Inches Low Turbulent Flow			12	14	16	20	24	28	32	36	42	48	54
Percent Lighter by Weight													
100	25 10	50 20	90 40	140 60	200 80	400 160	650 260	1000 400	1500 600	2200 900	3500 1400	5000 2000	7400 3000
50	10 5	20 10	40 20	60 30	80 40	160 80	280 130	430 200	650 300	930 440	1500 700	2200 1000	3100 1500
15	5 2	10 5	20 5	30 10	40 10	80 30	130 40	210 60	330 100	460 130	700 200	1100 300	1500 500

*

Appendix G Velocity Estimation Based on Field Observations

G-1. General

Another means of velocity estimation is based on field observations. Depth-averaged velocities at stages less than design stages are used to estimate depth-averaged velocities at design conditions. Limited data supporting this concept and the analytical relationship based on Manning's equation are shown in Plate G-1. These data were taken from a channel model bend having riprapped bed and banks (1V on 2H side slope) and from channel bends on the Sacramento River having 1V on 2H side slopes. More data are needed and it is almost certain that the lower the stage at observation, the poorer the estimate of velocities at the design conditions.

G-2. Relationship of Surface and Depth-Averaged Velocities

In conjunction with the extrapolation of depth-averaged velocities, tests were conducted to determine the relationship between surface velocities and depth-averaged velocities. Based on model and field results taken in channel bends near the downstream end of the bends, the depth-averaged velocity was roughly 85 percent of the

surface velocity. For the purpose of estimating velocities for riprap design, the surface velocities should be taken at various distances from the natural bank until the maximum is found. A complicating factor results from the fact that after an eroding bank is protected, the depth along the outer bank increases, which results in an increase in velocity. Techniques are not available to define this increase. A 25 percent increase is proposed until data become available.

G-3. Example

For example, suppose that at the time of observation of an eroding bank, the thalweg depth is approximately 15 ft. If the maximum surface velocities are determined to be 6 ft/sec, then the depth-averaged velocity for the observed condition will be $0.85(6) = 5.1$ ft/sec. If the thalweg depth at design conditions is 25 ft, then from Plate G-1 (using the design curve), the design velocity will be $1.5(5.1) = 7.7$ ft/sec. This velocity should then be increased by 25 percent to account for the increase in velocity after the bank is protected. The design velocity is $1.25(7.7) = 9.6$ ft/sec. It is obvious that many site-specific factors can cause this method to yield velocities that are substantially in error. Use of this method is recommended only when no other techniques for determining velocity are available.

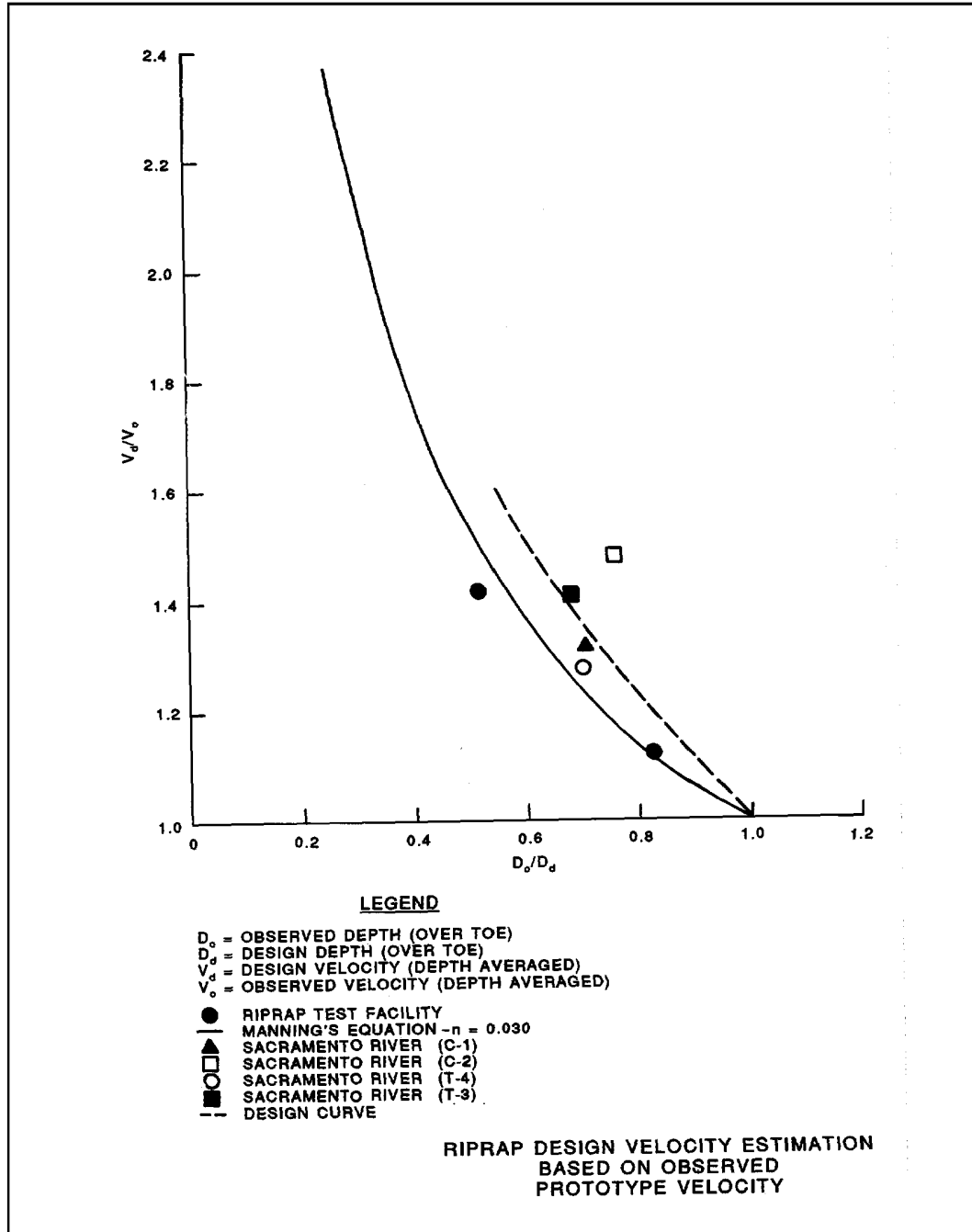


PLATE G-1

Appendix H Examples of Stone Size Calculations

H-1. Problem 1

a. Problem. Determine stable riprap size for the outer bank of a natural channel bend in which maximum velocity occurs at bank-full flow. Water-surface profile computations at bank-full flow show an average channel velocity of 7.1 ft/sec and a depth at the toe of the outer bank of 15 ft. The channel is sufficiently wide so that the added resistance on the outer bank will not significantly affect the computed average channel velocity (true in many natural channels). A nearby quarry has rock weighing 165 pcf and can produce the 12-, 18-, and 24-in. $D_{100}(\text{max})$ gradations shown in Table 3-1. A bank slope of 1V on 2H has been selected based on geotechnical analysis. A blanket thickness of $1D_{100}(\text{max})$ will be used in this design. Bend radius is 620 ft and water-surface width is 200 ft.

b. Solution. Using Plate 33, the maximum bend velocity V_{SS} is 1.48(7.1) or 10.5 ft/sec. The side slope depth at 20 percent up the slope is 12 ft. Using either Equation 3-3 or Plates 37 and 40, the required D_{30} is 0.62 ft. From Table 3-1, the 18-in. $D_{100}(\text{max})$ gradation is the minimum available gradation that has $D_{30}(\text{min})$ greater than or equal to 0.62 ft. This example demonstrates the added safety factor that often results from using standard gradations to avoid the extra production costs incurred by specifying a custom gradation for every design condition.

H-2. Problem 2

a. Problem. Determine stable riprap size in a bend of a trapezoidal channel with essentially uniform flow. Bank slope is 1V on 2H and both the bed and banks will be protected with the same size of riprap. The bottom width is 140 ft, slope is 0.0017 ft/ft, and the design discharge is 13,500 cfs. Use $1D_{100}(\text{max})$ thickness and the same quarry as in Problem 1. Bend radius is 500 ft and bend angle is 120 degrees.

b. Solution. In this problem the solution is iterative; flow depth, velocity, and rock size depend on each other. Use Strickler's equation $n = 0.036 (D_{90}(\text{min}))^{0.166}$ to estimate Manning's resistance coefficient. Bend velocity is determined using Plate 33.

(1) Assume trial gradation and solve for riprap size as shown in Tables H-1 and H-2. Use uniform flow computations listed in Table H-1.

(2) Use velocity estimation and riprap size equations to obtain riprap size in Table H-2.

This example demonstrates that the increasing rock size for the three trial gradations results in increasing depth and decreasing velocity. The minimum acceptable gradation is the 18-in. $D_{100}(\text{max})$.

EM 1110-2-1601
Change 1
30 Jun 94

Table H-1
Uniform Flow Computations

Trial D ₁₀₀ (max) in.	Manning's n	Normal Depth, ft ¹	Water- Surface Width, ft	Average Velocity fps ¹	Side Slope Depth, ft
12	0.034	10.6	182.4	7.9	8.5
18	0.036	11.0	184.0	7.6	8.8
24	0.038	11.3	185.2	7.3	9.0

¹ From iterative solution of Manning's equation $Q/A = (1.49/n)R^{2/3}S^{1/2}$.

* **Table H-2**
Velocity Estimation and Riprap Size

Trial D ₁₀₀ (max) in.	<u>Bottom Width</u> Depth	R/W	V _{SS} , ¹ fps	Computed D ₃₀ , ² ft	D ₃₀ (min) of trial ³ ft
12	13.2	2.74	9.9	0.59	0.48
18	12.7	2.72	9.5	0.53	0.73
24	12.4	2.70	9.2	0.48	0.97

¹ From Plate 33 using trapezoidal channel.

² From Equation 3-3 or Plates 37 and 40.

³ From gradation information given in Table 3-1.

*

**Appendix I
Notation**

		\bar{C}	Ratio of experimentally determined air volume to air plus water volume
		C_c	Contraction coefficient
		C_e	Expansion coefficient
		C_s	Stability coefficient
		C_T	Thickness coefficient
		C_V	Vertical velocity distribution coefficient
		C_1	Correction for unit stone weight other than 165 pcf
		C_2	Correction for side slope angle
		d	Depth of flow, ft
		d_a	Depth of air-water mixture, ft
		d_c	Critical depth of flow, ft
		d_w	Experimental water flow depth, ft
		$D_{\%}$	Equivalent-volume spherical stone diameter, ft
		D_{30}	Riprap size of which 30 percent is finer by weight, ft
		$D_{90(\text{min})}$	Size of stone of which 90 percent of sample is finer, from minimum or lower limit curve of gradation specification, ft
		f	Darcy-Weisbach resistance coefficient
		F	Froude number
		* F_g	Grain Froude number *
		F_1	Froude number in upstream channel of a rectangular channel contraction
		F_2	Froude number at intersection of wave fronts in transition of rectangular channel contraction
		F_s	Froude number for limit of stable flow
a	Undular wave height above initial depth, ft, maximum length of revetment stone		
* a_n	End area associated with subdivided area n *		
* A	Cross-sectional area, ft ² ; total end area of cross section *		
A_a	Cross-sectional area of upstream section, ft ²		
A_b	Cross-sectional area of downstream section, ft ²		
* A_i	End area of subdivided area i , subsection i *		
A_p	Cross-sectional area of pier obstruction, ft ²		
* A_r	Iwagaki coefficient for rough flow *		
* A_s	Iwagaki coefficient for smooth flow *		
A_1	Cross-sectional area of upstream channel, ft ²		
A_2	Cross-sectional area of channel within pier, section, ft ² ; cross-sectional area of downstream channel, ft ²		
A_3	Cross-sectional area of downstream channel, ft ²		
b	Channel bottom width, ft		
b_c	Confluence width, ft		
b_m	Average depth of flow at midpoint of the confluence, ft		
b_1	Upstream channel bottom width, ft		
b_3	Downstream channel bottom width, ft		
c	Maximum dimension of revetment stone parallel to the short axis		
C	Chezy's resistance coefficient; superelevation formula coefficient; weir coefficient; critical depth over crest		

EM 1110-2-1601

Change 1

30 Jun 94

g	Acceleration due to gravity, ft/sec ²	m_a	Total hydrostatic force of water in channel upstream section, lb
h_f	Energy loss due to friction, ft	m_b	Total hydrostatic force of water in channel downstream section, lb
h_1	Head loss between cross sections, ft	m_p	Total hydrostatic force of water on pier ends, lb
H	Total energy head, ft	M	Momentum per unit time, lb-sec/sec
H_e	Total specific energy of flow, ft	n	Manning roughness coefficient, ft
k and k_s	Effective roughness height, ft	n_b	Base n value *
k_c	Critical value of effective roughness height, ft	n_i	n value in subdivided area i , subsection i *
* K	Coefficient in Strickler's equation, ft; total conveyance in cross section *	n_N	n value in subdivided area n *
* K_i	Conveyance in subdivided area i , subsection i *	n_r	Ratio of Manning's n, model-to-prototype
K_1	Side slope correction factor	* n_1	Addition for surface irregularities *
L	Length of channel transition, ft, length of spillway crest, ft	* n_2	Addition for variation in channel cross section *
L_m	Length in model, ft	* n_3	Addition for obstructions *
L_p	Length in prototype, ft	* n_4	Addition for vegetation *
L_r	Length ratio, model-to-prototype	* \bar{n}	Composite n value for the section *
L_s	Length of spiral transition, ft	* N	Last subdivided area in the cross section *
L_1	Distance from beginning of transition to intersection point of wave fronts, ft	* p_N	Wetted perimeter in subdivided area n *
L_2	Distance from end of transition to intersection points of wave fronts, ft	P	Total wetted perimeter in the cross section
m	Total hydrostatic force of water in channel cross section, lb; air-water ratio; ratio for meandering *	P_1, P_2, P_3	Hydrostatic pressure forces acting on the control volume at the reference sections, lb
* m_1	Total hydrostatic force of water in upstream channel cross section, lb	P_f	total external force of frictional resistance along the wetted surface, lb
m_2	Total hydrostatic force of water in pier section, lb	q	Flow rate (discharge) per unit width of channel, ft ³ /sec/ft
m_3	Total hydrostatic force of water in downstream channel cross section, lb	Q	Total flow rate, discharge, cfs
		Q_n	Discharge in subsection, cfs

Q_T	Total discharge, cfs	\bar{V}	Flow velocity in subsection, fps
* Q_{mcb}	Discharge producing a stage near the tops of the midchannel bars *	V_{AVG}	Average channel velocity at upstream end of bend, fps
r	Center-line radius of bend, ft	V_c	Critical flow velocity, fps
r_L	Radius of left channel wall, ft	V_{SS}	Characteristic velocity for side slope equal to local average velocity over slope at a point 20 percent of the slope length up from toe of slope, fps
r_R	Radius of right channel wall, ft		
r_{min}	Minimum center-line radius of channel bend, ft	* V_{mcb}	Average channel velocity at the top of midchannel bars *
R	Hydraulic radius, ft; center-line radius of bend, ft	W	Channel width at elevation of center-line water surface, ft; water-surface width, ft; weight of the water in the control volume
* \bar{R}	Mean hydraulic radius *		
* R_c	Average hydraulic radius for the entire cross section *	$W_{\%}$	Weight of individual stone having diameter of $D_{\%}$, lb
* R_i	Hydraulic radius of subdivided area i , subsection i *	X	Longitudinal distance from beginning of expansion, ft
R_n	Reynolds number	y	Flow depth in straight channel, ft
* s_s	Specific gravity of sediment particles *	y_r	Vertical scale ratio, model-to-prototype
* S	Sine of angle of chute inclination; slope of bed *	\bar{y}	Distance from water surface to center of gravity of the flow section, ft
S_c	Critical slope, ft/ft	y_1	Flow depth in upstream channel of rectangular channel contraction, ft
S_f	Friction slope, i.e., slope of energy grade line, ft/ft; safety factor	y_2	Flow depth in transition at wave front intersection of rectangular channel contraction, ft
S_o	Slope of channel invert, ft/ft		
S_r	Ratio of model slope to prototype slope	Z	Side slope, horizontal to vertical, ft/ft; transverse distance from channel center line, ft
T	Thickness of riprap revetment, ft; sill submergence	α	Energy correction factor; angle of the channel slope ($\tan \alpha =$ channel slope); velocity head correction factor
U	Unknown reaction force exerted by the walls of the lateral in the upstream direction		
* U_*	Boundary shear velocity, fps *	α_1	Wave front angle from upstream channel wall in rectangular channel transition, deg
* V	Average flow velocity, fps; velocity of flow, fps; local depth-averaged velocity, V_{SS} for side slope riprap, length/time *		

EM 1110-2-1601

Change 1

30 Jun 94

α_2	Wave front angle from downstream channel wall in rectangular channel transition, deg	ζ	Depth-width ratio
β	Momentum correction coefficient; wave front angle	θ	Angle of side slope with horizontal, deg; wave-front reflected angle, deg; wall deflection angle in rectangular channel transition, deg; angle of intersection of the junction of side channel with main channel, deg
* γ and γ_w	Specific weight of water, pcf		
γ_s	Saturated surface dry specific weight of stone, pcf	ν	Kinematic viscosity of water, ft ² /sec
Δb_3	Required increase in channel width	ξ	Flow function, $Q/b^{5/2}$
Δh_v	Velocity head change from upstream to downstream-of transition, ft	σ	Geometric standard deviation of the sediment mixture
ΔP_1	Component in the main channel direction of the hydrostatic pressure acting over the width	ϕ	Angle of repose of riprap material, deg *
Δy	Superelevation of water surface in channel bend, ft		